POLLUTANTS IN ROAD-DEPOSITED SEDIMENTS: CHARACTERISTICS, MOBILITY, BIOAVAILABILITY AND REMEDIATION

By

THUY CHUNG NGUYEN

A Thesis submitted in fulfilment for the degree of

Doctor of Philosophy

School of Civil and Environmental Engineering

Faculty of Engineering & Information Technology

University of Technology Sydney

New South Wales, Australia

February 2016

CERTIFICATE OF AUTHORSHIP/ ORIGINALITY

I certify that the work in this thesis has not previously been submitted for a degree nor has it been submitted as part of requirements for a degree except as fully acknowledged within the text.

I also certify that the thesis has been written by me. Any help that I have received in my research work and the preparation of the thesis itself has been acknowledged. In addition, I certify that all information sources and literature used are indicated in the thesis.

Signature of Candidate:

Thuy Chung Nguyen

September 2015

Acknowledgement

I would like to express my deep gratitude to my principal supervisor Prof. Saravanamuthu Vigneswaran as my principal-supervisor for his support, enthusiasm and motivation when I undertook this thesis. My second deepest thanks go to my co-supervisor, Dr. Paripurnanda Loganathan and Dr Tien Vinh Nguyen for their tremendous help and support through my whole PhD study. I would also like to thank Professor Richard Lim, Dr Anne Colville, Dr Jaya Kandasamy and Dr Thi Thu Nga Pham for their help and support. I would also like to thank my colleagues and lab mates Dr. Jeong, Danious, Sukanya, Gayathri, Tram, Son and Hien Phuong in Centre of Technology for Water and Wastewater (CTWW). I would like to give a special mention to my team member and Senior Technical Officer of Environmental Engineering Laboratories, Md Abu Hasan Johir who had always been supportive in sharing his valuable time and ideas for my research.

I would like to show my gratitude to Prof. Ravi Naidu, Managing Director of Cooperative Research Centre for Contamination Assessment and Remediation of the Environment (CRC-CARE) and Mr. Andrew Beverage for the financial support. I owe my thanks to the academic and technical support of the University of Technology, Sydney and its staff, especially Phyllis for all my academic support. I would like to thank Smart Water Research Centre of Griffith University, Gold Coast, Australia and NSW Environment Protection Authority (EPA) for toxicity testing instruction and equipment supplies. I would like to give thankfulness to National Measurement Institute (NIM) for chemical analysis.

My most profound thanks, my most heartfelt appreciation; my deepest gratitude goes to my parents, without whom none of this could have been accomplished. At first, I heartily thank my parents for their blessings, love, care, sacrifices, suggestions, help and support not only for my PhD study for my whole life. It was my parents dream for me to get Doctorate degree and today I am going to get this degree because of them. I will never be able to thank my loving husband Nguyen Xuan Binh, who made me believe in myself and encouraged me through the whole process of research and always stayed beside me during my struggling periods. Thank you my dear husband for your selfless support in sharing the parenting and for loving me the way you do. I would like to thank my cutest and dearest daughter, Nguyen Thi Minh Ngoc who gave me every reason to complete this PhD through all hardships with happy and smiley face. She is my sunshine and great motivation for my life and study.

DEDICATION THIS THESIS

TO MY HUSBAND AND MY DAUGHTER

Journal papers Published

Journal publications

1. **Nguyen, T. C.**, P. Loganathan, T. V. Nguyen, S. Vigneswaran, J. Kandasamy, D. Slee, G. Stevenson, R. Naidu (2014). Polycyclic aromatic hydrocarbons in road-deposited sediments, water sediments, and soils in Sydney, Australia: Comparisons of concentration distribution, sources and potential toxicity. Ecotoxicology and Environmental Safety 104:339-348.
2. **Nguyen, T.C.**, P. Loganathan, T. V Nguyen, S. Vigneswaran, J. Kandasamy, R. Naidu. (2015). Simultaneous adsorption of Cd, Cr, Cu, Pb, and Zn by an iron-coated Australian zeolite in batch and fixed-bed column studies. Chemical Engineering Journal 270: 393-404.
3. **Nguyen, T.C.**, P. Loganathan, T.V. Nguyen, T.T.N. Pham, S. Vigneswaran, J. Kandasamy, M. Wu, and R. Naidu (2015). Trace elements in road-deposited and water bed sediments in Kogarah Bay of Sydney, Australia: Enrichment, sources, and fractionation. Soil Research 53(4): 401-411.

Conference papers and presentation

1. **Nguyen T.C.**, Loganathan P., Nguyen T.V., Vigneswaran S., Kandasamy J., Slee D., Naidu R. (2012) Polycyclic aromatic hydrocarbons and heavy metals in road-deposited sediments, water sediments and soils, FEIT Research Showcase 2012, UTS, Sydney, Australia September 12th-13th, 2012.

2. **Nguyen T.C.**, Loganathan P., Nguyen T.V., Vigneswaran S., Kandasamy J., Slee D., Naidu R. (2013). Heavy metals in road-deposited and water sediments at Kogarah bay, Sydney: Enrichment, sources, and fractionation, 5th IWA Specialist Conference on Metals and Related Substances in Drinking Water. Topic: "Metals in water – health protection and sustainability through technical innovation", Shanghai, China, November 6th-9th, 2013.

3. **Nguyen T.C.**, Loganathan P., Nguyen T.V., Vigneswaran S., Kadasamy J., Stevenson G., Naidu R. (2014). Polycyclic aromatic hydrocarbons and heavy metals in road-deposited sediments, water sediments and soils in Kogarah, Sydney, CRC Communication Conference, Adelaide, SA, Australia, 10th – 13th September, 2014.

4. **Nguyen T.C.**, Colville A., Lim R., Rahman M.A., Nguyen T.V., Loganathan P., Kandasamy J., Naidu R., Vigneswaran S. (2014) Aquatic toxicity assessment of road-deposited sediments in Sydney, Australia, 9th SETAC Asia/Pacific 2014 Conference, 14-17th, September 2014.

5. **Nguyen T.C.**, Loganathan P., Nguyen T.V., Vigneswaran S., Kandasamy J., Slee D., Naidu R. (2014). Simultaneous adsorption of heavy metals by a natural Australian iron coated zeolite, 5th IWA Young Professional Conference, Taipei, Chinese Taiwan, 7-10th, December 2014.

Awards

1. Certificate of completion in Professional Development Program in Civil and Environmental Engineering Research during 2012-2015 (University of Technology Sydney)
2. 2015 FEIT Research Publication Award 2015
3. 2013 FEIT Showcase Attendance Certificate

TABLES OF CONTENT

LIST OF FIGURES

CHAPTER 2

CHAPTER 3

CHAPTER 4

CHAPTER 5

CHAPTER 6

CHAPTER 7

LIST OF TABLES

CHAPTER 2

CHAPTER 3

CHAPTER 4

CHAPTER 5

CHAPTER 6

NOMENCLATURE

AET = apparent effects threshold

AhR = AhR aryl hydrocarbon receptor;

Ant = Anthracene

B[a]A = Benzo[a]anthracene

B[a]P = Benzo[a]pyrene

B[b]F = benzo[b]fluoranthene

B[ghi]P = benzo[g,h,i]perylene

B[k] = benzo[k]fluoranthene

BAET = benthic apparent effects threshold

BLS = Baseline soil

C_o = initial concentration of adsorbate (mg/L)

$Ca(OH)_2$ = Calcium hydroxide

Ca^{2+} = Calcium

CAFLUX = Chemically Activated Fluorescent Expression

C_e = equilibrium concentration of adsorbate (mg/L)

Chry = chrysene

C_o = inlet adsorbate concentration (mg/L)

C_s = the concentration on the external surface (mg/L)

C_t = concentration of adsorbate at time t (mg/L)

CYP1A1 = Cytochrome P450 1A1

DBA = dibenzo[a,h]anthracene

DOC = dissolved organic matter

DRE = dioxin response element

dw = dry weight

EC50 = estimated concentration needed to produce 50% of the maximal response

EROD = ethoxyresorufin O-deethylase

F = Fluorene

Fe^{3+} = Iron (III)

FeO = Zero-valent iron

Fl = Fluoranthene

FTIR = Fourier transform infrared spectroscopy

g/L = gram per litre

GAC = Granular activated carbon

HA = Humic acid

HACCP = Hazard Analysis and Critical Control Point

HAH = halogenated aromatic hydrocarbons

HCl = hydrochloric acid

HCO_3^- = bicarbonate

HFO = Hydrous ferric oxides

HMW PAH = high molecular weight PAHs

hr = hours

HSDM = Homogeneous surface diffusion model

ICZ = Iron-coated zeolite

IND = indeno[1,2,3-cd]pyrene

K^+ = Potassium

k_1 = equilibrium rate constant of pseudo-first-order sorption (1/min)

k_2 = equilibrium rate constant of pseudo-second-order (1/min)

kAB = kinetic constant, (L/mg.min)

KNO_3 = Potassium nitrate

KCl = Potassium chloride

KF = Freundlich constants (mg/g)

kf = the external mass transfer coefficient (m/s)

KH_2PO_4 = Monopotassium phosphate

KL = Langmuir constant related to the energy of adsorption (L/mg)

k_{Th} = Thomas rate constant (mL/min.mg)

k_{YN} = rate velocity constant (1/min)

LD50 = 50% lethal dose

LMW PAH = low molecular weight PAHs

LOEL = lowest observed effect level

M = mass of dry adsorbent (g)

m/h = meter per hour

mg/L = miligram per litre

MFO = mixed-function oxidase (or oxygenase) enzyme system

min = minutes

mL/min = millilitre per minute

MW = Molecular weight

Na^+ = Sodium

Na_2CO_3= Sodium carbonate

Na_2SO_4 = Sodium sulphate

NaCl = sodium chloride

$NaHCO_3$ = sodium bicarbonate

$NaNO_3$ = sodium nitrate

NaOH = Sodium hydroxide

Nap = Naphthalene

NOEL = No observed effect level

NOM = Natural organic matter

P450 = Cytochrome P450

PAH = Polynuclear aromatic hydrocarbon

PCB = Polychlorinated biphenyl

PCDDs = Polychlorinated dibenzo-p-dioxins

Phe = Phenanthrene

Pyr = Pyrene

RDS= Road-deposited sediments

TCDD = 2,3,7,8-tetrachlorodibenzo-p-dioxin

TCDF = 2,3,7,8-tetrachlorodibenzofuran

TEF = Toxic equivalency factor

TCDD TEQ = Dioxin TCDD toxic equivalent quotient

TPAH = Total PAHs

WBS = Water baseline sediments

WUSD = Water Sensitive Urban Design

μ = Solution viscosity

XRD = X-ray powder diffraction

SEM = Scanning Electron Microscopy

EDS = Energy Dispersive Spectroscopy

TEQ = toxicity equivalent quotient

ABSTRACT

Rapid urbanization and associated ever-increasing motor-traffic density have led to escalating amounts of pollution along road-ways in the form of aerosols and road-deposited sediments (RDS) in many parts of the world. RDS contain many pollutants such as heavy metals, metalloids and polycyclic aromatic hydrocarbons (PAHs) which are derived from vehicle exhaust emissions, vehicle tyres, brakes, body frames, asphalt road surfaces, deicing salt, paint markers, and pesticides and herbicides added to the pavement. During heavy rain, these pollutants are washed into stormwater and transported into natural water bodies and this can cause potentially toxicity to aquatic organisms.

Road-deposited sediments (RDS), water baseline sediments (WBS) and baseline soil (BLS) samples from major urban roads in Kogarah Bay area, Sydney, were analyzed for several heavy metals/metalloids and polycyclic aromatic hydrocarbons (PAHs). RDS had elevated concentrations of Pb, Cd, Cu, Cr, Ni, Zn, Fe and PAHs. Both correlation and principal component analysis showed that Zn, Cu, Cr, and Sb in RDS probably originated from vehicle brakes and tyre wear while V originated mainly from road asphalt surface. The heavy metal concentrations were similar in WBS and BLS. Heavy metal fractionation data showed that potential mobility, an indication of their transportation by stormwater, decreased in the order Fe > Mn, Zn > Cu, Pb > Cr, Ni, V, Cd, Sb. Ecological risk as assessed by ISQG (Interim Sediment Quality Guidelines) and the method developed by Hakanson (1980) was low to medium in RDS and low in BLS and WBS. Of the heavy metals in RDS, Cu had the highest potential risk, whereas Zn had the lowest.

The concentrations of sixteen polycyclic aromatic hydrocarbons (PAH mg/kg) in the RDS, WBS and BLS ranged from 0.40 to 7.49 (mean 2.80), 1.65 to 4.00 (mean 2.91), and 0.46 to 1.41 (mean 0.84), respectively. PAH compounds had higher concentrations of high molecular weight compounds with three or more fused benzene rings indicating that high temperature combustion processes were their predominant sources. The proportions of high molecular weight PAHs were higher in BLS than in RDS, whereas the low molecular weight PAHs were higher in RDS. All PAH compounds were observed to be the lowest in WBS. All PAHs (except naphthalene) were significantly correlated in BLS suggesting a common PAH source. The ratios of individual diagnostic PAHs showed that the primary source of PAHs in WBS and BLS was pyrogenic (combustion of petroleum (vehicle exhaust), grass, and wood) and in

RDS was petrogenic (unburned or leaked fuel and oil, road asphalt) as well as pyrogenic. The potential toxicities of PAHs calculated using toxicity equivalent quotients were all low but higher for BLS than for WBS and RDS.

This study also investigated the toxic effects of RDS and BLS in a range of bioassays, using water elutriates of sediments from different sites to simulate contaminated receiving waters, and solvent extracts to represent the total contaminant levels. Chemical analyses showed that the total concentrations of metals and PAHs in the RDS were above sediment quality guidelines, and were higher in the finer size fractions. Metal and PAH levels in the BLS were well below guideline levels. To establish baseline toxicity data, acute *Artemia* nauplii tests were carried out with putatively identified compounds (heavy metals and PAHs identified from chemical analyses of similar sediments in Sydney), spiked into aqueous solutions and elutriates. In these tests, low molecular weight PAHs showed greater toxicity than high molecular weight PAHs. For both metals and PAHs, the toxicity was significantly higher when they were tested in clean water than in elutriates. However, neither RDS nor BLS elutriates caused any toxicity in a 24-hour acute test with *Artemia* nauplii. In the Microtox® assay, both RDS and BLS elutriates showed some toxicity; RDS samples were more toxic than the BLS, but there was no significant difference between size fractions. The response patterns in the Microtox® assays suggested effects from both heavy metals and organic compounds. The AhR CAFLUX bioassay, which is sensitive to dioxin-like compounds including PAHs, showed relatively lower activity in solvent extracts of RDS, with slightly higher activity in the finer fractions of the sediment. There was no detectable AhR CAFLUX activity in BLS. The p53 GeneBLAzer® assay, a measure of genotoxicity, showed no effect from any elutriates or solvent extracts of RDS or BLS. The results indicate that the RDS presents a greater hazard than the BLS, particularly in the finer size fractions. Accumulation of RDS in estuarine sediment may pose a risk to benthic organisms, especially those that feed on and in the sediments.

Iron coated zeolite (ICZ) was synthesized by adding natural zeolite in an iron nitrate solution under strongly basic conditions. ICZ was found to adsorb significantly larger amounts of heavy metals than zeolite, because of thespecific adsorption of metals by the iron on the zeolite surface. The batch adsorption was satisfactorily explained using the Langmuir isotherm while the column adsorption data fitted reasonably well to the empirical Thomas model. Desorption of metals previously adsorbed on zeolite and ICZ columns by elution with

0.1 M HCl removed 62–90% and 58–85% of adsorbed metals in the first and second cycles of adsorption/desorption, respectively. Although the regeneration of ICZ reduced the adsorption capacity, partly because of the iron coatings being dissolved, the adsorption capacity of the regenerated ICZ was still higher than that of the original zeolite. In summary, the batch and fixed-column experimental results showed that ICZ is a potential adsorbent for removing heavy metals from aqueous solutions.

Industrial low-cost by-products such as blast furnace slag and fly ash were used to remove five heavy metals from water in batch and fixed bed column experiments. Increase of pH increased adsorption of all metals. Equilibrium adsorption of all metals was successfully modeled using Langmuir, Freundlich and Dubinin-Radushkevich models, with Freundlich model fitting the data the best. Langmuir adsorption maximum at pH 6.5 for fly ash ranged 3.4 - 5.1 mg/g with the adsorption capacity for the metals in the order, Pb > Cu > Cd, Zn, Cr. The corresponding values for furnace slag were 4.3 - 5.2 mg/g, and the order of adsorption capacities, Pb, Cu, Cd > Cr > Zn. The kinetics of adsorption fitted well to both the pseudo-first order and pseudo-second order models, but the fit was slightly better for the pseudo-second order model. The column experiments of furnace slags indicated that column process can be used for treating of waters containing a single heavy metal as well as for removal of mixtures of heavy metals. The effectiveness of the fixed bed columns with respect to heavy metal ions agreed well with the batch experiment. The mechanism of heavy metal removal may include ion exchange/adsorption and surface precipitation on the adsorbent.

CHAPTER 1

INTRODUCTION

CHAPTER 1

INTRODUCTION

Particles from vehicle emissions are not the only traffic-related factor that causes deterioration of air quality in cities. Road-deposited sediment (RDS) contain many types of inorganic and organic pollutants such as heavy metals, metalloids and polycyclic aromatic hydrocarbons (PAH). These pollutants originate from vehicle exhaust emissions, vehicle tyres, brakes and body frames, asphalt road surfaces, road fences, de-icing salt, paint markers, and pesticides and herbicides that end up on the pavement (Loganathan et al., 2013). During rain, storms, and other street-washing events, the RDS, associated heavy metals, and organic compounds are transported off-site in stormwater and can potentially end up in surface and sub-surface waters and become toxic to aquatic organisms Therefore stormwater needs to be treated so that these pollutants can be removed before they enter water bodies and affect the organisms living in them.

1.1. Pollutant enrichment

The degree of enriched pollutants close to roads has been shown to be very high because of the contribution from road-related activitescontribution. It can be assessed by comparing the pollutants' concentrations in RDS with those in nearby baseline soils (BLS) away from the roads with minimum contamination using different types of indices (pollutant indices, enrichment factors). Degree of enrichment has also been assessed by comparing the pollutants' concentrations in RDS with those in the Earth's crust (geo-accumulation index). The degree of pollutant enrichment in RDS decreases exponentially when one moves further away from the roads (Loganathan et al., 2013).

1.2. Pollutant sources

Source identification of the RDS pollutants is important so that correct measures to prevent pollution can be implemented. Pollutant sources are generally identified and apportioned

using multivariate statistical techniques such as correlation, cluster and principal component analyses (Mohammed et al., 2012; Yongming et al., 2006). If pollutants are highly correlated with each other or fall into the same group in principal component and cluster analyses, they are considered to have been derived from the same source. In the case of PAHs, the ratio of certain diagnostic individual PAHs can provide information on the PAH sources. Ratios between individual PAHs as well as between specific PAH isomers have been employed to identify the sources of PAHs (Yunker et al., 2002). In most cases, PAHs sources are identified as either petrogenic (unburned or leaked fuel and oil, road asphalt, and tyre particles) or pyrogenic (combustion of petroleum (vehicle exhaust), grass, and wood). Sources of heavy metals in RDS can be classified into geogenic (natural) and anthropogenic origin. Geogenic metals are derived from the parent materials of soils while anthropogenic sources are vehicles, roads, industry, buildings, and other activities in the vicinity of roads.

1.3. Pollutant mobility

During storm events, pollutants in RDS are transported to aquatic and terrestrial environments. The mobile fraction of the pollutants in RDS is transported by stormwater whereas the sediment-bound fraction, which is stored in the sediments may or may not move with the stormwater depending on the particle size of the sediments. The finer size particles tend to be transported by the stormwater and therefore carry the immobile fraction of the pollutants associated with them. Most of the coarser particles settle in drainage channels, canals, and gully pots. The proportions of the mobile and immobile fractions of pollutants alter during their transport as a result of changes in the biogeochemistry of sediments and water. The mobility and transport of the metals and metalloids and their bioavailability in the environment are functions of the chemical form of the metals and metalloids, which is governed by the physico-chemical and biological characteristics of the environmental system. However, most studies evaluating the adverse effects of RDS pollutants on the environment measure only the total pollutant concentration. To provide a more accurate measurement of the potential mobility and bioavailability of the metals and metalloids, some researchers have used sequential chemical extraction methods to measure the different chemical forms of the metals and metalloids. They have grouped them into fractions of different degrees of mobility and immobility (Mohammed et al., 2012; Rauret et al., 1999; Tessier et al., 1979).

1.4. Pollutant bioavailability and toxicity

Pollutants that are very mobile are also considered to have a high degree of bioavailability. Many heavy metals and metalloids and organic pollutants at high concentrations are acutely and chronically toxic and known to have adverse effects on humans and aquatic ecosystems. Many methods exist for assessing the bioavailability and toxicity of RDS pollutants. Sequential extraction chemical methods discussed in the preceding section are one means by which the degree of bioavailability of metals and metalloids can be indirectly determined. PAH toxicity evaluation has been conducted using relative toxicity values of individual PAH compounds as proposed by Nisbet and LaGoy (1992), and heavy metals bioavailability can be assessed by a similar method (Hakanson, 1980). Most toxicity assessments of RDS have been conducted using the dissolved form of pollutants leached from RDS using a multitude of species because this form of pollutants is the most easily available to the range of species (Khanal et al., 2014; Tang et al., 2013). These methods include exposing the different aquatic organisms to the urban stormwater; or tyre and road wear leachate using algae, daphnids or fish. A better method of assessing toxicity is to use the pollutants present in solution phase and the fraction that is eluted into the dissolved phase in toxicity assessments.

The majority of the above methods have the drawback that toxicity indices were obtained from experiments done on terrestrial animals such as mice (Nisbet and Lagoy 1992). To better assess stormwater pollutants' effects on natural water bodies, the toxicity effects on real aquatic organisms have to be determined. The toxic potential of RDS elutriate has been examined by some researchers using acute tests with *Vibrio fischeri* (Microtox®) and the brine shrimp *Artemia salina* as test models (Nguyen et al., 2009; Nunes et al., 2006). These includes urban runoff using sea urchin and water flea (Bay et al., 2003; Maltby et al., 1995), tire and road wear leachate using algae, daphnid, fish (Irealand et al., 1996; Wik et al., 2009), parking lot simulated runoff using sea urchin (Greenstein et al., 2004) and road runoff residues using using green algae (*Pseudokirchneriella subcapitata*) and daphnids (*Daphnia magna*) (Clement et al., 2010).

1.5. Stormwater pollutants remediation

Remediation measures used to reduce the pollutant load in RDS (street sweeping, water flushing, use of chemical suppressants, vegetation strips, filtration systems such as permeable pavements, buffer strips and grass swales, retention ponds or soil infiltration) have not been very successful in reducing these pollutants' concentrations in the stormwater, partly because dissolved pollutants can still move with the stormwater and by-pass these treatments (Loganathan et al., 2013). Adsorbents can be used to remove pollutants in stormwater, however, only a few studies have reported the removal of heavy metals and organic pollutants using low-cost adsorbents. Natural zeolite is one such adsorbent used for the removal of heavy metals. Though zeolite is locally Australian available and relatively cheap, the adsorption capacity is too low to effectively remove heavy metals. Therefore, some chemical modification of the adsorptive surfaces needs to be done in order to increase their adsorption capacity.

Adsorptive removal of heavy metals and PAHs from water has been previously studied using several adsorbents such as granular activated carbon (GAC), industrial by-products, and other mineral compounds in batch-type studies. A few studies using fixed-bed columns, which are more relevant to real operating systems on natural waters than batch studies, have been published (Han et al., 2009; Jeon et al., 2012; Nur et al., 2014). Results of batch adsorption studies which are conducted in static scenarios may sometimes be different from those conducted in dynamic column adsorption systems. Also, most studies have not comprehensively investigated the adsorption mechanisms and effects of solution factors such as pH of the water, and co-ions existing in water which may compete with the pollutants for adsorption. Neither have they investigated the level of competition among these heavy metals and PAH compounds that may influence the adsorption processes.

1.6. Necessity for the research

Numerous studies have been conducted on heavy metals, metalloids and PAH accumulation in RDS (Aryal et al., 2011; Li et al., 2010; Saeedi et al., 2012; Sojinu et al., 2010; Viñas et al., 2010) in many countries but few have been done on these pollutants in water sediments (Birch, 2011). No study appears to have compared heavy metal and PAH profiles in RDS, water baseline sediment (WBS) and BLS for any single catchment area. Yet this information is important for assessing the contributions of these pollutants carried by RDS and natural soils into local water bodies, so that control measures can be implemented to reduce pollution in these water bodies. The presence of chemical pollutants in RDS and the road runoff can cause adverse effects on aquatic organisms and also may pose a long-term chronic health risk to humans and other organisms using these waters. Information on the responses of aquatic organisms like fish abundance and community structure to toxic exposure is still insufficient. Consequently, it is necessary to evaluate the responses of these organisms to heavy metals and PAHs in urban runoff as well as in the sediment elutriates, in order to understand the hazardous impacts of these toxic compounds on aquatic ecosystems.

Sydney, the capital of New South Wales, is the political, cultural and commercial hub of Australia. The population of Sydney exceeded 5 million in 2012 and most of its people reside and work in the sprawling suburbs that surround the city centre. Heavy traffic in the city along the busy and congested roads causes continuous deposition of road sediments which may move to the water bodies causing damage to the aquatic environment. Kogarah Bay is an important semi-industrialised and urbanised area with several roads that experience heavy traffic. This is expected to create heavy metal and PAH pollution for Kogarah Bay. Detailed study of these pollutants' concentrations in RDS, WBS and BLS and their mobility and potential aquatic toxicity in this area is necessary. The natural set-up of roads, water channels, and bay within this bay catchment provides an ideal site for a study on investigating the effect of RDS pollutants on water bodies.

Removing the pollutants from stormwater by adsorption using filters containing low-cost adsorbents with high adsorption capacity for the pollutants is an attractive method. However, not enough information is currently available on specific adsorbents for removing heavy metals and PAHs under practical conditions such as adsorption in the presence of co-ions in column-based continuous dynamic adsorption system. Research on these aspects is necessary.

Low-cost adsorbents are economically attractive but they may not have a high adsorption capacity. Therefore research on increasing the adsorption capacity by chemical modification of the adsorbents is necessary. Regeneration of the adsorbents for reuse can also cut down the cost of operation. Research on this aspect is also necessary.

1.7. Objectives of the research

The objectives of this study are as follows. It will determine: (i) the distribution of nine heavy metals (Fe, Mn, Zn, Cu, Pb, Cd, Cr, Ni, V) and a metalloid (Sb) in RDS, WBS and BLS in a single catchment around Kogarah Bay in Sydney; (ii) heavy metals and metalloid enrichments in RDS and WBS by comparing their concentrations in RDS and WBS with those in the BLS reference; (iii) the potential mobility and bioavailability of these elements using a sequential chemical extraction method; (iv) the possible sources using statistical methods; (v) compare the concentration distribution, composition, possible sources and potential toxicity of PAHs found in RDS, WBS and BLS in the area of Kogarah Bay, Sydney; and (vi) the efficiency of adsorption technology in removing heavy metals and PAHs from synthetic solutions simulating RDS runoffs using batch and fixed-bed column experiments. Different adsorbents ranging from mineral to industrial by-products such as, GAC, zeolite, furnace slag and fly ash, will be assessed. This study will also determine the mechanism of adsorption and the most suitable mathematical models that can satisfactorily explain the adsorption data. A major aspect of this thesis is to investigate the best methods of regeneration of used adsorbents by completely desorbing the adsorbed pollutants so that the adsorbents can be used repeatedly in removing the pollutants. Furthermore it will determine the biotoxicity of the RDS elutriates and different reference compounds (5 heavy metals and 5 PAH compounds) using two toxicity tests (*Artemia salina* and the Microtox® test with *Vibrio fischeri*). Finally, this study aims to develop a modification of the method of alkaline unwinding assay so that the effect of heavy metals and PAHs on DNA damage in brine shrimp (*Artemia salina*) tissue under laboratory conditions can be assessed. This method will be used to evaluate the biotoxicity of RDS and BLS.

1.8. Outline of this thesis

A brief description of the contents of each chapter is presented below.

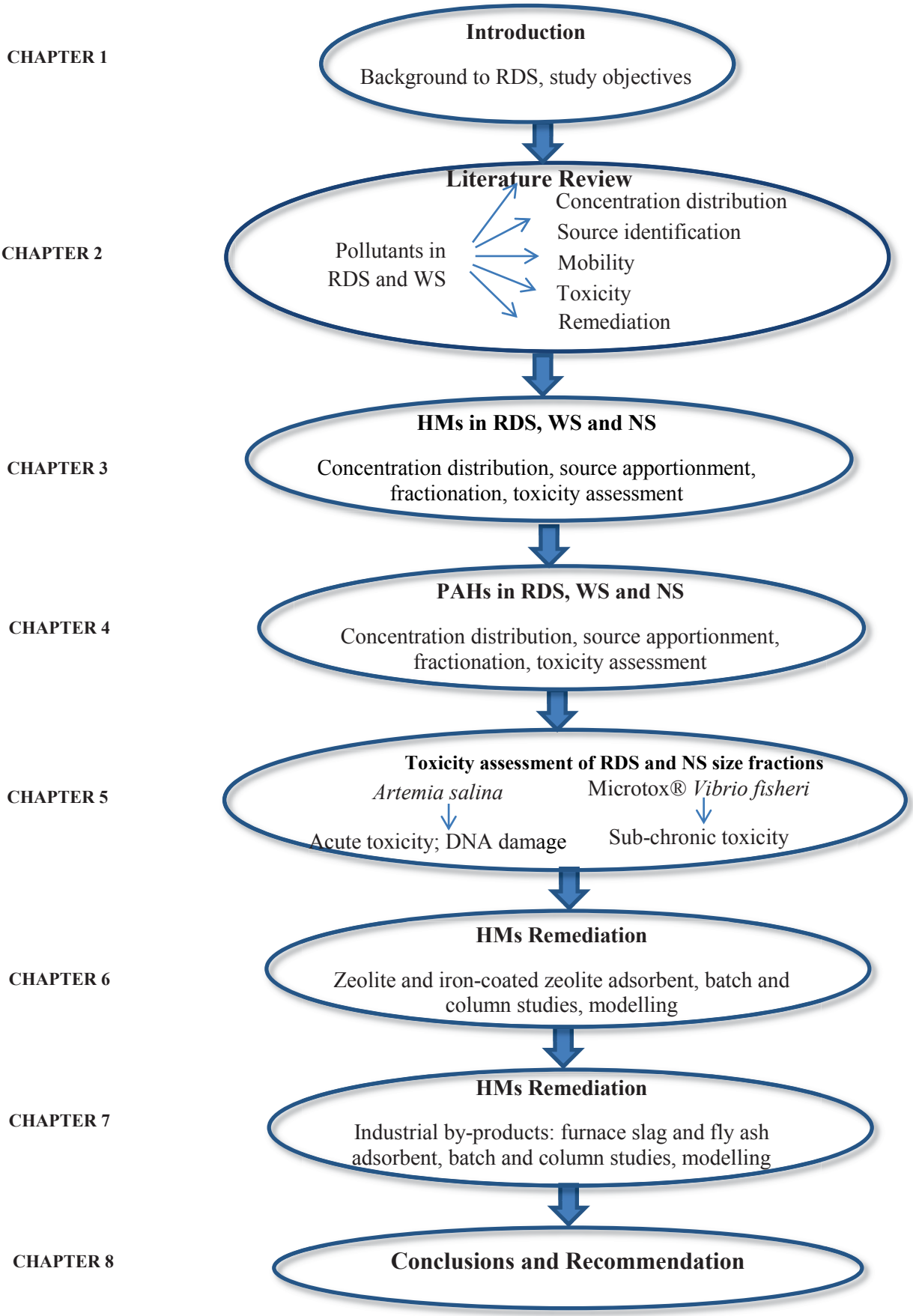
CHAPTER 1
Introduction
Background to RDS, study objectives
CHAPTER 2
Literature Review
Pollutants in RDS and WS
Concentration distribution
Source identification
Mobility
Toxicity
Remediation
CHAPTER 3
HMs in RDS, WS and NS
Concentration distribution, source apportionment, fractionation, toxicity assessment
CHAPTER 4
PAHs in RDS, WS and NS
Concentration distribution, source apportionment, fractionation, toxicity assessment
CHAPTER 5
Toxicity assessment of RDS and NS size fractions
Artemia salina
Acute toxicity; DNA damage
Microtox® Vibrio fisheri
Sub-chronic toxicity
CHAPTER 6
HMs Remediation
Zeolite and iron-coated zeolite adsorbent, batch and column studies, modelling
CHAPTER 7
HMs Remediation
Industrial by-products: furnace slag and fly ash adsorbent, batch and column studies, modelling
CHAPTER 8
Conclusions and Recommendation

CHAPTER 2

LITERATURE REVIEWS

CHAPTER 2

LITERATURE REVIEW

2.1. Road-deposited sediments (RDS)

RDS and the associated organic and inorganic pollutants such as heavy metals, metalloids and polycyclic aromatic hydrocarbons (PAH) and their effects on the environment have been investigated over the last few decades in many countries (Aryal et al., 2010; Loganathan et al., 2013; Murakami et al., 2008; Taylor and Owens, 2009). These pollutants are derived from vehicle exhaust emissions, vehicle tyres, brakes, body frames, asphalt road surfaces, road railings/fences, de-icing salt, paint markers, and pesticides and herbicides added to the pavement (Figure 2.1, Table 2.1). Many heavy metals, metalloids, and PAHs are acutely and chronically toxic and carcinogenic and known to have adverse effects on humans and terrestrial and aquatic ecosystems (Aryal et al., 2010; Kadıoğlu et al., 2010; Loganathan et al., 2013; Mohammed et al., 2012). Therefore, their concentrations in RDS and the road-runoff waters should be minimised.

Table 2. 1. Possible sources of pollutants in RDS (adapted from Aryal et al. (2010))

Pollutants	Brakes	Tyres	Frame and body	Fuel and oil	Pavement	De-icing salt	Litter
Cadmium		■					
Chromium		■	■				
Copper		■	■				
Iron	■	■	■				■
Lead			■				
Nickel		■	■				
Zinc	■	■	■				
Organic solids					■		■
Inorganic solids					■	■	■
PAHs		■		■	■		

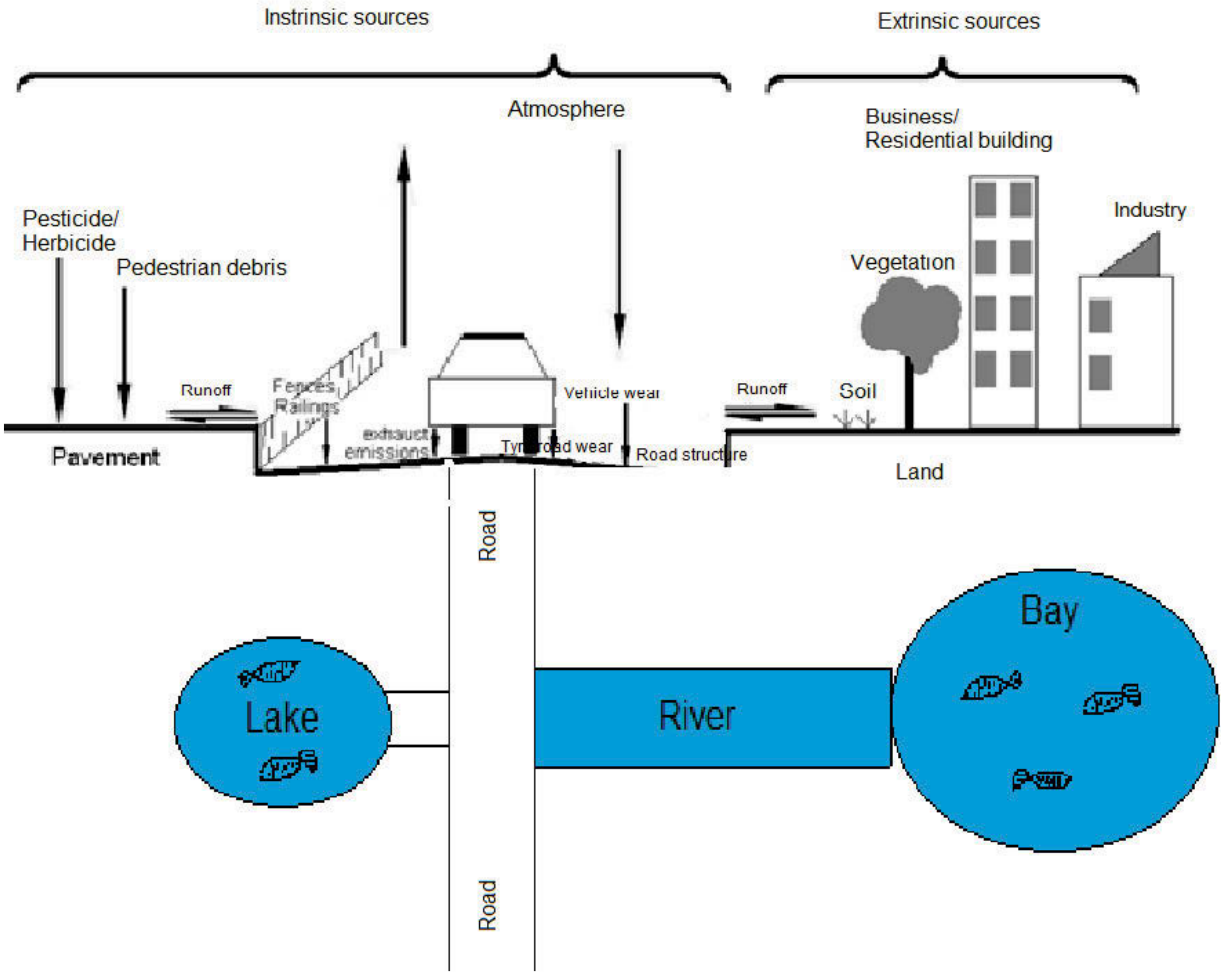

Figure 2. 1. Schematic illustration of the sources of road-deposited sediments (not to scale) (adapted from Loganathan et al. (2013) and Taylor (2007))

2.2. Pollutants in RDS

2.2.1. Heavy metals

During the last decade, several studies have reported that the levels of many heavy metals and metalloids (Cu, Mn, Zn, Cd, Pb, As, Cr, Fe, Hg, Ni, Pd, Pt, Rh, Sb, V) (Faiz et al., 2009; Joshi et al., 2009; Kuo et al., 2009; Lu et al., 2009; Wei et al., 2010; Wei and Yang, 2010; Zereini et al., 2007) and organic pollutants (PAH, nitro-PAH, phthalate esters) (Aatmeeyata and Sharma, 2010; Aryal et al., 2011; Dong and Lee, 2009; Wang et al., 2011; Zakaria et al., 2002; Zeng et al., 2009), many of which are considered to be biotoxic, existed in much higher concentrations in RDS and roadside soils compared to native soils away from the roads. Unlike in many earlier studies where only pollutant concentrations in RDS were reported (Gromaire-Mertz et al., 1999; Stone and Marsalek, 1996), in recent studies the pollutant concentrations in neighbouring uncontaminated soils were also reported and this enabled a comparison to made of the two concentrations. Also the pollutant enrichment factors could be determined (Chang et al., 2009; Duong and Lee, 2011; Faiz et al., 2009; Joshi et al., 2009; Kuo et al., 2009; Lu et al., 2009; Sutherland and Tolosa, 2000; Wei et al., 2010; Yang et al., 2010). The distribution patterns of heavy metals were related to level and type of traffic and its densities (Duong and Lee, 2011; Faiz et al., 2009; Saeedi et al., 2012). The reason for the higher concentration of heavy metals in RDS compared to native soils is that the vehicle parts, exhaust and asphalt surface of roads have high concentrations of heavy metals which are constantly released over a long period to the RDS (Table 2.2).

Table 2.2. Sources of heavy metals and metalloids, and their concentrations/or emission rates (adapted from Loganathan et al. (2013))

Heavy metals/metalloids	Source	Pollutant concentration/ emission rate	Reference
Cd	Brake lining/dust	8-12 µg/g	Westerlund (2001)
		<0.1–41 µg/g	Thorpe and Harrison (2008)
	Tyre tread	<0.05–2.6 µg/g	Thorpe and Harrison (2008)
Cr	Brake disc pad/dust	0.69–2.6%	von Uexküll et al. (2005)
	Brake lining/dust	73–151 µg/g	Westerlund (2001)
		<10–1320 µg/g	Thorpe and Harrison (2008)
		1.5% (mean)	Kadioğlu et al. (2010)
	Tyre tread	<1–30 µg/g	Thorpe and Harrison (2008)
	Unleaded gasoline exhaust	165 µg/g (mean)	Kadioğlu et al. (2010)
	Diesel exhaust	70 µg/g (mean)	Kadıoğlu et al. (2010)
Cu	Brake disc pad/dust	1.4–6.7%	von Uexküll et al. (2005)
	Brake lining/dust	5.1–11.8%	Westerlund (2001)
		11 µg/g–39%	Thorpe and Harrison (2008)
		6.6% (mean)	Kadioğlu et al. (2010)
	Tyre tread	<1-490 µg/g	Thorpe and Harrison (2008)
	Unleaded gasoline exhaust	212 µg/g (mean)	Kadioğlu et al. (2010)
	Diesel exhaust	47 µg/g (mean)	Kadioğlu et al. (2010)
Ni	Brake lining/dust	70–182 µg/g	Westerlund (2001)
		4–730 µg/g	Thorpe and Harrison (2008)
	Tyre tread	<1–50 µg/g	Thorpe and Harrison (2008)
	Asphalt bitumen	15–100 µg/g	Lindgren (1996)
Pb	Gasoline	1.2 g/L in 1970s, ≤ 0.15 g/L in 1980/1990s	Lovei (1998)
	Brake lining/dust	0.9–1.9%	Westerlund (2001)
		1 µg/g–11.9%	Thorpe and Harrison (2008)
	Tyre tread	1–160 µg/g	Thorpe and Harrison (2008)
	LPG exhaust	3096 µg/g (mean)	Kadioğlu et al. (2010)
Pd*	Vehicle exhaust	264 ng/km emission rate	Palacios et al. (2000)
Pt*	Vehicle exhaust	101 ng/km emission rate	Palacios et al. (2000)
Rh*	Vehicle exhaust	66 ng/km emission rate	Palacios et al. (2000)
Sb	Brake disc pad/dust	1.7– 4.6%	von Uexküll et al. (2005)
	Brake lining/dust	0.07–1.7%	Thorpe and Harrison (2008)
	Tyre tread	<0.2–0.9 µg/g	Thorpe and Harrison (2008)
			Thorpe and Harrison (2008)
			Thorpe and Harrison (2008)
Zn	Tyre tread	430–9640 µg/g	Westerlund (2001)
	Brake lining/dust	25 µg/g–18.8%	Kadioğlu et al. (2010)
		0.7–2.4%	Kadioğlu et al. (2010)
		7.9% (mean)	Kadioğlu et al. (2010)
	Unleaded gasoline exhaust	3225 µg/g (mean)	Kadioğlu et al. (2010)
	LPG exhaust	1074 µg/g (mean)	
	Diesel exhaust	466 µg/g (mean)	

(*) Platinum group metals used as catalytic convertor in vehicles

2.2.2. PAHs

Polycyclic aromatic hydrocarbons (PAHs) are chemical compounds that consist of fused aromatic rings (benzene rings which share one or more sides) and do not contain a heteroatom or carry substituents (Dong and Lee, 2009) (Table 2.3, Figure 2.2). The number of rings ranges from 2 to 6. PAHs with few rings have low molecular weight, are highly volatile and soluble in water (Table 2.3). They are highly persistent, toxic, and widespread environmental pollutants and are of major concern regarding the damage they can do (Wang et al., 2009a). Many PAHs are considered to be mutagenic or carcinogenic and are believed to cause health problems, such as cataracts, kidney and liver damage, and jaundice (Dong and Lee, 2009; Su et al., 1998; Zhao et al., 2014). Due to their potential toxicity, and widespread distribution in the environment, such as air, water, soils, and sediments, some PAHs are listed as priority monitoring pollutants by the United States Environmental Protection Agency (EPA Test Method, 1982; (Li et al., 2010; Long, 2006) (Figure 2.2). Generally, the high molecular weight PAHs consisting of more than three aromatic rings are more toxic than low molecular weight PAHs containing two or three aromatic rings (Nisbet and LaGoy, 1992). As with heavy metals, PAHs are also emitted from diverse sources. Likewise major sources emit many types of PAHs. The sources of PAHs and their emission rate to the environment are listed in Table 2.4.

Aryal et al. (2011) reported that the total and individual PAHs contents were highest in the finest size fraction (< 75 μm) and in the winter season compared to the other seasons when analysing 18 RDS samples for 16 PAHs from Sydney, Australia. Longer the dry weather period the higher the total PAHs content. They also found that the concentrations of high molecular weight PAHs (4 and 5 rings) were much higher than the concentrations of low molecular weight PAHs (2 and 3 rings).

Table 2.3. Physical and chemical characteristics of PAHs

PAH	Cycles	Vaporisation	Solubility	TEF values (*)
Napthalene	2	very	high	0.001
Acenapthylene	2	very	high	0.001
Acenapthene	3	very	medium	0.001
Fluorene	3	very	medium	0.001
Phenanthrene	3	very	medium	0.001
Anthracene	4	insignificant	low	0.01
Fluoranthene	4	same	low	0.001
Pyrene	4	same	low	0.01
Benzo(a)anthracene	4	same	low	1
Chrysene	5	same	low	0.01
Benzo(b+k)flouranthrene	5	same	low	0.1
Benzo(a)pyrene	5	same	low	1
Indeno(1,2,3-cd)pyrene	5	same	low	0.1
Dibenzo(a,h)anthracene	6	same	low	5
Benzo(g,h,i)perylene	6	same	low	0.01

(*) Toxicity equivalency factor (TEF) values proposed by Nisbet and LaGoy (1992)

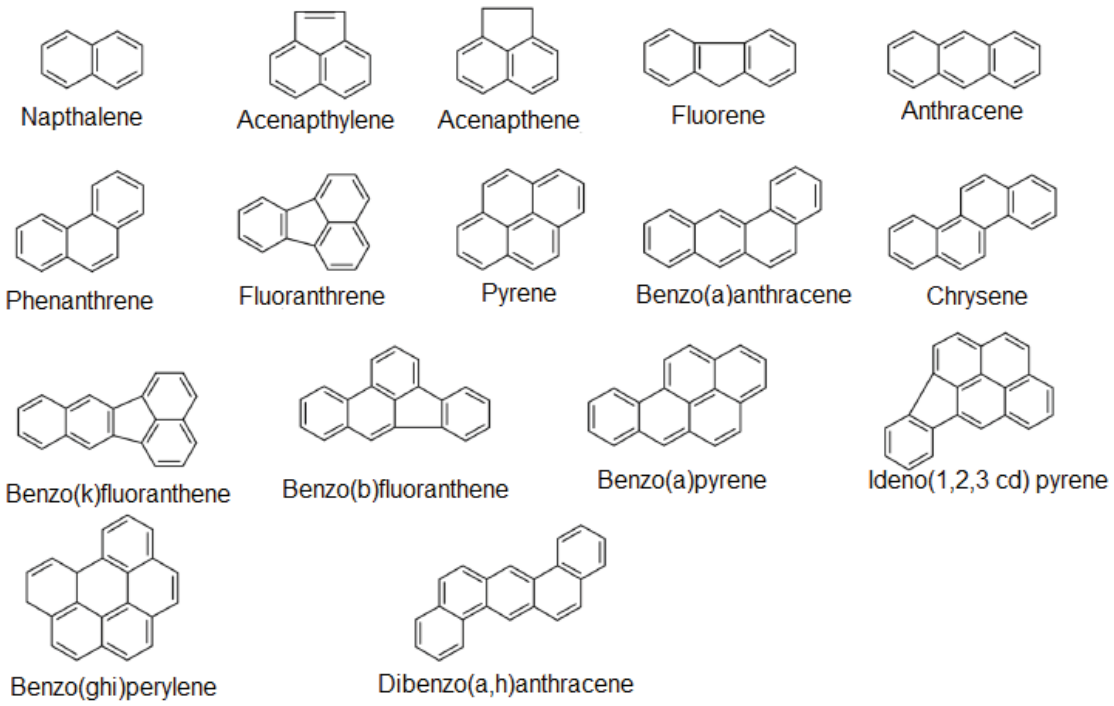

Figure 2.2. US. EPA 16 priority PAH compounds (US EPA, 1992)

Table 2. 4. Sources of PAHs and PAHs concentration or emission rate (adapted from Loganathan et al., 2013)

Pollutant	Source	Pollutant concentration/emission rate	Reference
PAHs	Vehicle exhaust	1476 ng/g	Mostafa et al. (2009)
	Fresh lubricating oil	2926 ng/g	
	Used lubricating oil	1428 ng/g	
	Tyre particles	364 ng/g	
	Asphalt	1596 ng/g	
	Diesel vehicle exhaust	415–8868 µg/g	Takada et al. (1990)
	Asphalt	4–9 µg/g	
	Tyre	378 ng/tyre/km	Aatmeeyata and Sharma (2010)
	Vehicle exhaust, oil combustion	NR	Dong and Lee (2009)
	Vehicle exhaust, tyre	NR	Pengchai et al. (2005)
Nitro-PAH	Diesel exhaust particles	2.0–4.1 µg/g	Murakami et al. (2008)

NR = not reported

2.3. Pollutant source identification

In order to formulate adequate measures to reduce environmental risk caused by heavy metals and PAHs, it is necessary to determine quantitatively the contributions of the various sources of these pollutants. The methods used in identifying the sources of heavy metals and PAHs are discussed in this section.

2.3.1. Heavy metals

It is not easy to identify the major sources of some heavy metals because a heavy metal can originate from multiple sources. The origins of a heavy metal may differ depending on the road surfaces (asphalt versus concrete) and vehicle type (heavy duty trucks using diesel versus passenger vehicles using petrol). Sources of heavy metals are generally identified by using statistical techniques such as principle component analysis (PCA), cluster analysis (CA), correlation coefficient analysis (CCA) and depending on types of vehicle, and road surface in the area (Table 2.5).

When comparing the heavy metals in RDS from a concrete highway with those from asphalt highway under a similar vehicle density, Duong and Lee (2011) found that Cd, Ni and Pb concentrations in RDS were higher along the concrete highway RDS. They explained these results as due to higher tyre abrasion that occurs in concrete highway. The minerals make-up of different rock materials varies in the metal contents. Therefore the concentration of the metals released to the RDS varies widely (Lindgren, 1996). Duong and Lee (2011) also found that heavy metals concentrations in RDS at rotary areas of the highway were higher than those in other areas. They stated that the high concentrations of heavy metals in RDS in rotary areas may be due to the substantial increase in traffic volume and stopping and idling while waiting at traffic lights. Heavy metal concentrations in RDS can be variable (Table 2.5), however, it is clearly shown that urban metal loadings often exceed those found in industrial zones, highway areas. Consequently, there is the possibility of heavy metal loading from sources other than vehicles (Mohammed et al., 2012).

Table 2. 5. Studies on pollutants source identification and apportionment and methods used (adapted from Loganathan et al., 2013)

Study area	RDS sampling/ analysis and method used for source identification	Source identified/apportionment	Reference
Ankara, Turkey	9 RDS samples: brake pads, exhaust dust of vehicles	Cr, Mn, Cu, Zn, and Sn from brake pads; As and Pb from exhaust dust	Kadıoğlu et al. (2010)
California, USA	56 tyre and 53 brake samples; 28 element samples analysed. Grouped by PCA	Zn, Pb, Cu from tyres; Cu, Mn, and Cd (Cd-plated brake rotor) from brakes	McKenzie et al. (2009)
Maryland, USA	Pb, Cu, Cd and Zn analysis of building siding and roofs; brakes; tyres; oil leakage; atmospheric deposition	Building siding, all 4 metals; brake, Cu; tyre, Zn; atmosphere, Cd, Cu, Pb	Davis et al. (2001)
Sweden	Asphalt bitumen and stone materials analysed for 8 elements	Stone material major source; bitumen minor source; caused by studded tyre use in winter	Lindgren (1996)
Taiwan	RDS from steel plant, coal-fired power plant, industrial park and main roads; grouped by PCA	Fe, Zn, and Pb steel plant; Cu, Cr and Ni road intersection; Zn and Ni industrial park	Chang et al. (2009)
Urumqi, China	169 samples from different roads. Geostatistic/Kriging interpolation method of data analysis/mapping	Cu, Pb, Cr, Zn traffic related; Ni, Mn industrial activity; Cd commercial, industry, phosphate fertilizer	Wei et al. (2009)
Republic of Korea	12 RDS samples from different industrial complex (IC) areas	Cd, Cu, Pb mainly in non-ferrous metal IC, followed by petrochemical IC, Ni, Zn petrochemical IC	Dong and Lee (2009
Germany	54 RDS samples (2004) analysed for Pt group metals and compared with 1994 values	Pt, Rh, 2 and 1.6 times higher but Pd 15 times higher. Metals use in 1993 or earlier as catalytic convertors in vehicles	Zereini et al. (2007)

Urumqi, China	169 RDS samples; 10 elements analysed; statistics: CCA, PCA, CA	U, Mn, Co natural soils; Cu, Pb, Zn, Cr mainly traffic and partly industry; Ni, Be mainly industry	Wei et al. (2010)
Istanbul,Turkey	41 RDS analysed for 3 elements; heavy traffic and industrial areas; CCA	Pb, Zn, Cu strong correlation, common source, Vehicle traffic main source	Guney et al. (2010)
Islamabad, Pakistan	13 RDS samples analysed for Cd, Cu, Ni, Pb, Zn: CCA	Cu, Pb high correlation, similar anthropogenic source (vehicle)	Faiz et al. (2009)
China	23 RDS, 17 elements; Shanghai(commercial, industry(I)), Beijing (I), Hong Kong (traffic, metropolis)	Finger printing metals in RDS; Cr, Cu, Ce, Zn higher in Hong Kong RDS due to higher traffic	Tanner et al. (2008)
Xi'an, China	65 urban dust samples; 6 metals analysed; CCA, PCA, CA	Cr, Cu, Pb, Sb, Zn mainly industry, Pb, Zn also traffic; Ag, Hg commercial, domestic; As, Mn mainly soil	Yongming et al. (2006)
Wuhan, China	97 RDS samples;10 elements, magnetic properties	Cu, Fe, Ni mainly traffic related	Yang et al. (2010)
Manchester, England	Electron microscope/ microporobe/ Raman spectroscopy on RDS grains	4 types of grains (Si, Alumino-Silicate, Fe oxides, Fe-rich glass, Accessory grains) Elements distributed to them	Taylor and Robertson (2009)
Manchester, England	9 inner city and 10 outer city RDS samples; chemical and mineralogical analysis	Fe, Zn, Pb, Cu, Mn magnetic component of RDS; vehicular source	Robertson et al. (2003)

CA- Cluster analysis; PCA- Principle component analysis; CCA: Correlated coefficient analysis

The main source of Pb in RDS decades ago was leaded gasoline but with the reduction/removal of Pb additives in gasoline, more recently the source of Pb has changed to tyres (McKenzie et al., 2009), brakes (Davis et al., 2001), fuel tanks, spark plugs and piston coatings (Maher et al., 2008). However, elevated concentrations of Pb continue to be observed in soils close to roads and this was considered to be not only to the new sources of Pb but also to Pb from gasoline added to soils in the past. It has been strongly adsorbed to the soils and persists for a long time (Guney et al., 2010; Hjortenkrans et al., 2006). Recently, Mohammed et al. (2012) found that RDS in highways in and around Sydney, Australia were significantly enriched with Cu and Zn. This was explained as due to a contribution from vehicle components such as brake linings and tyre wear, respectively, which contain high concentration of these metals. They also reported that correlation and cluster analyses suggested that Fe, Mn, Cr and Ni in RDS had primarily a lithogenic origin.

Yongming et al. (2006) studied the possible sources of heavy metals in RDS in central China. Using PCA and CA, they found that, Ag and Hg had commercial and domestic sources; Cu, Sb, Pb, Zn and Cr were mainly from industrial sources, combined with traffic sources; Mn and As were from soil sources. The metal groupings identified using cluster analysis of the metal concentrations are shown in Figure 2.3. Another investigation in a regional city of Urumqi, China by Wei et al. (2010) found that the sources of Cu, Pb, Cr and Zn were mainly roads with heavy traffic. Ni, Mn and Cd were mainly from the industries; Co and U were from the soil material, and Be was from railway activity.

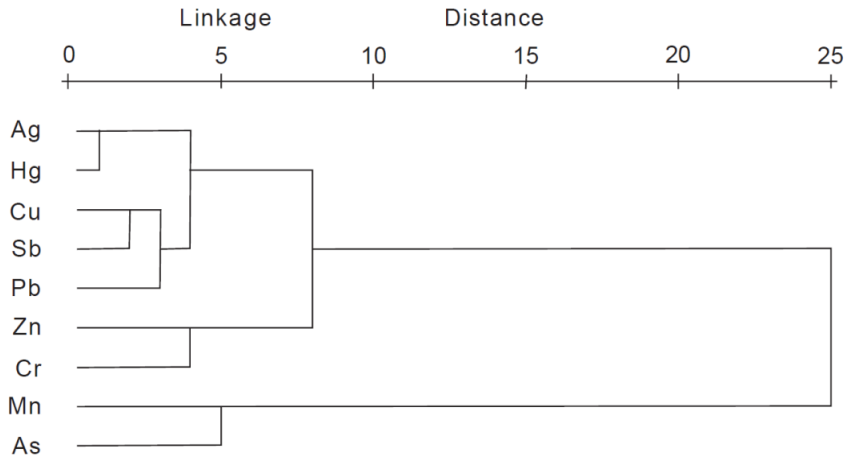

Figure 2.3. Cluster analysis of heavy metals in RDS in central China (re-drawn from Yongming et al., 2006)

2.3.2 PAHs in RDS

Sources of PAHs are commonly categorised into pyrogenic and petrogenic groups (Lee, 2010; Wang et al., 2009; Yunker et al., 2002). Pyrogenic sources are those where PAHs are generated by high temperature combustion of fossil fuel (coal and petroleum) such as vehicle exhaust particles and biomass (burning of grass, and wood, bush fires) (Saeedi et al., 2012b; Wang et al., 2009; Yunker et al., 2002), whereas petrogenic sources are derived from crude oil and its refined products (oil, petrol, and diesel leaks, tyre particles, deteriorating asphalt or asphalt sealant) (Lorenzi et al., 2011; Sojinu et al., 2010; Wang et al., 2009). Asphalt contains approximately 95% mineral aggregates and the majority of the remaining 5% is bituminous binder which is the main source of PAH in asphalt (Thorpe and Harrison, 2008).

2.3.2.1 PAHs source identification using ratios of individual PAHs

Ratios between low and high molecular weight PAHs as well as between specific PAH isomers have been used to identify the sources of PAHs (Saeedi et al., 2012; Viñas et al., 2010; Wang et al., 2011; Wang et al., 2009; Yunker et al., 2002). For example, Lorenzi et al. (2011) used the ratios of anthracene / (anthracene+phenanthrene); fluoranthene / (fluoranthene+pyrene); benzo(a)anthracene / (benzo(a)anthracene + chrysene); and, indeno(1,2,3-cd)pyrene / (indeno (1,2,3-cd) pyrene + benzo (g,h,i) perylene) to determine whether the sources of PAHs were petrogenic or pyrogenic in RDS from Newcastle-upon-Tyne, England (Figure 2.4). The classification of these sources according to the PAHs ratio was developed by Yunker et al. (2002) (see Table 2.6).

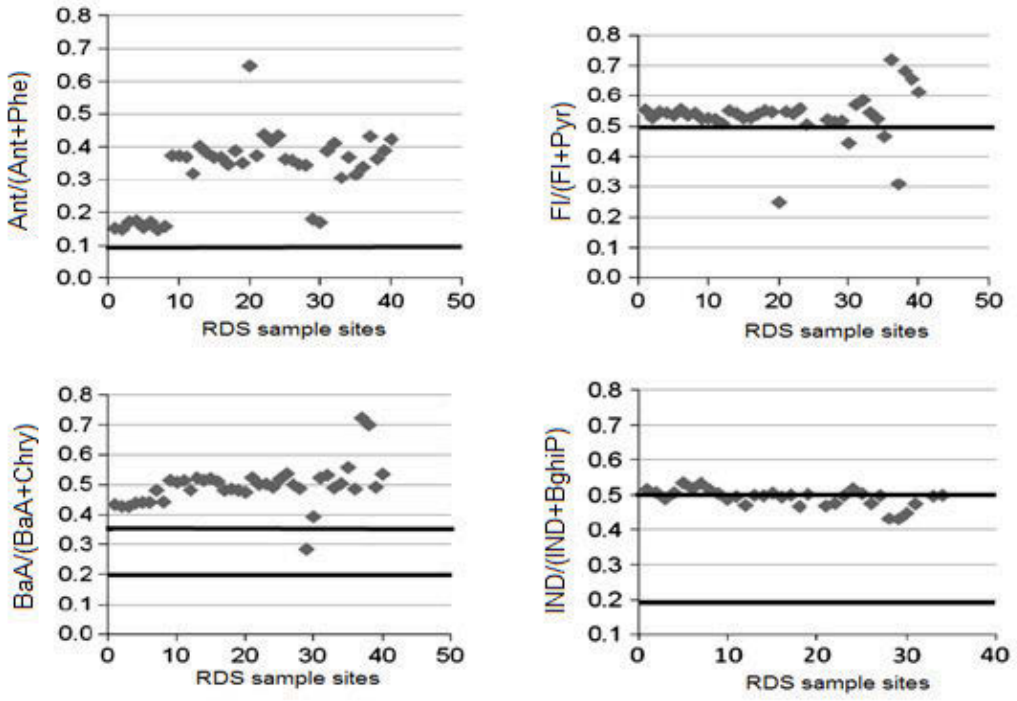

Figure 2.4. Use of ratios of different PAHs compounds for source identification. Horizontal lines demarcate petrogenic from pyrogenic sources according to the classification of Table 2.6 (re-drawn from Lorenzi et al. (2011))

Ant-Anthracene, Phe- Phenanthrene, Fl- Fluoranthrene, Pyr-Pyrene, BaA- Benzo(a)anthracene, Chry-Chrysene, IND- Indeno(1,2,3) c,d pyrene, BghiP- Benzo(g,h,i)Perylene

Table 2. 6. Indicative ratios to distinguish petrogenic and pyrogenic sources of PAHs in RDS (adapted from Lozenzi et al., 2011; Yunker et al., 2002)

Ratio	Petrogenic source	Petroleum or combustion source	Pyrogenic source
Anthracene/(Anthracene + Phenanthrene)	< 0.1		> 0.1
Fluoranthrene/ (Fluoranthrene + Pyrene)	< 0.5		> 0.5
Benzo(a)anthracene/Benzo(a)anthracene + Chrysene)	< 0.2	0.2 – 0.35	> 0.35
Ideno(1,2,3) c,d pyrene/(Ideno(1,2,3) c,d pyrene + Benzo(g,h,i)perylene	< 0.2	0.2 – 0.5 (liquid fossil fuel combustion)	> 0.5

Yunker et al. (2002) also reported that Fluoranthrene/(Fluoranthrene + Pyrene) and Ideno(1,2,3) c,d pyrene /(Ideno(1,2,3) c,d pyrene + Benzo(g,h,i)perylene) ratios can be used as indicators to discriminate fossil fuel from other biomass combustions. Low ratios of these PAHs (<0.40 and <0.20) signifies petroleum sources; intermediate ratios (0.40–0.50 and 0.20–0.50) indicates liquid fossil fuel (vehicle and crude oil) combustion whereas ratios higher than 0.50 are considered as signals of wood or coal combustion. Other ratios such as Anthracene/(Phenanthrene+Anthracene), Fluoranthrene /(Pyrene+ Fluoranthrene), and Ideno(1,2,3) c,d pyrene /(Ideno(1,2,3) c,d pyrene + Benzo(g,h,i)perylene) have also been used to distinguish PAH pollution originating from petroleum products, petroleum combustion and biomass or coal burning (Tobiszewski and Namieśnik, 2012; Zhang et al., 2015).

2.3.2.2. PAH source identification using principle component analysis (PC

As in the case of heavy metals, both PCA and multivariate linear regression analysis have been employed to identify the primary sources of PAHs and for estimating their contributions to RDS. Peng et al. (2011) studied the possible sources of 16 PAHs compounds found in RDS in central China and through PCA, separated them into distinct groups based on factor loadings (Figure 2.5). In this separation of PAHs, phenanthrene, anthracene, fluoranthene, pyrene, benzo(a)anthracene, and chrysene occurred in one PC group (70.7%) with high loadings, and they were considered to have originated from coal combustion. The other group

(20.7%) which contained napthalene and acenapthene was considered to have derived from long-range atmospheric migration.

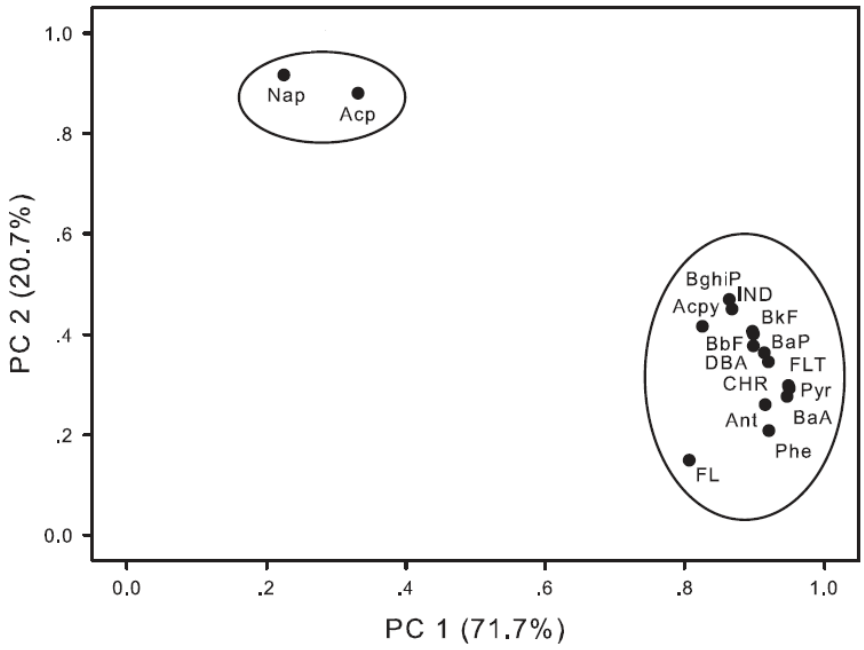

Figure 2.5. Principal component (PC) analyses loadings plot for 16 individual PAHs (re-drawn from Peng et al., 2011)

2.4 Pollutant enrichment factors

The degree of pollutants contamination in RDS arising from roads and vehicles has been generally assessed by comparing the pollutant concentrations in RDS with nearby natural soils with minimum contamination. Pollution index (PI), enrichment factor (EF) and geoaccumulation index (I_{geo}) are three indices that have been popularly used for this purpose (Faiz et al., 2009; Lu et al., 2009; Mohammed et al., 2012).

2.4.1 Heavy metals

2.4.1.1. Pollution index (PI)

The PI is defined as the ratio of heavy metal concentration in RDS to the corresponding heavy metal background concentration in the nearby soils. The pollution index PI is defined as follows:

$$PI = \frac{C_n}{B_n}$$

where C_n and B_n are the concentrations of element n in RDS and uncontaminated soil away from the roads, respectively. PI is classified as follows: PI ≤ 1: low level of pollution; 1 < PI ≤ 3: middle level of pollution; PI > 3: high level of pollution (Faiz et al., 2009; Lu et al., 2009).

Mohammed et al. (2012) reported that heavy metal pollution in RDS in Sydney, Australia, had mean (± standard errors) PI values for Cu, Zn, Cr, Cd, Pb, Fe, Mn, and Ni of 8.1 ± 1.6; 7.3 ± 1.2, 3.4 ± 0.8, 3.1 ± 0.5, 2.3 ± 0.5, 2.0 ± 0.6, 1.7 ± 0.4, and 0.7 ± 0.2, respectively. Corresponding median PI values were 7.4, 6.9, 3.5, 3.0, 2.0, 1.9, 2.0, and 0.4. The PI values indicate that Cu and Zn had moderate to high enrichment in the RDS compared with other metals which had lower values. In Baoji, China, Lu et al. (2009) also reported that PI index in RDS was high for Zn and Cu. Faiz et al. (2009) studied the PI values in RDS in Pakistan and documented the order of the values was Cu > Pb > Cd ~ Zn > Ni.

2.4.1.2. Enrichment factor (EF)

The EF is determined by a similar method to that used for the PI, with the exception that the measured metal concentrations in RDS and background soils are normalised against a reference metal. The EF is calculated using the following equation:

$$EF = [C_x/C_{ref}]sample/[C_x/C_{ref}]background$$

where C_x is the concentration of the examined heavy metal in the sample and the background soil, and C_{ref} is the concentration of the reference element in the sample and the background soil. Five enrichment categories are recognised on the basis of the EF: < 2 denotes deficiency to minimal enrichment; 2–5: moderate enrichment; 5-20: significant enrichment; 20-40: very high enrichment; > 40: extremely high enrichment (Lu et al., 2009; Yongming et al., 2006).

In the calculation of EF, a reference metal is used to normalise the metal enrichment because the composition of soils is inherently variable. The reference metal used is often characterised by low occurrence variability and of natural origin. Common metals used as reference include Al, Fe, Mn, Si, and Ti (Joshi et al., 2009; Lu et al., 2009; Yongming et al., 2006). In a study in China, using Mn as reference metal, Ag, Hg, Pb and Zn in RDS were found to have mean EFs higher than 5, which means significant contamination; while Cr, Cu and Sb, with their mean EFs between 2 and 5, were classified as moderately contaminated (Yongming et al., 2006). Mohammed et al. (2013) reported that RDS samples from Sydney, Australia had both PI and EF highest for Cu and Zn with EF value for Cu: 6.1±1.5 (mean 5.2) and Zn: 3.8±0.8 (mean 3.4). They also reported that inputs of Cu and Zn to RDS were likely to be mainly the result of brake and tyre wear, respectively. In Tehran, Iran, Saaedi et al. (2012) discovered that - using Mn as the reference metal - the EF values in RDS samples were in the order Cd > Pb > Zn > Cu.

2.4.1.3. Geo-accumulation Index (Igeo)

The geo-accumulation index was originally used with bottom sediments. It is computed by the following equation (Faiz et al., 2009; Lu et al., 2009; Wei et al., 2010):

$$I_{geo} = log_2\left[\frac{C_n}{1.5B_n}\right]$$

where C_n represents the measured concentration of the element n and B_n is the geochemical background value of the element n in fossil argillaceous sediment or in soil. The geo-accumulation index is classified as follows:

$I_{geo} \leq 0$ unpolluted

$0 < I_{geo} \leq 1$ unpolluted to moderately polluted

$1 < I_{geo} \leq 2$ moderately polluted

$2 < I_{geo} \leq 3$ moderately to strongly polluted

$3 < I_{geo} \leq 4$ strongly polluted

$4 < I_{geo} \leq 5$ strongly to extremely polluted, and Igeo > 5 extremely polluted.

Wei et al. (2010) examined the enrichment of heavy metals in RDS from different locations in China using I_{geo} as a measure of the enrichment. They found that the average I_{geo} of metals ranged from 0.18 to 2.64 with the highest value for Cd and lowest value for Cr (Table 2.7). Among the cities studied, Guangzhou and Hongkong generally had the highest I_{geo} values for most of the heavy metals and this was explained as due to higher population density and more vehicles on the road in these two cities. Jiang et al. (2009) stated that average I_{geo} values for heavy metals in RDS from Beijing urban areas were 0.24 for Cr, 0.75 for Ni, 1.01 for Cu, 0.61 for Zn, 3.17 for Cd and 1.50 for Pb. They found that the RDS in different areas had different I_{geo} values. On this basis, Cd was considered to be "heavily contaminated", indicating that the RDS were obviously polluted by Cd. The average I_{geo} for Zn was 0-1, which was ranked as an "uncontaminated to moderately contaminated" level.

The values obtained for the three indices used to determine enrichment of heavy metals in RDS in various countries were presented by Loganathan et al. (2013). They are summarized in Table 2.8.

Table 2.7. Geo-accumulation index of heavy metals in urban RDS in different cities of China (adapted from Wei et al., 2010)

City	Cr	Cu	Pb	Zn	Ni	Cd
Xi'an	0.60	1.03	1.78	1.33	-	-
Hangzhou	-0.78	1.18	1.68	1.05	-0.61	2.18
Shanghai	0.35	1.52	2.04	1.77	0.59	1.84
Shanghai1	-	1.45	1.93	1.68	0.61	-
Shanghai2	0.25	1.49	1.97	1.73	0.61	-
Guangzhou	0.04	1.93	1.49	2.11	-0.56	3.77
Baoji	-	1.29	2.35	1.86	0.19	-
Urumqi	-0.31	0.86	0.61	1.05	0.08	1.87
Hongkong	-	1.63	1.53	2.57	-	3.25
Mean	0.18	1.48	1.81	1.48	0.34	2.64

Table 2.8. The ranges of EF, PI and I_{geo} values of some heavy metals reported in literature from several countries (data from Loganathan et al., 2013)

Metals	Enrichment Factor	Pollution Index	Geoaccumulation index
Cu	3-90	5-10	< 1
Pb	2-20	5-15	1-3
Cd	2-9	2-9	1
Zn	2-90	6-30	2-3
Cr	0-9	2-12	< 0
Ni	2-90	3-10	< 0
Mn	0-11	-	0

2.4.2. PAHs

Only a few attempts have been made to quantify the enrichment of PAHs in RDS (Brown and Peake, 2006; Maltby et al., 1995; Zechmeister et al., 2006). Fang et al. (2004) in their analysis of PAHs species distribution in RDS in central Taiwan, showed that Phenanthrene,

Fluoranthrene, Pyrene, and Benzo (g,h,i) Pyrene were the most abundant PAHs in the roadside RDS samples. In a study in Kuala Lumpur, Malaysia, Omar et al. (2002) reported that lower molecular weight PAHs, Phenanthrene, Fluoranthrene and Pyrene, were the predominant PAHs in RDS samples. Venkataraman and Friedlander (1994) reported that vehicular emissions are a source contributing to particulate PAH concentrations throughout the Los Angeles air basin. Lower molecular weight PAHs were more enriched in RDS particles, whereas high molecular weight PAHs were more abundant in atmospheric particles. They explained this as being due to lower molecular weight PAHs predominating in larger particles, which deposit more quickly whereas high molecular weight ones predominate in the smaller particles that deposit more slowly from the atmosphere.

2.5. Pollutant concentration distribution

Pollutant concentration distribution in RDS and the neighbouring soils varies with the distance from the roads, traffic density and speed, temporal changes, heterogeneity of the roads, and RDS particle size.

2.5.1. Distance from road

Studies have shown that there is a significant decrease in pollutant concentrations of RDS with increasing distance from the road (Davis et al., 2001; Snowdon and Birch, 2004; Zereini et al., 2007). For example, Birch and Scollen (2003) studied the RDS in Sydney and found that the concentration of Cr, Cu, Ni, Pb, and Zn was shown to decline with distance from 30 to 150 m from the roads. Higher concentrations of pollutants near the roads were explained as due to the constant high velocity wind generated by vehicles on roads and flushing from pavement runoff into the adjacent soils. A similar trend has also been found for PAHs concentrations which decreased exponentially with distance from roads in Brisbane, Queensland (Pathirana et al., 1994). In this study the concentrations of total PAHs as well as individual PAHs decreased exponentially with distance from roads up to 30 m.

2.5.2. Traffic density/speed and road surface

Increase of traffic density and speed increases RDS pollutant concentration mainly because of

the high exhaust emissions from increased engine emissions and road abrasion by high speed vehicles (Duong and Lee, 2011). In Sydney, Davis and Birch (2011) detected a good relationship between average daily deposition fluxes of Cu, Pb, and Zn and traffic density. Similarly, Tanner et al. (2008) reported that the higher traffic density in Hong Kong compared to Shanghai and Beijing caused extraordinarily higher concentrations of Cr, Cu, Pb and Zn in RDS in Hong Kong than in the other two cities. The speed of vehicles also plays an important role in controlling the pollutant concentrations in RDS.

2.5.3. Road site locations

Many studies have shown that in road environment where there is frequent vehicle braking and sudden deceleration/acceleration activity, RDS metal concentrations can be higher than at other locations along the road. For example, Hjortenkrans et al. (2006) reported that in decelerating environments such as roads with traffic lights, roundabouts and intersections in Sweden the RDS concentrations of Cu and Sb, the major input from brake linings, were more than eight-fold compared to background levels. Similarly, Awato et al. (2009) studying the variability of the RDS chemistry in different urban environments in Spain, reported that Cu, Sb, Zn and Mo were sharply concentrated at locations with braking activities. This revealed a strong relationship with the wear of brake pads and tyres.

2.5.4. RDS particle size

Pollutant concentration and total amount in different particle size fractions of RDS are important parameters for assessing the transport of sediment-bound pollutants (Stone and Marsalek, 1996). The finer fraction of RDS is easily transported in runoff but the coarser particles are more effectively controlled. The largest sized fraction that mostly stays on the road surface is removed by street cleaning or is retained in the sediment storage areas (sewer inlets and gully pots) and not transported through the entire drainage system.

Many studies have shown that concentrations of heavy metals (Cu, Fe, Cd, Mn, Ni, Pb, Zn) decrease when particle size increases with the highest concentrations found in the finest fraction <63–75 μm (Birch and Scollen, 2003; Ewen et al., 2009; Singh, 2011; Stone and Marsalek, 1996). As observed for the heavy metals, the concentrations of PAHs in RDS were also higher in the finer sized fraction (Dong and Lee, 2009; Murakami et al., 2005). Dong and

Lee (2009) reported that the PAHs concentration in the smaller sized particles (<75 μm and 75−180 μm) were much higher than those in the larger sized particles (180−850 μm and 850−2000 μm).

2.6. Pollutant mobility

2.6.1. Pollutants movement to water bodies via stormwater

Pollutants in RDS are transported to aquatic and terrestrial environments during storm events. The mobile fraction of the pollutants in RDS is transported by stormwater whereas the immobile fraction, which is stored in the sediments, may or may not move with the stormwater depending on the particle size of the sediments. The finer size particles tend to be transported by the stormwater and therefore carry the immobile fraction of the pollutants associated with them.

Birch and Scollen (2003) studied the distribution of heavy metals in RDS, gully pits and parkland soils in a highly urbanised sub-catchment of Port Jackson, New South Wales. They found that a large proportion of heavy metals was associated with the mobile fine fraction (< 62.5 μm). The heavy metals concentrations in solid and aqueous phases in stormwater runoff vary widely depending on various factors such as location, seasons, temperature and pH. In Sweden, both Westerlund et al. (2003) and Hallberg et al. (2007) found that dissolved fractions of Al, Cd, Co, Cr, Mn and Ni were significantly higher in winter compared to summer.

2.6.2. Sequential extraction of metals from RDS

Several studies have been conducted to assess the mobile and immobile fractions of heavy metal in RDS. The methods used in these studies can be classified into two main groups. In one group, single extractions such as 0.5 M HCl and 2 M HNO_3 were used to dissolve metals and the amounts dissolved are considered to be the mobile fraction (Joshi et al., 2009; Kartal et al., 2006; Stone and Marsalek, 1996). In the other group, reagents are used in a sequential order to extract different chemical forms of the metals. Each step in the sequential extraction

is more destructive than the previous step and hence the metal fractions extracted are in decreasing order of mobility. Two sequential extraction methods have generally been utilised. The method devised by Tessier et al. (1979) is a five-step sequential extraction method which uses reagents to extract the following fractions in decreasing order of mobility: exchangeable, carbonate-bound, Fe/Mn oxide-bound, organic-bound, and residual (Table 2.9).

Table 2.9. Five-step sequential extraction scheme for fractionation of metals (Tessier 1979)

Step	Phase	Extractant
1	Exchangeable metals	1 M $MgCl_2$
2	Metals bound to carbonates	1 M NaOAc + Acetic acid
3	Metals bound to Fe-Mn oxides	0.3 M $Na_2S_2O_4$ + 0.175 M Na-citrate + 0.025 M H-citrate
4	Metals bound to organic matter	0.02 M HNO_3 + 30% H_2O_2 + 3.2 M NH_4OAc
5	Residual	HF-$HClO_4$

The other sequential extraction method is a three-step procedure developed by the Standards, Measurements, and Testing program of the European Union (Rauret et al., 1999; Sahuquillo et al., 1999; Kartal et al., 2006). This method extracts exchangeable, reducible (Fe/Mn oxide-bound) and oxidisable (organic- and sulfide-bound) fractions. The residual fraction is determined by subtracting the sum of these three fractions from the total metal concentration measured independently. In both these methods, exchangeable fraction is considered to be mobile and the residual fraction is the least mobile fraction. The modified sequential extraction method is presented in Table 2.10.

Residual fraction originates mainly from natural geological materials whereas the other fractions originate mainly from anthropogenic sources such as industry, vehicles and road surfaces. The single and sequential extractions of RDS generally showed Cd or Zn to be the most mobile metal and Fe, Mn, Ni, and Pb to be the most immobile metals (Kumar et al., 2010; Robertson et al., 2003; Tokalio˘glu et al., 2003).

Mohammed et al. (2012) analysed 9 RDS samples collected from major motorways in Sydney, Australia and found that the mean metals concentration decreased in the order: Fe > Mn > Zn > Cu > Cr > Pb > Ni > Cd. Sequential extraction of metals showed 50-95 % of Cr and Fe to be present in the residual fraction, whereas 15-65 % Zn was contained in the exchangeable fraction.

Table 2.10. The modified BCR sequential extraction method used for the fractionation of metals (Kartal et al., 2006)

Step	Fraction	Extractant
1	Water and acid soluble and exchangeable	0.11 M CH_3COOH
2	Reducible	0.5 M $HONH_2 \cdot HCl$ (pH 2)
3	Oxidisable	8.8 M H_2O_2 (pH 2)
		1 M NH_4OAc (pH 2)
4	Residual	Aqua regia

2.7. Toxicity assessment

US EPA (1992) defined ecological risk assessment as being "evaluation of the likelihood that adverse ecological effects may occur or are occurring as a result of exposure to one or more stressors"*. This assessment process combines the information from toxicity tests (ecological effects), the exposure information, assumptions, and uncertainties in a way that helps the risk assessor understand the relationships between the ecological effects and the stressors (heavy metals and PAHs) and helps support decision-making. Common methods used to assess toxicity of heavy metals and PAHs are discussed in this section.

2.7.1. Ecological risk assessment

2.7.1.1. Heavy metals

The method of determining ecological risks of heavy metals originally introduced by Hakanson (1980) has recently been used in many studies on RDS. The ecological risk of heavy metals contaminated sites is mainly based on the concentration and toxic potential of the metal (Qiu et al., 2010; Sun et al., 2010; Saeedi et al., 2012). This method was adopted to assess the ecological risks (RI – risk index) of heavy metal pollution in RDS as follows:

$$RI = \sum_{i=1}^{m} Er$$

$$Er = T_r \times C_f \text{ and } C_f = C_r / C_b$$

where C_r is heavy metal concentration in RDS and C_b is heavy metal concentration in uncontaminated soils. Er is the ecological risk of each metal. Tr is defined as a "toxic-response factor" for a given heavy metal. Hakanson (1980) reported the values for this factor for Cd, Cu, Pb, Cr and Zn to be 30, 5, 5, 2 and 1, respectively. These values are related to the degree of toxicity per unit concentration of the heavy metal. On this basis, Cd is the most toxic and Zn is the least toxic. Tr values obtained from experiments on mice and rats are normally used. Therefore, while this may not be directly applicable to determine toxicity assessment on aquatic organisms, it can indicate to some extent the degree of toxicity. The risk classification of Er and RI values is presented in Table 2.11.

Table 2.11. Indices and grades of potential ecological risk assessment

Er value	Grades of potential ecological risk of single heavy metal	RI value	Grades of potential ecological risk of the environment
Er < 40	Low risk	RI < 150	Low risk
40 < Er < 80	Moderate risk	150< RI < 300	Moderate risk
80 < Er < 160	Considerable risk	300 <RI < 650	Considerable risk
160 < Er < 320	High risk	RI > 600	Very high risk
Er > 320	Very high risk		

In Tehran, Iran, Saaedi et al. (2012) found very high ecological risk in RDS from industrial areas (highest for Cd, Er 1596.2-1647.0). Similarly, most RDS samples from Urumqi, China were reported to have high potential ecological risk with mean RI of 430.5 (43.0 – 3734.7)

(Wei et al. 2010). In another study in Shanghai, China, it was reported that the urban RDS had higher values of Er and RI for all metals and total environment than in suburban RDS (Shi et al., 2010).

2.7.1.2. PAHs

PAH toxicity evaluation is generally conducted using relative toxicity values of individual PAHs proposed by Nisbet and LaGoy (1992). They assigned toxicity equivalent factors (TEF) to the various PAHs by assuming a relative value of 1 for Benzo(a)pyrene which is considered to be one of the most potent carcinogens in the PAH group. The values for the other PAHs were derived by reviewing published literature on their doses related toxicities found mainly on rats and mice. The toxicity equivalent quotient (TEQ) of contaminated site is then calculated by summing the products of each individual PAH concentration (Ci) and it's TEF value, as follows:

$$TEQ = \sum_{i=1}^{n} (C_i * TEF_i)$$

Duong and Lee (2009) calculated TEQ of RDS in different sites of Ulsan, South Korea and found that the range of TEQ values of PAHs in RDS from industrial areas and urban areas were 0.93-16.74 µg/g and 4.37- 68.84 µg/g, respectively. Wang et al. (2011) reported high TEQ values (0.84-12.3 µg/g) in the bustling commercial streets of Guangzhou, China where the high concentrations of PAHs may have resulted from the accumulation of PAHs from the emissions of slow moving vehicles and the limited dispersion of pollutants. Recently, Wang et al. (2015) reported that the TEF concentrations of ∑16 PAHs of RDS in suburban areas of Nanjing, China ranged from 2.34 to 1430 ng/g, with a mean value of 215 ng/g which were much lower than in rural areas. TEF concentration of ∑16PAHs ranged from 2.65 to 465 ng/g, with a mean value of 130 ng/g in rural areas.

2.7.2. Biological methods

The toxic potential of various stormwater runoff has been examined by conducting tests of acute lethality or immobilisation using classical bio-indicators such as *Vibrio fischeri*, *Daphnia magna*, *Artemia salina* and Medaka fish (*Oryzias latipes*) (Beasley and Kneale, 2002; Nguyen et al., 2009; Svensson et al., 2005) (Table 2.12). *Vibrio fischeri* (Microtox®) has been widely used to estimate acute toxicity and several commercial test kits are commercially available (Parvez et al., 2006). *Artemia salina* (Artemia) has been used as test

organism for assessing acute and chronic toxicity of different kinds of contaminated water (Svensson et al., 2005). Artemia is widely used in toxicity studies and a large database is available on the toxicity of different contaminants on Artemia, which is applicable for a range of environments. Regulatory authorities have favoured the use of biological indicators rather than chemical methods for assessing the potential toxicity of environmental pollutants (Nunes et al., 2006). Table 2.12 presents LC50 and EC50 values for toxicity risk assessment of different pollutants on aquatic organisms.

Table 2.12. LC50 and EC50 values for toxicity risk assessment of pollutants

Pollutant name	Animal/ Organism	Plant	Concentrations of LC50/EC50(μg/L)	Reference
Cu (Copper sulfate)	*Artemia salina*		LC50= 4450	Gaete et al. (1996)
		Lemna minor	LOEC=12	Olette et al. (2008)
Pb (Lead nitrate)	*Artemia salina*		LC50= 1700	Gajbhiye and Hirota (1990)
		Lemna minor	EC_{50}= 3000	Borek et al. (1998)
Cd (Cadmium nitrate)	*Artemia franciscana*		EC_{50}= 112440	Blust et al. (1995)
		Lemna minor	BCF(1500)= 1000	Hutchinson (1975)
Zn (Zinc sulfate)	*Artemia salina*		LC50= 50500	Crisinei et al. (1994)
		Lemna minor	LC50= 67700	Brown and Rattigan (1979)
Cr (Sodium dichromate)	*Ceriodaphnia reticulata*		LC50= 195	Elnabarawy et al. (1986)
		Lemna minor	EC50= 195	Taraldsen and Norberg-King (1990)
BaP (Benzo[a]pyrene)	*Daphnia magna*		LC50= 250	Atienza et al. (2006)
		Lemna gibba	EC50= 560	Huang et al. (1995)
BbF (Benzo[b]fluoranthene)	*Daphnia magna*		EC50= 1024	Wernersson and Dave (1997)
		Plant	NA	
BkF (Benzo[k]fluoranthene)	*Daphnia magna*		BCF= 14	Newsted and Giesy (1987)
		Lemna minor	NA	
DBA (Dibenz[a,h]anthracene)	*Daphina magna*		EC50= 496	Wernersson and Dave (1997)
		Lemna gibba	EC50= 2000	Krylov et al. (1997)
Fl (Fluoranthene)	*Artemia salina*		EC50= 39.6	Diamond et al. (2000)
		Lemna minor	EC50= 166	Spehar et al. (1999)
Pyr (Pyrene)	*Artemia salina*		LC50= 99.10	Abernethy and Mackay (1987)
		Lemna gibba	LC50=166	Huang et al. (1995)

Another method used to assess the toxicity of pollutants on organisms is the alkaline unwinding of DNA technique which is based on the time-dependent partial unwinding of DNA when the organism is exposed to pollutants. It makes it possible to determine the ratio of conversion of double-stranded DNA (dsDNA) to single-stranded DNA (ssDNA) (Dixon

and Wilson, 2000). The alkaline unwinding assay has proved to be a rapid and sensitive method of assessing DNA strand breakage in the cells of marine invertebrate caused by pollutants, under both laboratory and field conditions (Dixon and Wilson, 2000). Nacci and Nelson (1992) used this assay to detect DNA damage in the gill tissues of *M. edulis* and *Crassostrea virginica* that had been transplanted into an urban estuary setting contaminated with polychlorinated biphenols, PAH and heavy metals. This study showed that increased DNA strand breaks resulted from acute exposures to sublethal concentrations of the genotoxic agent N-methyl-N'-nitro-N-nitrosoguanidine. Other studies on the alkaline unwinding assay include investigations on *M. galloprovincialis* (Viarengo et al., 1991) and starfish *Asterias rubens* (Everaarts, 1995). Everaarts (1995) showed that the low integrity of DNA indicated the extent of damage occuring due to interaction of various pollutants with DNA from the seastars. Such a low integrity of DNA could be due to enhanced concentration of PAHs, PCBs, and metals like Cd, Pb, Cu in the bulk sediments. Goumenou et al. (2004) reported a modified DNA alkaline elution procedure with the optimised fluorometric determination of ssDNA and applied this technique to liver tissue from both untreated and treated Wistar rats. This method proved to be an accurate and reliable approach for determining *in vivo* induced ssDNA strand breaks.

2.8. Permissible limits for heavy metals and PAHs in water

There are several guidelines for restricting heavy metals and PAHs compounds in water and sediments in many countries worldwide. Because recycled water provides a viable opportunity to supplement water supplies, alleviate environmental loads as well as the sources (Chen et al., 2013). These guidelines are used as a general tool for assessing water quality and are the key to determining water quality objectives that protect and support the designated environmental values of water resources. In 1980, for example, US EPA developed ambient water quality criteria to protect people's health from the carcinogenic effects of PAH exposure. EPA sets a maximum contaminant level (MCL) for benzo(a)pyrene, the most carcinogenic PAH, at 0.2 µg/L. Different organisations/agencies have recommended a permissible limit on the concentrations of heavy metals and PAHs in water, above which toxicity to aquatic organisms is likely. The limits proposed for heavy metals are presented in Table 2.13.

Table 2. 13. Permissible limits and health effects of some heavy metals in potable water (adapted from Ahmaruzzaman. 2011)

Metals	Permissible limits for potable water (mg/L)				Health hazards
	Australian standard (ADWG, 2011)[a]	WHO[b]	US.EPA[c]	EU standard[d]	
Ni	0.02	0.02	0.1	0.02	Causes chronic bronchitis, reduced lung function, cancer of lungs.
Zn	5.0	3.0	5.0	-	Causes short-term illness called "metal fume fever" and restlessness
Cu	2.0	2.0	1.3	2.0	Long term exposure causes stomach ache, irritation of nose,
Cd	0.005	0.003	0.005	0.005	Carcinogenic, cause lung fibrosis, dyspnoea
Pb	0.01	0.01	0.015	0.01	Suspected carcinogen, anaemia, muscle and joint pains, kidney problem and high blood pressure
Cr	0.05	0.05	0.1	0.05	Suspected human carcinogen, producing lung tumours

a. ADWG 2011 Australian Drinking Water Guidelines (2011)
b. http://www.gemswater.org.
c. http://www.lenntech.com
d. General standards for discharge of environment pollutants: effluent. Gazette notification of MoEF (Organization, 2015)

Sediments are important, both as a source and sink of dissolved contaminants. As well as influencing surface water quality, sediments represent a source of bioavailable contaminants to benthic biota and hence potentially to the aquatic food chain. It is therefore desirable to define situations in which contaminants associated with sediments represent a likely threat to ecosystem health. Sediment quality guidelines are being actively considered by regulatory agencies worldwide.

The World Health Organization has established a very strict legislation for PAH compounds (WHO, 2011). The permissible limit in this legislation for Benzo (a) Pyrene (BaP) was 0.7 x 10^{-3} mg/L. An Australian and New Zealand guideline (ANZECC, 2000) recommended the trigger values of Napthalene for freshwater as 2.5 µg/L and for marine water as 50 µg/L (99% level of protection). According to the US EPA (1992), maximum concentration level of BaP should not exceed 200 ng/L. In addition to BaP, the European Union in Directive 98/83/EC has regulated benzo[b]fluoranthene (BbF), benzo(k)fluoranthene (BkF), benzo(g,h,i)perylene (B(g,h,i)P) and indeno(1,2,3-c,d)pyrene (IND). Maximum contaminant level values were set at 10 ng/L for the highly toxic BaP and 100 ng/L for the sum of the remaining PAH. Limits for naphthalene (1200 ng/L), fluoranthene (100 ng/L) and anthracene (100 ng/L) were also included in this directive. The summary of sediment quality guidelines with toxicity threshold metals concentrations for aquatic organisms is presented in Table 2.14 and for PAHs in Table 2.15.

Table 2. 14. Sediment quality guidelines - toxicity threshold metals concentrations for aquatic organisms (mg/kg) (adapted from Burton (2002))

SQG	As	Cd	Cr	Cu	Pb	Hg	Ni	Zn	Reference
TEL[1]	5.9	0.6	37.3	35.7	35	0.17	18	123	a
ERL	33	5	80	70	35	0.15	30	120	a
LEL[2]	6	0.6	26	16	31	0.2	16	120	a
MET[3]	7	0.9	55	28	42	0.2	35	150	a
CB TEC	9.79	0.99	43.4	31.6	35.8	0.18	22.7	121	a
EC-TEL[4]	7.24	0.68	52.3	18.7	30.2	0.13	15.9	124	b
NOAA ERL[5]	8.2	1.2	81	34	46.7	0.15	20.9	150	c
ANZECC ERL[5]	20	1.2	81	34	47	0.15	21	200	d
ANZECC ISQG-low[5]	20	1.5	81	65	50	0.15	21	200	d
SQAV TEL-HA28[6]	11	0.58	36	28	37	-	20	98	e
SQO Netherlands Target	2.9	0.8	-	36	85	0.3	-	140	d
Hong Kong ISQG-low[7]	8.2	1.5	80	65	75	0.15	40	200	d
Hong Kong ISQV-low[7]	8.2	1.5	80	65	75	0.28	40	200	f
Flanders RV X[8]	28	1	43	20	0.1	35	28	168	g
EQS Human Health Items	0.01	0.01	0.05	-	0.01	0.0005	-	-	h
Slightly Elevated StreamSediments[9]	8	0.5	16	38	28	0.07	-	80	i

SQG, Sediment quality guideline; TEL, threshold effect level; ERL, effects range low; LEL, lowest effect level; MET, minimal effect threshold;
CB, Consensus Based; TEC, threshold effect concentration; EC, Environment Canada; NOAA, National Oceanic and Atmospheric Administration;
ANZECC, Australian and New Zealand Environment and Conservation Council; ISQG, Interim Sediment Quality Guidelines; SQAV, Sediment Quality Advisory Value; SQO, Sediment Quality Objective; ISQV, Interim Sediment Quality Value; RV, Reference Value; EQS, Environmental Quality Standard; MEL, Median Effect Level; FEDP, Florida Department of Environmental Protection

[1] Same as Canadian Freshwater Sediment Guidelinesd
[2] Same as Ontario Ministry of Environment Screening Level Guidelinesd
[3] Same as MEL in SQAVse
[4] Same for FDEP Guidelinesd and Canadian Marine Sediment Quality Guidelinesd
[5] Some values in NOAA and ANZECC are the same
[6] All other SQAVs are the same as SQGsa
[7] ISQG and ISQV are the same for all metals except Hg
[8] Reference values and class limits for rivers in Flanders; _X class 1, _Y class 2, _Z class 4, _Z class 5
[9] Classification of Illinois Stream Sediments

a MacDonald et al. (2000)
b Smith et al. (1996)
c NOAA (1999)
d ANZECC (1997)
e Swartz (1999)
f Chapman et al. (1987)
g De Cooman et al. (1999)
h Design Prefecture (2001)
i Classification of Illinois Stream Sediments

Table 2. 15. Sediment quality guidelines - toxicity threshold PAHs concentrations for aquatic organisms (µg/kg) (adapted from Burton (2002))

Substance	SLC	TEL[1]	ERL	LEL	MET	CB TEC 95% CI	Ontario Minimum Environmental Screening Level-low	NOAA freshwater TEL[3]	NOAA TEL marine[2]	NOAA ERL[1]
Acenaphthene	60	10	20						6.71	16
Acenaphthylene	50	10	40						5.87	44
Anthracene	160	50	90						46.85	85.3
Fluorene	100	20	20						21.17	19
Napthalene	410	30	160					41.9	34.57	160
Phenanthrene	270	90	240						86.68	240
LMW PAHs								31.7	311.7	552
B(a)anthracene	260	70	260						74.83	261
Benzo(b) fluoranthrene	320	70	320							
Benzo(k) fluoranthrene	280	60	280							
Benzo(a)pyrene	400	90	430					31.9	88.81	430
Dibenzo(a,h)anthracene									6.22	63.4
Chrysene	380	110	380					57.1	107.77	384
Fluoranthene	640	110	600					111	112.82	600
Pyrene	660	150	660					53	152.66	665
HMW PAHs									655.34	1700
Total PAHs	4090	870	3500			1190-4610	2000		1684.06	4022
Reference	a	a	a	a	a	a	b	c	c	b,c

SLC, screening level contamination; TEL, threshold effect level; ERL, effects range low; LEL, lowest effect level; MET, minimal effect threshold;
CB, Consensus Based; TEC, threshold effect concentration; CI, confidence interval; NOAA, National Oceanic and Atmospheric Administration;
LMW, low-molecular-weight; PAHs, polycyclic aromatic hydrocarbons; HMW, high-molecular-weight; DDD, dichlorodiphenyldichloroethane;
DDE, dichlorodiphenyldichloroethylene; DDT, dichlorodiphenyltrichloroethane; PCBs, polychlorinated biphenyls; ISQG, Interim Sediment
Quality Guidelines; ISQV, Interim Sediment Quality Value; ANZECC, Australian and New Zealand Environment and Conservation Council;
FDEP, Florida Department of Environmental Protection
[1] Same as Hong Kong ISQG-lowb, does not include DDT, DDE, DDT, chlordane, dieldrin, endrin, heptachlor epoxide, and lindane
Same as Hong Kong ISQV-lowd, does not include DDT, DDE, DDT, chlordane, dieldrin, endrin, heptachlor epoxide, and lindane
Same as ANZECC ISQG-lowb, does not include heptachlor epoxide
Same as ANZECC guidelines for sediments sea disposalb, screening level effects range low, except Chlordane and Dieldrin
[2] Same as Canadian sediment quality criteriae
Same as FDEP Guidelinesb
Same as Canadian Marine Sediment Quality Guidelinesb
[3] Same as Canadian Freshwater Sediment Quality Guidelinesb
a Swartz (1999)
b ANZECC (1997)
c NOAA Administration) (1999)
d Smith et al. (1996)

2.9. Technologies for reducing concentrations of heavy metals and PAHs in stormwater

2.9.1. Management of RDS

One method of reducing the concentration of heavy metals and PAHs in stormwater is to reduce the amount of RDS. This can be done by adopting preventive treatment or mitigating strategies. Preventive measures are improvement of roads (resurfacing, paving the access to unpaved lots), and road traffic restrictions (Kadıoğlu et al., 2010). Mitigating measures are used to remove or bind RDS already present by sweeping, water flushing and applying chemical suppressants. Use of dust suppressants such as salts, polymers, resins, and bitumen have been tried, mainly for unpaved roads but this is not a widely used method. Furthermore, some of these suppressants can pose environmental hazards and their application may be costly (Amato et al., 2010).

2.9.2. Stormwater treatment

Stormwater best management practices (BMPs) are widely used for reducing the adverse effects of stormwater (Braune and Wood, 1999). Although most BMPs are developed to control the water flow in order to alleviate peak flows and avoid flooding, more attention has recently focused on developing BMPs that also remove pollutants. The most common BMPs are the use of ponds, basins, wetlands and swales. Of these, some are built to infiltrate stormwater, whereby pollutants are either accumulated in the soil or transported to the groundwater. Others are built as active scavengers for pollutants associated with particles. The primary inadequacy of such systems is that the colloidal and truly dissolved fractions cannot be removed via settling; hence, there is a need for secondary treatment of stormwater, after passing through a pond, basin or wetland. Filtration of the stormwater, where both colloidal and truly dissolved heavy metal fractions are primarily removed via adsorption, is preferred over the other methods because of the advantages of having a small space usage in filtration. Furthermore, a very high filtration rate can be used in filtration through adsorbents packed in filter-beds (Tsihrintzis and Hamid, 1997). Without appropriate stormwater treatment devices, the resulting impacts of these pollutants on receiving waters can be devastating, not only for aquatic ecosystems but also to community values such as aesthetics, recreation, economics and health of receiving water bodies.

Various chemical and physical treatment methods have been developed for removing heavy metals from wastewater which can be applied to stormwater treatment (Table 2.16). There are four classes of chemical separation technologies: chemical precipitation, electrolytic recovery, adsorption/ion exchange and membrane filtration. These major classes involve various specific methods that include chemical treatment, caustic oxidation and reduction, ion-exchange, adsorption, reverse osmosis, solvent extraction, membrane filtration and electrochemical treatment. The advantages and disadvantages of these methods are presented in Table 16. Of these methods, adsorption/ion exchange is one of the most promising technologies in the wastewater treatment process because it is efficient, cost effective and a reliable treatment process (Bhatnagar and Sillanpää, 2011; Loganathan et al., 2014). Furthermore, it produces a minimum amount of waste unlike other processes.

Table 2. 16. Treatment technologies for heavy metals removal from wastewater/stormwater involving physical or chemical processes (adapted from Ahmaruzzaman (2011))

Methods	Advantages	Disadvantages
Oxidation	Rapid process for toxic pollutants removal	High energy costs and formation of by-products
Ion-exchange	Wide range of heavy metals can be removed	Adsorbent requires regeneration or disposal
Membrane filtration technologies	High efficiency of removing the heavy metals	Concentrated sludge production, expensive
Adsorption	Flexibility and simplicity of design, ease of operation and intensitivity to toxic pollutants	Adsorbents requires regeneration
Coagulation/flocculation	Economically feasible	High sludge production and formation of large particles
Electrochemical treatment	Rapid process and effective for certain metal ions	High energy costs and formation of by-products
Ozonation	Applied in gaseous state: alteration of volume	Short half life
Photochemical	No sludge production	Formation of by-products

Irradiation	Effective at lab scale	Required a lot of dissolved O_2
Electrokinetic coagulation	Economically feasible	High sludge production
Fenton's reagents	Effective and capable of treating variety of wastes and no energy input necessary to activate hydrogen peroxide	Sludge generation
Biological treatment	Feasible in removing some metals	Technology yet to be established and commercialised

Although applications of adsorbents for treating heavy metals have been extensively investigated (Bhattacharya et al., 2006; Kragović et al., 2012), studies on removing PAHs compounds and other organic pollutants have emerged only in recent years (Kong et al., 2012; Valderrama et al., 2008; Yakout and Daifullah, 2013). Figure 2.6 illustrates various kinds of adsorbents used for removing pollutants such as heavy metals and PAHs from stormwater. Some of these adsorbents are waste materials and therefore they are of low cost. However, their adsorption capacities are poor and therefore they may not remove much of the pollutants from highly contaminated water. On the other hand, some adsorbents have very high adsorption capacities and can effectively remove pollutants in highly contaminated water. However, these adsorbents are often very expensive but nonetheless the cost of adsorbents can be overcome if they are regenerated many times without compromising their adsorption capacities.

Most studies on removal of pollutants using adsorbents have been conducted on static batch mode of adsorption in closed system and relatively few on fixed-bed column mode of adsorption, which is dynamic and more practical and commonly used in waste water treatment plants. However, the batch method is simple and information can be obtained quickly on the effects of many solution variables on adsorption by conducting a number of batch adsorption experiments simultaneously (Loganathan et al., 2014). Many studies on adsorption investigated the effects of physical and chemical factors influencing adsorption. Some of these factors are pH, concentrations of co-ions, and temperature (Ahmaruzzaman, 2011; Babel and Kurniawan, 2003; Gupta and Ali, 2012).

In equilibrium adsorption studies, the heavy metals adsorption in batch studies have been fitted to models such as Langmuir isotherm, Freundlich isotherm, and Dubinin–Radushkevich

isotherm (Dimirkou and Doula, 2008; Doula, 2009; Mishra and Patel, 2009; Sounthararajah et al., 2015). Batch kinetic data for the adsorption of heavy metals have been fitted to pseudo-first order, pseudo-second order and diffusion models (Kocaoba et al., 2007; Taparcevska et al., 2010; Wang et al., 2008). Kinetics of PAHs adsorption have also been described by pseudo-first order and pseudo-second order in some studies (Cabal et al., 2009; Xi and Chen, 2014) and equilibrium adsorption using the Langmuir and Freundlich isotherms (Crisafully et al., 2008; Yakout et al., 2013). Column adsorption data of heavy metals have been modelled using the Thomas model (Han et al., 2009; Sounthararajah et al., 2015), Bohart-Adam model (Jusoh et al., 2007), and Yoon-Nelsoon model (Baral et al., 2009; Tabakci and Yilmaz, 2008). In adsorption studies generally the mechanisms of adsorption are investigated using zeta potential (Abdel Salam et al., 2011; Sounthararajah et al., 2015) and spectroscopic (FTIR, EDX) (Doula, 2009; Han et al., 2009; Mozgawa, 2000; Vidal et al., 2011) measurements.

Most previous studies on heavy metal adsorption considered a single metal at a time. However, very often, ions of more than one metal are present in stormwater. Therefore, it is important to understand the behaviour of this mixture of ions in the solution and to explore the effect of the concentration of one metal ion on the adsorption of other metal ions. This can be achieved by investigating equilibrium isotherms of multicomponent systems (Bayat, 2002; Doula, 2009; Minceva et al., 2007). Such competitive adsorption of heavy metals has been analysed for some adsorbents (Bayat, 2002; Doula, 2009; Jeon et al., 2012; Minceva et al., 2007; Sounthararajah et al., 2015).

With reference to PAH compounds, adsorption of individual PAHs has been studied by many researchers (Cabal et al., 2009; Crisafully et al., 2008; Gong et al., 2007) but not as a mixture of PAHs. As in the case of heavy metals, adsorption of mixture of PAHs is important because in stormwaters, many PAHs occur simultaneously and therefore there can be competition for adsorption among them.

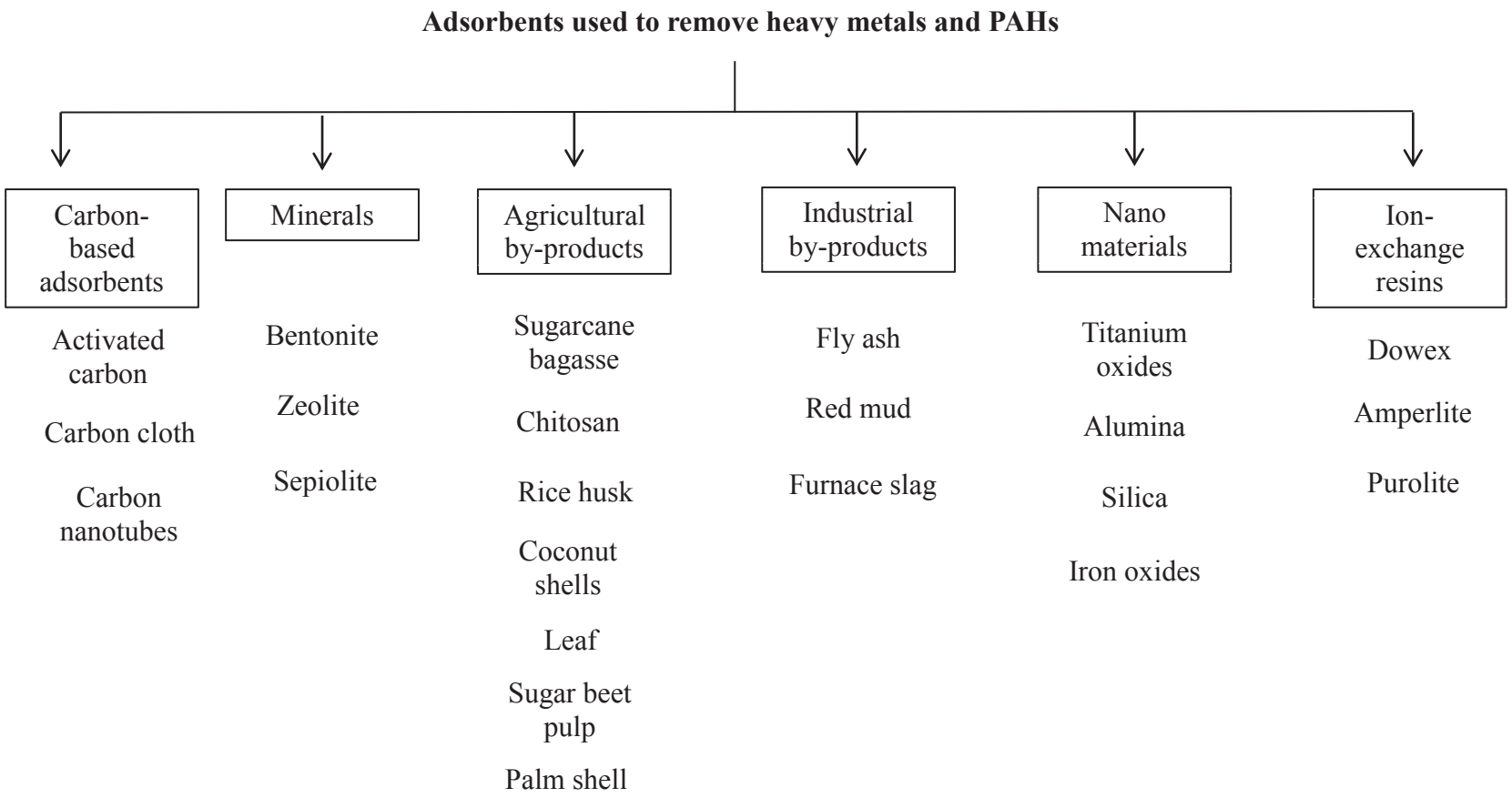

Figure 2.6 . **Different adsorbents used in removing pollutants from stormwater**

2.10. Conclusions

RDS and the associated organic and inorganic pollutants such as heavy metals, metalloids and polycyclic aromatic hydrocarbons (PAH) and their effects on the environment have been investigated over the last few decades in many countries (Aryal et al., 2010; Loganathan et al., 2013; Murakami et al., 2008; Taylor and Owens, 2009). The degree of enrichment of heavy metals and PAHs in RDS that were derived from roads and vehicles has been calculated by comparing their concentrations in RDS and natural soils using enrichment factors such as pollution index, geological indices. Many heavy metals, metalloids, and PAHs are acutely and chronically toxic and carcinogenic and known to have adverse effects on humans and terrestrial and aquatic ecosystems. RDS constitute a potentially significant source of pollution to surface water, marine sediments, and consequently the food chain because pollutants are often transported in stormwaters to water bodies. However, the health risk and toxicity effects of heavy metals and PAHs in RDS are still not well understood.

Statistical methods such as principal component analysis, cluster analysis and Pearson correlation analysis have been successfully used to identify the heavy metals and PAHs sources (road asphalt surface, brakes, tires, vehicle exhaust, local industry, bush fires, etc.) so that adequate measures can be taken to reduce the environmental risk posed by these pollutants. In the case of PAHs, diagnostic ratios of specific PAH species have also been used. Numerous studies have been conducted on PAH and heavy metals accumulation in RDS in many countries. However, no study appears to have compared the heavy metals and PAHs profiles in RDS, water sediments, and natural soils for any single catchment area. Yet this type is important in assessing the pollutants contribution of RDS and natural soils to local water bodies, so that control measures can be implemented to reduce pollution of water bodies.

The finest size fraction of RDS has been shown to contain the highest concentration of pollutants. The mobile fraction of the pollutants is transported in dissolved form by stormwater whereas the immobile fraction is largely stored in the sediments. However, the finest size particles tend to be transported by the stormwater and therefore carry the immobile fraction of the pollutants associated with them. Sequential extraction techniques have been used to assess the mobile fraction of heavy metals in RDS. No study appears to have been

conducted on relating the different fractions of metals to the metals concentrations in water sediments.

At elevated concentrations of heavy metals and PAHs, RDS can cause toxicity to aquatic organisms. Ecological risks have been evaluated using risk indices derived from experiments on rats and mice. These indices may not be directly applicable to risk on aquatic organisms. Some studies used classical bio-indicators such as *Vibrio fischeri*, *Daphnia magna*, *Artemia salina* and medaka fish (*Oryzias latipes*). Only a few studies have investigated the DNA damage which can serve to detect the molecular toxic effects of heavy metals and PAHs in the stormwater runoff. This test needs further development as it is more relevant to assessing toxicity to aquatic organisms.

Pollutants that enter the water bodies through stormwater runoff need to be removed to protect the aquatic environment of the receiving water. Several adsorbents have been used to remove these pollutants. The use of low-cost adsorbents is preferred to costly ones. Adsorptive removal of metals and PAHs is influenced by pH, concentrations of co-ions, and temperature. The majority of previous studies on heavy metal and PAHs adsorption considered one metal or one PAH at a time. However, very often, more than one metal or one PAH are present in stormwater. Subsequently, it is important to understand the behaviour of these mixed pollutants and how one pollutant influences the adsorption of another. Most studies on the removal of pollutants using adsorbents have been conducted using static batch mode of adsorption in a closed system, while relatively few have been done on fixed-bed column mode of adsorption. The latter is dynamic and more practical and commonly used in waste water treatment plants. More studies are required using fixed or fluidised bed column mode of adsorption.

CHAPTER 3

University of Technology, Sydney

HEAVY METALS IN ROAD-DEPOSITED SEDIMENTS AND WATER BED SEDIMENTS IN KOGARAH BAY OF SYDNEY, AUSTRALIA: ENRICHMENT, SOURCES AND FRACTIONATION

Much of this chapter was published in T.C. Nguyen, P. Loganathan, T.V. Nguyen, T.T.N. Pham, S. Vigneswaran, J. Kandasamy, M. Wu, and R. Naidu (2015). Trace elements in road-deposited and water bed sediments in Kogarah Bay of Sydney, Australia: Enrichment, sources, and fractionation. Soil Research 53(4): 401-411.

CHAPTER 3

HEAVY METALS IN ROAD-DEPOSITED SEDIMENTS AND WATER BED SEDIMENTS IN KOGARAH BAY OF SYDNEY, AUSTRALIA: ENRICHMENT, SOURCES AND FRACTIONATION

3.1 Introduction

The escalating rate of vehicle usage as a result of the urban population's rapid growth is causing increasing amounts of RDS in many parts of the world. RDS contain high concentrations of inorganic and organic pollutants, and of these, heavy metals constitute a major component (Loganathan et al. 2013). Many of the heavy metals at elevated concentrations have harmful effects on humans and aquatic environments (Hakanson 1980; Lynam and Pfeifer 1991; Scanlon 1991). The sources of the heavy metals in RDS are vehicle parts and exhaust emissions, road surfaces, and lithology of the area (Taylor and Owens 2009; Loganathan et al. 2013). The mobile fraction of heavy metals in RDS can easily be dissolved in stormwater and can potentially be transported into adjacent water bodies. Other fractions can also be transported along with suspended solids in the water. Trace elements stored in water baseline sediments (WBS) are released slowly over time and become bioavailable to aquatic organismms.

The degree of heavy metals enrichment in RDS depends on the relative contribution of the various sources of heavy metals such as BLS, vehicle activities and abrasion of road surfaces. The contribution of vehicle activities and roads can be assessed by comparing the heavy metals concentrations in RDS with those in nearby BLS away from the roads with minimum contamination using different types of indices, for example: a geo-accumulation index (I_{geo}) (Faiz et al. 2009; Lu et al. 2009), an enrichment factor (EF) (Lu et al. 2009), and a pollution index (PI) (Faiz et al. 2009; Lu et al. 2009).

Source identification of heavy metals is important so that the correct measures to prevent pollution are implemented. Multivariate statistical approaches such as correlation coefficient,

cluster and principal component analyses have been employed for source identification (Yongming et al. 2006; Mohammed et al. 2012). In these analyses, heavy metals which are inter-correlated to form principal components are considered to have originated from common sources.

The mobility and bioavailability of heavy metals in RDS, WBS, and BLS depends mostly on the chemical forms in which the metals exist, rather than on the total concentration. Sequential extraction methods are one method by which the operationally defined readily mobile, less mobile and immobile fractions can be determined. Two general sequential extraction procedures have been used previously. The methods commonly used to determine these fractions were described in Chapter 2.

Numerous studies have been conducted on heavy metals accumulation in RDS (Taylor and Owens 2009; Loganathan et al. 2013). However, very few studies have been reported on comparing metal concentrations between RDS, WBS, and BLS within a single catchment area (Birch 2011). Such a study is important in assessing the RDS and BLS contribution of heavy metals load contributions to local water bodies, so that control measures can be adopted, if necessary, to reduce RDS polluting the water bodies. The aims of the study were to determine heavy metals: (1) distributions in RDS, WBS, and BLS; (2) enrichments in RDS and WBS by comparing concentrations in RDS and WBS with those in BLS reference; (3) potential mobility and bioavailability using a sequential chemical extraction method; and (4) possible sources using statistical methods.

3.2 Materials and methods

3.2.1. Sediments and soils sampling

Samples used in this study were samples of those collected for another study conducted to determine the polycyclic aromatic hydrocarbons distribution in the same area (Nguyen et al. 2014). Eleven samples each of RDS and WBS, and 7 samples of BLS were collected in and around Kogarah Bay, Sydney, the largest and most populated city in Australia. The sites where the samples were collected are shown in Figure 3.1. No major industries were presented close to the catchment. RDS were collected during summer months on asphalted pavement within the shoulder of the roads excluding the gutters within an area of

approximately 2 m^2. Two to three weeks of dry weather were allowed for sufficient RDS to accumulate at each site before samples were collected. The areas were carefully brushed using a clean plastic dustpan and then transferred into self-sealing polyethylene bags for transport to the laboratory for analysis.

Most parts of the catchment area had roads and buildings, leaving only very small areas under bushland which had minimum effect from the above sources with no visible signs of contamination. These sites were 200 to 2000 m away from the various RDS sampling sites. Due to the limited land area available under bushland a smaller number of BLS samples were collected. Before collection of BLS samples, the vegetation on the land was removed and approximately 1 kg soil collected to a depth of 0.1 m depth from each of three areas 10 m apart using a stainless steel spade. The samples were mixed thoroughly and subsamples of 1 kg soil were transported to the laboratory for analysis.

A total of 11 WBS samples were collected. Six samples were collected (top 0.1 m depth) during summer season using a stainless steel grab sampler in canals that carry stormwaters from the roads (Figure 3.1). Each sample was a composite of 3-5 samples collected at 1 m apart. Similarly, five WBS samples were collected (top 0.1 m depth) within the bay at distances of 10 to 100 m from the places where the canals drains to the bay. The depth of water at the sampling sites was 0.2-0.5 m in the canals and 1-2 m in the bay. The bay is > 7 km from the coastline of the Pacific Ocean.

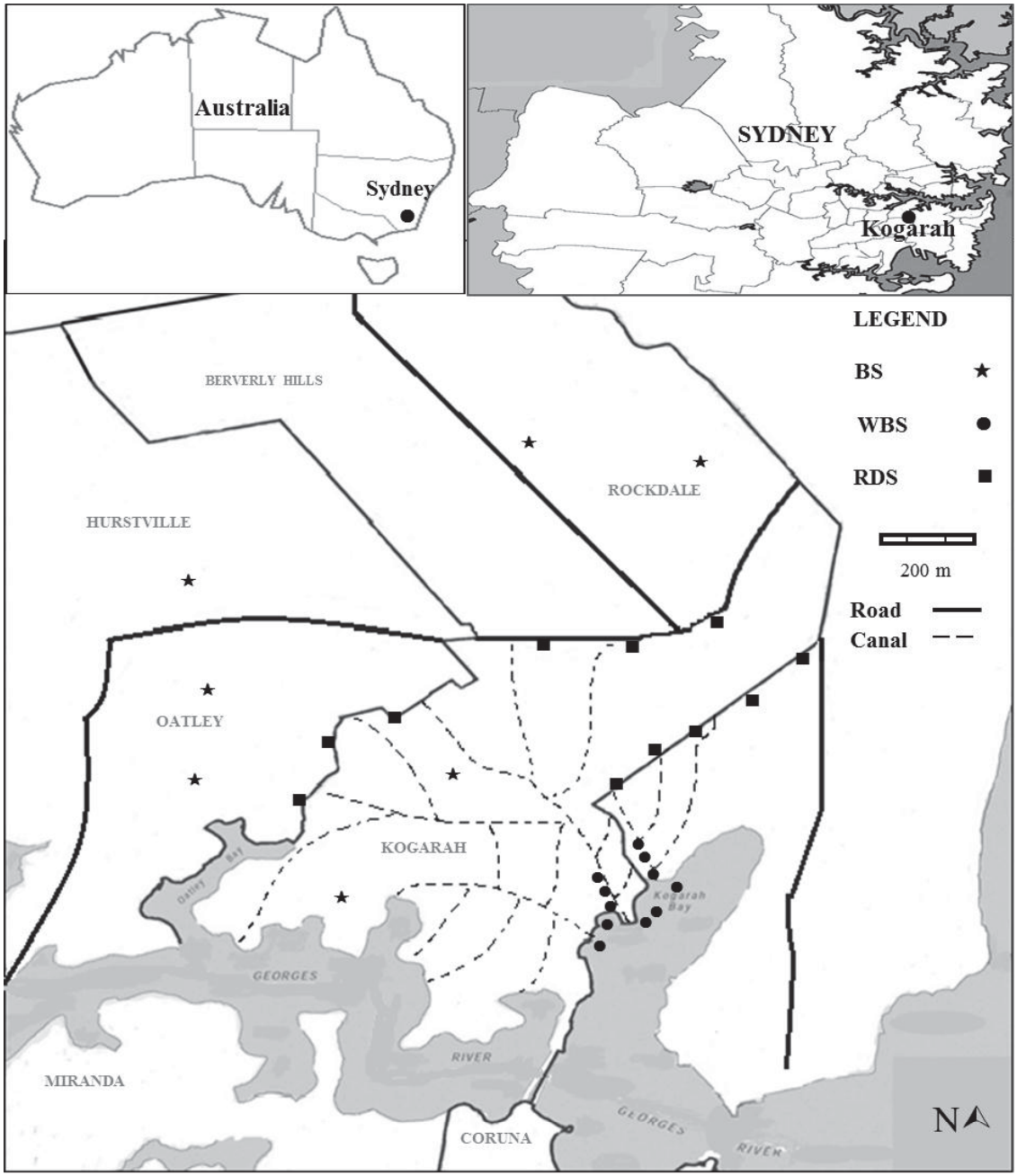

Figure 3.1. Map of sampling sites

3.2.2. Chemical analysis

The soil and sediment samples were dried at 40^{o}C inside an oven. The dried samples were ground to pass through a 2 mm stainless steel sieve and samples of approximately 50 g each were ground using a stainless steel electric grinder before the heavy metals analysis. Pseudo-total concentrations of Cd, Cr, Cu, Fe, Mn, Ni, Pb, Sb, V, and Zn were determined by digestion of 0.5-1.0 g soil or sediment sample using 3 mL 70% HNO_3 and 3 mL 32% HCl for 2 h at 100^{o}C. Of these heavy metals, Sb is a metalloid, V is a light metal, and the rest are te. The digestion was followed by analysis of the diluted digests using ICP-OES and ICP-MS at the National Measurement Institute, Sydney, Australia. The instruments used were Varian 730-ES ICP-OES and Perkin Elmer DRC 2 ICP-MS. An Australian 'national certified reference standard' (river sediment sample AGAL-10) analysed in parallel with the unknown samples indicated 92-108% recovery of heavy metals (Table 3.1). The near-100% recovery suggests that the extraction method and chemical analysis used in the study are suitably accurate.

Asphalt samples were collected from three roads in the study area to determine the concentration of V. In each road, approximately 100 g composite samples from five points at distances of 1-5 m apart were collected. The samples were processed, acid digested, and analysed as described for soil and sediments.

Fractionation of the heavy metals was conducted according to the Standards, Measurements and Testing Program of the European Union (Rauret *et al*. 1999; Kartal *et al.* 2006). In this procedure, exchangeable and water and weak-acid soluble heavy metals were extracted first by acetic acid (0.1 M, pH 2.85), followed by extraction of the reducible heavy metals fraction by hydroxylamine hydrochloride (0.5 M, pH 2), and finally extraction of the oxidisable heavy metals fraction by hydrogen peroxide (8.8 M)/ammonium acetate (1 M, pH 2). The concentration of heavy metals in the residual fraction was determined by subtracting the sum of the above three fractions' concentrations from the pseudo-total heavy metals concentration. Heavy metals concentrations in the fractions were measured using ICP-OES and ICP-MS.

Table 3. 1 Comparison of measured heavy metals concentrations (mg/kg) obtained using HNO_3/HCl digestion and certified values on the Australian reference standard

Certified material reference (AGAL-10)					
Heavy metals	Measured values (mg/kg)		Certified values (mg/kg)		Recovery (%)
	Mean	S.D	Mean	S.D	
Cd	10.1	1.0	9.33	0.64	108
Cr	87.0	5.0	82.0	11	106
Cu	23.6	2.0	23.2	1.9	102
Fe	18880	1160	19950	1170	95
Mn	230	20	241	11	96
Ni	18.3	2.0	17.8	2.7	103
Pb	41.4	3.0	40.4	2.7	102
Sb	5.90	3.0	6.40	3.2	92
V	25.1	5.0	25.3	4.0	99
Zn	61.0	5.0	57.0	4.2	107

Recovery = (measured value/certified value) x 100

3.2.3. Pollution index and ecological risk

The Pollution Index (PI) (Faiz et al. 2009; Lu et al. 2009) and ecological risk using Hakanson method (Hakanson (1980)) as described in Chapter 2 were determined. These methods were adopted to assess the PI values and ecological risk of heavy metal pollution in RDS and WBS.

3.2.4. Statistical analysis

Correlation analysis was conducted between heavy metals separately for RDS, WBS and BLS to determine their inter-element relationships (Chang et al. 2009). Pearson correlation coefficients were employed to examine the degree of significance of the above relationships. A significant and positive correlation between heavy metals often indicates that they are derived from the same sources (Yongming et al. 2006; Chang et al. 2009; Faiz et al. 2009).

Principal component analysis (PCA) is a multivariate statistical tool employed to reduce a set of original variables to extract a small number of latent factors called principal components for analysing relationships among the observed variables. Variables with similar characteristics are grouped into factors and factors with eigenvalues greater than one are selected as the principal components. The analysis provides information on the percentage of variance explained by each factor and the factor loadings for each variable. The results of PCA reveal the primary portion of the data variance through these factors; consequently, the heavy metals representative of each factor can be selected as source tracer. Factors having high loading values (high variance percentage of variance) represent the possible heavy metals sources.

The correlation and PCA were done using Predictive Analysis Software (PASW) Statistics version 20, previously called SPSS Statistics.

3.3. Results and discussion

3.3.1. Heavy metals concentrations and enrichments

Concentrations of heavy metals in RDS, WBS and BLS in this study were generally in the lower half of the concentration ranges reported in other countries (Table 3.2).

The concentrations of most of the heavy metals in BLS did not vary much as evidenced by the low standard errors of means of concentrations (Cd 0.2 ± 0.03, Sb 0.7 ± 0.09, V 8.4 ± 1.8, Cr 4.4 ± 0.9, Cu 19.2 ± 3.9) which indicates that the mineral composition among the different sampling points in BLS was similar. Mean concentrations of all heavy metals were generally higher in RDS than in BLS (Figure 3.2), indicating that vehicle activity and road surface abrasion have contributed to the accumulation of heavy metals in RDS. The pollution index (PI), the ratio of heavy metals concentration in RDS to that in BLS, was more than 3 for Zn, Cu, V, Cr, and Sb in all samples (Figure 3.3 and Figure 3.4).

Furthermore the medians of the values were more than 5 indicating that these heavy metals were highly enriched in RDS according to the classification of Faiz et al. (2009) and Lu et al. (2009). Vehicle brakes and tyre wear might have been the possible predominant sources for Zn, Cu, Cr, and Sb in RDS and mainly road surface for V (Ozaki et al. 2004; McKenzie et al. 2009; Loganathan et al. 2013). Vanadium can also be contributed by brake linings (Figi et al. 2010) and tyres (Ozaki et al. 2004). Many others also reported enrichment of Zn, Cu, and Sb in RDS (Sweden, Cu, Zn, and Sb, Hjortenkrans et al. 2006; NW China, Cu and Zn, Lu et al. 2009; Pakistan, Cu and Zn, Faiz et al. 2009; Australia, Cu and Zn, Mohammed et al. 2012). The heavy metals concentrations in WBS were the same or marginally higher than in BLS for all heavy metals except Pb (median PI lower than ≤ 2 for all heavy metals, except for Pb it was 5), probably because WBS originated from both RDS and BLS with the latter being the larger contributors.

Table 3.2. Mean or range of concentration of heavy metals (mg/kg) in road deposited sediments in Sydney area and other cities in the world

Sample	City	Cd	Cr	Cu	Ni	Pb	Mn	Fe	Zn	Sb	V	Reference
RDS	Sydney, Australia	0.2	42	263	14	165	567	19645	544	6.5	65	This study
	Sydney, Australia	0.2-1.7	49-486	314-730	20-208	36-379	489-3966	22036-103000	557-2117	-	-	Mohammed *et al.* (2012)
	Sydney, Australia	-	34	160	27	880	-	-	850	-	-	Birch and Scollen (2003)
	Tokyo, Japan	0.5	0.3	30	53	11	-	-	1450	1.1	35	Ozaki *et al.* (2004)
	Birmingham, UK	1.6	-	467	41	48	-	-	534	-	-	Charlesworth *et al.* (2003)
	Coventry, UK	0.9	-	226	130	47	-	-	680	-	-	Charlesworth *et al.* (2003)
	London, UK	3.5	-	155	-	1030	-	26000	653	-	-	Schwar *et al.* (1988)
	Manchester, UK	-	-	113	-	265	-	8767	653	-	-	Robertson *et al.* (2003)
	Oslo, Norway	1.4	-	123	41	180	833	-	412	-	-	De Miguel *et al.* (1997)
	Madrid, Spain	-	61	188	44	1927	362	-	476	-	17	De Miguel *et al.* (1997)
	Aviles, Spain	22.3	42	183	28	514	1661	42200	4892	-	28.1	Ordonez *et al.* (2003)
	Lulea, Sweden	0.1	13	24	8	34	-	-	60	-	-	Karlsson and Viklander (2008)
	Amman, Jordan	1.7	-	177	88	236	-	7132	358	-	-	Jiries (2003)
	Istanbul, Turkey	1.9	-	208	32	212	398	-	521	-	-	Sezgin *et al.* (2003)
	Tokat, Turkey	5.4	41	38	128	266	415	-	98	-	-	Tuzen (2003)
	Kayseri, Turkey	10.1	-	67	57	165.5	274	-	-	-	-	Al-Khashman (2007)
	Bahrain	72	144	-	-	697	-	-	152	-	-	Akhter and Madany (1993)
	Dhaka, Bangdalesh	-	136	104	35	53	-	-	169	-	-	Ahmed *et al.* (2007)
	Tehran, Iran	10.7	33	225	35	257	1215	47935	873	-	-	Saaedi *et al.* (2012)
	Luanda, Angola	1.1	26	42	10	351	258	-	317	-	20	Baptista and De Miguel (2005)
	Ottawa, Canada	0.4	43	66	15	39	431	-	113	-	34	Ramussen *et al.* (2001)
	Hawaii, USA	-	273	167	177	106	-	-	434	-	-	Sutherland *et al.* (2000)
	Urumqui, China	1.2	54	95	43	54	926.6	-	294	-	-	Wei *et al.* (2010)
	Xian, China	-	167	95	-	231	687	-	421	-	-	Han *et al.* (2006)
	Baoji, China	-	126	123	49	433	804	-	715	89	-	Lu *et al.* (2009)

Table 3.2 (cont.)

	Beijing, China	0.6	69	72	26	202	-	-	219	-	-	Du *et al.* (2013)
	Hangzhou, China	3.6	60	212	28	194	-	-	709	-	-	Zhang and Wang (2009)
	HongKong	3.8	-	173	-	181	-	-	1450	-	-	Li *et al.* (2001)
	Taiwan	-	-	51	17	102	338	25467	227	-	-	Kuo *et al.* (2009)
	Singapore	2.4	1245	9069	186	338	-	-	1696	-	-	Joshi *et al.* (2009)
WBS	Sydney, Australia	0.2	13	48	7	45	72	11329	117	0.2	23	**This study**
	Sydney, Australia	-	20	110	20	200	-	-	260	-	-	Birch and Scollen (2003)
	Sydney, Australia	-	59	180	15	310	-	-	640	-	-	Birch and Mc Cready (2009)
	Alberoni, Italia	0.4	82	31	26	60	360	20	-	-	-	Sfriso *et al.* (1995)
	Venice, Italia	2.5	82	57	31	60	430	22	480	-	-	Sfriso *et al.* (1995)
	Manzala, Egypt	85	-	315	-	135	420	2430	22	-	-	Saeed and Shaker (2008)
	Tamar, UK	1.0	47	330	44	235	59	35124	452	-	-	Bryan and Langston (1992)
BLS	Sydney, Australia	4.4	0.2	19	3	59	108	5972	74	0.7	8	**This study**
	Sydney, Australia	-	16	51	15	330	-	-	330	-	-	Birch and Scollen (2003)
	Sydney, Australia	-	20	62	12	410	-	-	340	-	-	Snowdon and Birch (2004)
	Sydney, Australia	0.0-0.5	10-79	6-225	27-242	24-198	16-2460	6175-47210	71-238	-	-	Mohammed *et al.* (2012)
	Brisbane, Australia	0.1	0.0	8	0.0	272	1	61	353	-	-	Gunawardana *et al.* (2012)
	Earth's crust	0.2	100	50	80	14	950	41000	75	-	-	Karbassi *et al.* (2005)
	Beijing, China	0.2	76	28	-	18	-	-	-	-	-	Liu *et al.* (2005)
	Chengdu, China	0.4	60	43	-	77	-	-	-	-	-	Liu *et al.* (2006)
	Hainan, China	0.3	23	30	16	48	-	-	52	-	-	Zhao *et al.* (2007)
	Kunshan, China	0.2	88	34	31	30	-	-	105	-	-	Chen and Pu (2007)
	Taiwan	-	-	12	132	20	298	27110	68	-	-	Kuo *et al.* (2009)

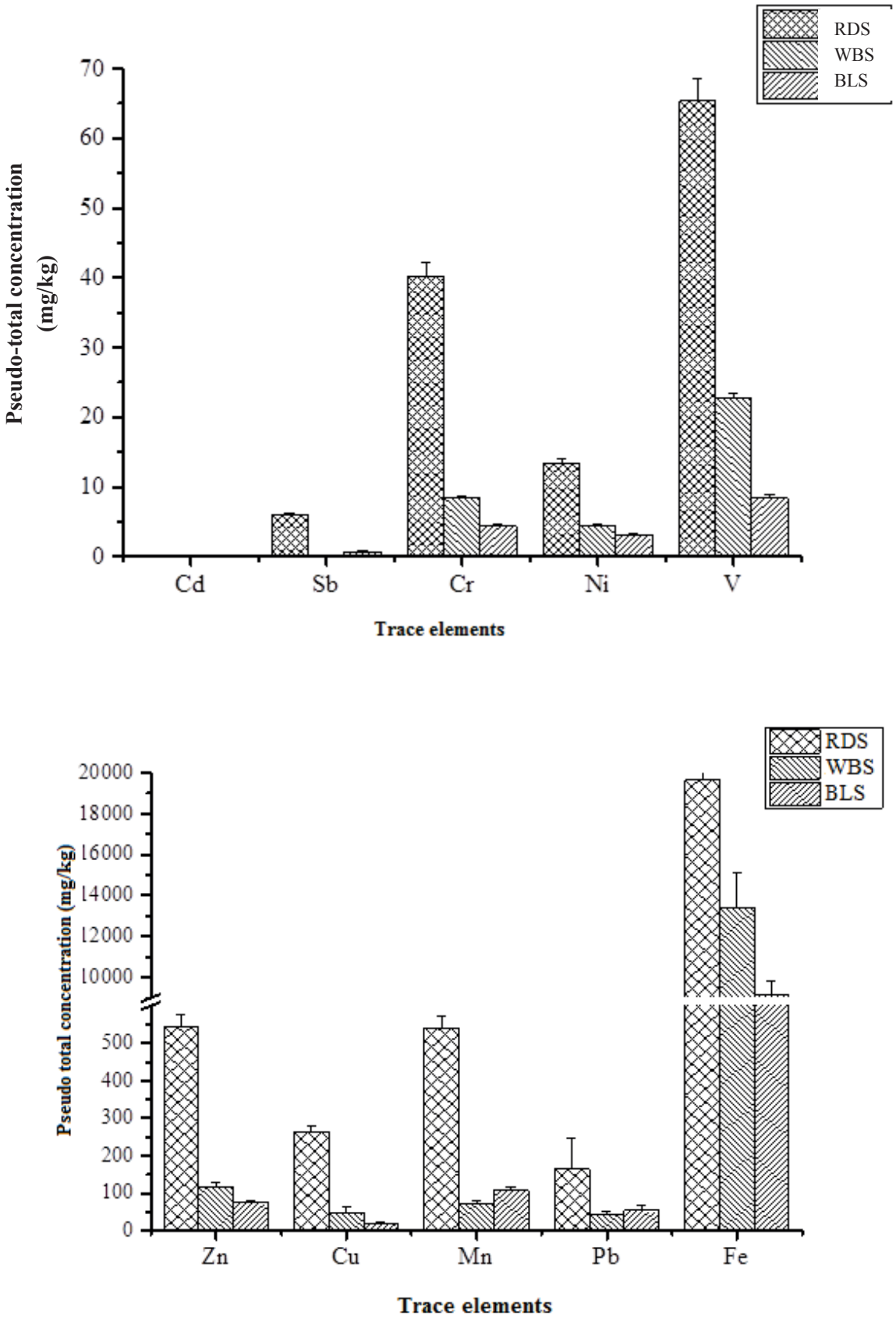

Figure 3.2. Mean heavy metals concentrations in RDS, WBS and BLS samples. Capped lines are standard errors

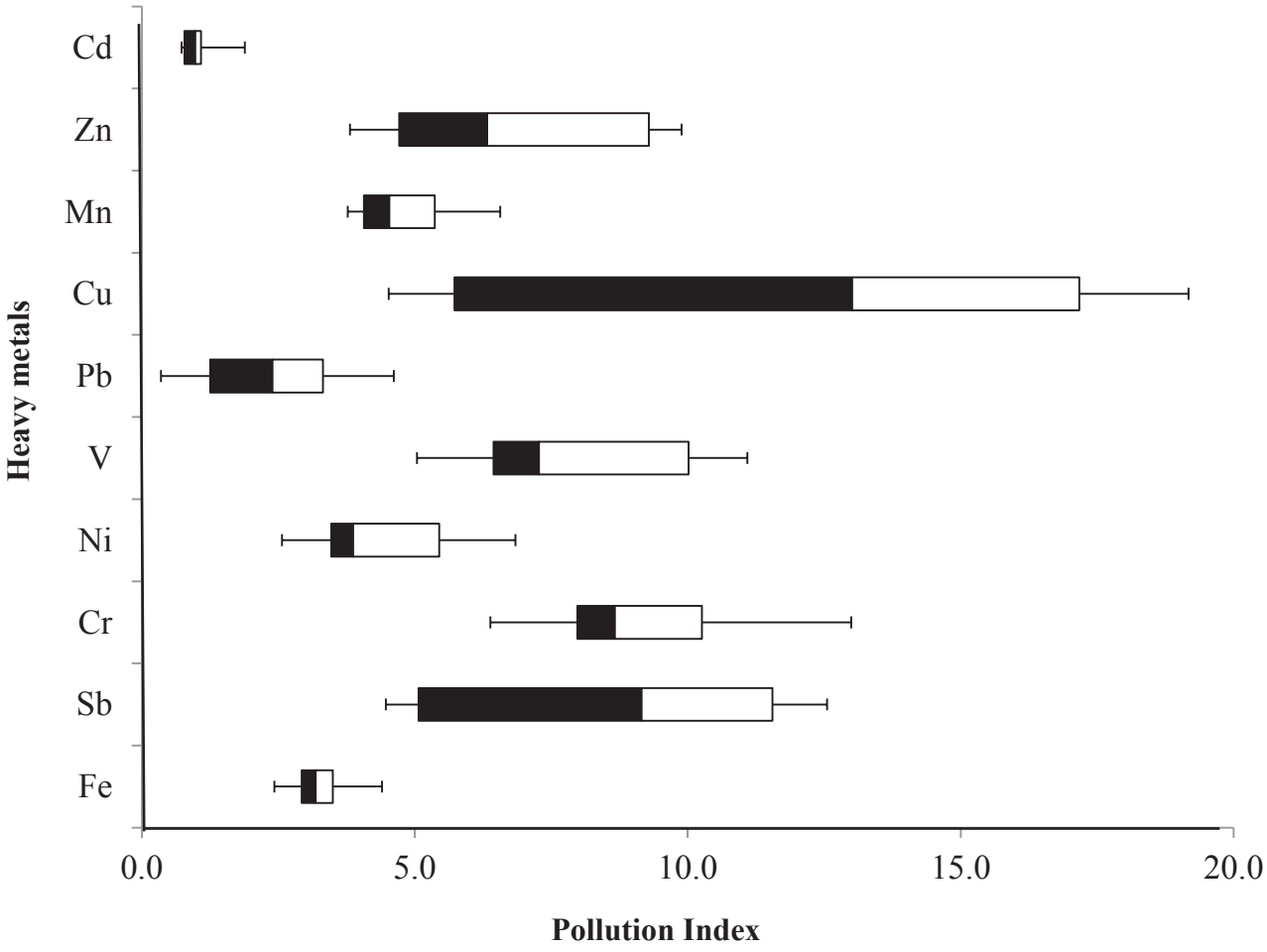

Figure 3.3. Box-plot of pollution indices for RDS samples. The line separating the dark and light shaded area inside the box represents the median; the boxes mark the 25th and 75th percentiles; the horizontal line outside the box, the whisker, denotes the maximum and minimum values

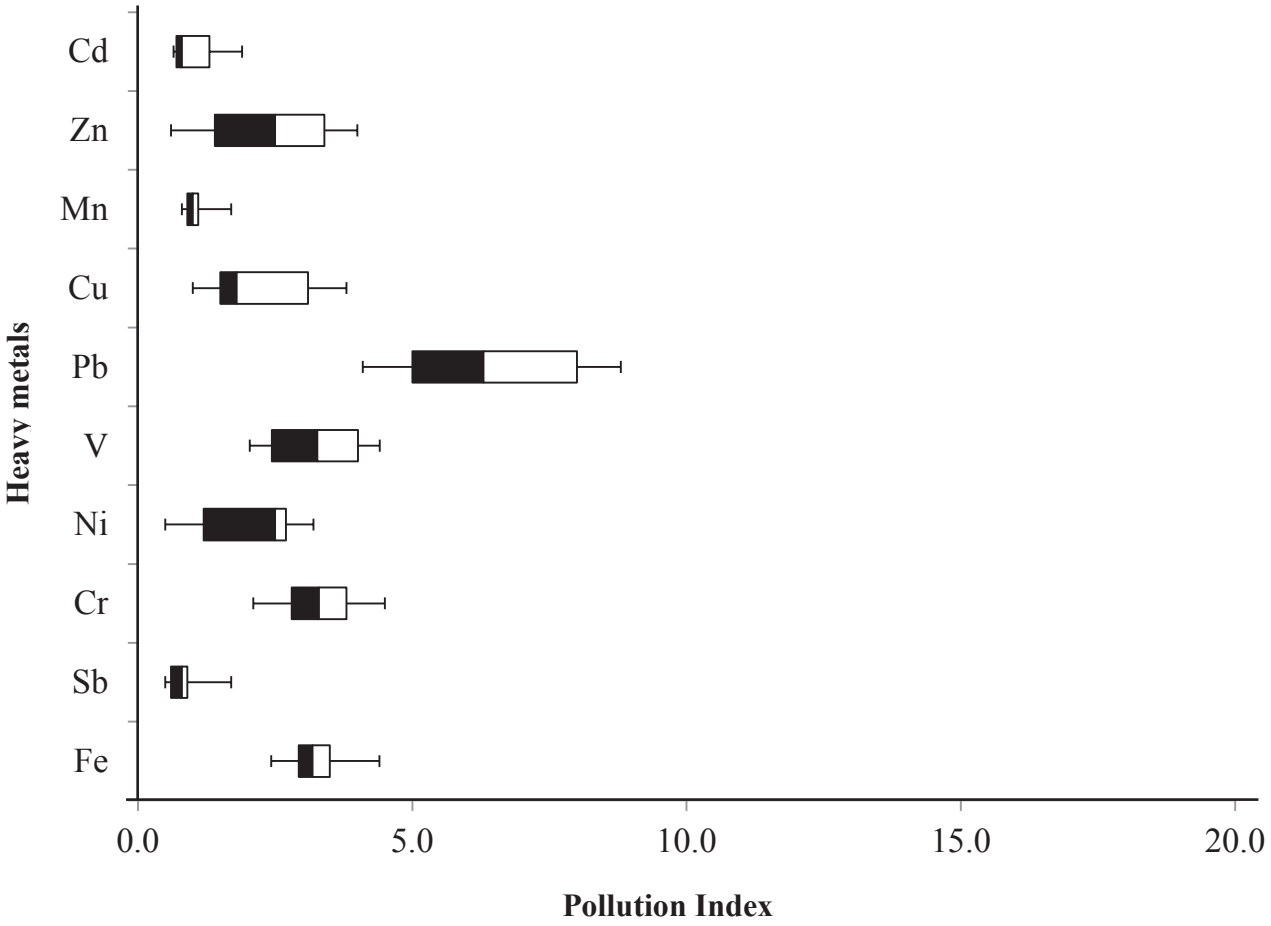

Figure 3.4. Box-plot of pollution indices for WBS samples. The line separating the dark and light shaded area inside the box represents the median; the boxes mark the 25th and 75th percentiles; the horizontal line outside the box, the whisker, denotes the maximum and minimum values

3.3.2. Metal sources

Pearson's correlation coefficient analysis showed that in BLS, the metals Sb and Cd had no significant correlation with any of the metals (Table 3.3). In RDS, however, Sb was significantly correlated to Pb, Cu, Zn, Cd, and Cd to Sb, Pb, and Zn. This suggests that Sb, Pb, Cu, Zn, and Cd in RDS might have derived from vehicle activities. These metals are components of tyre treads/or brake linings (Loganathan *et al.* 2013). Therefore these vehicle components would have contributed to these heavy metals in RDS. However, of these heavy metals, only Cu, Zn, and Sb were enriched in RDS when their concentrations were compared to BLS producing high PI values (Figure 3.3 and Figure 3.4).

Vanadium was significantly correlated with Pb, Cu, Zn, Fe, Cr, and Ni in BLS but only with Mn in RDS (Table 3.3). Therefore, V in RDS would have originated from a source other than BLS, possibly from the erosion of asphalt road surface which contains V (Lindgren 1996; Ozaki *et al*. 2004; Béze *et al.* 2012) by abrasion during vehicle transport. The mean V concentration of the asphalt samples from three roads in the study area was 121 ± 11 mg/kg. This value is nearly double the value of the V concentration in RDS (65 ± 5 mg/kg) and much higher than the value of 8 ± 2 mg/kg for BLS.

The correlation data for WBS is more similar to BLS than RDS. For example, Sb had no significant positive correlation to any other metal in both WBS and BLS, but was significantly correlated to Pb, Cu, Zn, Cd, and Fe in RDS. These results show that BLS would have contributed to the heavy metals load in WBS more than RDS did.

Table 3.3. Inter-element correlation in RDS, WBS and BLS samples at Kogarah, Sydney

(values represent correlation coefficient)

	Heavy metal	Sb	Cr	Ni	V	Pb	Cu	Mn	Zn	Cd	Fe
RDS	Sb	1.00									
	Cr	0.24	1.00								
	Ni	0.19	0.62(*)	1.00							
	V	0.20	0.67(*)	0.34	1.00						
	Pb	0.71(*)	0.01	0.22	0.18	1.00					
	Cu	0.72(*)	0.68(*)	0.73(*)	0.38	0.57	1.00				
	Mn	-0.12	0.54	0.05	0.77(*)	0.02	0.13	1.00			
	Zn	0.81(**)	-0.01	-0.06	0.34	0.72(*)	0.42	0.14	1.00		
	Cd	0.67(*)	0.02	0.10	0.23	0.79(*)	0.48	-0.09	0.70(*)	1.00	
	Fe	0.65(*)	0.72(*)	0.58	0.48	0.41	0.87(**)	0.22	0.42	0.37	1.00

(*) correlation is significant at the 0.05 level (2 tailed)
(**) correlation is significant at the 0.01 level (2 tailed)

Table 3.3. (Continued)

Heavy metal	Sb	Cr	Ni	V	Pb	Cu	Mn	Zn	Cd	Fe
WBS	1.00									
Cr	-0.75(*)	1.00								
Ni	-0.30	0.74(*)	1.00							
V	-0.82(**)	0.94(**)	0.59	1.00						
Pb	-0.54	0.67(*)	0.57	0.67(*)	1.00					
Cu	-0.09	0.36	0.09	0.76(**)	-0.14	1.00				
Mn	-0.18	0.39	0.04	0.32	-0.19	0.86(**)	1.00			
Zn	-0.56	0.82(**)	0.87(**)	0.44	0.86(**)	-0.10	-0.08	1.00		
Cd	0.02	0.27	0.33	0.19	0.72(*)	-0.09	-0.16	0.49	1.00	
Fe	-0.82(**)	0.94(**)	0.69(*)	0.97(**)	0.75(*)	0.14	0.22	0.87(**)	0.21	1.00

(*) correlation is significant at the 0.05 level (2 tailed)
(**) correlation is significant at the 0.01 level (2 tailed)

Table 3.3. (Continued)

BLS

Heavy metals	Sb	Cr	Ni	V	Pb	Cu	Mn	Zn	Cd	Fe
Sb	1.00									
Cr	-0.27	1.00								
Ni	-0.21	0.87(**)	1.00							
V	-0.15	0.90(**)	0.72(*)	1.00						
Pb	-0.09	0.85(**)	0.65	0.99(**)	1.00					
Cu	-0.15	0.77(*)	0.63	0.95(**)	0.96(***)	1.00				
Mn	0.33	0.50	0.35	0.60	0.63	0.45	1.00			
Zn	-0.12	0.94(**)	0.95(***)	0.80(**)	0.74(*)	0.66	0.59	1.00		
Cd	0.35	0.11	0.50	0.05	0.02	0.13	0.16	0.36	1.00	
Fe	0.10	0.57	0.43	0.86(**)	0.90(**)	0.89(**)	0.67	0.51	0.02	1.00

(*) correlation is significant at the 0.05 level (2 tailed)
(**) correlation is significant at the 0.01 level (2 tailed)

The principal component analysis of RDS, WBS, and BLS data grouped the metals into two statistically significant components that together explained 72.5%, 79.6%, and 79.8% of the total variance of metal concentrations in RDS, BLS, and WBS, respectively (Table 3.4, Table 3.5, and Table 3.6). In BLS, the metals, Sb and Cd had high factor loadings in component 2, whereas the other metals had high loadings in component 1 (Table 3.4 and Table 3.5, Figure 3.6, Figure 3.7, and Figure 3.8). This is in agreement with the correlation data where these two metals had no significant correlation with the rest whereas the other metals were related to each other. These results suggest that there are two sources for the metals in BLS. Sb and Cd may have mostly originated from one source whereas the other metals form another sources. The sources could be different parent rocks from which the soils were formed. In RDS the heavy metals, Sb, Pb, Cu, Zn, Cd, and Fe which were significantly correlated in the correlation analysis fitted into one component with high factor loadings in PCA (Table 3.4, Figure 3.6). These metals formed components of 1 and 2 of BLS and therefore originated from the BLS. In addition, since they are constituents of the vehicles (Table 2.2), they may have also originated from vehicles. However, the analysis is not able to distinguish the origin of the metals from these two sources.

Similarly, V which was significantly correlated with many metals in BLS, formed a common component with these metals in PCA but separated from them in RDS into another component. Therefore PCA, as concluded in the correlation analysis, suggests that of the five heavy metals enriched in RDS, Zn, Cu, Cr, and Sb originated from one source and V from another. Though V in RDS could have been derived - like Zn, Cu, Cr, and Sb from brake linings and tyres - because it is separated into a different component from the latter four elements, the dominant source of V is considered to be asphalt road surface which contains significant amounts of this element.

Table 3.4. Principal component analysis for trace element concentrations of the road-deposited sediment (RDS)

Element	RDS		
	PC1	PC2	Comm.
Sb	**0.81**	-0.45	0.85
V	0.60	0.51	0.62
Cr	0.62	**0.73**	0.91
Cu	**0.91**	0.12	0.84
Ni	**0.68**	-0.52	0.50
Mn	0.28	0.61	0.45
Pb	**0.72**	-0.53	0.79
Fe	**0.86**	0.22	0.80
Cd	**0.67**	-0.56	0.76
Zn	0.56	0.44	0.74
Initial Eigen values	4.78	2.47	4.78
Variance (%)	47.8	24.7	47.8
Cumulative variance (%)	47.8	72.5	47.8

Comm : Communalities; Bold numbers indicate statistical significance at $P < 0.05$

Table 3.5. Principal component analysis for trace element concentrations of the road-deposited sediment (WBS)

Element	WBS		
	PC1	PC2	Comm.
Sb	-0.76	-0.15	0.59
V	**0.94**	0.25	0.95
Cr	**0.96**	0.22	0.97
Cu	0.19	**0.86**	0.77
Ni	**0.77**	-0.15	0.61
Mn	0.22	**0.91**	0.88
Pb	**0.83**	-0.45	0.88
Fe	**0.97**	0.59	0.94
Cd	0.41	-0.50	0.41
Zn	**0.92**	-0.32	0.95
Initial Eigen values	5.68	2.28	
Variance (%)	56.84	22.75	
Cumulative variance (%)	56.84	79.60	

Comm : Communalities; Bold numbers indicate statistical significance at $P < 0.05$

Table 3.6. Principal component analysis for trace element concentrations of the road-deposited sediment (BLS)

Element	BLS		
	PC1	PC2	Comm.
Sb	-0.10	**0.83**	0.73
V	**0.98**	-0.12	0.70
Cr	**0.92**	-0.12	0.98
Cu	**0.91**	-0.19	0.87
Ni	**0.81**	-0.01	0.87
Mn	0.67	0.55	0.66
Pb	**0.96**	-0.09	0.75
Fe	**0.83**	0.02	0.94
Cd	0.12	**0.85**	0.69
Zn	**0.89**	0.11	0.80
Initial Eigen values	6.18	1.80	
Variance (%)	61.77	17.98	
Cumulative variance (%)	61.77	79.75	

Comm : Communalities; Bold numbers indicate statistical significance at $P < 0.05$

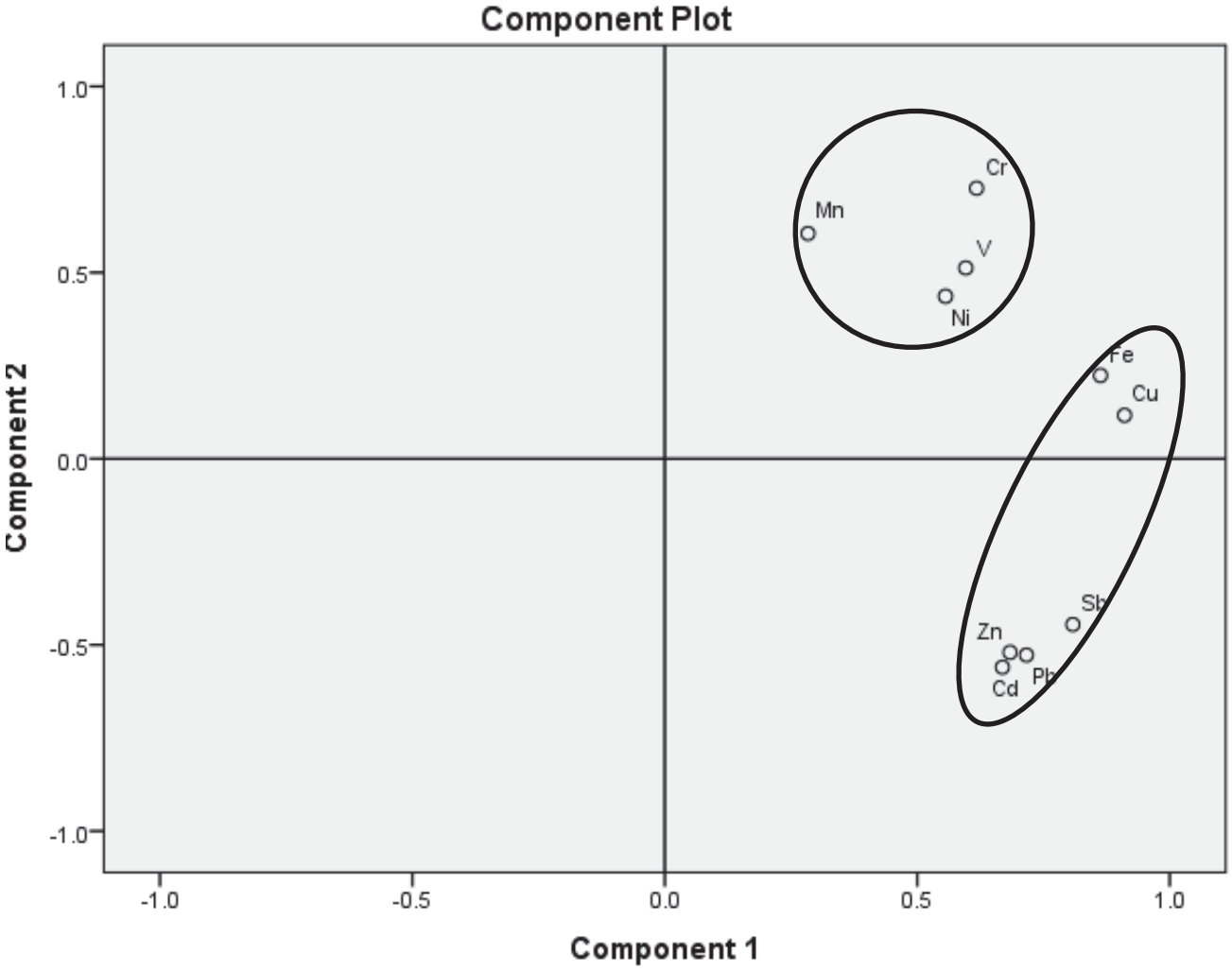

Figure 3.5. Principal component analysis of trace element concentrations in RDS

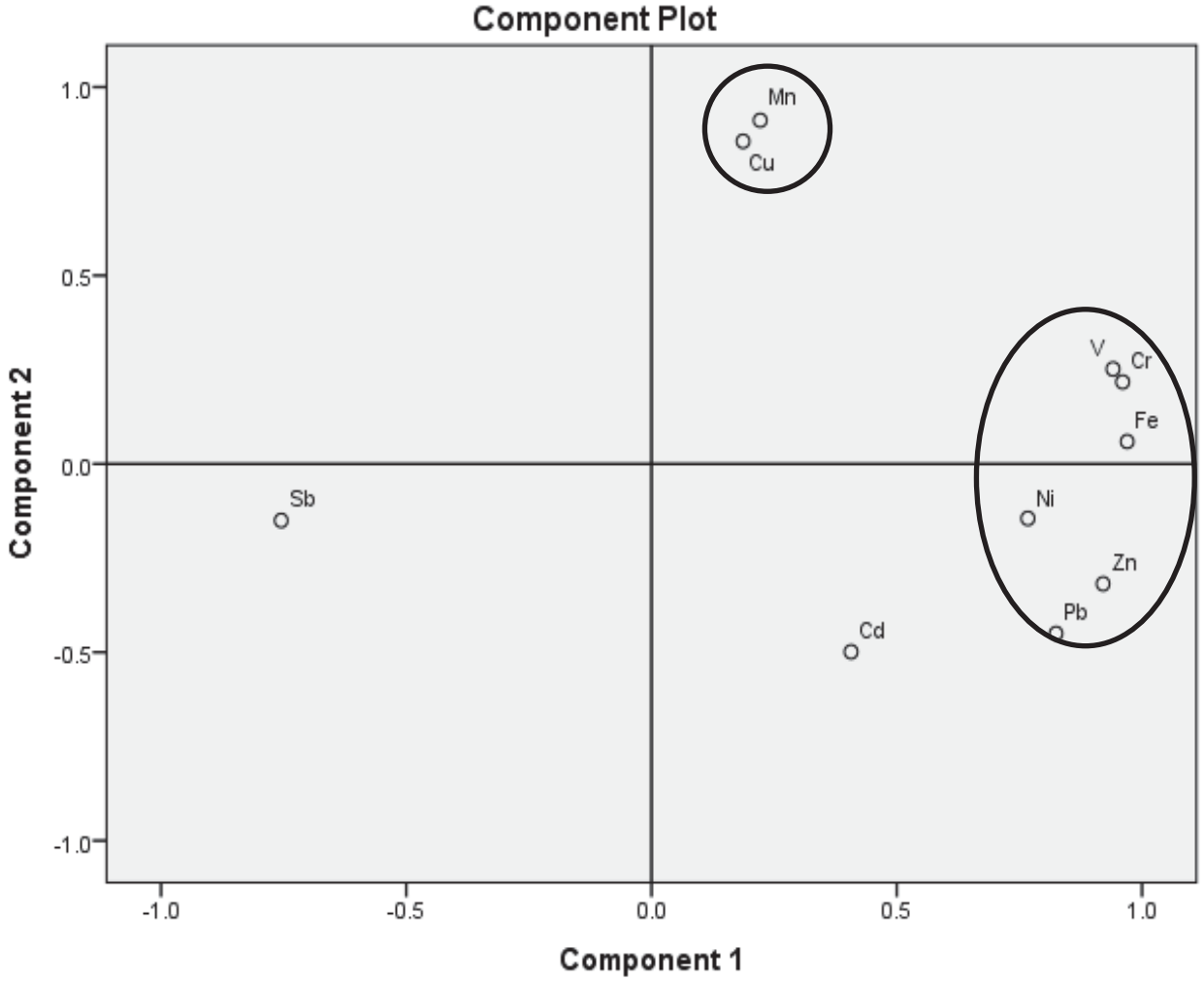

Figure 3.6. Principal component analysis of trace element concentrations in WBS

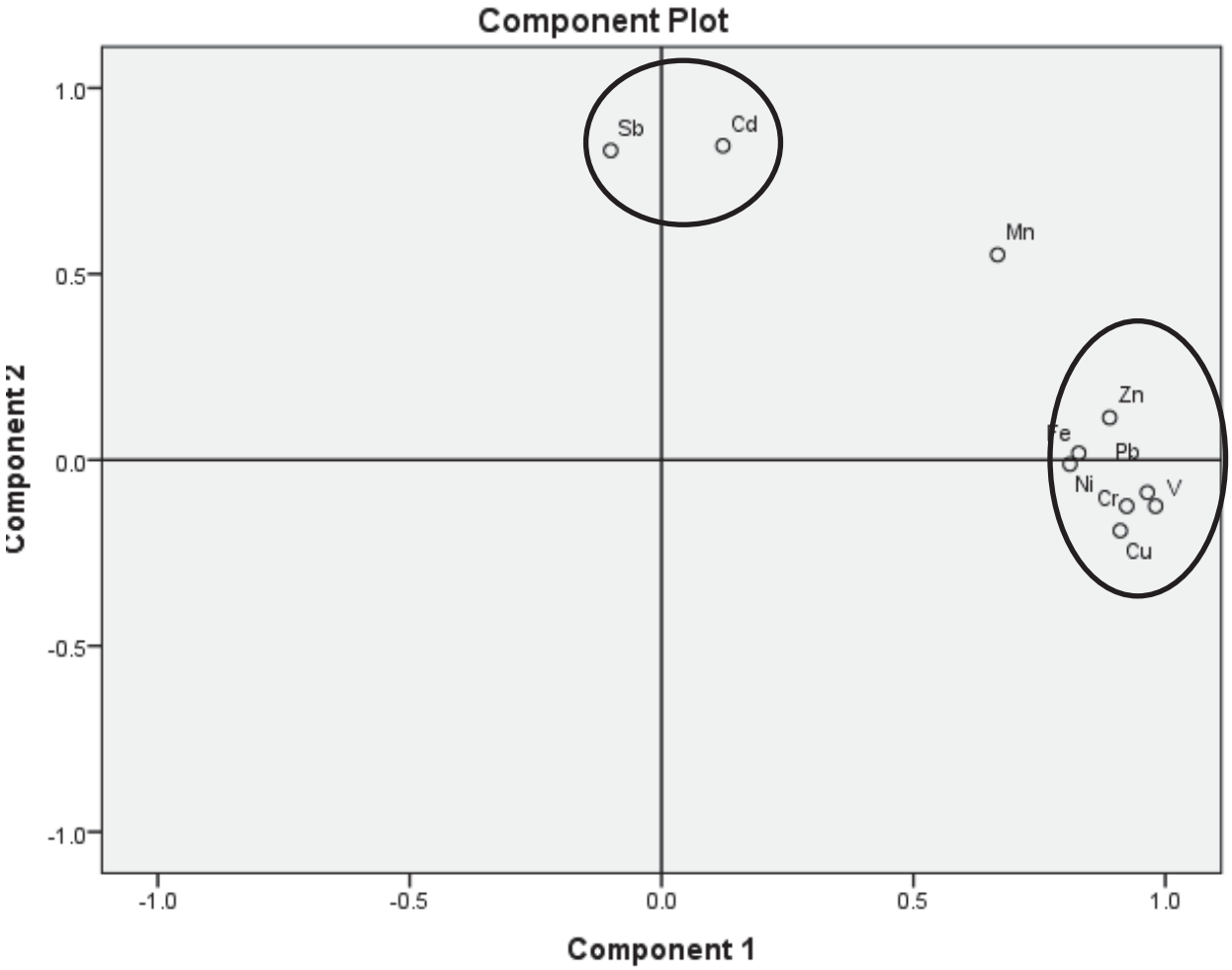

Figure 3.7. Principal component analysis of trace element concentrations in BLS

3.3.3. Metal fractionation

Fractionation data for RDS showed that the concentration of the most mobile of the four fractions, the exchangeable heavy metals fraction (Fraction 1), decreased in the order Fe > Mn, Zn > Cu, Pb > Cr, Ni, V, Cd, Sb (Figure 3.5). The mobile fraction as a percentage of total concentration was, however, lowest for Fe and highest for Cd, because of the high total concentration of Fe and low total concentration of Cd. Zinc was found to be the second largest percentage of mobile fraction. Other studies also reported Cd or Zn to be the most mobile heavy metals (Charlesworth et al. 2003; Mohammed et al. 2012). Considering the total concentration of mobile fraction, Fe, Mn, Zn, Cu, and Pb from RDS were expected to have been transported more than the other heavy metals to the neighbouring water bodies by stormwaters. Transportation of other fractions may have also occurred through the movement of suspended particles in stormwater. However, no major difference in total concentration between WBS and BLS was noticed for these or other heavy metals probably due to: firstly, the low amounts of heavy metals transported from RDS compared to the amounts already present in WBS; and secondly, the wider distribution of transported heavy metals between the sediments and large volume of water in the bay (Figure 3.9).

3.3.4. Ecological risk

The Australian and New Zealand Interim Sediment Quality Guidelines (ISQG) concentrations for heavy metals reported to be at low risk based on a battery of biological toxicity tests were 1.5, 2.0, 21, 50, 65, 80, and 200 mg/kg for Cd, Sb, Ni, Pb, Cu, Cr, and Zn, respectively (McCready et al. 2006). The corresponding concentrations for high risk were 10, 25, 52, 220, 270, 370, and 410 mg/kg. Based on these guidelines, all WBS and BLS sites were at low risk for all heavy metals. In RDS sites, however, Sb, Pb, Cu, and Zn concentrations were between the low and high risk values. It is interesting to note that of these four heavy metals, Zn, Sb, and Cu were enriched in RDS as shown by the PI index (Figure 3.3 and Figure 3.4).

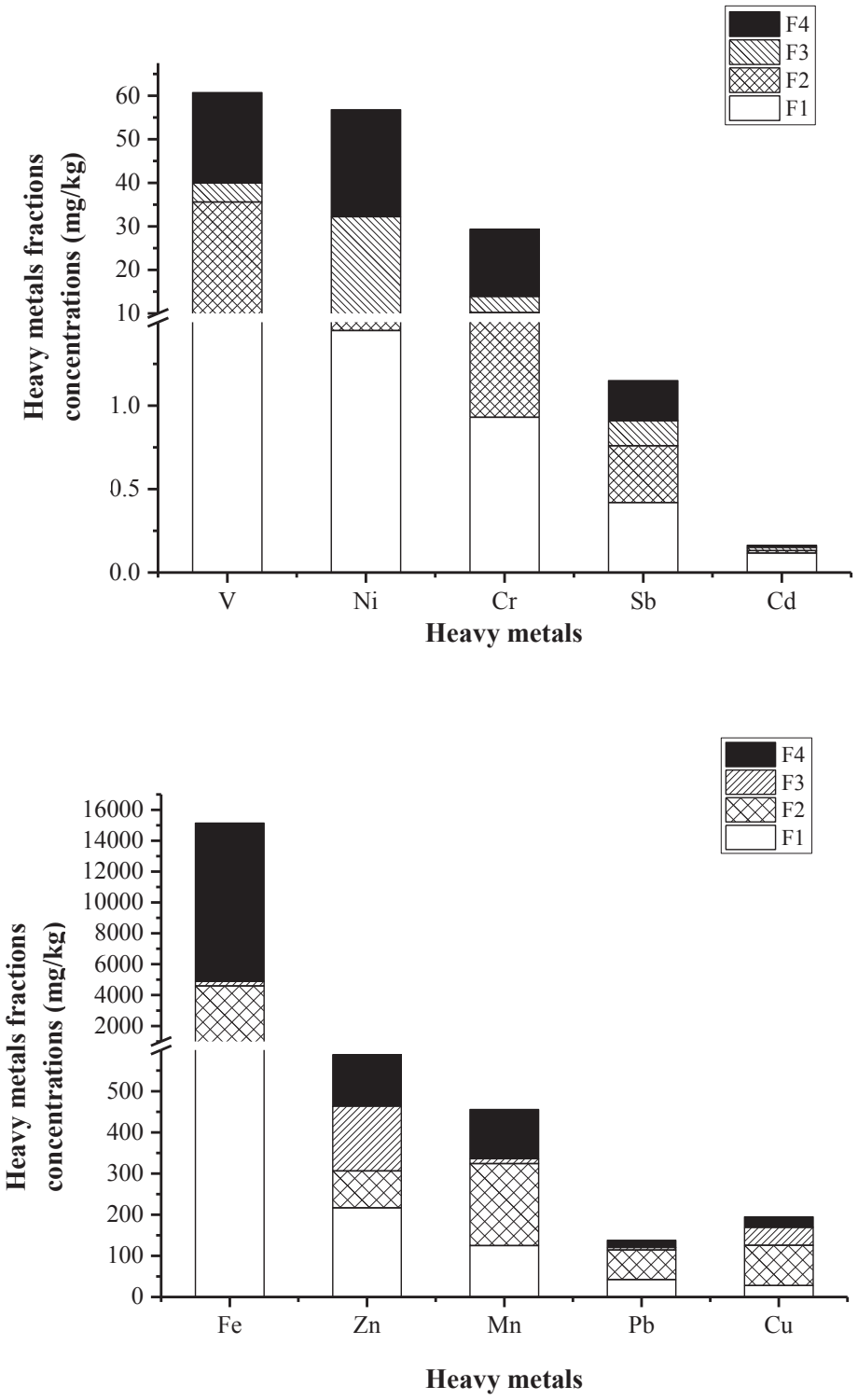

Figure 3.8. Concentrations of heavy metals fractions in RDS

(F1, exchangeable + water and acid soluble; F2, reducible; F3, oxidisable; F4, residual)

Table 3.7. The potential ecological risk indices (RI)* for RDS from different sampling sites in Kogarah, Sydney

	Sampling site	Mean value of Er					RI	Ecological risk
		Cr	Pb	Cu	Cd	Zn		
RDS	1	12.8	5.0	28.6	15.7	3.8	65.8	Low
	2	18.7	5.3	33.8	28.2	2.8	88.8	Low
	3	22.3	12.0	96.3	17.2	5.7	153.5	Moderate
	4	20.5	8.5	19.0	15.7	4.7	68.4	Low
	5	16.4	6.3	24.7	26.6	6.7	80.8	Low
	6	26.0	24.9	140.5	36.0	6.3	233.8	Moderate
	7	17.3	16.6	65.1	29.8	10.1	138.8	Low
	8	16.4	34.1	75.5	40.7	12.0	178.7	Moderate
	9	15.0	29.5	85.9	36.0	9.7	176.1	Moderate
	10	29.2	12.0	119.7	28.2	9.4	198.5	Moderate
	11	16.0	12.9	65.1	31.3	9.3	134.5	Low
	Ave.						**138.0**	**Low-moderate risk**

* Calculation of RI is described in Section 2.7.1.1., page 34 of the thesis

Table 3.8. The potential ecological risk indices (RI) for WBS from different sampling sites in Kogarah, Sydney

	Sampling site	Mean value of Er					RI	Ecological risk
		Cr	Pb	Cu	Cd	Zn		
WBS	1	1.9	1.8	2.9	15.7	0.7	22.9	Low
	2	3.6	3.3	6.2	15.7	1.2	30.0	Low
	3	4.2	1.9	41.6	15.7	0.7	64.2	Low
	4	2.2	2.3	5.7	15.7	1.5	27.4	Low
	5	5.9	4.0	7.5	36.0	1.6	55.1	Low
	6	12.8	5.2	28.6	31.3	2.3	80.2	Low
	7	4.4	4.1	6.8	18.8	1.3	35.4	Low
	8	8.2	5.3	9.1	23.5	2.0	48.1	Low
	9	9.1	5.5	12.2	18.8	2.2	47.8	Low
	10	6.4	5.3	7.5	29.8	1.8	50.8	Low
	11	5.9	7.1	8.6	72.1	2.0	95.7	Low
	Ave.						**46.6**	**Low risk**

Ecological risk assessments of heavy metals determined using Hakanson's (1980) method showed that the RDS sampling sites had low to moderate risk (Table 3.7 and Table 3.8). The range of risk index (RI) values for RDS (65-234) are similar to those (46-353) reported for different functional areas in seven districts of Shenyang in China (Sun et al. 2010). The RI values for RDS are, however, much lower than the values reported for RDS in Tehran, Iran (Saeedi et al. 2012). This is probably due to the smaller concentrations of the heavy metals in this study compared to the study in Iran. The much lower risks in WBS sites are due to the smaller concentrations of Cr, Pb, Cu, and Zn at these sites than at RDS sites (Figure 3.2). Of the heavy metals in RDS, Cu had the highest potential ecological risk (Er value) and Zn the least.

3.4. Conclusions

Road-deposited sediments contained elevated concentrations of heavy metals. The ratio of heavy metals concentration in RDS to that in BLS was more than 5 for Zn, Cu, V, Cr, and Sb. Both the correlation and principal component analyses showed that Zn, Cu, Cr and Sb in RDS originated mainly from one source, probably vehicle brakes and tyre wear and V mainly from another source, likely to be road asphalt surface abrasion. The heavy metals concentrations were similar in WBS and BLS. Heavy metals fractionation data showed that heavy metals' potential mobility, an indication of their transportation by stormwater, decreased in the order Fe > Mn, Zn > Cu, Pb > Cr, Ni, V, Cd, Sb. However, the mobile fraction as a percentage of total heavy metals concentration was highest for Cd and Zn, and lowest for Fe, Cr, Ni and V. Ecological risk as assessed by ISQG and the method developed by Hakanson (1980) was low to medium in RDS but low in BLS and WBS. Of the heavy metals in RDS, Cu had the highest potential ecological risk while Zn had the lowest.

CHAPTER 4

POLYCYCLIC AROMATIC HYDROCARBONS IN ROAD-DEPOSITED SEDIMENTS IN SYDNEY WATER SEDIMENTS, AND BASELINE SOILS IN SYDNEY, AUSTRALIA

Much of this chapter was published in Nguyen, T. C., P. Loganathan, T. V. Nguyen, S. Vigneswaran, J. Kandasamy, D. Slee, G. Stevenson, R. Naidu (2014). Polycyclic aromatic hydrocarbons in road-deposited sediments, water sediments, and soils in Sydney, Australia: Comparisons of concentration distribution, sources and potential toxicity. Ecotoxicology and Environmental Safety 104:339-348.

CHAPTER 4

POLYCYCLIC AROMATIC HYDROCARBONS IN ROAD-DEPOSITED SEDIMENTS, WATER SEDIMENTS, AND BASELINE SOILS IN SYDNEY, AUSTRALIA

4.1 Introduction

RDS is an important sink for PAHs originating from vehicle transport activity and road surface abrasion (Aryal et al., 2010; Loganathan et al., 2013; Mostafa et al., 2009; Murakami et al., 2005). This makes RDS a significant source of PAHs entering neighbouring water bodies as a result of stormwater runoffs and wind dispersion. At elevated concentrations the PAHs in water can be toxic to aquatic organisms and humans (Loganathan et al., 2013). Generally, the high molecular weight PAHs consisting of more than three aromatic rings are more carcinogenic than low molecular weight PAHs containing two or three aromatic rings (Nisbet and Lagoy, 1992). However, in aquatic environment the low molecular weight PAHs are more toxic because of their higher solubility in water.

Numerous studies have been conducted on PAH accumulation in RDS (Loganathan et al., 2013; Saeedi et al., 2012) but few have been done on PAHs pollution of water sediments (Aryal et al., 2011; Li et al., 2010; Sojinu et al., 2010; Viñas et al., 2010). However, no study appears to have compared PAHs profiles in RDS, water bed-sediments (WBS), and baseline soils (BLS) for any single catchment area. Yet this type is important in assessing the PAHs contribution of RDS and BLS to local water bodies, so that control measures can be implemented to reduce pollution of water bodies.

In order to formulate adequate measures to reduce environmental risk caused by PAHs, it is necessary to determine quantitatively the contributions that various sources of PAHs make. Sources of PAHs are commonly catergorised into pyrogenic and petrogenic groups (Wang et al., 2009; Yunker and Macdonald, 2003). Pyrogenic sources are those where PAHs are generated by high temperature combustion of fossil fuel (coal and petroleum) such as vehicle exhaust particles and biomass (burning of grass, and wood, bush fires) (Lorenzi et al., 2011;

Wang et al., 2009; Yunker et al., 2002), whereas petrogenic sources are derived from crude oil and its refined products (oil, petrol, and diesel leaks, tyre particles, deteriorating asphalt or ashphalt sealant) (Lorenzi et al., 2011; Sojinu et al., 2010; Wang et al., 2009). Ratios between low and high molecular weight PAHs as well as between specific PAH isomers have been used to identify the sources of PAHs (Saeedi et al., 2012; Viñas et al., 2010; Wang et al., 2009; Wang et al., 2011; Yunker et al., 2002). Statistical procedures including principal component analysis, cluster analysis, and multiple linear regression analysis have been employed to quantify the source contribution of PAHs (Dong and Lee, 2009; Long et al., 2013; Wang et al., 2009).

The aim of this study is to compare the concentration distribution, composition, possible sources and potential toxicity of PAHs found in RDS, WBS and BLS in the catchment area of Kogarah Bay, Sydney. The study not only expands on our limited knowledge in Australia of PAHs concentrations in RDS and water sediments (Aryal et al., 2011; McCready et al., 2000; Pathirana et al., 1994), more importantly, for the first time it compares PAHs profiles, likely sources, and potential toxicities in RDS, WBS, and BLS, within a catchment. The study compliments that of heavy metals distribution in the same study area described in Chapter 3.

4.2 Materials and methods

4.2.1. RDS, WBS, and BLS sampling

Eleven samples of RDS, 7 samples of BLS (0-10 cm depth), and 11 samples of WBS (0-10 cm depth) were collected in and around Kogarah Bay, Sydney, from July 2012 to January 2013 (as shown in the map in Chapter 3). Description of the site, samples collection and sample preparation procedures were described in Chapter 3.

4.2.2. Chemical analysis

Sixteen PAHs compounds (Nap: Napthalene; AcPy: Acenapthylene; Ace: Acenapthene; Fl: Fluorene; Phe: Phenanthrene; Ant: Anthracene; Flu: Fluoranthene; Pyr: Pyrene; BaA: Benz(a)anthracene; Chr: Chrysene; B(b)F: Benzo(b)fluoranthrene; B(k)F: Benzo(k)fluoranthrene; BaP: Benzo(a)pyrene; IND: Indeno(1,2,3-cd)pyrene; DBA: Dibenzo(a,h)anthracene; BghiP: Benzo(g,h,i)perylene) were analysed in all samples at the

National Institute of Measurement laboratory, Sydney. B(b)F and B(k)F co-eluted and therefore were quantified together as was done by Wang et al. (2011). The National Institute of Measurement Laboratory had ISO 17025 : 2005 accredited for these analyses and participates in international inter-laboratory studies to benchmark performance.

A sample of approximately 10 grams was extracted using a solvent mix of dichloromethane and acetone (1:1 by volume, pesticide grade, Merck). The samples were subjected to end-over-end tumbling (30 min, approximately 1 cycle per second) followed by soaking overnight. The extract was filtered through sodium sulphate followed by a concentration using Turbovap (Caliper Life Sciences) at 40°C. The extracts were spiked with the USEPA8270 internal standard mix (Supelco, Sigma Aldrich, USA) and analysed by gas chromatography mass spectrometry (Agilent 5975, USA) with capillary column DB5ms (30 m x 0.25 μm X 0.25 micron film, J&W, USA). The GC/MS was operated in Selected Ion Mode with helium as the carrier gas (1 mL/min, BOC gases). The oven temperature was kept constant at 40°C for 1 min, increased to 310°C at 18°C per min and then maintained for 7 min at this temperature Laboratory procedural blanks were analysed with each batch of samples, and analytes were not reported in samples unless greater than three times larger than the blank levels. Duplicate samples, laboratory control samples (LCS) and matrix spikes were analysed with each batch, with all analytes within ±20% RPD for duplicates (at the 10 x LOR level), and recoveries of 95-117% for LCS.

Organic carbon in sediments can strongly influence the accumulation of PAHs in soils and sediments through its adsorptive properties. Viñas et al. (2010) reported a significant positive relationship between PAHs concentration and total organic carbon content in sediments. Total organic carbon (TOC) was determined at National Institute of Measurement in Sydney using Elementar Vario Max C Elemental Analyser.

4.2.3. Potential toxicity evaluation

PAH toxicity evaluation was conducted using relative toxicity values of individual PAHs proposed by Nisbet and LaGoy (1992). Nisbet and LaGoy (1992) assigned toxicity equivalent factors (TEF) to the various PAHs by assuming a relative value of 1 for B(a)P which is considered to be one of the most potent carcinogens in the PAH group. The values for the other PAHs were derived by reviewing published literature on their doses related toxicities

found mainly on rats and mice. The value for Nap, AcPy, Ace, Fl, Phe, Flu and Pyr is 0.001. That for Ant, Chr, BghiP is 0.01. That for BaA, B(b+k)F and IND is 0.1. That for BaA, B(b + k)F and IND is 0.1. That for DBA is 1.0.

The toxicity equivalent quotient (TEQ) of contaminated site is then calculated by summing the products of each individual PAH concentration (Ci) and it's TEF value, as follows:

$$TEQ = \sum_{i=1}^{n} (C_i * TEF_i)$$

4.2.4. Statistical analysis

Correlation analysis was conducted between each of the PAHs separately for RDS, BLS, and WBS to determine inter-relationships between PAHs. Pearson correlation coefficients were used to examine the degree of significance of the above relationships. A significant and positive correlation between PAHs often indicates that the PAHs are derived from the same sources (Saeedi et al., 2012; Wang et al., 2011).

Cluster analysis and principal component analysis (PCA) were done to complement correlation analyses and further classify PAHs according to their sources of origin. Cluster analysis is a multivariate analysis, also known as data segmentation, which groups PAHs into subsets (called clusters) so that PAHs in the same cluster (subsets) are more closely related in terms of their concentration patterns to one another than PAHs assigned to different clusters. The analysis is based on Ward's method of hierarchical algorithm using the square Euclidean distance as a similarity measure to establish clusters (Poulton, 1989). The similarity of PAH concentration patterns in a cluster is considered to have been caused by the PAHs originating from common sources, viz. soils or traffic activity (Golobočanin et al., 2004).

PCA is a multivariate statistical tool used to reduce a set of original variables to extract a small number of latent factors called principal components for analysing relationships among the observed variables (Golobočanin et al., 2004). The principles and applications of this method were described in Chapter 3. The results of PCA show the primary portion of the data variance through these factors; consequently, the PAHs representative of each factor can be

selected as source tracers. Factors having high loading values (high variance percentage of variance) represent the possible PAH sources (Fang et al., 2004; Khalili et al., 1995; Wan et al., 2006).

The correlation, cluster analyses and PCA were performed using Predictive Analysis Software (PASW) statistics version 18, previously called SPSS statistics.

4.3. Results and discussion

4.3.1. PAH composition and concentrations

The composition and concentrations of PAHs in RDS, WBS and BLS in Kogarah Bay catchment are shown in Figure 4.1. The total PAHs concentrations (mg/kg) in BLS, RDS, and WBS ranged from 0.40 to 7.49 (mean 2.80), 1.65 to 4.00 (mean 2.91), and 0.49 to 5.19 (mean 1.76), respectively. These concentrations are lower than the Australian/New Zealand threshold concentration of 40 mg/kg above which adverse biological effects are expected to occur more frequently (Simpson et al., 2005) but generally similar to those reported in other countries with the exceptions that higher concentrations were reported for: NS in Hong Kong and India (Agra); RDS in Ghana (Kumasi), Hong Kong, and South Korea (Daejeon); and WBS in Germany (Mosel River) and The North West USA (Table 4.1). The slightly lower total PAHs concentration in WBS compared to RDS and NS is probably due to the PAHs in RDS and BLS particles being removed by the stormwater before the particles were deposited in the bay. The very large volume of water in the bay may have also caused part of the PAHs in WBS to be desorbed into the water.

The PAHs were dominated by high molecular weight compounds (4-6 rings) with fluoranthene and pyrene being the most abundant ones, which is similar to the findings in RDS and BLS of Dalian, China (Wang et al., 2009). The high abundance of the high molecular weight PAHs is explained by the general predominance of high temperature combustion processes as the primary sources (pyrogenic sources) of PAHs (McCready et al., 2000). The low molecular weight PAHs which are mainly derived from oil and fuel leaks and road asphalt abrasion and tyre deterioration may have become volatilised and degraded.

Therefore they do not persist for a long period of time in soils and sediments. Compared to RDS, BLS had higher concentrations of high molecular weight PAHs. This is probably due to the presence of a higher proportion of PAHs derived from pyrogenic sources (wood and grass burnings) in BLS.

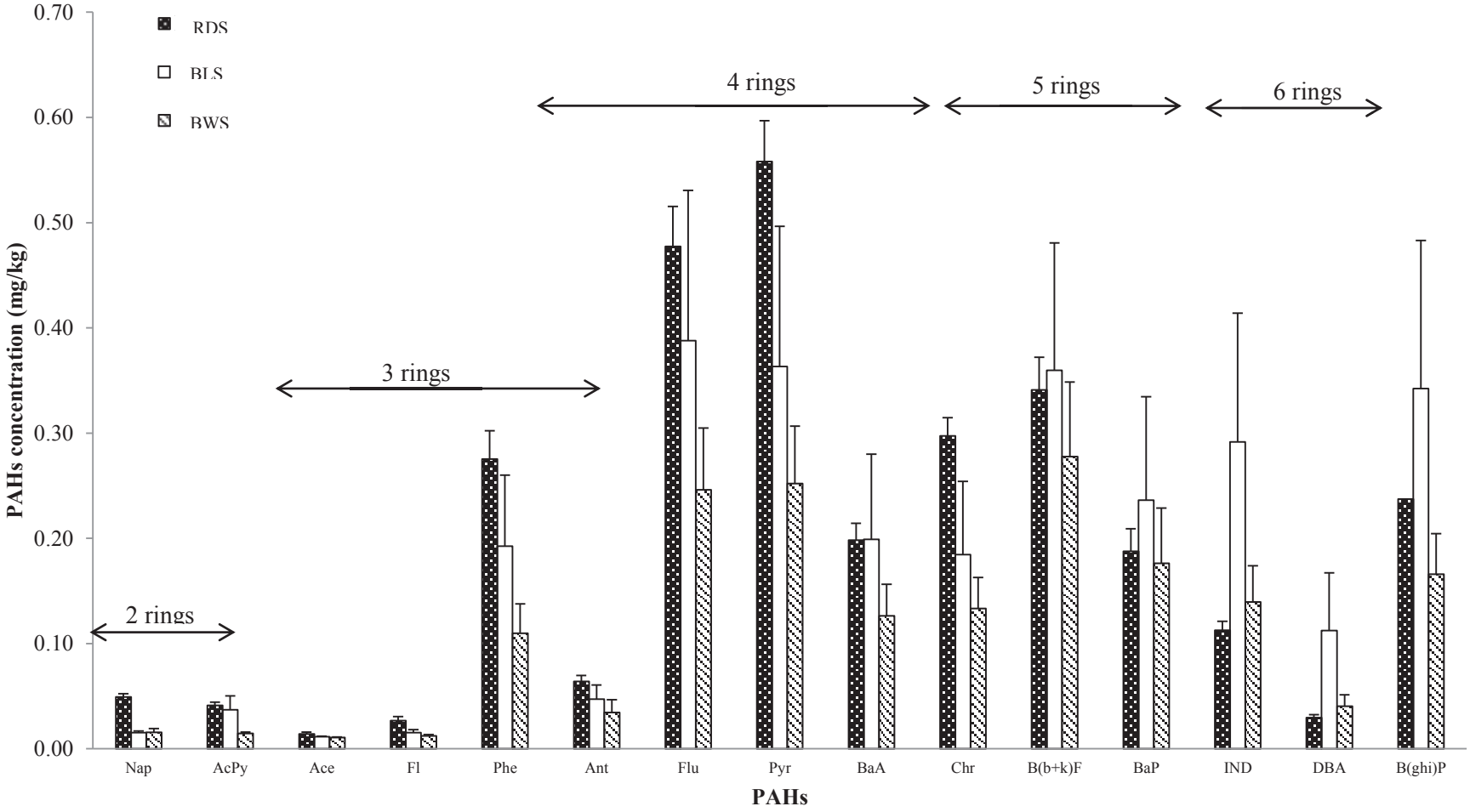

Figure 4.1. Concentrations of PAHs in RDS, WBS and BLS at Kogarah, Sydney (the number of fused benzene rings in the PAHs is shown by horizontal arrow)

Table 4.1. PAHs concentrations in soils, RDS and WBS in different regions of the world (mg/kg)

Country	Region	Source types	BLS			RDS			WBS			Reference
			No of PAHs	Mean	Range	No of PAHs	Mean	Range	No of PAHs	Mean	Range	
China	Beijing	Urban Soil		1.64	0.46-5.47							Li et al. (2006)
		Urban soil		3.92	0.22-27.83							Tang et al. (2006)
		Street dust				16	0.9					Wang et al. (2009)
		Street dust				16	1.2	0.1-13.1				Peng et al. (2011)
		Sub-urban soil		1.31								Ma et al. (2005)
		Rural		0.46								
	East of China	River soil		0.40	0.01-3.88							Ping et al. (2007)
	Guangzhou				0.42-11.2							Chen et al. (2005)
						16	1.8	0.7-15.4				Wang et al. (2011)
	Guanting Reservoir	Rural		0.39	0.06-4.11							Jiao et al. (2009)
	Huanan	Street dust				16	8.8					Long et al. (2013)
	Huizhou					16	0.3					Ma et al. (2011)
	Lanzhou	Yellow River							13		0.01-0.13	Li et al. (2006)
		Yellow River							16		0.46-2.62	Xu et al. (2007)
	Nanjing	Agriculture		0.18	0.02-0.53							Yin et al. (2008)
	Shanghai	Urban		3.29	0.35-17.9							Jiang et al. (2009)
		Street dust				16	8.4					Doong and Lin. (2004)
		Surface soil	18	1.7								Liu et al. (2010)
		Park soils				22	2.5	1.2-4.9				Ma et al. (2011)
		Road side				22	7.1	0.7-19.7				Jiang et al. (2009)
		Commercial district				22	2.4	0.6-6.3				
		Residential district				22	1.5	0.5-4.61				
		Green belts				22	3.0	0.44-10.9				
	Shantou	Agriculture		0.32	0.02-1.25							Hao et al. (2007)
	Wenzhou	Sediment							15	0.79		Li et al. (2010)
		Soils	15	1.18								
	Zhanjiang					16	0.6					Li et al. (2006)
France	Biscay Bay	Coastal area							15		0.02-5.16	Tronczynsky et al. (2004)
	Gironde Esturary								17		0.02-4.89	Budzinski et al. (1997

Table 4.1. (Continued)

	Aquitaine							14		0.0-0.84	Soclo et al. (2000)
	Arcachon Bay							16		0.03-4.12	Baumard et al. (1998)
Germany	Mosel river	Depth (0-20cm)						45	33.9	18.3-43.3	Pies et al. (2008)
		Depth (20-40cm)						45	44.3	17.9-85.7	
		Depth (40-60cm)						45	65.7	21.9-87.0	
		Depth (60-80cm)						45	83.9	52.8-115.1	
	Berlin	Street dust						16	0.8		Agarwal et al. (2009)
Ghana	Kumasi	Road dust				16	478.6				Essumang et al. (2006)
HongKong		Grassland									
		Farmland	14	31.30							Zhang et al. (2006)
		Wetland	14	33.60							
		Urban area				14	169.0				
India	Agra	Urban		12.14	3.1-28.5						Masih and Taneja (2006)
Iran	Tehran	Road dust				16	0.3				Saadie et al. (2012)
Jordan	Amman	Road dust				14	20.1				A. Jiries et al. (2003)
Japan	Tokyo					15	9.55	0.5-292.4			Zakaria et al. (2002)
		Paddy soils		0.50	0.05-2.18						Honda et al. (2007)
	Tokushima	Soils	13		0.61						Yang et al. (2002)
Macao		Street dust				16	10.6				Soclo et al. (2000)
		Pnai river	15	0.08							Zakaria et al. (2002)
		Pinang esturary	15	0.92							
		Port Klang	15	0.39							
Malaysia	Coastal area	Klang esturary	15	0.23	0.02-0.43						
		Klang Coast	15	0.02	0.0-0.04						
		Malacca						15	0.02	0.0-0.1	
Nepal	Kathmandu	Urban		1.56	0.18-10.3						Aichner et al. (2007)
Nigeria	Niger Delta	Oil installation	28		0.02-0.12			28		0.06-0.33	Sojinu et al. (2010)
Norway	Bergen	Urban	16	1.60							Haugland et al. (2008)
		Soils		0.15	0.01-1.05						Nam et al. (2008)
Serbia and Montenegro	Novi Sad	Soils	16	47.9							Skrbic et al. (2002)
		Road dust									Lee et al. (2011)
South Korea	Seoul					16	0.03				

Table 4.1. (Continued)

		Industrial complex				16	88.4					Duong et al. (2011)
	Daejon	Petrochemical complex				16	55.3					
		Mechanical area				16	112.1					
		Heavy traffic area				16	91.9					
		Downtown				16	148.8					
		Residential area				16	45.8					
		Agriculture	16	0.24	0.02-2.83							Nam et al. (2003)
	Northern of Spain	Coastal area							13		0.02-67.14	Vinas et al. (2010)
	Asturias								13		0.05-47.53	
	Cantabria								13		0.02-1.34	
Spain	Basque country								13		0.08-67.14	
	Guipuzcoan coast								26		0.43-1.45	Grimaldi et al. (1992)
	Bilbao estuary										1.49-47.48	Prieto et al. (2008)
	Urdaibai Estuary								16		0.0-0.14	Cortazar et al. (2008)
	Santander Bay								16		0.02-344.6	Viguiri et al. (2002)
	Tarragona	Urban	16	1.00								Nadal et al. (2004)
Switzeland		Soils			0.01-0.6							Bucheli et al. (2004)
Thailand		Sediment				14		0.01-8.40				Ruchaya et al. (2006)
UK		Soils		0.64	0.04-11.20							Nam et al. (2008)
USA	New Orleans	Urban	16		0.91-7.29							Mielke et al. (2004)
	Wiscosin	Street dust				16	4.5					Su et al. (1998)
	The North West	Urban lake							40	2590		Kim et al. (2008)
		Harbor							40	47.7		
		Shipping waterway							40	25.6		
		Remote lake							40	6.54		
Australia	Sydney	Traffic sites				16		8.7-105.4				Aryal et al. (2011)
	Sydney Harbor	Urban area							16		0.1-380.0	McCready et al. (2000)
	Sydney	Urban area	15	2.80	0.4-7.49	15	2.91	1.7-4.0	15	1.76	0.49-5.19	**This study**

4.3.2. PAHs sources

4.3.2.1. Correlation coefficient analysis

In RDS and WBS, the concentrations of most of the high molecular weight PAHs (4 – 6 rings) were significantly correlated to each other (RDS, correlation coefficient r = 0.06 to 0.98; WBS, r = 0.93 to 0.99), unlike the low molecular weight PAHs (2 – 3 rings) (RDS, R^2 for Nap, AcPy, Ace against all PAHs = -0.18 to 0.79; WBS, R^2 for Nap, AcPy against all PAHs = -0.31 to 0.01). Wang et al. (2011) found the same correlation pattern in RDS samples from Guangzhou, China. They suggested that the reason for the difference in the correlations obtained for low and high molecular weight PAHs was due to these two groups of PAHs having different origins. In contrast to RDS and WBS, all PAHs in BLS, besides Nap, did significantly correlate (R^2 = 0.81 to 0.99, $p < 0.05$-0.01, Nap R^2 = 0.30 to 0.65) to each other, which suggests a common PAH source. Because Nap has the smallest number of benzene rings, lowest molecular weight, and highest vapour pressure, it might have been easily volatised/or degraded by the microorganisms from the soils and sediments. This process would have prevented it from maintaining the relationships it may have had in the original source.

4.3.2.2. PAHs diagnostic ratio analysis

To determine the likely sources of PAHs in soils and sediments, the ratios of low to high molecular weight PAHs (Ant/(Ant + Phe), Flu/(Flu + Pyr), BaA/(BaA + Chr), and IND/(IND + BghiP)) are generally used as tools to discriminate between the petroleum (petrogenic source, unburned and leaked oil and fuel, asphalt) and combustion (pyrogenic, fuel and oil combustion and grass and wood combustion, bush fire) sources (Yunker et al., 2002; Ma and Zhou, 2011; Lorenzi et al., 2011).

Considering the ratio Ant/(Ant + Phe), all samples of BLS, WBS, and RDS fall into the pyrogenic source category with the ratios for BLS and WBS in the range 0.12-0.50, while those for RDS are in the range 0.15-0.22 (Figure 4.2 A). The ratio Flu/(Flu + Pyr), however, distinguished the sources of RDS from those of WBS and BLS. The RDS samples had the ratio in the petrogenic region (0.40-0.50), whereas those of WBS in both pyrogenic and petrogenic regions (0.45-0.52) and BLS only were in the pyrogenic region (0.50-0.53). These

results suggest that the source of RDS is mainly petrogenic, probably unburned leaked fuel and oil, road asphalt, and tyre particles, whereas that of BLS is mainly pyrogenic, probably a combustion of grass and wood, and bush fires. The source of WBS seems to be both petrogenic and pyrogenic with the latter serving as the predominant contributor. This is because WBS was derived from both BLS and RDS transported by stormwater, thus reflecting the combined sources of BLS and RDS.

The BaA/(BaA + Chr) and IND/(IND + BghiP) ratios fall into an intermediate region in between petrogenic and pyrogenic sources, representing mixed sources (Yunker et al., 2002; Lorenzi et al., 2011) (Figure 4.2 B). All WBS and BLS samples had BaA/(BaA + Chr) greater than 0.35, indicating the predominant PAH sources of these samples were pyrogenic. The ratio for most of the RDS samples was also greater than 0.35, but some samples were on the borderline between mixed and pyrogenic sources. The IND/(IND + BghiP) ratios for all samples fitted in the mixed source category (0.20-0.50) with the RDS close to the petrogenic source region and BLS and WBS close to the pyrogenic region.

Considering all four diagnostic ratios, it appears that the PAHs in RDS were derived from both petrogenic and pyrogenic sources, whereas the PAH in BLS and WBS were derived predominantly from pyrogenic sources.

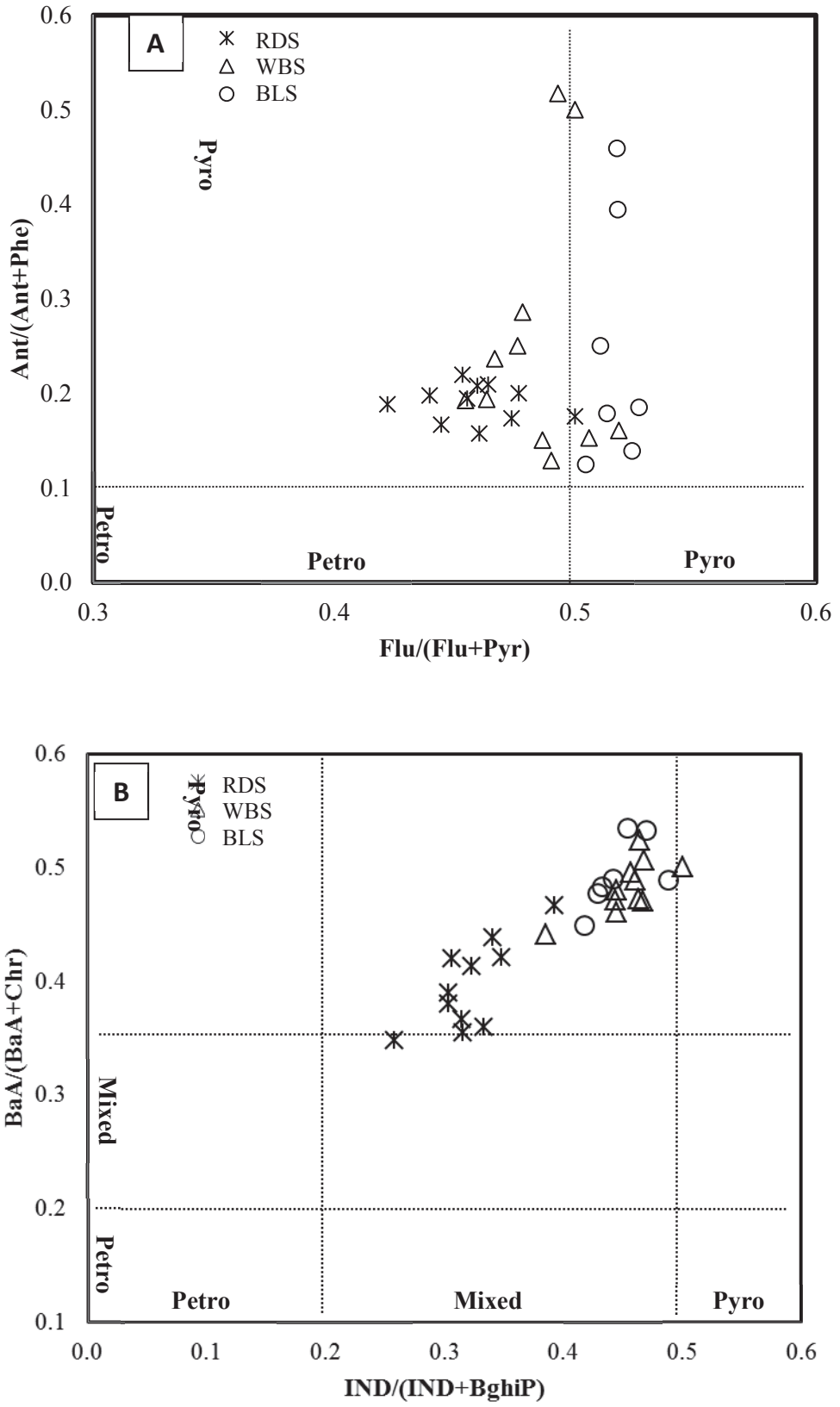

Figure 4.2. Diagnostic PAHs ratios in RDS, WBS and BLS (petro - petrogenic sources, pyro -pyrogenic sources, mixed – mixed sources)

4.3.2.3. Principal component analysis

The concentrations of PAHs in soils and sediments not only depend on the amount of PAHs derived from various sources such as vehicle activity, road surface, and combustion processes that occurred in the natural soils. They also rely on the adsorption of PAHs on soils and sediments. Organic matter is considered to be the major component of soils and sediments which adsorb PAHs (Viñas et al., 2010; Wang et al., 2009). The TOC content (%) ranges in RDS, WBS, and BLS were 0.8 – 6.8, 0.3–3.0, and 1.8–3.8, respectively. The ranges of coefficient of determinations (R^2) between individual PAHs and TOC for RDS, WBS, and BLS were 0.41–0.81 (except Nap, AcPy, Ace, $R^2 < 0.20$), 0.44–0.82 (except Nap, AcPy, $R^2 < 0.06$), and 0.45–0.85 (except Nap, $R^2 = 0.35$), respectively. The low degree of correlation between PAH concentration and TOC for Nap, AcPy and Ace is probably due to the high solubility and high volatility (Table 2.3) of these low molecular weight PAHs which reduce their adsorption to organic matter in the sediments. However, the coefficient of determination between total PAH and TOC for RDS, WBS and BLS were higher (RDS: 0.808; BWS: 0.807; BLS: 0.742) (Figure 4.3, Figure 4.4 and Figure 4.5). Before identifying the PAH sources using PCA and cluster analysis, the TOC effect on PAH concentration has to be reduced. This is done by normalising the PAH data which necessitates dividing the PAH concentration at each site by the TOC concentration where ever the R^2 value for PAH vs TOC was high ($R^2 > 0.45$).

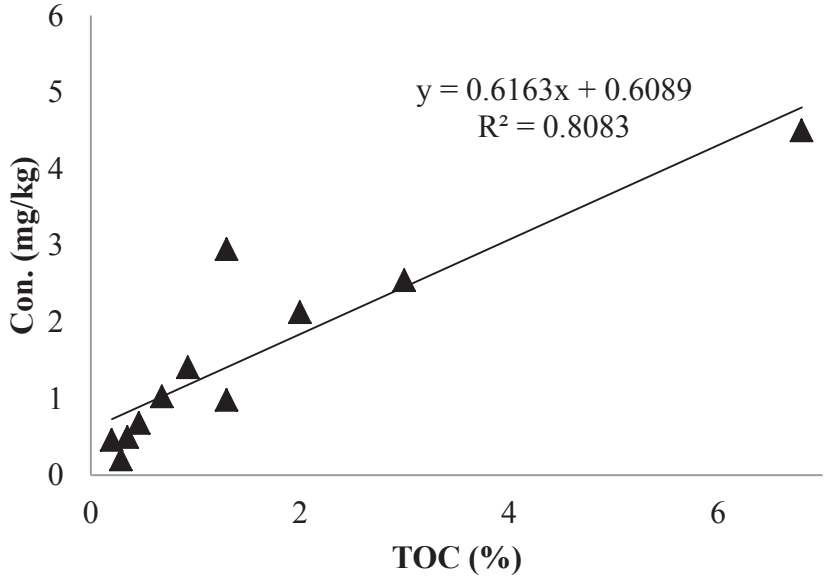

Figure 4.3. TOC versus Total PAHs concentration in RDS

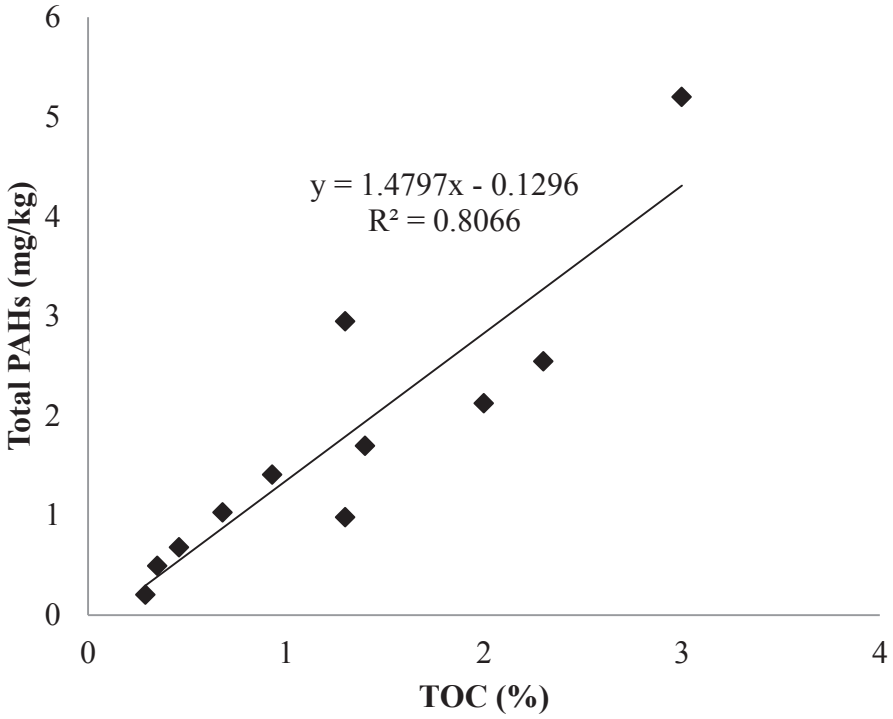

Figure 4.4. TOC versus Total PAHs concentration in WBS

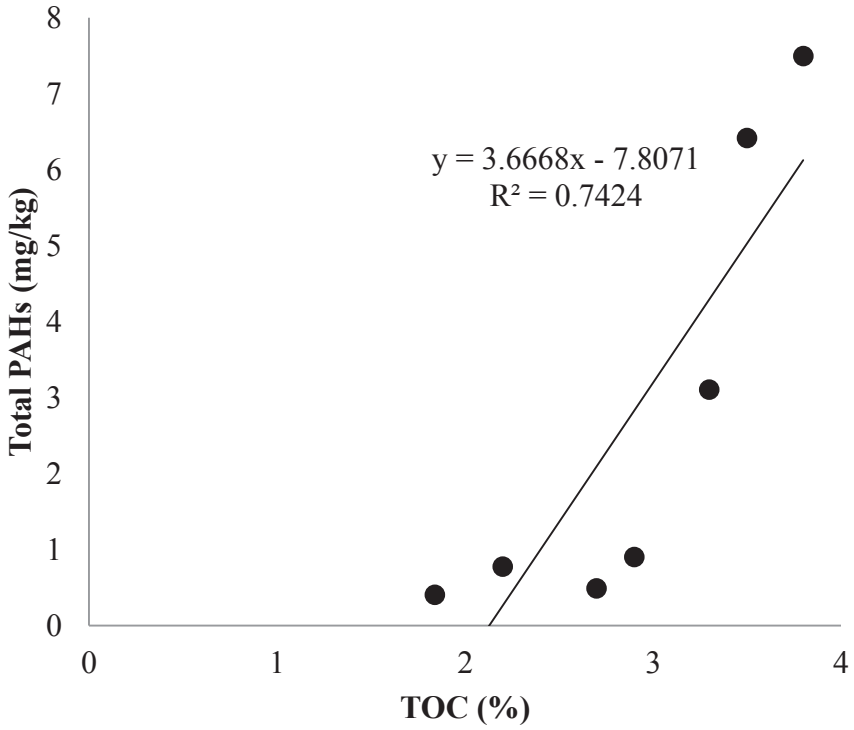

Figure 4.5.TOC versus Total PAHs concentration in BLS

The PCA-based factor loading for each PAH resulted in two distinct PCs for BLS, RDS, and WBS describing 94%, 80%, and 75% of the total variance of the data, respectively (Figure 4.6, Figure 4.7 and Figure 4.8). The PC1 is dominated by high molecular weight PAHs (4-6 rings), whereas the PC2 is generally dominated by low molecular weight PAHs (2-3 rings). The PC1 and PC2 of BLS explained 85% and 9% of the variance, respectively. Ace is the dominant of the two PAHs in PC2, which is highly volatile and petrogenic in origin and may have originated from vehicle activity on the neighbouring roads and easily transported through the atmosphere and deposited in the soils. The components of PC1 consist of PAHs from pyrogenic sources (high molecular weight PAHs). Their origin is mainly biomass combustion such as grass, wood burning and bush fires.

The cumulative variances in RDS are slightly different from those of BLS, cumulative variance for RDS was smaller percentage (70%) than that for BLS (85%). Cumulative variances has less loadings of high molecular weight PAHs (pyrogenic) in RDS compared to BLS, which has been reported by Wang et al. (2009). The sources of these high molecular weight PAHs are combustion of fuel and exhaust emissions. Four PAHs were grouped into PC2 of RDS compared to one in NS. They consist of two 2-3 ring Nap and Ace, and two 5 rings B(b-k)F and BaP. The 2-3 rings probably derived from oil and fuel spills and low temperature or incomplete combustion (Dong and Lee, 2009; Wang et al., 2009). Table 4.2, Table 4.3 and Table 4.4 show a summary of the two factors of the RDS, WBS and BLS, i.e. the loadings of the three matrices: RDS samples (Table 4.2), BWS samples (Table 4.3) and BLS samples (Table 4.4). The variance explained by the dominant principal component (PC1) (63%) in WBS is less than that in RDS (70%) and BLS (85%). The PAHs of low molecular weight had high PC1 loadings in RDS (Table 4.2), whereas the PAHs of high molecular weights had high PC1 loadings in BLS. This is because PAHs of petrogenic origin (vehicle activities and asphalt road) predominated in RDS. In contrast PAHs of pyrogenic origin (biomass combustion (grass and wood burning and bush fire)) predominated in BLS. The WBS had PAHs of high molecular weights having high loadings in PC1, similar to BLS indicating that the PAHs sources in WBS are similar to those of BLS.

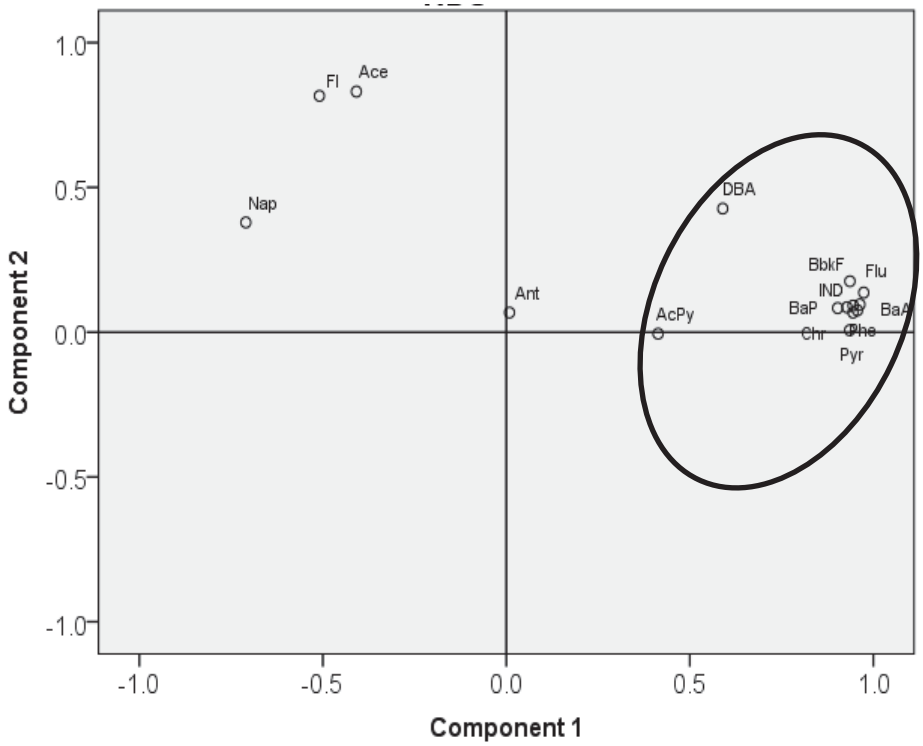

Figure 4.6. PCA analysis results of RDS

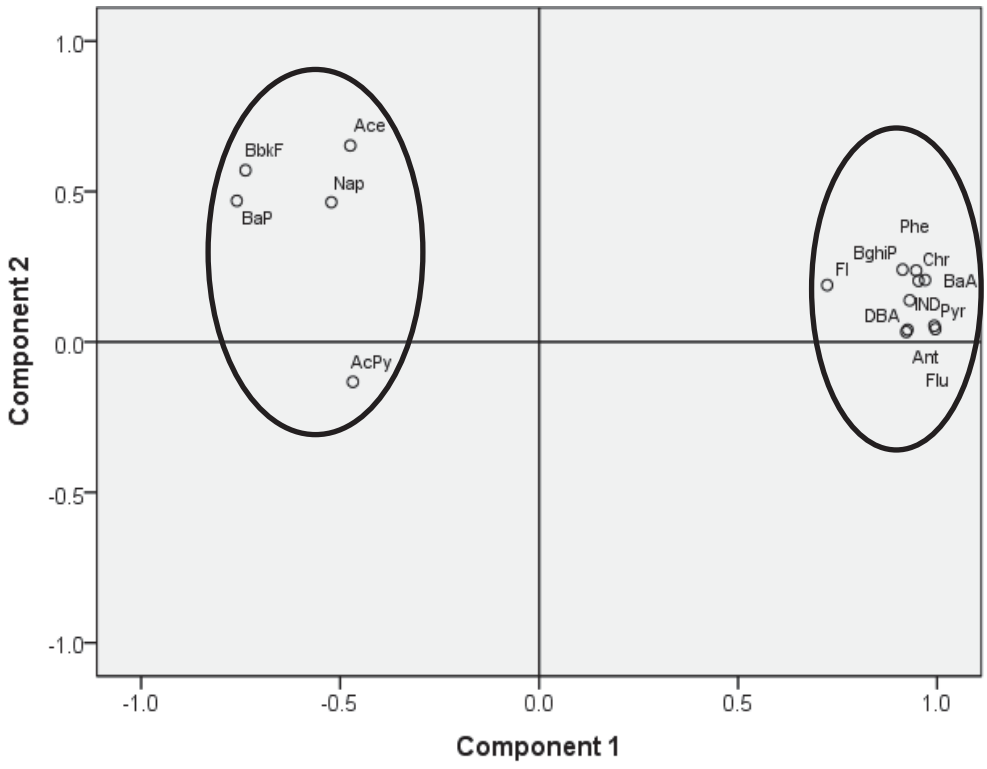

Figure 4.7. PCA analysis results of WBS

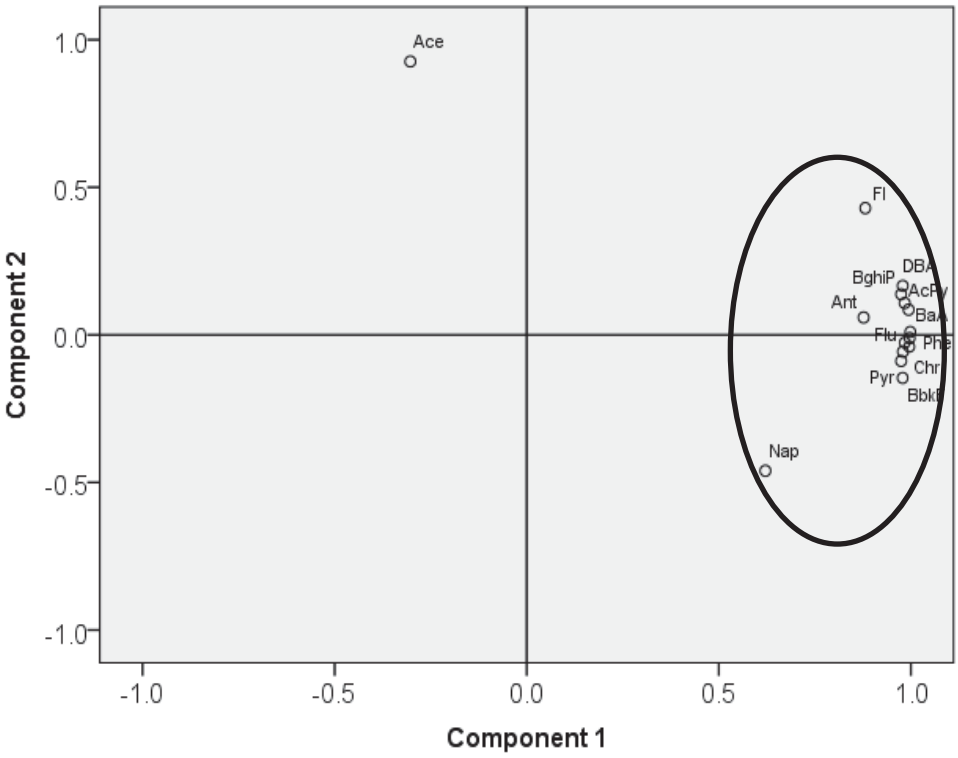

Figure 4.8. PCA analysis results of BLS

Table 4.2. Principal component analysis for PAHs concentrations of the RDS

Element	RDS		
	PC1	PC2	Comm.
Pyr	0.996	0.043	0.75
Flu	0.993	0.054	0.56
BaA	0.970	0.206	0.84
Chr	0.953	0.203	0.97
Phe	0.947	0.237	0.31
IND	0.931	0.138	0.78
Ant	0.926	0.041	0.68
DBA	0.922	0.033	0.64
BghiP	0.913	0.240	0.51
BaP	-0.760	0.469	0.35
BbkF	-0.738	0.571	0.86
Fl	0.724	0.189	0.52
Nap	-0.522	0.464	0.52
AcPy	-0.468	-0.133	0.43
Ace	-0.475	0.653	0.85
Initial Eigen values	1.43	3.75	
Variance (%)	1.465	9.765	
Cumulative variance (%)	10.496	69.975	

Comm : Communalities

Table 4.3. Principal component analysis for PAHs concentrations of the WBS

Element	WBS		
	PC1	PC2	Comm.
Pyr	-0.710	0.379	0.46
Flu	0.414	-0.005	0.87
BaA	-0.409	0.831	0.77
Chr	-0.509	0.816	0.47
Phe	0.957	0.076	0.68
IND	0.009	0.068	0.71
Ant	0.963	0.096	0.75
DBA	0.944	0.068	0.84
BghiP	0.974	0.137	0.45
BaP	0.928	0.086	0.89
BbkF	0.936	0.176	0.36
Fl	0.903	0.083	0.44
Nap	0.945	0.092	0.75
AcPy	0.590	0.427	0.15
Ace	0.935	0.007	0.67
Initial Eigen values	3.53	2.15	
Variance (%)	1.779	11.857	
Cumulative variance (%)	9.453	63.021	

Comm : Communalities

Table 4.4. Principal component analysis for PAHs concentrations of the BLS

Element	BLS		
	PC1	PC2	Comm.
Pyr	0.621	-0.461	0.53
Flu	0.994	0.085	0.91
BaA	-0.303	0.926	0.92
Chr	0.881	0.429	0.46
Phe	0.984	-0.026	0.63
IND	0.877	0.059	0.82
Ant	0.979	-0.057	0.44
DBA	0.975	-0.089	0.92
BghiP	0.998	0.010	0.48
BaP	0.996	-0.040	0.67
BbkF	0.978	-0.146	0.57
Fl	0.996	-0.011	0.59
Nap	0.984	0.108	0.20
AcPy	0.979	0.166	0.39
Ace	0.974	0.138	0.56
Initial Eigen values	2.01	4.12	
Variance (%)	1.358	9.053	
Cumulative variance (%)	12.701	84.672	

Comm : Communalities

4.3.2.4. Cluster analysis

The cluster analysis, like the PCA, grouped the PAHs into two major classes in NS, RDS and WBS (Figure 4.9, Figure 4.10 and Figure 4.11). The linkage distance between these two clusters is high implying there is a significant difference between them. The PAHs in the two clusters are mostly the same as in the two PCAs. Therefore the interpretations proposed for the possible sources of PAHs in PCA also apply to the cluster analysis results.

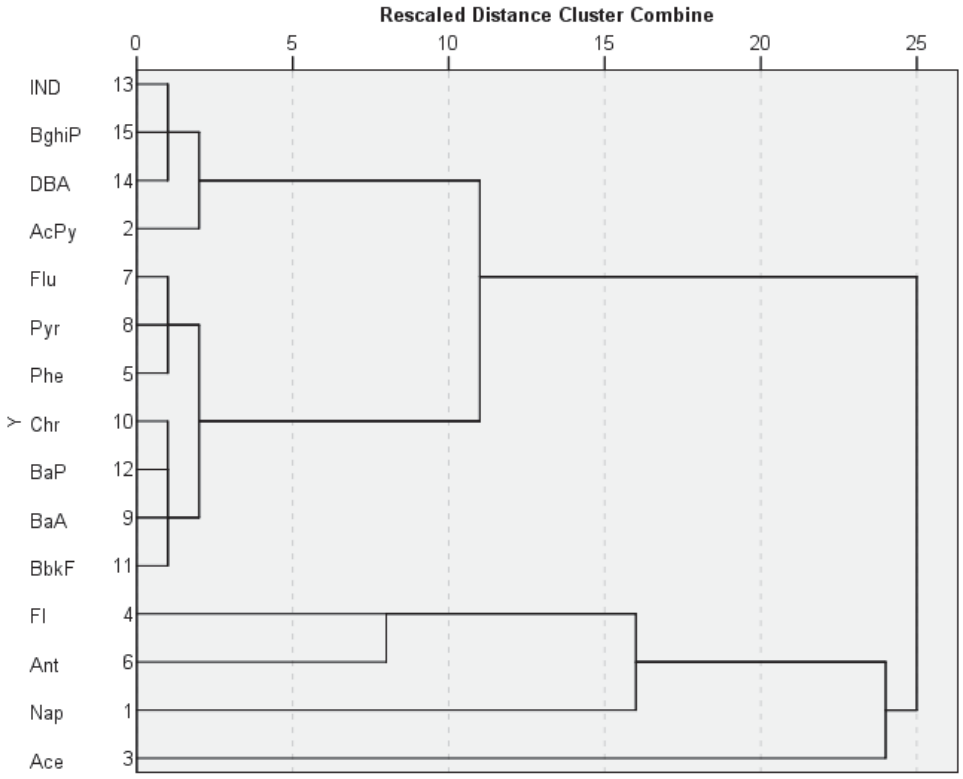

Figure 4.9. Cluster analysis results of RDS

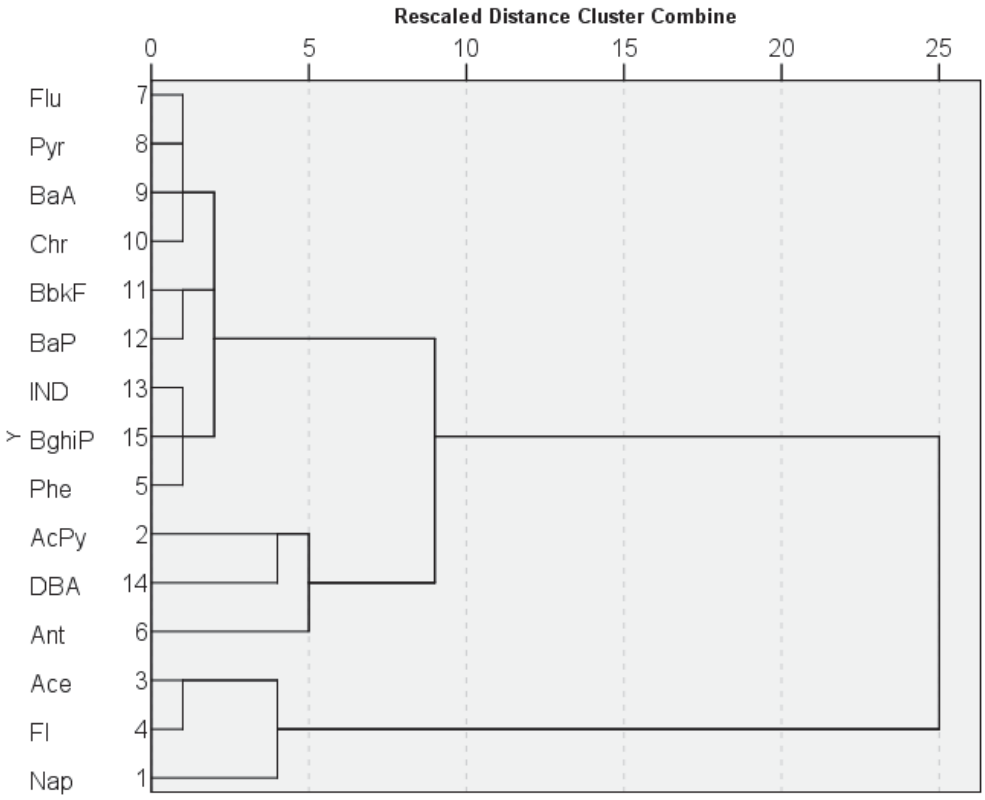

Figure 4.10. Cluster analysis results of WBS

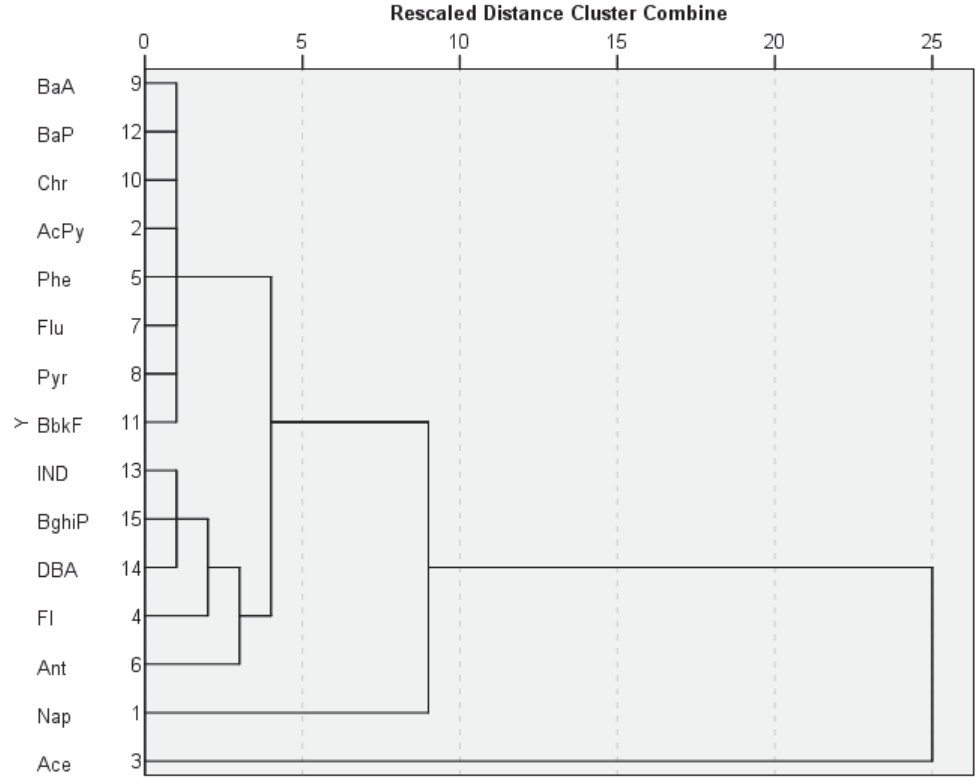

Figure 4.11. Cluster analysis results of BLS

4.4. Potential PAH toxicity

Potential toxicity of PAHs depends on the natural toxicity rating of the PAH and its concentration (Equation 1). Table 4.5 shows that the total TEQs of all PAHs in RDS, WBS and BLS were respectively, 0.29, 0.28, and 0.44 mg/kg. These values are much lower than the values reported in Sydney (1.6-25.3 mg/kg, Aryal et al., 2011) and in Ulsan, South Korea (2-70 mg/kg, Dong and Lee, 2009). The low potential toxicity of PAHs in the RDS, WBS and BLS at Kogarah is due to the very low PAHs concentrations at these sites. Higher TEQ values obtained for BLS compared to those for RDS and WBS are due to the presence of greater concentrations of high molecular weight PAHs in BLS which are more toxic (higher TEF, Table 4.5) than the low molecular weight PAHs.

Table 4.5. Toxic equivalent quotients (TEQ) of RDS, WBS and BLS

Compound	TEF	TEQ (mg/kg)		
		RDS	WBS	BLS
Nap	0.001	0.00005	0.00002	0.00002
AcPy	0.001	0.00004	0.00002	0.00004
Ace	0.001	0.00001	0.00001	0.00001
Fl	0.001	0.00003	0.00001	0.00002
Phe	0.001	0.00028	0.00011	0.00019
Ant	0.01	0.0006	0.00035	0.0005
Flu	0.001	0.00048	0.00025	0.00039
Pyr	0.001	0.00056	0.00025	0.00036
BaA	0.1	0.02	0.01260	0.02
Chr	0.01	0.003	0.00133	0.0018
B(b+k)F	0.1	0.034	0.02780	0.036
BaP	1	0.19	0.17600	0.24
IND	0.1	0.011	0.01400	0.029
DBA	1	0.03	0.04100	0.11
BghiP	0.01	0.0024	0.00166	0.0034
Total TEQ		**0.29**	**0.28**	**0.44**

4.5. Conclusions

This study showed that in a catchment area consisting of roads, natural soils, and a bay the total concentration of 16 PAHs did not differ much between RDS, WBS, and BLS. However, the PAH composition and source from where they originated differed between these three sites. The total concentrations were similar to those in 70 world wide sites but smaller than those in 6 sites. PAHs in RDS, WBS, and BLS were dominated by relatively high molecular weight compounds with more than three fused benzene rings, indicating that high temperature combustion processes were their predominant sources. The proportion of high molecular weight PAHs with 5 or 6 rings were higher in BLS than in RDS, whereas the low molecular weight PAHs proportions were higher in RDS.

Principal component and cluster analyses showed that the PAHs can be divided into two groups which together can explain 94%, 80%, and 75% of the total variance of the data in BLS, RDS, and WBS, respectively. The sources for one group are predominantly pyrogenic (vehicle exhaust and combustion of grass and wood and bush fires) while those for the other group are petrogenic (unburned or leaked fuel and oil, road asphalt, and tyre particles). Diagnostic PAHs ratios investigations revealed that the predominant sources of BLS and WBS were pyrogenic and those of RDS were a mixture of pyrogenic and petrogenic.

Finally, the potential toxicities of PAHs calculated using toxicity equivalent quotient (sum of the products of each PAH concentration and natural toxicity rating of the PAH) were all low. This is probably due to the low concentrations of the highly toxic high molecular weight PAHs.

CHAPTER 5

BIOAVAILABILITY AND TOXICITY OF POLLUTANTS IN EXTRACTS FROM ROAD DEPOSITED SEDIMENTS

CHAPTER 5

BIOAVAILABILITY AND TOXICITY OF POLLUTANTS IN EXTRACTS FROM ROAD DEPOSITED SEDIMENTS

5.1. Introduction

Road-deposited sediments (RDS) are known to contain several inorganic and organic pollutants such as heavy metals, metalloids and polycyclic aromatic hydrocarbons (PAH), herbicides, nutrients and polychlorinated biphenyl (PCBs) (Cheung et al., 1997; Loganathan et al., 2013; Taylor, 2007). Heavy metals and polycyclic aromatic hydrocarbon compounds (PAHs) are known to be toxic to animals and humans and have potential for carcinogenic, mutagenic or allergenic effects (Adams and Rowland, 2003; Eriksson et al., 2007; Marsalek et al., 1999). Urban stormwater runoff has been considered a major source of water pollution by many authors (Beasley and Kneale, 2002; Boyd et al., 2004; Kayhanian et al., 2008). Stormwater quality data has been collected across the world, and worldwide data sets have been analysed for trends in traditional pollutants such as suspended solids, nutrients, heavy metals and organic compounds (Aryal et al., 2010). Discharges of urban runoff to aquatic environments have been documented to show that it causes accumulation of heavy metals and different organic chemicals in the water phase (Beasley and Kneale, 2002; Lau et al., 2009; Mahler et al., 2014; Pengchai et al., 2004). The chemical composition of road runoff can vary enormously between sites (composition, speciation, etc), making it difficult to assess its toxic potential and treatment (Aryal and Lee, 2009). Regulatory authorities have favoured the use of biological indicators as an essential means of assessing potential toxicity of environmental pollutants (Nunes et al., 2006).

High levels of heavy metals such as Cu, Pb and Zn in urban street dusts have been reported in many countries (Burton et al., 2000; Stone and Marsalek, 1996). Heavy metals such as Cu, Zn, Fe and Mn are normal constituents of marine and estuarine environments and are essential elements for organisms. However, when high concentrations of heavy metals enter receiving water, they become potentially toxic and may interfere with the ecology of a particular environment (Bryan and Langston, 1992). The mobility and transport of heavy metals and their bioavailability in the environment is a function of the chemical form of the metals. However, many studies evaluating the adverse effects of metals on the environment

measure only the total metal concentrations (Wei and Yang, 2010). The exposure of aquatic organisms to toxic levels of metal pollutants can cause damage to tissue, inability to regenerate damaged tissue, growth inhibition, damage to DNA (Everaarts, 1995; Neumann and Galvez, 2002). Metal ions can penetrate inside the cell, interrupting cellular metabolism and in some cases can enter the nucleus. Metals cations can bind to DNA and cause DNA damage. Metal carcinogenicity is proved to be mediated by the generation of reactive free radicals (especially hydroxyl radicals and reactive oxygen species) (Valavanidis and Vlachogianni, 2010).

PAHs (polycyclic aromatic hydrocarbons) arise mainly from the incomplete combustion of fossil fuels, organic materials, and wood and are also found in petroleum (Loganathan et al., 2013). They have been shown to cause carcinogenic and mutagenic effects and are potent immune-suppressants (Bihari et al., 2006). For instance, the resistance of PAH compounds to oxidation, reduction, and vaporisation increases with increasing molecular weight, whereas the aqueous solubility of these compounds decreases. PAHs can be divided into two groups based on their physical, chemical, and biological characteristics. The lower molecular weight (LMW) PAHs (e.g., 2 to 3 ring group of PAHs such as naphthalenes, fluorenes, phenanthrenes, and anthracenes) have significant acute toxicity to aquatic organisms, whereas the high molecular weight (HMW) PAHs, 4 to 7 rings (from chrysenes to coronenes) do not. However, several HMW PAHs are known to be carcinogenic. Effects of PAHs have been documented on immune system development, immunity and on host resistance (Miller and Ramos, 2001; White, 2002). PAHs may be considered complete carcinogens in the sense that a role in both initiation (DNA damage fixed as a mutation) and promotion of carcinogenesis (increased cell growth and proliferation) is possible for these compounds (Boström et al., 2002). In particular, benzo[a]pyrene (BaP) can be converted to its metabolite benzo[a]pyrene-diolepoxide through a series of biotransformations (pathways of BaP detoxification or activation). This metabolite is highly carcinogenic (Pastorelli et al., 1998). Many PAH compounds induce cytochrome P4501A1 (CYP1A1) by binding to the AhR (aryl hydrocarbon receptor) in the cytosol. It is generally reported that LMW PAHs (e.g. naphthalenes, fluorene) are more toxic than HMW compounds, partly because the lower molecular weight compounds are more water soluble and are more bioavailable than the HMW PAH compounds (Roberts et al., 1989). A range of studies have demonstrated relationships between PAH exposures and effects on different types of organisms in road runoff and sediment extracted elutriate (Bihari et al., 2006; Li et al., 2013; Tang et al., 2013).

Toxicity tests give more information than just chemical analysis, are more realistic and can take into account the interactions and effects of the natural environment. They also can measure the toxicity of unmeasured components in the sediments. The toxic potential of various stormwater runoffs has been examined previously, usually using a battery of toxicity tests to assess different aspects such as acute lethality, sub-lethality or immobilisation using classical bio-indicators such as *Vibrio fischeri, Daphnia magna, Artemia salina* and medaka fish (*Oryzias latipes*). This study aims to assess the toxicity of sediments by measuring acute toxicity to *Artemia salina*, and sublethal toxicity to Microtox®, AhR CAFLUX and p53 GeneBLAzer®. Because the receiving waters at some of the study sites in this thesis were estuarine, two assays that were applicable to saline conditions (*Artemia* and Microtox) were included. A summary of the characteristics of these assays is presented in Table 5.1.

Table 5.1. Summary of test assays used in this study

Assay	Organism	Mode of action	Target chemical	Measured end point	Reference compound
Brine shrimp acute toxicity test	*Artemia salina*	Acute toxicity test (24 h)	Heavy metals PAHs	Lethality	Cd, Benzo[a] pyrene
Microtox®	*Vibrio fischeri*	Sub-lethal toxicity test for 5, 15 and 30 mins	Heavy metals PAHs	Decrease in light emission	Phenol, $ZnCl_2$
AhR CAFLUX*	Hepa1c1 7 hepatoma cell	AhR activation indicative of xenobiotic metabolism	Dioxin-like chemicals including PAHs	AhR dependent green fluorescent protein expression, fluorescence	TCDD
p53 Gene-BLAzer®**	p53RE-*bla* HCT-116	Agonists/ antagonists of the p53 signaling pathway	DNA damage/ genotoxic agents	p53 dependent β-lactamase expression, cleaving the fluorescent substrate and changing the wavelength of light emission	Mitomycin

* Jin et al. (2015); Tang et al. (2014. **Escher et al. (2013)

Artemia salina has been widely used as a test organism for assessment of saline environments because it is tolerant to high concentrations of chloride ions (Svensson et al., 2005). The *Artemia* nauplii acute toxicity test is expected to be sensitive to heavy metals and PAHs, and requires small volumes of test sample, whereas other tests such as amphipod or sea urchin tests require much larger volumes (Nunes et al., 2006). *Vibrio fischeri* (Microtox®) is a suitable tool for detection of non-specific toxicity, has been widely used for acute toxicity estimation and several commercial test kits are available (Parvez et al., 2006). In addition to the low cost and simplicity of the assay, its application for various water types is well established in the literature, providing a large volume of comparative information (Phyu et al., 2005). For detection of toxicity in sediment organic extracts, the Microtox bioassay was performed by other authors (Bihari et al., 2006; Wells et al., 1997). The EC50 value (the concentration that causes a 50% reduction in light emission from the bacteria) of copper to *V. fischeri* after a 30 min exposure ranged between 0.5 and 2.0 mg/L (Choi and Meier, 2001; Vasseur et al., 1984) and that for zinc was 0.7 mg/L (Miller et al., 1985). The EC50 value for hexavalent chromium after a 30 min exposure of *V. fischeri* was between 16 to 58 mg/L (Vasseur et al., 1984). These values give a measure of the likely sensitivity of the assay.

AhR CAFLUX (AhR chemically activated fluorescence expression) and GeneBLAzer® are two cell-based methods which measure the response of cultured cell lines to pollutants in water samples or sediment extracts, and allow high-throughput screening of samples. Cell-based assays generally require smaller volumes than whole-organism tests, may have high sensitivity, and are time- and cost-effective for a range of environmental applications. AhR CAFLUX is a method for measuring compounds that interact with the AhR. The binding of compounds to the AhR is followed by transportation of the PAH-AhR complex into the nucleus of the cell and subsequent binding to specific sequences (dioxin responsive elements, DREs) in the DNA. Binding of the chemical-receptor complex to the RE triggers the expression of DRE-associated genes. The structure of the AhR pathway is presented in Figure 5.1. The AhR CAFLUX cells contain a DRE linked to an enhanced green fluorescent protein (EGFP) reporter gene; a positive response is measured by the amount of fluorescence emitted (Escher and Leusch, 2012; Nagy et al., 2002; Zhao et al., 2010). The detailed methodology was described in Jin et al. (2015).

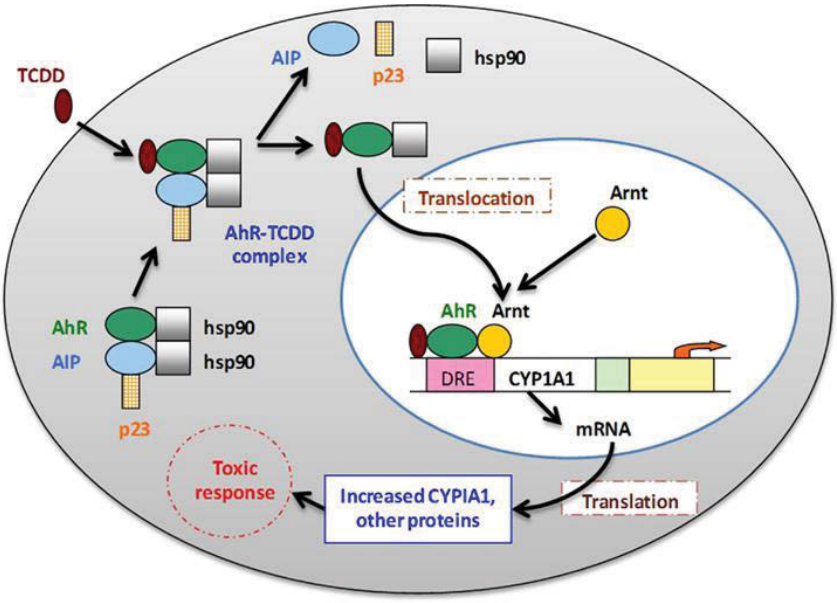

Figure 5. 1. The AhR signaling pathway

Key components and events in AhR signaling pathway activation. AIP: Aryl hydrocarbon receptor interacting protein; hsp90: heat-shock protein 90; Arnt: aryl hydrocarbon receptor nuclear translocator; DRE: dioxin-responsive element (Bhattacharya et al., 2012)

The p53 GeneBLAzer® detects agonists and antagonists of the p53 signalling pathway (Invitrogen, 2010). The p53 protein is induced in cells in response to a range of stimuli including DNA damage; the p53 binds to DNA and acts as a protective mechanism and tumour suppressor (Harris and Levine, 2005). Induction of p53 is used as an indicator of genotoxicity, i.e. that DNA damage may occur due to toxic compounds in a sample (Molendijk, 2013). Alternative options for genotoxicity testing include the comet assay, alkaline unwinding assay and Ames test (Escher and Leusch, 2012). The p53 GeneBLAzer® assay was carried out according to the p53 CellSensor® p53RE-bla HCT-116 cell-based protocol from Invitrogen Corporation (Invitrogen, 2010). CellSensor® p53RE-bla HCT-116 cell line (epithelial cell) can be used to detect agonists and antagonists of the p53 signaling pathway. p53RE-bla HCT-116 cell line has been shown to respond to Mitomycin and can be used to probe p53 signaling, which is involved in DNA repair, cell cycle arrest, and in some cases, apoptosis (Poulsen et al., 2011). The mechanism and toxic action of Gene BLAzer® assay are shown in Figure 5.2.

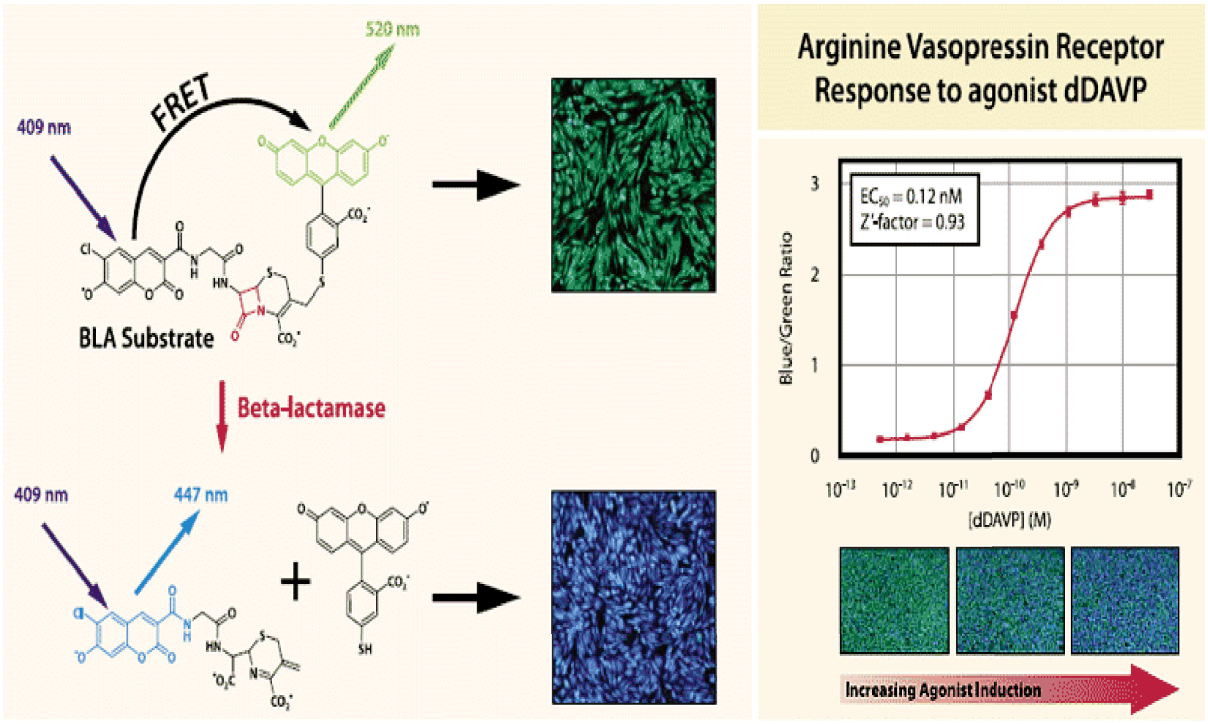

Figure 5.2. Schematic illustration of GeneBLAzer® assay (Invitrogen, 2010)

Each physicochemical and biological test requires a specific amount of sediment for chemical analyses, depending on the detection limits attainable and extraction efficiency by the procedure, and for biological testing, depending on the test organisms and test method (EPA, 2001). Under certain programs, some analytical procedures and toxicity test protocols necessitate specific manipulations (e.g., seawater or solvent extractions for effluent toxicity test). Bioassay test conditions use a combination of whole sediment extraction, solvent extraction and passive chemical spiking toxicity testing to identify the causes of sediment toxicity (Cheung et al., 1997; Hurst et al., 2004; Khanal et al., 2014). Whole sediment is sediment plus associated pore water which have had minimal manipulation while spiked sediment is a sediment to which a material has been added for experimental purposes (EPA, 1996). Previous studies comparing different bioassays showed toxicity values obtained with organic solvent extracts correlated better with the concentrations of sediment pollutants than the values obtained with water extracts (Guzzella, 1998; Persoone and Janssen, 1993), but solvent extracts are likely to overestimate the concentrations of pollutants partitioning into the water phase in the environment, where they are available to cause toxicity to organisms.

There have been several studies which included toxicity bioassays for the monitoring of heavy metals and PAHs compounds in runoff water or sediment in and around Sydney (Rawson, 2008; Tang et al., 2012) but the number of studies is very limited. The overall objectives of this study were (i) to compare the potential toxicity of RDS and BLS to aquatic organisms if the sediments are washed into waterways, and (ii) to examine whether the toxicity could be explained by the measured pollutants, or whether there are other factors influencing the results (unmeasured toxicants, interactions with other factors). This study assessed four toxicity endpoints, and used aqueous extractions that reflected environmental exposures, rather than solvent extractions which would give much higher concentrations than organisms would be exposed to naturally through water solubility. Sea water elutriates were used to reflect the conditions in estuarine receiving waters. The effects of particle size of the sediments were examined because much research showed there were significant differences among samples with fine and coarser sediments. The profiles of the heavy metals and PAHs in RDS and BLS are believed to differ among fractions of different particle sizes (Khanal et al., 2014) so the study determined the difference among size fractions of RDS and BLS. In addition, in some bioassays, solvent extracts of sediments were also tested to give a measure of the "worst case scenario" if the entire organic pollutant load was extracted into the exposure solutions. The toxicity values of the sediments were compared with the chemistry results, and the toxicities of spiked reference compounds in test water and in elutriates, to assess the likely causes of toxicity, and whether there were factors in the elutriates that influenced the toxicity.

5.2. Materials and methods

The study examined chemical concentrations and biological toxicity of RDS from The Comenarra Parkway, a busy urban road in Sydney, Australia, and BLS samples from nearby bushland. Heavy metal and PAH analyses were carried out on sea water elutriates, and solvent and acid extracts of whole and fractionated sediments. *Artemia* toxicity tests and Microtox® tests were carried out with sea water elutriates of the sediments. The cell-line bioassays for quantification of CYP1A1 activity (AhR CAFLUX), and genotoxicity (p53 GeneBLAzer®) were carried out on diluted mineral water elutriates, and solvent extracts of sediments. For the *Artemia* and cell line tests, spiked reference compounds were also analysed for comparison with the sediment results.

5.2.1. Sediment and soil sampling

RDS and BLS samples were collected from The Comenarra Parkway, Turramurra, Sydney New South Wales, Australia (GPS: 33°43'52.7"S and 151°05'60.0"E) (Figure 5.3). Sampling sites had been selected and moved from Kogarah to Comenarra Parkway, because logistical problems at the Kogarah sampling site meant that we could not collect enough samples. Sediment samples were collected on five occasions (from September, 2013 to June, 2014). RDS samples were collected from the asphalted road surface (excluding the gutters). On each sampling occasion, two to three weeks of dry weather were allowed for sufficient RDS to accumulate before samples were collected. The RDS were carefully brushed into a clean plastic dustpan and then transferred into self-sealing polyethylene bags for transport to the laboratory for analysis. BLS samples (top 0.1 m depth) were collected in nearby bushland with no visible signs of contamination, approximately 50 - 100 m away from the RDS sampling site, using a stainless steel spade, and bagged and transported as above. Samples were pooled to make composite samples from all collection times and then air-dried at room temperature and passed through a 2 mm stainless steel sieve. A portion was reserved as a whole RDS and BLS sample, and the remainder was fractionated by passing through sieves of different pore sizes to give fractions designated as follows: "< 75" = ≤ 75 μm, "< 150" = 76 – 150 μm, "< 300" = 151 – 300 μm, "< 425" = 301 – 425 μm, "< 600" = 426 – 600 μm. All samples were stored at 4°C until analysis.

Figure 5.3. Sampling site at Comenarra Parkway, Turramurra, Sydney

5.2.2. Chemical analysis

Analytical characterisation was conducted for total sediments and fractionated sediments of the RDS and BLS samples. They were analysed for heavy metals (Cd, Cr, Cu, Fe, Mn, Ni, Pb, antimony (Sb), V, and Zn) and 16 priority compounds of PAHs (Nap: Naphthalene; AcPy: Acenaphthylene; Ace: Acenaphthene; Fl: Fluorene; Phe: Phenanthrene; Ant: Anthracene; Flu: Fluoranthene; Pyr: Pyrene; BaA: Benz[a]anthracene; Chr: Chrysene; B[b&k]F: Benzo[b+k]fluoranthrene; BaP: Benzo[a]pyrene; IND: Indeno[1,2,3-cd]pyrene; DBA: Dibenzo[a,h]anthracene; BghiP: Benzo[g,h,i]perylene) selected according to criteria given in Yan et al. (2004). Pseudo-total concentrations of these heavy metals were determined by digestion of 0.5 - 1.0 g soil or sediment sample using 3 mL 70% HNO_3 and 3 mL 32% HCl for 2 h at 100°C. The digestion was followed by analysis of the diluted digests using ICP-OES and ICP-MS at the National Measurement Institute, Sydney, Australia. The instruments used were Varian 730-ES ICP-OES and Perkin Elmer DRC 2 ICP-MS. For PAH analysis, a sample of approximately 10 g was extracted using 100 mL of a solvent mix of dichloromethane (DCM) and acetone (1:1 by volume, pesticide grade, Merck). The samples were subjected to end-over-end tumbling (30 min, approximately 1 cycle/s) followed by soaking overnight. The extract was filtered through sodium sulfate followed by concentration

using a Turbovap (Caliper Life Sciences) at 4°C. The extracts were spiked with the US EPA 8270 internal standard mix (Supelco, Sigma Aldrich, USA, Product No 861238) and analysed by gas chromatography mass spectrometry (Agilent 5975, USA) with capillary column DB-5ms (30m, 0.25 mm ID, 0.25 μm film, J&W, USA). The recoveries of all compounds were between 75-110 %.

Elutriate extracts were prepared according to the US EPA protocol (EPA, 2001). 10 g sediment (whole and fractionated as described in section 5.2.1) was added to the artificial sea water (Ocean Nature, Aquasonic) with concentration 30 ‰. The solutions were analysed for their heavy metal (Cd, Cu, Pb, V, Mn, Fe, Cr, Zn and V) content by inductively coupled plasma-atomic emission spectroscopy (ICP-AES), and PAH content (Nap; AcPy; Ace; Fl; Phe; Ant; Flu; Pyr; BaA; Chr; B[b&k]F; BaP; IND; DBA; BghiP) by Gas chromatography mass spectroscopy (GC-MS), respectively.

5.2.3. Toxicity tests

5.2.3.1. Acute toxicity test on brine shrimp nauplii (*Artemia salina*)

Elutriates were prepared with artificial sea water according to the method described in section 5.2.2 from dried RDS and BLS (whole sediment and 5 size fractions, see section 5.2.2) according to the US EPA protocol (EPA, 2001). RDS and BLS samples were mixed with artificial seawater 30‰ (Ocean Nature® Aquasonic sea salt) in the ratio 1:4 (weight:volume), and shaken at 120 RPM for 1 h, then centrifuged at 10 000 g. Elutriates were filtered with Whatman nylon syringe filters, pore size 0.45 μm, before use for toxicity testing. The pH of the extracts was measured using a pH meter (Hanna Instruments).

Reference compounds for both metals (Cu, Cd, Zn, Pb and Cr) and PAHs (Chr, Fl, BkF, Pyr, BaP) were spiked into sea water and the elutriate at concentrations approximately 0.2x, 1x and 10x the 24-h LC50 for *Artemia* as determined from literature values (see LC50 values in Chapter 2, Table 2.5). *Artemia* nauplii were prepared by hatching *Artemia* eggs in 30 g/L artificial sea salts (Ocean Nature). Eggs (10 g) were placed in a plastic bottle with rapid aeration at 25°C with illumination. After 24 h, the nauplii were collected for use.

Experimental exposures were carried out in 4-mL glass vials containing 2 mL test solution. The test was conducted under laboratory lighting at room temperature (23°C). Elutriates were tested at 100%, 50% and 25% dilutions with artificial sea water and artificial sea water controls, three replicates of each treatment. Artificial sea water (30 g/L) and whole sediment elutriate (100%) were spiked with metals and PAHs in the concentration ranges shown in Table 5.2.

Table 5. 2. Spiked concentrations of heavy metals and PAHs into the sea water elutriates for determination of LC50s in the *Artemia* test

Metal	µg/L in sediment elutriate (100%)	µg/L in artificial sea water	PAH	µg/L in sediment elutriate (100%)	µg/L in artificial sea water
Cu	0 - 10000	0 - 8000	BaP	0 - 2000	0 - 500
Zn	0 - 15000	0 - 8000	BkF	0 - 4000	0 - 2000
Pb	0 – 8000	0 - 8000	Chr	0 – 1000	0 - 1000
Cd	0 - 4000	0 - 4000	Pyr	0 - 1000	0 - 1000
Cr	0 - 3000	0 - 1000	Fl	0 - 1000	0 - 1 000

Five 24-h-old brine shrimp (*Artemia salina*) nauplii were added to each container and incubated for 24 h. Physico-chemical parameters (temperature, pH, conductivity and DO) were measured in all treatment solutions at the beginning of the test. These measurements were carried out in a separate container to avoid damage to the nauplii by the sensor probe. The nauplii were unfed for the duration of the test; at that development stage they live off the nutrients in the yolk sac and do not feed. Mortality (failure of the organism to move upon gentle stimulation) was measured as a final endpoint. Mortality was assessed as the failure of the organism to exhibit any form of movement (under 40x microscope) within a 24 h observation period. If the control mortality did not exceed 10% in the nauplii tests, they were considered valid.

5.2.3.2. Sub-lethal toxicity on Microtox (*Vibrio fischeri*)

The extracted sediment sea water elutriates prepared for the *Artemia* tests were also used for the Microtox® tests. The test was performed at Environmental Forensics – Ecotoxicology Team, Office of Environment & Heritage, Lidcombe, NSW, using a Microtox® toxicity analyser (M500, Azur Environmental, Carlsbad, USA) following the standard operating procedure for the basic or 100% test, as supplied by the company. The Microtox toxicity test system exposes luminescent bacteria (*Vibrio fischeri*) to increasingly concentrated solutions of test sample. The bacterial luminescence, the endpoint of this assay, was measured for all samples after 5, 15, and 30 mins of exposure at 15°C. The reduction in the light output of the luminescent bacteria reflecting the toxicity of the sample is monitored in a temperature-controlled photometer. Phenol was used for the organic reference compound, and $ZnCl_2$ was used as the heavy metal reference compound. The Microtox® toxicity tests were carried out on elutriates of 5 size fractions of RDS and BLS and the whole sediment. Each test consisted of treatments with five nominal dilutions (80%, 40%, 20%, 10% and 5% of original elutriate), a Microtox diluent water control and an artificial sea water control.

5.2.3.3. Cell based assays: AhR CAFLUX and p53 GeneBLAzer®

a. Preparation of the sediment elutriates

Sediment elutriates for these assays were prepared using diluted mineral water (DMW; Reverse osmosis water containing 20% Perrier® mineral water) prepared according to EPA (2002). Four litres of Perrier® water was added to 16 litres of Milli-Q® deionised water. The mixture was then aerated vigorously for 24 h to stabilise the medium. It was not possible to use sea water elutriates for the cell-based assays because the high salinity would be toxic to the cells.

Forty mL of diluted mineral water was added to 10 g of sediment in 250-mL flasks and shaken for 1 h, then centrifuged at 1500 g for 15 mins and the supernatant was collected for use in tests. The supernatant was filtered through a 0.45 μm nylon syringe filter (Whatman® GD/X), the first 5-10 mL were discarded and the remaining filtrate was collected for use. A diluted mineral water blank without sediment was used in these tests as the control.

b. Preparation of solvent extracts of sediments

Solvent extracts of the sediments were prepared according to the method given in Hurst et al. (2004). Ten grams of sediment sample were extracted with 10 mL dichloromethane (DCM) in 50-mL beakers covered by a watch glass to reduce evaporation, and shaken in a Heidolph Unimax 1010 shaker for 30 mins, then sonicated in a ultrasonic cleaner bath sonicator (PCI Analytics Ltd) for 10 mins. The slurry was then transferred to 50-mL capped glass centrifuge tubes and centrifuged in a UNICO 24 place Rotor centrifuge at 4000 g for 10 mins. The DCM supernatant was then transferred to a 50-mL beaker. This process was then repeated twice more (total 3 times). The supernatants were combined and were then concentrated to dryness using an N_2 evaporator (MX C8624 (CM24)). The residue was dissolved in 100 μL dimethyl sulfoxide (DMSO) and stored at 4°C for the bioassay. A solvent blank control (without sediment) was also prepared by the same procedure.

c. Extract spiking

Diluted mineral water elutriates of total RDS and total BLS were spiked with PAHs and metals at environmental concentrations as measured in solvent or acid extracts of the RDS and BLS sediments. The concentrations are listed in Table 5.3. These samples were intended to replicate the “worst case scenario” if all the pollutant was extracted into the water elutriate.

Table 5.3. Spiking concentrations of heavy metals and PAHs into the RDS and BLS elutriate for cytotoxicity assays

Metal	mg/L in 100% RDS elutriate	mg/L in 100% BLS elutriate	PAH	mg/L in 100% RDS sediment elutriate	mg/L in 100% BLS sediment elutriate
Cu	32	1.2	BaP	0.44	0.01
Zn	39	3	BkF	0.28	0.02
Pb	27	8.7	Chr	0.14	0.02
Cd	11	3.9	Pyr	0.27	0.02
Cr	1	0.5	Fl	0.52	0.01

5.2.3.4. AhR CAFLUX (AhR Chemically Activated Fluorescent Expression)

The AhR CAFLUX assay was performed according to the protocol used in the Smart Water Research Centre at Griffith University, Gold Coast, Qld. Hepa1c1c7 mouse hepatoma cells were cultured in DMEM (Dulbecco's modified Eagle's medium) with GlutaMAX (supplemented with 10% dialysed FBS, HEPES and NEAA). The cells were washed twice in PBS, trypsinised, resuspended and diluted in DMEM and transferred to 96 well clear bottom black microplates to give a final concentration in the wells of 3.0×10^5 cells/mL (3.0×10^4 cells/well).

2,3,7,8 TCDD standards at concentrations from 10^{-13} M to 10^{-8} M were used as the reference standard. Samples were diluted and 100 µL of each diluted sample, DMSO blank or TCDD standard was added to the relevant wells of the microplate. Each sample was run in triplicate, and a standard curve and a range of controls was run on each microplate. The plate was read at the start (T = 0), then incubated for 48 h at 37°C. After 24 h and 48 h the plate was read again for comparison with the background fluorescence measurement at T = 0. The fluorescence in each well of the plate was measured in a microplate fluorometer (Fluostar Galaxy, BMG Labtechnologies, Offenburg, Germany) with an excitation wavelength of 485 nm and an emission wavelength of 520 nm. The relative fluorescence units (RFU) values in AhR CAFLUX was determined by subtracting fluorescence measured at T=0 h from fluorescence at T = 24 h and T = 48 h. The ΔRFU was plotted against log TCDD

concentration to determine the EC50 value, and the ΔRFU TCDD top and bottom values were used to express the sample data as % induction relative to TCDD using the follow equation:

$$\%\ Induction = \frac{(\Delta RFU_{sample} - \Delta RFU_{TCDD\ bottom})}{(\Delta RFU_{TCDD\ top} - \Delta RFU_{TCDD\ bottom})}$$

5.2.3.5. p53 GeneBLAzer®

The p53 GeneBLAzer® assay was carried out according to the Invitrogen protocol (Invitrogen, 2010), modified to suit 384-well microplates. CellSensor™ p53RE-bla HCT-116 cells (containing a beta-lactamase reporter gene under control of the p53 response elements stably integrated into HCT-116 cells) were cultured in culture medium with Blastocidin. The cells were harvested and resuspended in assay medium according to the protocol, and used to seed the wells of a 384-well black-wall, clear-bottom microplate (except for cell-free wells which received assay medium only). The plate was incubated at 37°C/5% CO_2 for 6 h. Samples were then added to sample wells, Mitomycin was used as a positive control, and blanks included blank water and solvent extracts, DMSO controls and cell-free wells. The plate was incubated for 40 h. This was longer than the standard protocol (16 h), to try to increase sensitivity. Substrate (LiveBLAzer™ -FRET B/G Substrate (CCF4-AM) made up according to the protocol) was then added to all wells and the plate was incubated for a further 2.5 h at room temperature in the dark.

The fluorescence was measured in the blue channel with excitation wavelength 409 nm/20 nm bandpass width and emission wavelength 460 nm/40 nm and fluorescence in the green channel was measured at excitation wavelength 409 nm/20 nm and emission wavelength 530 nm/30 nm. Each water sample, reference chemical, cell-free media, DMSO control, and DMSO-free control was assayed in triplicate on each plate. The AhR CAFLUX and GeneBLAzer® experiments were carried out with all equipment and instruction at Smart Water Research Centre of Griffith University, Gold Coast, Australia.

5.2.4. Statistical analysis

Dose-response curves were generated from the acute mortality/toxicity data, and analysed using various regression equations. The LC50 values for the *Artemia* tests were calculated by the Trimmed Spearman-Karber Method (EPA, 1993). For the Microtox assay, the EC50s were calculated using the software provided with the instrument, except in some samples where outliers caused problems; these values were calculated with RegTox (Vindimian, 2012) with outliers removed. For AhR CAFLUX, all experimental data were evaluated with concentration−response regressions (sigmoidal with defined maximum (100%) and minimum response (0%)). Dose response curves were fitted using the sigmoidal dose-response model from GraphPad Prism 6.0 (GraphPad, San Diego, CA, USA), and the EC50 and EC20 values (the effect concentrations inducing 50% and 20% of the maximum effect respectively) were calculated. For the p53 GeneBLAzer® test, the ECIR1.5 (effect concentration causing an induction ratio IR of 1.5) was used for comparison of samples. The ECIR1.5 is appropriate for all reporter gene assays where no maximum response can be obtained.

5.3. Results and discussion

When assessing the toxicity of a sediment and attempting to identify chemicals causing sediment toxicity, it is important to consider the bioavailability of pollutants. Although a chemical may be found in high concentrations in a sediment, it may not be responsible for the observed sediment toxicity because some mechanisms, such as adsorption and absorption, can effectively reduce the freely dissolved concentrations of toxic chemicals in sediment interstitial waters and the ability of these chemicals to cause toxicity (Perron et al., 2010). Therefore this study determined the sources, distribution and toxicity of poly aromatic hydrocarbons (PAHs) in elutriates or solvent extracts in the RDS and BLS samples.

5.3.1. Pollutant contamination

5.3.1.1. Total heavy metals contamination in the RDS and BLS

The concentrations of six heavy metals (Cr, Cu. Pb, Ni. V and Zn) in RDS and BLS, as well as the sediment quality ISQG guidelines (McCready et al., 2006) are presented in Figure 5.4 and Figure 5.5 respectively. Interim sediment quality guidelines (ISQGs) for heavy metals for threshold and probable effects levels were compared with the chemistry results for RDS and BLS. The detailed data of the heavy metal concentrations can be found in the Appendix 1. A comparison of the heavy metal concentration in RDS revealed that Pb > V > Zn > Cr. The Cd concentration was lower than the detection limit (0.1 mg/kg). The finest fraction (< 75 μM) had higher concentrations than other coarser fractions. Cu and Pb in RDS fractions were higher than ISQG limit.

The concentrations of all metals in the BLS were lower than in the RDS (Figure 5.5).. A negligible amount of Ni and Cu was present in the BLS samples. Similarly, Cr and Cu content in soils were low (10 times) and were about < 8 mg/kg and 0.5 mg/kg respectively These observations confirm that Zn, Cu, Ni, Cr would have originated from traffic related activities in RDS. Mean concentrations of all heavy metals were generally higher in RDS than in BLS, indicating that vehicle activity and road surface abrasion have contributed to the accumulation of heavy metals in RDS. Metal concentrations increased markedly in the finer material in RDS and BLS samples from sampling sites with high concentrations in finer fractions (Figure 5.4 and 5.5).

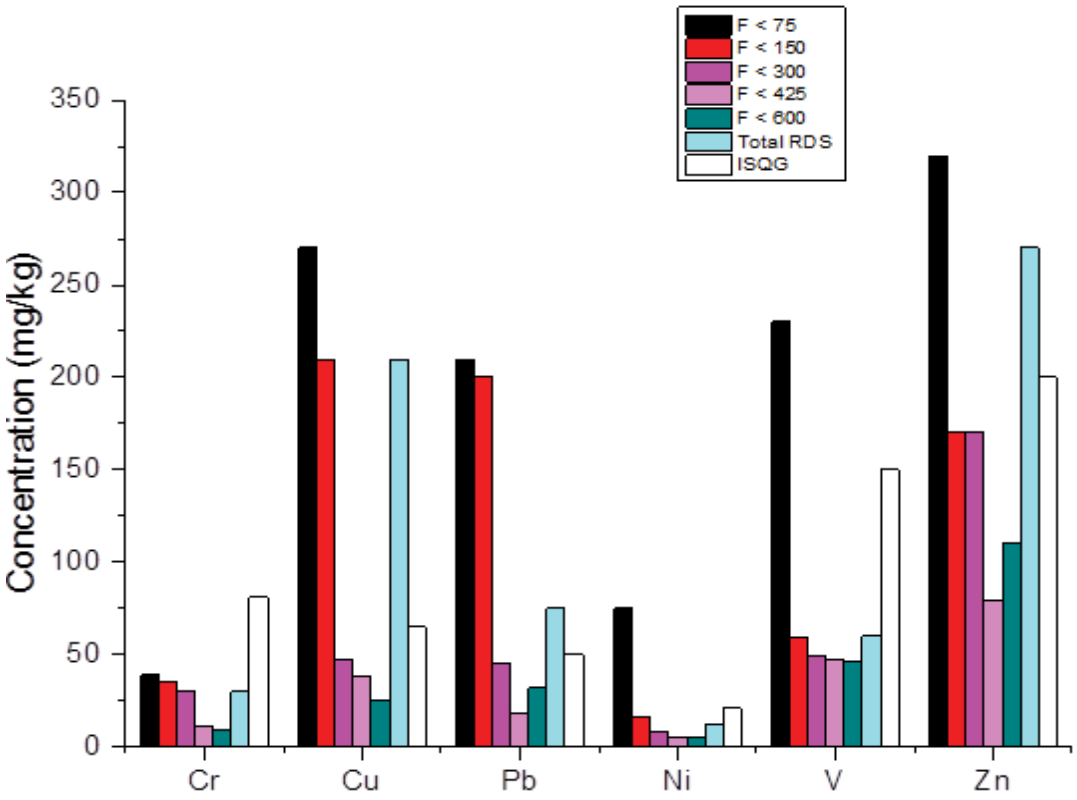

Figure 5.4. Heavy metal concentrations in RDS for different sediment size fractions and composite sample (total) compared with Interim sediment quality guidelines (ISQG)

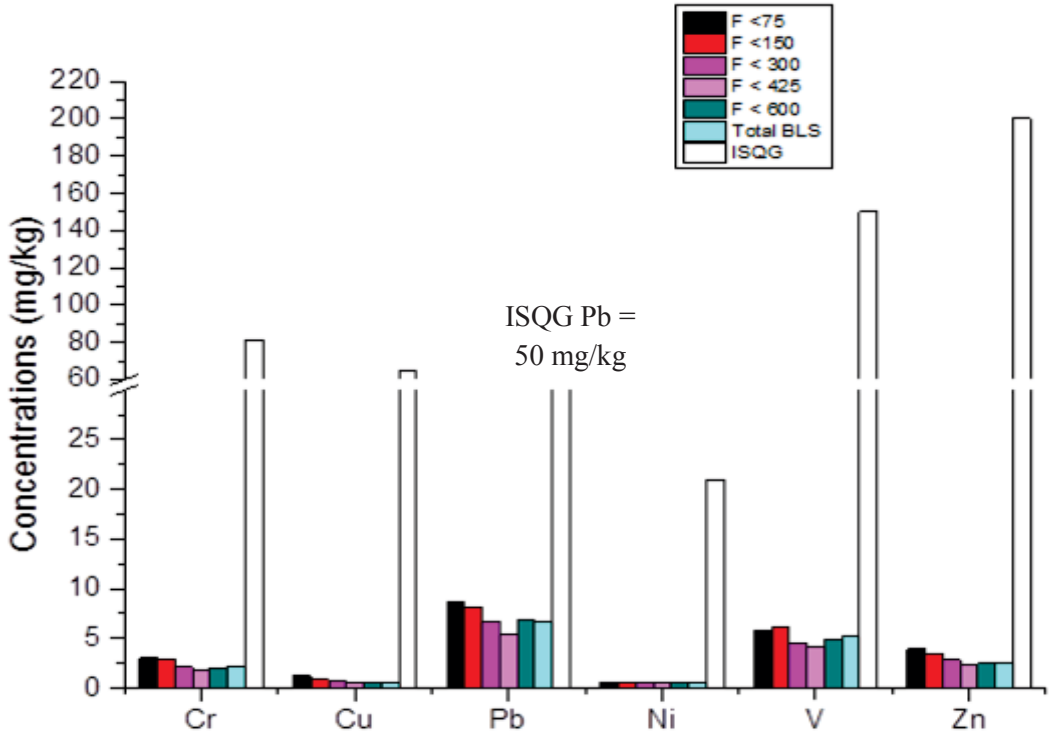

Figure 5. 5. Heavy metal concentrations in BLS for different sediment size fractions and composite sample (total) compared with Interim sediment quality guidelines (ISQG)

5.3.1.2. Total PAH contamination in the RDS and BLS

Figure 5.6 shows the total, HMW and LMW PAHs plotted for each particle-size fraction and weighted average for the total samples of sediments. The total concentrations of PAHs in the fractionated and total RDS and BLS samples are shown in Figure 5.6A. The detailed results of the PAH concentrations for each compound are presented in Appendix 2. The total PAH concentration (mg/kg) in the RDS was highest in the finest fraction (<75 μm, 2.37 mg/kg); concentrations decreased in the coarser fractions. The calculated weighted mean concentration (total) in RDS was 1.25 mg/kg. Concentrations in the BLS fractions ranged from 0.2 mg/kg in the finest fraction to 0.16 mg/kg in the 600 μm fraction. These concentrations were all lower than sediment quality guideline (ISQG, total PAH = 2.26 mg/kg, LMW = 1.21 mg/kg and HMW = 1.05 mg/kg). The measured concentrations of total PAHs, HMW and LMW of total fraction were higher than the calculated weighted concentrations, probably because the extraction method could not extract well for the fine particle fractions, in which much of the sediment was floating during the extraction procedure. In the total fraction, the presence of the larger particles seemed to grind up the finer particles and improve the extraction, thus giving a higher extraction efficiency.

Figure 5.6 B and C shows the differences between the HMW and LMW PAHs in the RDS and BLS and fractions. The overall concentrations of PAH were much lower in the BLS than in RDS. All HMW in RDS samples had higher concentrations than LMW and the trend was similar in BLS samples.

HMW PAHs are more stable (Amodu et al., 2013) and less volatile than the LMW PAHs, and therefore are more likely to accumulate on road surfaces and in the sediments. As discussed in Chapter 4 of this thesis, the LMW PAHs, which are mainly derived from oil and fuel leaks and road asphalt abrasion and tyre deterioration, are likely to have been volatilised and degraded. To determine the likely sources of PAHs in RDS and BLS, the ratios of low to high molecular weight PAHs Flu/(Flu+Pyr), BaA/(BaA+Chr), and IND/(IND+BghiP)) are generally used as tools to discriminate between the petroleum and pyrogenic sources (Yunker et al., 2002). When the ratio of Ant/(Ant+Phe) was calculated from the data in Appendix 5, all samples of RDS and BLS fell into the pyrogenic source category with the ratios for RDS in the range 0.13–0.18, while those for BLS were in the range 0.27–0.57. The BaA/(BaA+Chr) and IND/(IND+BghiP) ratios of both RDS and BLS fell into an intermediate

region in between petrogenic and pyrogenic sources, representing mixed sources. This is probably due to the presence of higher proportion of PAHs derived from pyrogenic sources (wood and grass burnings) in BLS. This suggests that the sources of PAHs in RDS mainly came from tyres, road pavement, asphalt, and diesel exhaust particles.

As with the total PAH concentrations, the HMW and LMW PAHs were higher in the finer fractions than in the coarser fractions. The research literature reports the relationship of PAH concentrations with specific size ranges of particulates. Evans et al. (1990) reported that PAHs were associated with organic matter. In the size fractions for the RDS and BLS, the fine fractions were higher in organic content (see appendix 6), which parallels the PAH distribution in both sediments. The PAH result of this study result also agreed well with Allen et al. (1996) which reported a PAH maximum in the fine size followed by the middle and coarse silt fractions.

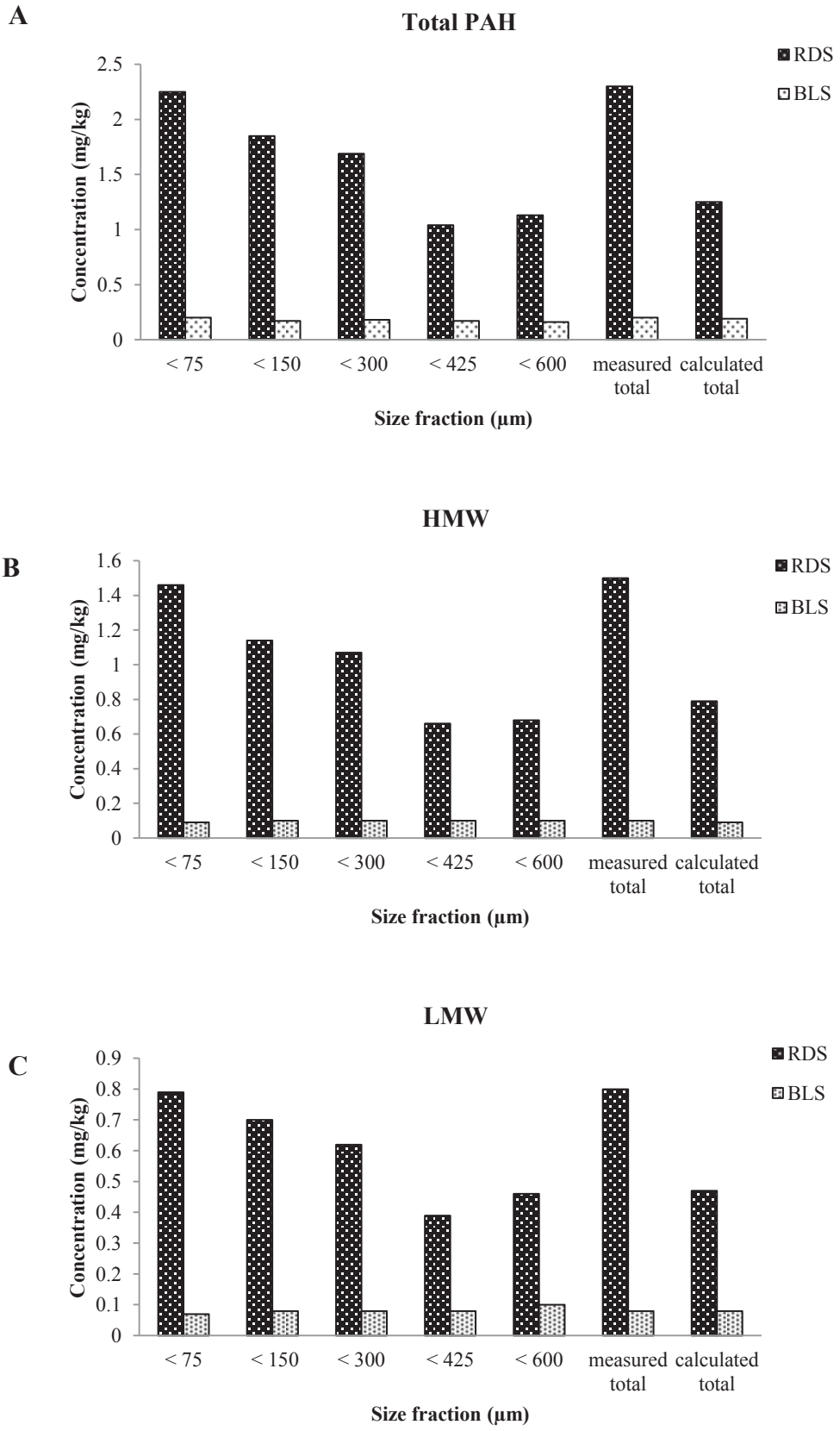

Figure 5.6. Total PAH concentrations (A), HMW (B) and LMW (C) in RDS and BLS for different sediment size fractions and composite sample (total)

5.3.1.3. Heavy metal contamination in the RDS elutriates in comparison with BLS elutriates

Table 5.4 lists the measured metal concentrations of the sediment elutriates. In general, all the elutriates contained rather low levels of heavy metals and Cd and Ni in the BLS elutriates were below detection limits (< 0.01 mg/L). Cu, Cd, Cr and Zn were generally higher in RDS than in BLS, however Pb was similar in both. The concentrations of heavy metals in elutriates were much lower when compared with the total original heavy metals in sediment because of low solubility in the water (metal partition coefficients (log Kd) in sediment/water with low total metal concentrations).

5.3.1.4. PAH concentrations in the RDS and BLS elutriates

Table 5.4 presents the PAHs concentrations in artificial sea water elutriates from RDS and BLS. The PAHs in the RDS seawater elutriates were dominated by the presence of HMW compounds with fluoranthene and pyrene as the most abundant ones, similar to the findings in RDS and BLS of road dust in China (Wang et al., 2009). The procedure to prepare the elutriate extracted very little of the PAHs, because PAH compounds hardly dissolved in the salty water. The PAH concentrations in BLS elutriates were lower than RDS. In Chapter 4 of this thesis, the results also revealed the great difference between PAH concentrations in RDS and BLS.

Table 5.4. Summary of elutriate concentrations and toxicity data for *Artemia* acute tests

Compound	Molecular weight	Measured concentration in RDS elutriate (mg/L)	Measured concentration in BLS elutriate (mg/L)	*Artemia* LC50 (mg/L, nominal) for compounds spiked in sea water	*Artemia* LC50 (mg/L, nominal) for compounds spiked in RDS elutriate	*Artemia* LC50 (mg/L, nominal) for compounds spiked in BLS elutriate
Cd	112	0.0113	-	1.00	3.50	4.20
Cu	64	0.0422	0.0148	1.20	4.20	5.70
Pb	211	0.0134	0.0104	0.89	3.70	3.98
Zn	65	0.0658	0.0234	5.50	11.00	12.65
Cr	52	0.0134	-	0.79	2.40	2.25
Fl	166	0.00012	0.0005	0.20	0.40	0.48
Pyr	202	0.0009	0.0001	0.23	0.33	0.52
Chr	228	0.0005	0.0001	0.19	0.37	0.42
BbF	252	0.0002	0.0001	1.40	1.70	1.80
BaP	252	0.00010	0.00003	0.34	0.65	0.75

(-): not detected. Detection limit for PAHs: 10^{-4} mg/L and for heavy metal: 10^{-2} mg/L)

5.3.2. *Artemia salina* nauplii acute toxicity assay

The *Artemia* nauplii tests were carried out on elutriates of the RDS and BLS total and fractionated sediments. To determine the possible effects of detected compounds, and to investigate the effects of the elutriate on toxicity, heavy metals and PAHs were also spiked into artificial sea water and whole sediment elutriates, at concentrations bracketing LC50 values identified from the literature (From Chapter 2, Literature Reviews).

None of the RDS nor the BLS elutriates (fractionated or whole sediments) showed any lethality to *Artemia* nauplii because of much lower concentrations of metals and PAHs in the elutriates than the LC50 values. The results of the assays of spiked metals and PAHs are shown in Table 5.4. Note that the lower the EC50 or LC50, the higher the toxicity. The order of toxicity of compounds spiked into sea water was as follows: for metals, Cr^{6-}> Pb^{2+} > Cd^{2+} > Cu^{2+} > Zn^{2+} and for PAHs, Chrysene ~ Fluoranthene > Pyrene > Benzo[a]pyrene > Benzo[b]fluoranthene. LMW PAHs showed greater toxicity than HMW PAHs, this result agreed with some previous research (Blust et al., 1995; Hadjispyrou et al., 2001; Nunes et al., 2006). When spiked into the elutriates, the toxicity was considerably lower than for spiked compounds in sea water (Figure 5.7 and Table 5.4). It is likely that the toxicity was reduced by binding of the toxicants to colloid materials and organic compounds (such as humic acid) in the elutriates. The pH was a little higher in the elutriates and that could contribute to reducing the solubility, particularly for the heavy metals (pH of sea water was 8.0±0.3, but the average pH of the elutriates was 8.5±0.2). The toxicity of heavy metals depends mostly on a free ion (Nguyen et al., 2009) i.e. on a soluble metal compound concentration rather than on the total metal concentration. The insoluble, colloid-bound, and complexed metal compounds are less bioavailable and less toxic.

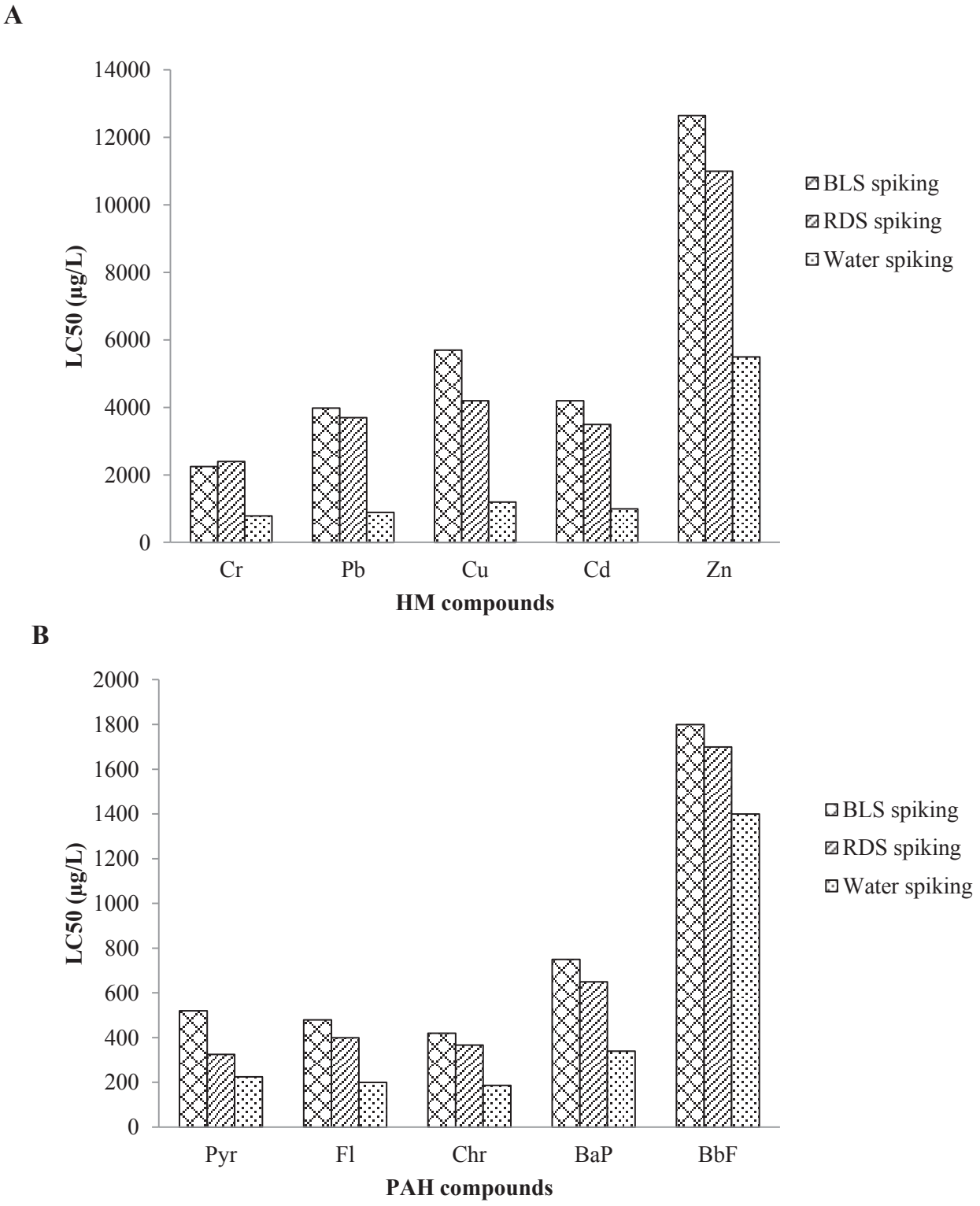

Figure 5. 7. *Artemia salina* acute 24-h toxicity test with heavy metals (A) and PAHs (B) spiked into the BLS and RDS elutriates and artificial sea water. LC50 values were calculated by the Spearman-Karber method.

5.3.3. Microtox® (*Vibrio fischeri*) sub-lethal toxicity assay

The Microtox® assay with *V. fischeri* was performed on RDS and BLS sediment elutriates of 5 size fractions and total sediments to get the EC50 concentrations after 5 minutes, 15 minutes and 30 minutes exposure in order to observe the toxicity of the extracts towards the bacteria. The results are reported in Figure 5.8 in the form of toxic units (TUs), calculated from the EC50 of the samples. For the Microtox® test, one toxic unit is the concentration that will reduce the light output of *Vibrio fischeri* by 50%; a solution containing two TUs will have the same effect when diluted by 1/2.

For all samples in the Microtox® test, almost all samples showed toxicity, and the toxicity of RDS was significantly higher than BLS samples (paired t-test, 17 df, t Critical two-tail = 2.11, $p = 0.00003$). The Microtox® results for 30 min gave TU values between 1.1-3.5 for RDS samples and 0.0-1.8 for BLS. The BLS elutriate of the whole fraction showed a slight response, but not enough to be measurable. In most of the samples, the toxicity increased with time of exposure in the Microtox® (TU values at $5<15<30$ mins). This increase of toxicity with time is characteristic of metal toxicity (Ruiz et al. (1997); Utgikar et al. (2004), suggesting that metals contributed to the measured toxicity.

There was a slight tendency for greater toxicity in the finer fractions, but this was not significantly different in either RDS or BLS (ANOVA, $p > 0.05$).

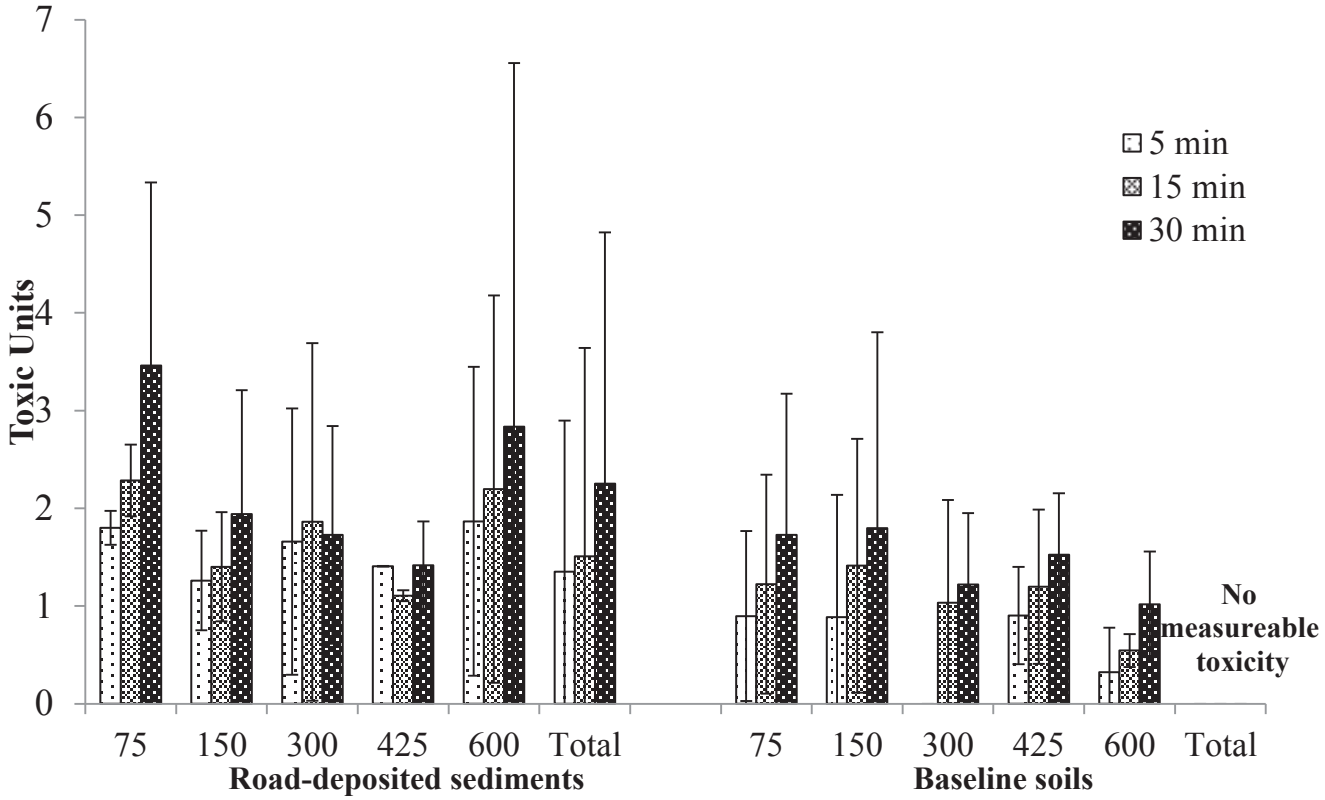

Figure 5.8. Microtox® toxicity test on RDS and BLS

5.3.4. AhR CAFLUX (Chemically Activated Fluorescent Expression) bioassay

For measuring the AhR signaling with specific receptor-mediated activity, the EC50s and EC20s that cause 50% or 20% respectively of the maximum induction for TCDD for AhR were derived. The EC50 and EC20 values obtained for TCDD in the AhR CAFLUX were within acceptable limits (TCDD 24 h EC50 = 11.7 pM ± 3.0 and 48 h EC50 = 11.09 pM ± 0.4). The standard curve for TCDD is shown in Figure 5.9. The toxic effect for the TCDD standard was greater after 48 h than at 24 h. This result was similar to previous research (Jin et al., 2015; Nagy et al., 2002; Tang et al., 2014), and was within the laboratory QA requirements. The toxicities of the sample extracts were all below the EC50 values, so the results are reported as the EC20 values, and the TCDD equivalents were calculated.

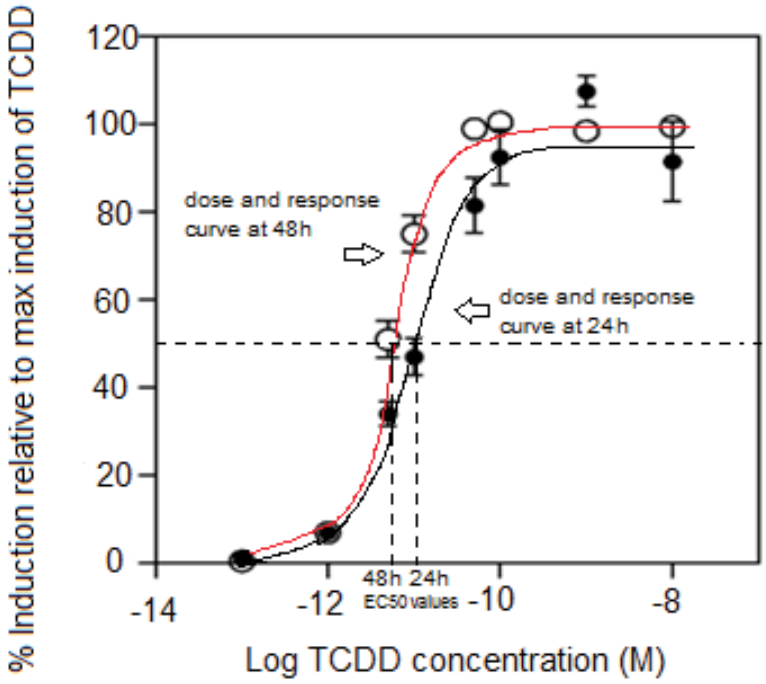

Figure 5.9. TCDD concentration-response curves at 24 and 48 h in the AhR CAFLUX assay (based on 4 test bioassays)

The response curves in the AhR CAFLUX for the solvent extracts of RDS and BLS are shown in Figure 5.10. All fractions of RDS gave measurable responses in the assay, and induced AhR CAFLUX fluorescence activity in cells to the same maximal activity as that of TCDD. BLS samples were all below detection limits. The response at 48 h was markedly lower than at 24 h, suggesting that the cells were possibly detoxifying the compounds.

The EC20s and calculated TCDD equivalents of the AhR CAFLUX assays on solvent extracts of whole and fractionated sediments, and unspiked water extract of total RDS, and spiked water-extract of whole sediments, are presented in Table 5.5. The TCDD equivalent concentrations of the RDS solvent-extracted samples ranged up to 3.79×10^{-14} moles TCDD/g sediment. These levels are consistent with though lower than other previous estimates of aryl hydrocarbon receptor activity in natural samples, such as 0.3×10^{-9} moles TCDD in urban stormwater (Kennedy et al., 2010; Tang et al., 2013). As seen in Figure 5.10, the BLS samples were too low for quantification. In the RDS samples, the <75 μm and the <150 μm fractions showed higher TCDD equivalents than the coarser size fractions. As with the chemistry results (see Figure 5.6 above), the measured TCDD equivalents in the total fraction gave higher values in the AhR CAFLUX than the value calculated from the weighted average of the size fractions. This suggests that the extraction efficiency for the fractionated samples was less than in the total fractions, possibly because the large particles in the total fraction assisted in grinding up the fine particles and releasing more of the pollutant compounds.

A

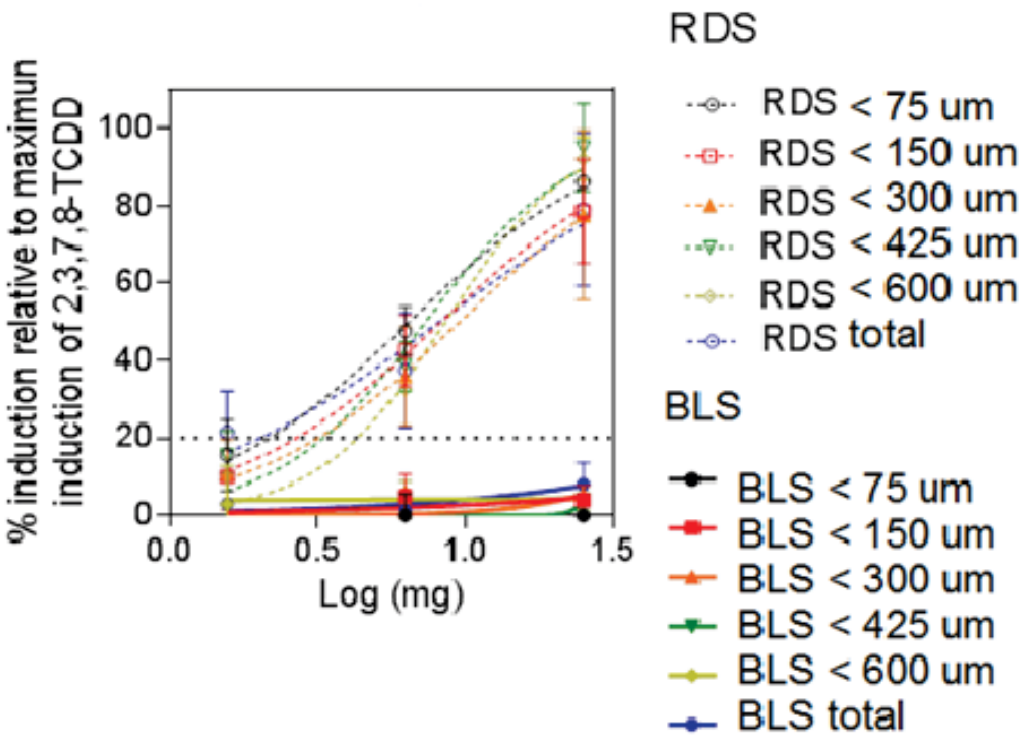

B

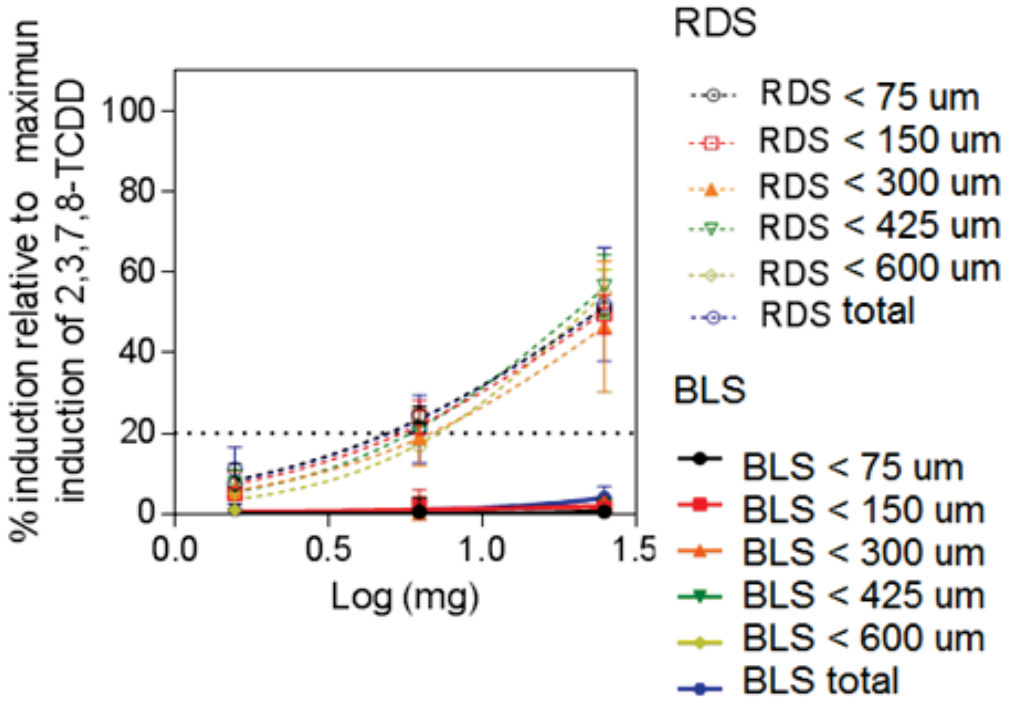

Figure 5.10. AhR CAFLUX of solvent-extracted samples after 24 h (A) and 48 h (B)

Diluted mineral water elutriates of both RDS and BLS showed negligible induction of AhR receptor activity in the AhR CAFLUX assay; the result of the whole RDS water elutriate is shown in Table 5.5, (other results not shown). To estimate the maximum effects that might be produced by the total measured concentrations of PAHs and metals in the sediments, water elutriates were spiked with these concentrations, alone, and in a mixture of total PAHs and total metals. The results (Table 5.5) show that the results were not consistent, probably because the quantity of aqueous samples that could be added to the assay mixture was very low (2 μL of sample into 100 μL well volume), so the errors in the assay were very high.

Table 5.5. Results of EC20 and TCDD equivalent of AhR CAFLUX on solvent extracts of sediments and fractions, and spiked and unspiked water elutriates after 24 h

	Fraction		BLS EC20 (g sediment/mL)	BLS TCDD equivalents (moles TCDD/g sediment)		RDS EC20 (g sediment/mL)	RDS TCDD equivalents (moles TCDD/g sediment)
Solvent extract	< 75		> 16.89	< 1.83E-16		**0.11360**	**2.72E-14**
	< 150		> 5.36	< 5.77E-16		**0.10820**	**2.86E-14**
	< 300		> 1.19	< 2.59E-15		**0.12810**	**2.41E-14**
	< 425		> 5.02	< 6.16E-16		**0.13340**	**2.32E-14**
	< 600		> 4.45	< 6.94E-16		**0.17390**	**1.78E-14**
	total		Sample lost	Sample lost		**0.08161**	**3.79E-14**
	Compound	**Spiked conc. into BLS water elutriate (mole/g sediment)**	**BLS EC20 (g sediment/mL)**	**BLS TCDD equivalents (moles TCDD/g sediment)**	**Spiked conc. into RDS water elutriate (mole/g sediment)**	**RDS EC20 (g sediment/mL)**	**RDS TCDD equivalents (moles TCDD/g sediment)**
Water extract only		0.00	-	-	0.00	> 0.00666	< 4.64E-13
PAH spiking	Fl	4.95E-05	> 0.01004	< 3.08E-13	2.57E-03	> 0.00313	< 9.87E-13
	BkF	7.94E-05	**0.00266**	**1.16E-12**	1.11E-03	> 0.00554	< 5.58E-13
	BaP	3.97E-05	**0.00033**	**9.46E-12**	1.75E-03	> 0.00166	< 1.87E-12
	Chr	8.77E-05	> 0.00103	< 3.00E-12	6.14E-04	**0.00120**	**2.58E-12**
	Pyr	9.90E-05	> 0.02929	< 1.05E-13	1.34E-03	> 0.00222	< 1.39E-12
	Mixture of all compounds	3.55E-04	-	-	7.38E-03	0.00005	< 5.62E-11
Metal spiking	Cd	6.27E-01	> 0.00251	< 1.23E-12	7.65E-02	> 0.00125	< 2.47E-02
	Cu	4.22E-01	**0.00208**	**1.48E-12**	1.88E-02	> 0.00274	< 1.13E-12
	Pb	5.31E-02	> 0.00581	< 5.32E-13	4.20E-02	**0.00150**	**2.07E-12**
	Zn	8.93E-03	> 0.00827	< 3.74E-13	4.46E-03	> 0.01053	< 2.93E-13
	Cr	6.00E-01	> 0.00418	< 7.40E-13	4.62E-02	> 0.03103	< 9.96E-14
	Mixture of all compounds	6.09E-01	> 0.01401	< 1.23E-12	5.06E-02	-	-

(-): sample lost. Values in bold are within the quantifiable range. Values are given as > or < are estimated by extrapolation

5.3.5. p53 GeneBLAzer®

The p53 GeneBLAzer® assay was carried out on the same samples as the AhR CAFLUX. For this assay, the response can be induced without apparent limit until the compounds become cytotoxic. Without a defined maximum response, the ECIR1.5 that causes 1.5-fold induction relative to control signals was derived for these assays. The general toxicity endpoints measured included cell viability and genotoxic potency. Mitomycin was used as the reference compound. The p53 cell line showed a dose response to mitomycin with appropriate ECIR1.5 values. (0.74×10^{-4} mg/mL), which was acceptable within the laboratory QA requirements (Figure 5.11).

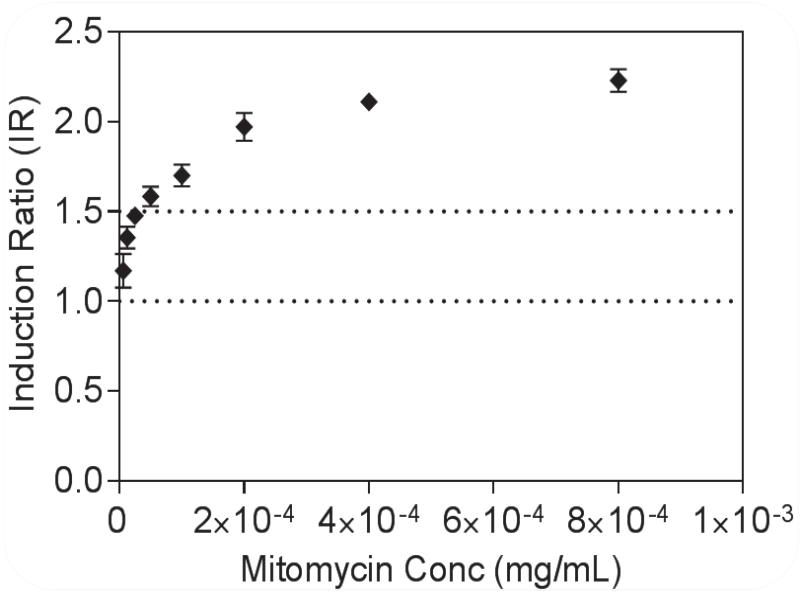

Figure 5.11. Dose response (relative to solvent control) of GeneBlazer® for mitomycin

There was no evidence of cytotoxicity in the GeneBLAzer® assay, and the induction did not exceed the 10% effect threshold in any sample, indicating that both RDS and BLS were nontoxic to the cells and caused no genotoxicity. This is not surprising because Escher et al (2013) have found that this assay was not as responsive as some other assays (e.g. AhR-CAFLUX, umuC). This bioassay is relatively new, and requires further validation work to improve the detection limit (Escher et al., 2013).

5.3.6. General discussion

The overall results indicated that the contamination in the RDS was higher than in the BLS, and the observed toxicity was also higher in RDS than in BLS. Chemical analyses indicated that concentrations of metals and PAHs were higher in the RDS than in BLS, and finer fractions had higher concentrations than coarser fractions. There was no acute toxicity to *Artemia* in either RDS or BLS seawater elutriates. Water elutriates of RDS showed higher toxicity in the Microtox® assay than BLS elutriates. Solvent extracts of RDS showed measurable induction in AhR CAFLUX,, but there was no measureable response from solvent extracts of BLS. There was no cytoxicity or genotoxicity in any extracts of RDS or BLS in the p53 GeneBLAzer. Attempts to simulate a "worst case scenario" with samples spiked with heavy metals and PAHs at concentrations equal to the total measured concentrations in the sediments showed very little effect in the AhR CAFLUX or GeneBLAzer, probably because the volume that could be tested was very small.

Comparison with the Guidelines (ISQG (McCready et al., 2006)) indicated that the RDS sediment concentrations were all above levels of concern for both metals and PAHs. This was not reflected in any acute toxicity to *Artemia*, but *Artemia* has often been reported to be relatively insensitive (Dvorak et al., 2012). However, toxicity was detected in Microtox®, as expected because of the chemistry results. Microtox did not detect significant differences among the size fractions of RDS or BLS, although it is possible that there is a slight trend in Figure 5.8. Repetition of the experiment with more replicates might detect this trend. In AhR CAFLUX, however, there was a trend for stronger effects in the finer fractions, which would be explained by the chemistry PAH trend in the fractions.

The bioavailability of organic contaminants in sediment to benthic animals is influenced by physical and chemical properties of the compounds in sediment, particularly its organic matter content, composition and grain size distribution (Bott and Standley, 2000). The fine fractions move differently in runoff. Coarse fractions drop out early, and fine, more heavily contaminated fractions can be carried a long way, so pollutants may be concentrated in fine muddy sediments. Fine fractions may be eaten by sediment-feeding organisms, allowing uptake of toxicants via the gut pathway, as well as by water contact, increasing the potential bioavailability. It was, however, observed that the toxicity of spiked compounds to *Artemia*

was less in the elutriates compared with the toxicity in artificial sea water (Figure 5.7). In the environment, the toxicity of pollutants may be ameliorated by the presence of the sediments.

Effects of light on the cytotoxicity and genotoxicity of Benzo[a]pyrene have been described in many studies (Botta et al., 2009; Fernandez and I'Haridon, 1994; Jiang et al., 2007). Light-irradiated PAHs are excited to upper energy states at the origin of electron or energy transfer to oxygen and biological molecules and produce reactive species which may induce DNA damage by several mechanisms. In the environment, exposure to light would therefore increase the toxicity of PAH-containing sediments..

5.4 Conclusions and future study

The toxic effects of RDS and BLS were studied in a range of bioassays, using water elutriates of sediments to simulate polluted receiving waters, and solvent extracts to represent the total contaminant levels. Chemical analyses showed that the total concentrations of metals and PAHs in the RDS were above the interim sediment quality guidelines, and were higher in the finer size fractions. Metal and PAH levels in the BLS were well below ISQG. To establish baseline toxicity data, acute *Artemia* nauplii tests were carried out with putatively identified compounds (heavy metals and PAHs identified from chemical analyses of similar sediments in Sydney), spiked into aqueous solutions and elutriates. The toxicity order of spiked RDS elutriates to *Artemia salina* was as follows: Cr^{6-}>Pb^{2+}>Cd^{2+}>Cu^{2+}>Zn^{2+} and Fl>Pyr>Chr>BaP>BbF. LMW PAHs showed greater toxicity than HMW PAHs. For spiked metals and PAHs, the toxicity to *Artemia* was significantly higher when they were tested in clean water than in elutriates. However, neither RDS nor BLS elutriates caused any toxicity in a 24-hour acute test with *Artemia* nauplii. In the Microtox® assay, both RDS and BLS elutriates showed some toxicity with TU values between 1.1-3.5 for RDS samples and 0.0-1.8 for BLS. RDS samples were more toxic than the BLS, but there was no significant difference between size fractions. The response patterns in the Microtox® assays suggested effects from both heavy metals and organic compounds. The AhR CAFLUX bioassay, which is sensitive to dioxin-like compounds including PAHs, showed relatively low activity in solvent extracts of RDS, with slightly higher activity in the finer fractions of the sediment. In all samples of BLS, no detectable AhR CAFLUX activity was observed. The p53 GeneBLAzer® assay showed no cytotoxic or genotoxic effects from any elutriates or solvent extracts of RDS or BLS.

The results indicate that the RDS presents a greater hazard than the BLS, particularly in the finer size fractions. The sediments are unlikely to be acutely toxic to aquatic organisms, but there was some non-specific sublethal toxicity and induction of the AhR response. The AhR activity is indicative of dioxin-like toxicity, which can result in effects such as teratogenesis, immunosuppression and tumour promotion, as well as endocrine disruption (Mimura et al 2003)(Mimura and Fujii-Kuriyama, 2003). Accumulation of RDS in estuarine sediment may pose a risk to benthic organisms, especially those that feed on and in the sediments.

Some of the assays used in this study proved to show little sensitivity to the elutriates of the RDS and BLS. This suggests low toxicity, but it would be advisable to extend the study with more sensitive assays. In spite of its frequent use in toxicological testing, earlier studies refer to *Artemia* as a less sensitive species for ecotoxicity testing (Dvorak et al., 2012; Sorgeloos et al., 2001). Other tests species such as sea urchin, copepods, amphipods, may be more sensitive. The GeneBLAzer assay also showed no effects in this study. DNA damage and genotoxicity can also be measured by the umuC test (Kennedy et al., 2010), the alkaline unwinding assay (Georgiou et al., 2009) and the comet assay (Slameňová et al., 1999). The umuC test can also be used to measure the genotoxicity after metabolic activation of different PAH compound (such as Benzo[a] pyrene) (Macova et al., 2011). These assays can be valuable tools in assessing general toxicity endpoints including cell viability and genotoxicity as well as specific endpoints including adaptive stress response activation and can replace the GeneBLAzer® in future studies.

A major factor that was beyond the scope of this study, was the marked increase in toxicity of PAHs caused by the effects of light (Arfsten et al., 1996). It would be highly recommended that the effects of light on the toxicity of the sediments should be tested in future work. This was not possible with the Microtox, AhR CAFLUX or p53 GeneBLAzer, but it would be possible to adapt the protocols for the *Artemia*, sea urchin, copepod, or amphipods tests, to include exposing the organisms to sunlight or controlled levels of UV radiation.

CHAPTER 6

ZEOLITE AND IRON-COATED ZEOLITE ADSORBENTS FOR REMOVING HEAVY METALS FROM RUNOFF WATER

Much of this chapter was published in Nguyen, T.C., P. Loganathan, T. V Nguyen, S. Vigneswaran, J. Kandasamy, R. Naidu. (2015). Simultaneous adsorption of Cd, Cr, Cu, Pb, and Zn by an iron-coated Australian zeolite in batch and fixed-bed column studies. Chemical Engineering Journal 270: 393-404.

CHAPTER 6

ZEOLITE AND IRON-COATED ZEOLITE ADSORBENTS FOR REMOVING HEAVY METALS FROM WATER

6.1. Introduction

The study reported in Chapter 3 shown that some heavy metals (Cu, Zn and Pb) accumulated in the RDS in Sydney and these heavy metals can be transported to nearby water bodies by stormwater. Therefore, these heavy metals need to be removed from the stormwater. There are many chemical and physical processes to remove heavy metals from water. Of these, adsorption is one of the promising technologies due to its high removal efficiency, and simplicity, provided easy availability of low-cost adsorbent can be found locally. Locally available zeolites have been utilized as low-cost adsorbents for the removal of heavy metals in many countries (Baker et al., 2009; Hamidpour et al., 2010; Wang and Peng, 2010). Wang and Peng (2010) presented the adsorption capacities of natural zeolites from several countries reported in literature for Cd, Cr, Cu, Co, Mn, Ni, Pb, and Zn. They stated that these information were obtained from adsorption in solutions containing only one metal which may not be directly applicable to real wastewater system where there are several metal ions co-exist and they may compete with each other for adsorption. The difference in adsorption capacities between metals are commonly explained using hydration energy, hydrolysis constant, electro-negativity, and hydroxide solubility product of the metals (Minceva et al., 2007).

Some studies have shown that modification of zeolite surface by coating with iron (ICZ) can enhance the adsorption capacity of the zeolite for heavy metals (Dimirkou and Doula, 2008; Doula, 2009; Han et al., 2009; Jeon et al., 2012; Kragović et al., 2012). In batch experiments, Han et al. (2009) found that an iron oxide coated zeolite had greater adsorption capacity than zeolite for Cu. They reported that of the three models used, Thomas model described the adsorption of Cu on the iron oxide coated zeolite in fixe-bed column the best at all flow rates, initial Cu concentrations, and bed depths. Similarly, Kragović et al. (2012) showed that an iron oxide coated zeolite had higher adsorption capacity than zeolite for Pb. In contrast to the

above single-metal adsorption studies, Doula (2009) reported that an iron modified zeolite had higher adsorption capacities than unmodified zeolite for Cu, Zn, and Mn from a solution containing all these metals in batch studies. At high metals concentrations, Mn adsorption by both modified and unmodified zeolite decreased due to competition from Zn and Cu. They also found that Zn adsorption marginally decreased and Cu adsorption was similar to the adsorption pattern of Cu-only solution. The affinity of the metals for both modified and unmodified zeolite followed the order, Cu > Zn > Mn.

Most of the studies using zeolite or ICZ were conducted only in static batch experiment or on individual metals. Studies using fixed-bed column which are more relevant to real operating systems on natural waters are necessary. Results of batch adsorption studies which are conducted under static condition may sometimes be different from those conducted in dynamic column adsorption system (Loganathan et al., 2014). For example, Baker et al. (2009) reported that the metal adsorption capacity for a Jordanian zeolite followed the order Pb > Cd > Cu > Zn but the order in column adsorption system was Cd > Zn > > Pb > Cu. As many metals co-exist in water they can compete with each other for adsorption and therefore it is important to consider the simultaneous removal of co-existing metals. Therefore, the aim of this research was to determine the adsorption behaviour of Cd, Cu, Cr, Pb, and Zn individually and simultaneously on an Australian natural zeolite with and without iron-coating, after their thorough characterisation, in batch and column experiments and determine the mechanisms of adsorption. Desorption of the adsorbed metals and stability of the iron-coatings were also determined. Simultaneous adsorption of several heavy metals in fixed-bed columns and their modelling, and an investigation of the iron-coatings' stability in zeolite during desorption of metals are novel features of this study.

6.2. Materials and Methods

6.2.1. Preparation of iron-coated zeolite (ICZ)

The zeolite used in this study was obtained from an Australian natural deposit at Werris Creek, New South Wales and supplied by Zeolite Australia Pty Ltd., Australia, locally available low cost material. The ICZ was prepared by a method similar to that of Doula's method (Doula, 2009) by mixing 20.0 g of zeolite, 100 mL of freshly prepared 1 M $Fe(NO_3)_3$, and 180 mL of 5 M KOH in a 2 L glass flask. KOH solution was added rapidly to $Fe(NO_3)_3$

with continued stirring. The suspension was diluted to 2 L with deionized water and was held for 60 hours in the closed polyethylene flask at 70^{o}C. At the end of this period the reaction vessel was removed from the oven, and the precipitate was centrifuged, washed with distilled water (until free of NO_3^- ions) and then dried. During the 60 h period the suspension was observed to be converted from a red brown colour to a compact red-brown precipitate. This change was explained by Doula (Doula, 2009) to be a conversion of ferrihydrite to geothite.

6.2.2. Characteristic of the materials

The mineralogy of the zeolite was determined using a XRD Shimadzu S6000 (Japan) diffractometer on powder samples of the zeolite and ICZ. The X-ray diffractometer was equipped with a Cu target operated at 40 kV and 30 mA with a setting of 5–45^{o} (2θ), step time 2^{o}/min. Scanning electron microscopy (SEM), Fourier transform infrared (FTIR) spectroscopy, surface area, and porosity measurements were also conducted on zeolite and ICZ. For the SEM analysis, the samples were imaged, uncoated, in a Zeiss Evo LS15 SEM using its variable pressure mode and an accelerating voltage of 15 kV. FTIR pattern was recorded using a Nicolet 6700 FT-IR Spectrometer equipped with a room temperature DLaTGS detector and a Nicolet FT-IR Smart System with Smart Accessories using a diamond crystal HATR.

Surface area and porosity were determined by nitrogen-sorption measurements carried out at 77 K with a Micromeritics 3 Flex surface characterization analyser. The BET method was used to calculate the specific surface area. The pore size distribution was derived from the adsorption branch of the isotherm by using the Barrett–Joyner–Halenda (BJH) method.

Samples of zeolite and ICZ were analysed by Energy-dispersive X-ray spectroscopy (EDS). An EDS system called JED-2300/2300F Analysis Station was used to determine the chemical elemental composition.

Zeta potentials were measured on the suspensions of zeolite and ICZ in deionised water at an ionic strength of 10^{-3} M $NaNO_3$ and initial pH ranging from 3.0 to 9.0. The pH adjustment was made utilising 0.1 M NaOH or 0.1 M HNO_3 solutions and the pH was measured using a portable pH meter. The suspensions were agitated in a flat shaker at a shaking speed of 120 rpm at room temperature (25 ± 2^{o}C) for 8 h. At the end of the period, the pH (equilibrium

pH) and zeta potential were determined. Zeta potential was measured using a zeta sizer nano instrument (Nano ZS Zen3600, Malvern, UK).

6.2.3. Chemical analysis

All chemicals used were of analytical reagent grade. Heavy metal nitrates, NaOH, and HNO_3 were supplied by Sigma-Aldrich, Australia (reagent grade) and they were used as received. Stock solutions of Pb, Zn, Cu, Cd and Cr were prepared using $Pb(NO_3)_2$, $Zn(NO_3)_2$ $6H_2O$, $Cu(NO_3)_2$ $5H_2O$, $Cd(NO_3)_2$ $4H_2O$, and $Cr(NO_3)_3$ $9H_2O$, respectively. The initial pH of the test solutions was adjusted to the desired value by using dilute solutions of 0.1 M NaOH and 0.1 M HNO_3. Heavy metal analyses were made using a Microwave Plasma-Atomic Emission Spectrometer (MP-AES- 4100 Agilent).

6.2.4. Batch adsorption experiment

6.2.4.1. Equilibrium experiments

Batch mode experiments on adsorption of heavy metals on zeolite and ICZ from solutions containing single and mixed metals at an initial concentration of 50 mg/L and ionic strength of 10^{-3} $NaNO_3$ was conducted at a temperature of 25 ± 2°C. Zeolite or ICZ were added to 100 mL metal solutions contained in glass bottles to provide adsorbent loading rates of 1.0 to 25.0 g/L. The bottles were sealed and agitated at 120 RPM for 24 hours in an orbital shaker. The pH of the suspension was maintained at 6.5 ± 0.2. The suspensions were filtered through a 0.45 µm nylon syringe filter (Cole-Parmer) and heavy metals concentrations were measured using a Microwave Plasma-Atomic Emission Spectrometer (MP-AES- 4100 Agilent). The amount of heavy metal adsorption at equilibrium, q_e (mg/g), was calculated using equation (1),

$$q_e = \frac{(C_o - C_e)\,V}{M} \qquad (1)$$

where, C_o = initial concentration of heavy metal (mg/L); C_e = equilibrium concentration of the heavy metal (mg/L); V = volume of the solution (L) and M = mass of adsorbent (g). The adsorption data were fitted to the Langmuir, Freundlich and Dubinin–Radushkevick adsorption isotherm which are described in Table 6.1.

Table 6. 1. The models and equations used for the description of batch and column adsorption of heavy metals (HM) by zeolite and ICZ

Method	Model	Equation	Graphical method used to calculate model constant
Batch	Langmuir	$q_e = \frac{q_{max} K_L C_e}{1 + K_L C_e}$	$\frac{C_e}{q_e} = \frac{1}{q_{max} K_L} + \frac{C_e}{q_{max}}$
		C_e = equilibrium concentration of HM (mg/L), q_e = amount of HM, C_e = equilibrium concentration of HM (mg/L), q_e = amount of HM adsorbed (mg/g), q_{max} = maximum amount of HM adsorbed (mg/g); K_L = Langmuir constant related to the energy of adsorption (L/mg)	
	Freundlich	$q_e = K_F C_e^{1/n}$	$lnq_e = lnK_F + \frac{1}{n} \ln C_e$
		C_e = the equilibrium concentration of the adsorbate (mg/L); q_e = the amount of adsorbate adsorbed per unit mass of adsorbent (mg/g); and K_F, n = Freundlich constants.	
	Dubinin–Radushkevick isotherm	$q_e = q_m \exp(-\beta\varepsilon^2)$	$\ln(q_e) = \ln(q_m) - \beta\varepsilon^2$
		q_e = the amount of heavy metal adsorbed per unit dosage of the adsorbent (mg/g); q_m= the monolayer capacity, and β is the activity coefficient related to mean sorption energy and ε is the Palanyi potential described as: $\varepsilon = RT \ln[1 + (\frac{1}{Ce})$	
	Pseudo-first order kinetic	$\frac{dq_t}{dt} = k_1(q_e - q_t)$	$\ln (q_e - q_{t)} = \ln q_e - k_1 t$
		q_e = amount of HM adsorbed at equilibrium (mg/g); q_t = amount of HM adsorbed at time, t (min) (mg/g) and k_1 = equilibrium rate constant of pseudo-first order sorption (1/min)	

	Pseudo-second order kinetic	$\frac{dq_t}{dt} = k_2(q_e - q_t)^2 \quad \frac{t}{q_t} = \frac{1}{k_2 q_e^2} + \frac{t}{q_e}$ q_e = amount of HM adsorbed at equilibrium (mg/g); q_t = amount of HM adsorbed at time, t (min) (mg/g) and k_2 = equilibrium rate constant of pseudo-second order (1/min)
	Weber and Morris	$q_t = k_p t^{0.5} + C$ q_t = amount of HMs adsorbed at time t (min) (mg/g); k_p = intra-particle diffusion rate constant; C = a constant
Column	Thomas	$\ln(C_o/C_t) - 1 = k_{Th} q_0 M/Q - k_{Th} C_o t$ k_{Th}= Thomas rate constant (mL/min mg), q_o= equilibrium HM uptake per g of zeolite (mg/g), C_0 = inlet HM concentration (mg/L), C_t= outlet HM concentration at time t (mg/L), M = mass of zeolite (g), Q = filtration velocity (mL/min) and t = filtration time (min)

6.2.4.2. Kinetic experiments

Batch adsorption kinetic experiments were conducted on single and mixed metals solutions at a heavy metal concentration of 5 mg/L each in a set of glass flasks containing 100 mL of heavy metal solution and adsorbent dosage of 2.0 g/L at an ionic strength of 10^{-3} M $NaNO_3$ and pH 6.5. The suspensions were agitated in a flat shaker at 120 RPM for 72 hours at room temperature (25 ± 2°C). Aqueous samples were taken at different time intervals and the concentrations of heavy metals were measured. The amounts of heavy metals adsorption at time t, q_t (mg/g), were calculated using equation (2):

$$q_t = \frac{(C_o - C_t)\,V}{M} \qquad (2)$$

where C_o = the initial concentration of heavy metals (mg/L); C_t = the concentration of heavy metals at time t (mg/L); V = the volume of the solution (L) and M = the mass of dry adsorbent (g).

The adsorption data were analysed using pseudo-first and pseudo-second order kinetic models and the intra-particle diffusion model of Weber and Morris (Weber and Morris, 1963). The equations for these models and the methods of calculating the model parameters are presented in Table 6.1.

6.2.5. Column experiments

Fixed-bed columns used in this study were made up of 2.5 cm inner diameter Pyrex glass tube with a stainless steel sieve attached to the bottom of the column, followed by a layer of glass beads in order to provide a uniform flow of the solution through the column. A known quantity (40 g) of the zeolite or ICZ was packed in the column to yield a bed height of 10 cm. Heavy metals solutions containing individual or mixed metals at concentrations of 5 mg/L, each were pumped downward through the column at a filtration velocity of 0.52 m/h (8 mL/min) to yield a bed volume of 0.038 L and an empty bed contact time of 11.5 min, controlled by a peristaltic pump (Figure 6.1). The effluents at the outlet of the column were

collected at regular time intervals and the heavy metals concentrations were measured using a Microwave Plasma-Atomic Emission Spectrometer (MP-AES- 4100 Agilent).

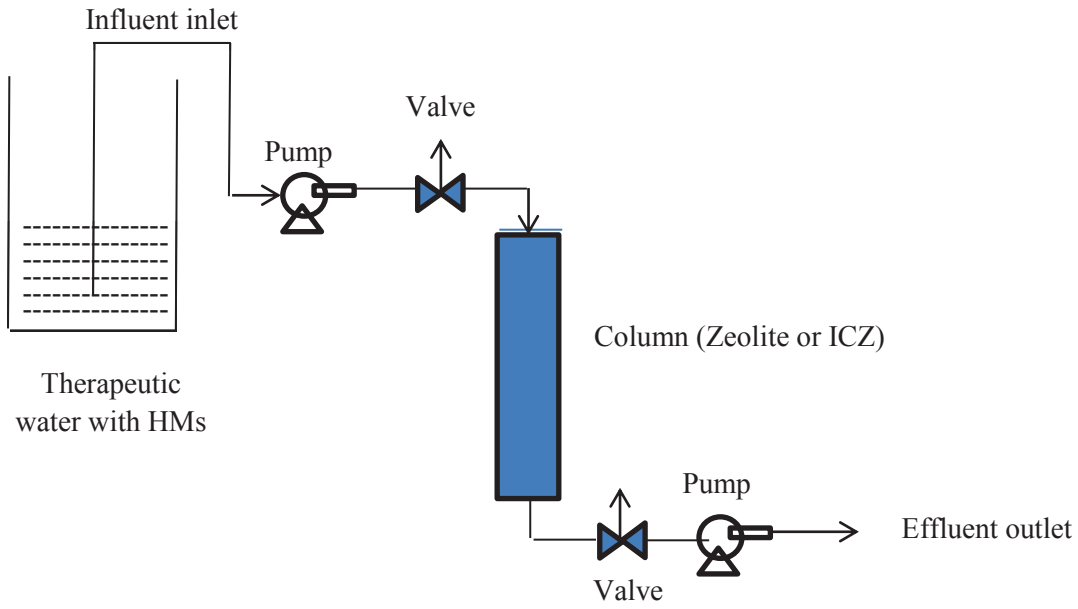

Figure 6.1. Column experimental set-up

6.3. Results and discussion

6.3.1. Characteristics of materials

The XRD and FTIR patterns of ICZ were similar to those of zeolite and therefore only patterns of zeolite are presented (Figure 6.2 and 6.3). The XRD spectra of zeolite showed that the zeolite comprised primarily of heulandite (2θ: 10.0^o, 19.0^o, 22.7^o, 30.0^o) (Deshpande and Bhoskar, 2012; Treacy and Higgins, 2007) and small amount of quartz (2θ: 21.0^o, 27.0^o, 36.5^o) (Figure 6.2) (Jamil et al., 2010; Mozgawa, 2000). X-ray diffractograms of ICZ revealed no notable change in the basic zeolite diffraction peaks, indicating no detectable damage to the zeolite framework, or the presence of additional Fe oxidic or oxo-hydroxidic crystalline phases resulting from the iron oxide coating of the zeolite. However, XRD cannot detect any amorphous Fe species that may have formed on the zeolite surface. Therefore the Fe coatings might have present as amorphous Fe oxides.

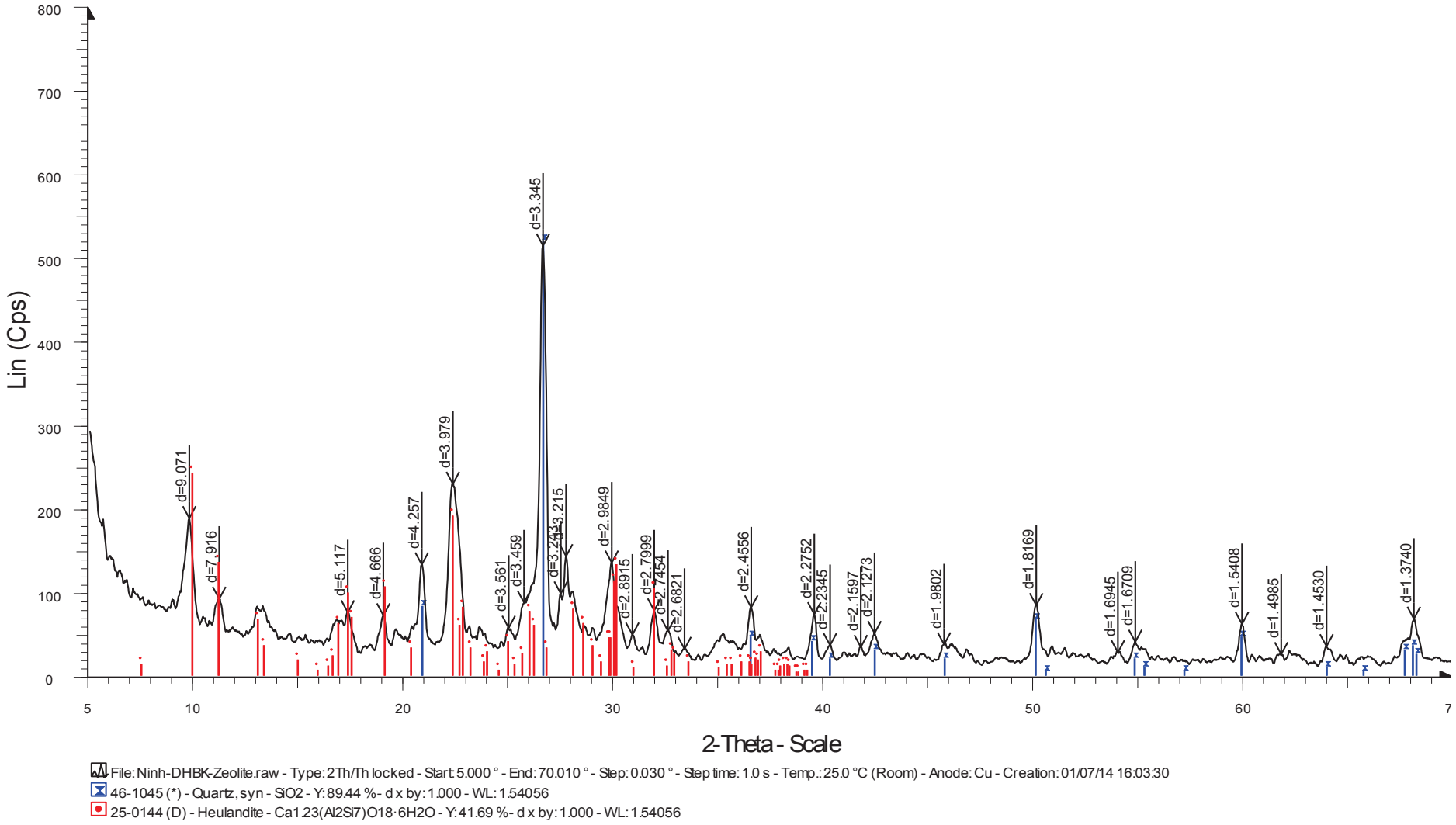

Figure 6.2. XRD patterns of zeolite

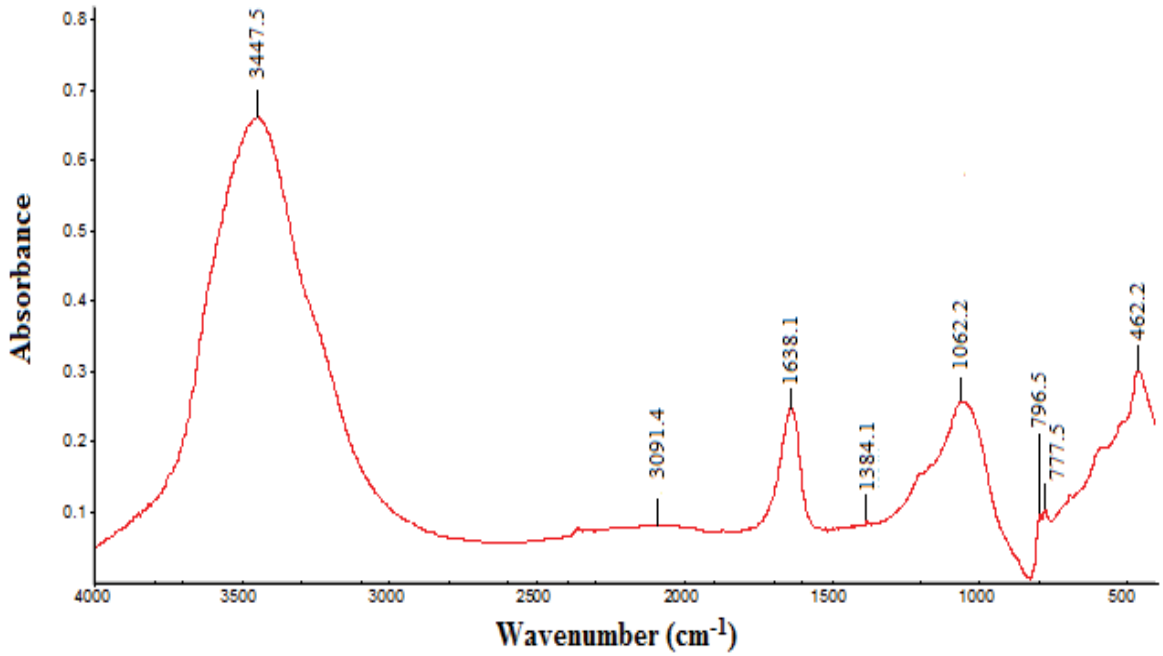

Figure 6.3. FTIR spectra of zeolite

Figure 6.3 shows the FTIR spectra for zeolite. The peak at 1048 cm^{-1} is attributed to asymmetric O–T–O stretching vibration (vO-T-O) where T represent Si or Al (Doula et al., 2002). The peak at 462 cm^{-1} is probably from the bending of the bonds inside TO_4 (Doula, 2007). The peaks at 3447 cm^{-1} and 1638 cm^{-1} can be assigned to the stretching vibration mode of lattice water and hydroxyl groups and OH bending vibration mode of adsorbed water molecules (Nur et al., 2014).

The surface area (BET) of zeolite and ICZ were 15.4 g/m^2 and 7.51 g/m^2, respectively. The lower surface area of ICZ compared to zeolite is probably due to the blockage of the pores in zeolite by the iron oxide coatings. EDS data showed that the Fe content of ICZ was 8.46% while that of zeolite was only 1.03 % (Figure 6.4).

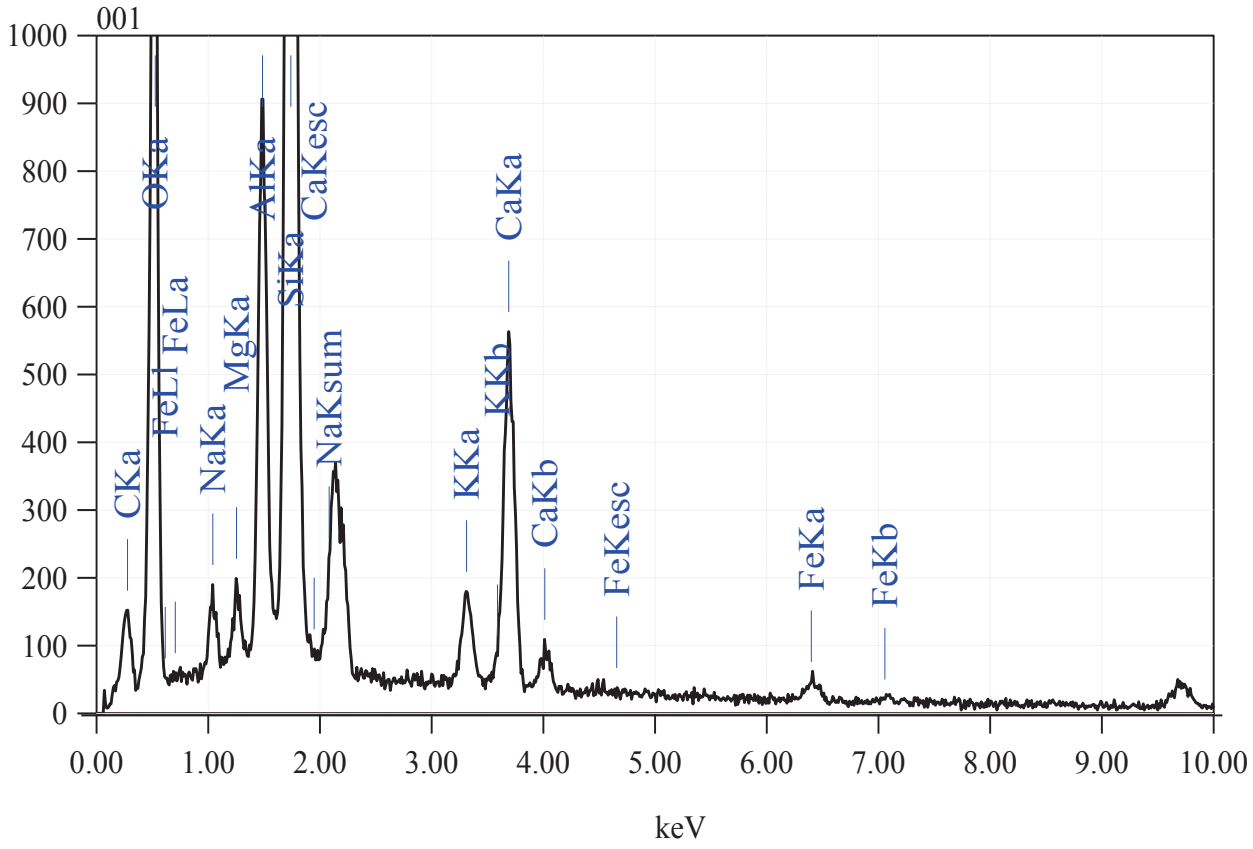

Figure 6. 4 (A). EDS results of Zeolite

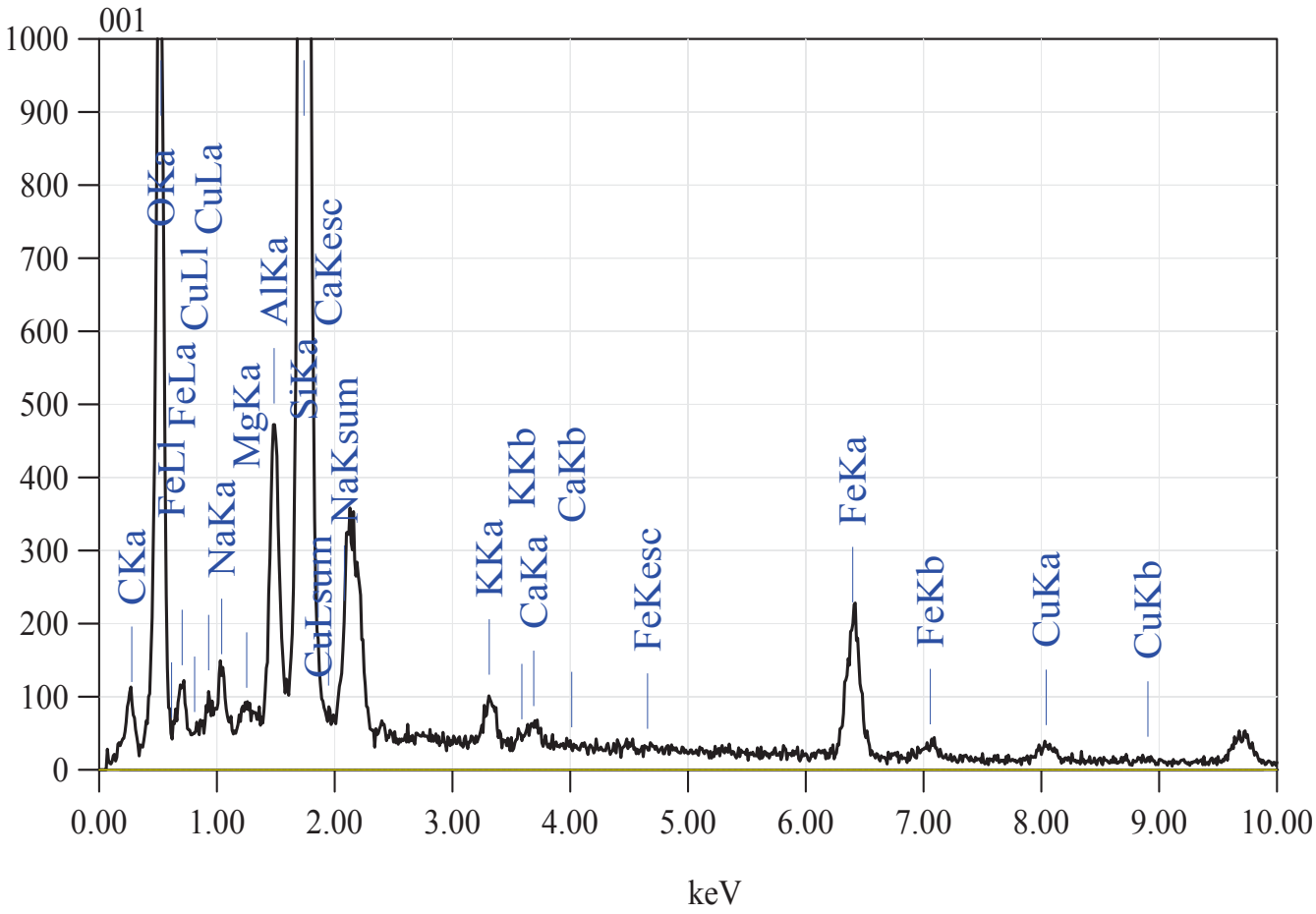

Figure 6.4 (B). EDS results of ICZ

A distinct difference in the surface morphology of zeolite and ICZ can be observed in the SEM photographs (Figure 6.5). The coated zeolite surfaces were apparently occupied by clusters of newborn iron oxides, which were formed during the iron oxide coating process.

The negative zeta potentials of zeolite at all pHs (pH 3.0 to 9.0) were higher than those of ICZ (Figure 6.6). The zero point of charge (pH at which the net surface charge on the particle is zero) of zeolite was approximately pH 2.2 whereas that of ICZ was nearly pH 5.6. This shows that more negative charges were available in zeolite than in ICZ. Therefore, zeolite is expected to adsorb more heavy metals cations than ICZ if the adsorption is due to electrostatic attraction (coulombic forces). However, ICZ may adsorb more heavy metals than zeolite if the adsorption is dominated by specific adsorption (chemical adsorption) on the iron oxides at the zeolite surface.

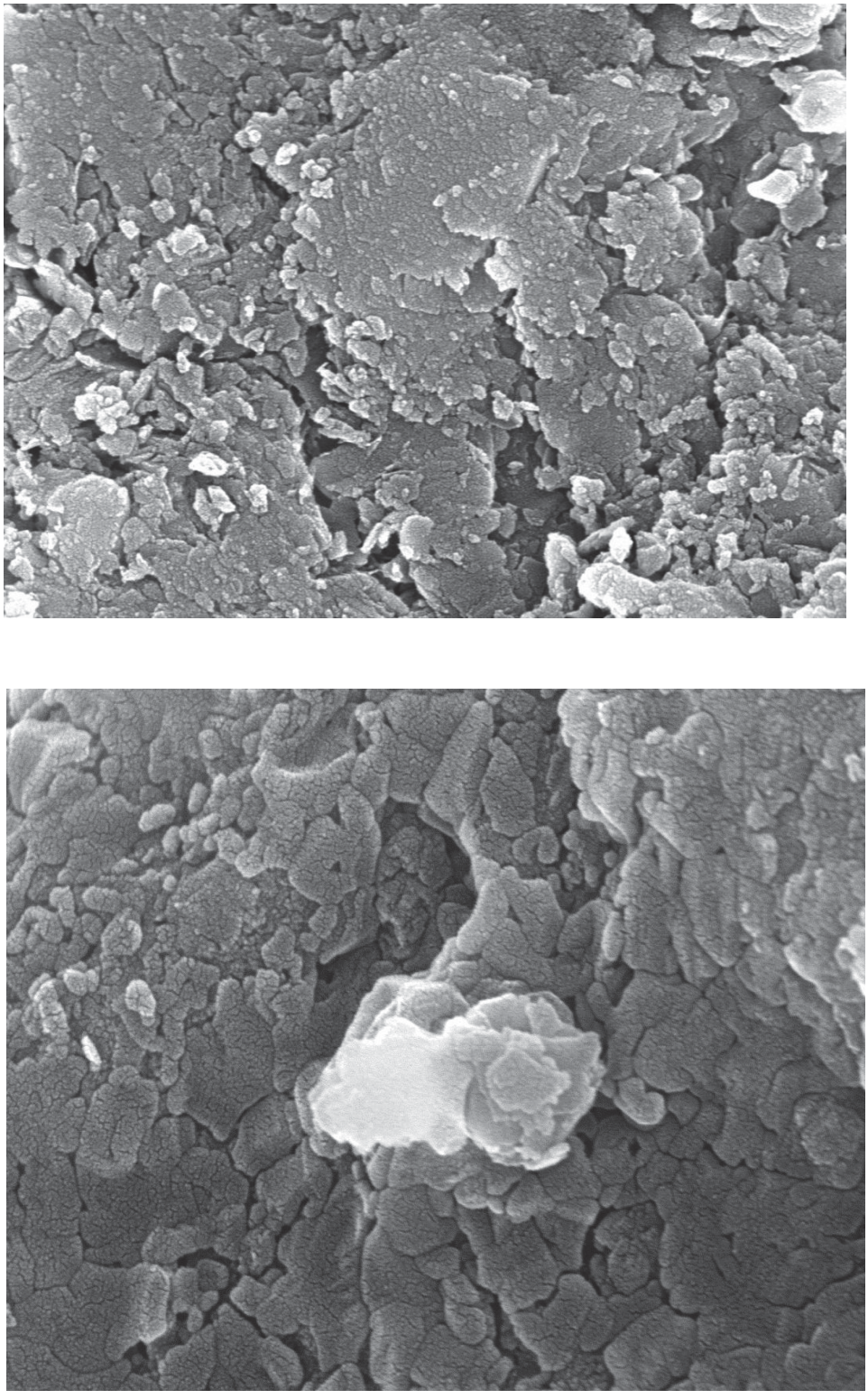

Figure 6.5. SEM images of zeolite (up) and ICZ (down) at 40.000 X magnification

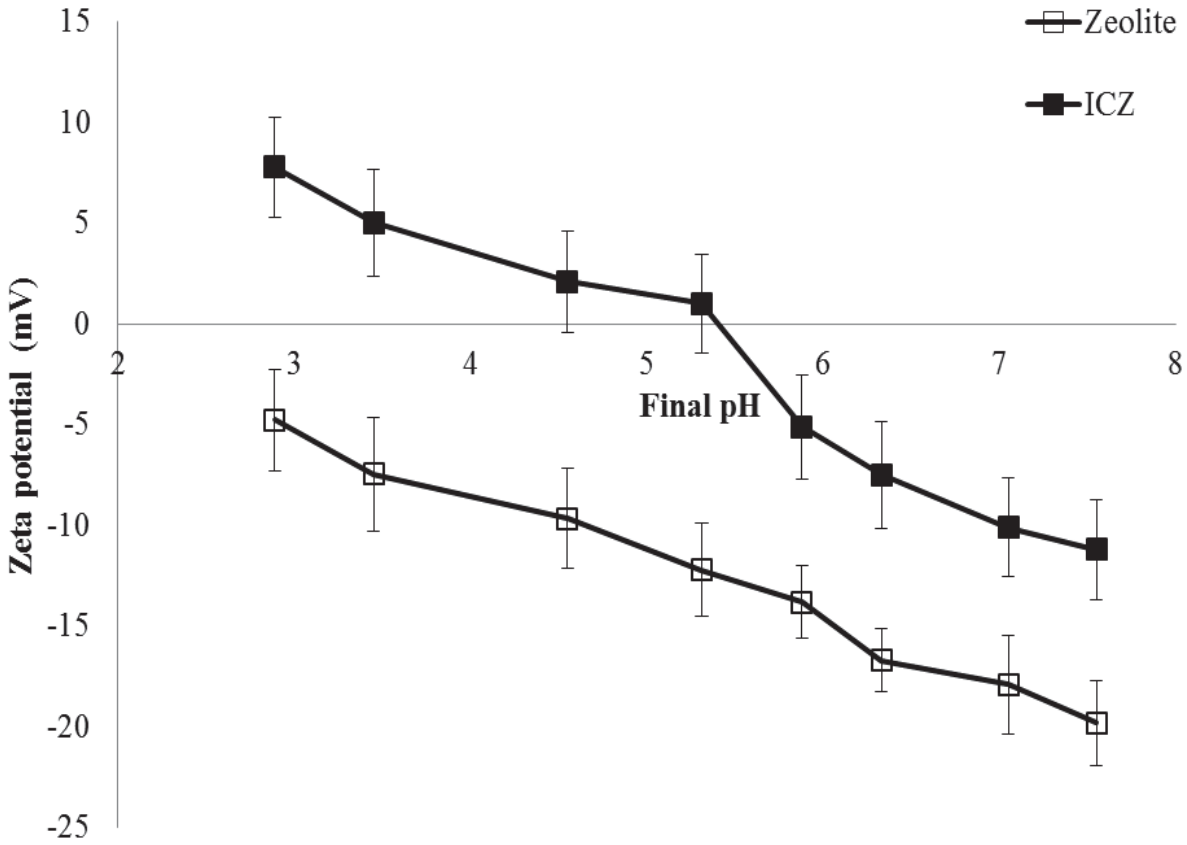

Figure 6.6. Zeta potential of zeolite and ICZ suspensions at an ionic strength 10^{-3}M $NaNO_3$

6.3.2. Batch experiment

6.3.2.1. Batch equilibrium adsorption modelling

The adsorption isotherms for individual and mixed metals showed that the adsorption capacity decreased in the following order: Pb > Cu > Cd > Zn, Cr (Figure 6.7 and Figure 6.8) and the adsorption of the metals capacities on ICZ was higher than those on zeolite. The data for the adsorption of all metals from single metal solution as well as from the mixed metals solution satisfactorily fitted to the Langmuir adsorption models. However, the fits were better for single metal solutions than for mixed metal solution probably because of competition for adsorption between metals in the mixed metals solution (Table 6.2). Competition for adsorption of metals is reflected in the lower Langmuir adsorption capacity for each metal in mixed metals system than in single metal system. The data fits to two other adsorption models, i.e. Freundlich (single metal solution, R^2 = 0.905-0.985; mixed metals solution, R^2 = 0.450-0.876) and Dubinin-Radushkevich models (Karthikeyan et al., 2009) (single metal solution, R^2 = 0.526-0.870; mixed metals solution, R^2 = 0.682-0.971) were less satisfactory than the Langmuir model fits (Table 6.3 and Table 6.4).

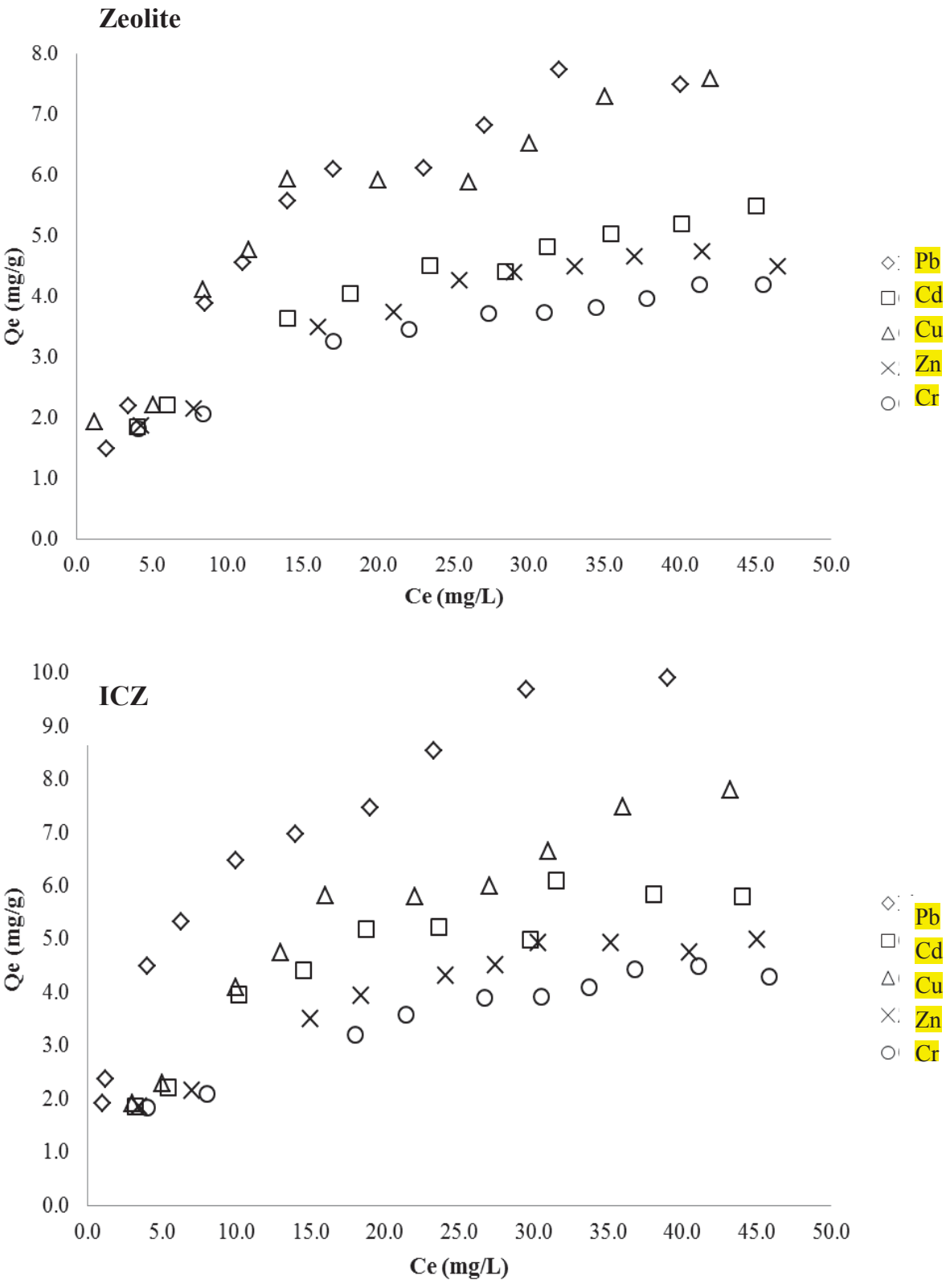

Figure 6.7. Batch adsorption isotherms for individual metals on zeolite and ICZ at ionic strength 10^{-3} M $NaNO_3$ and pH 6.5

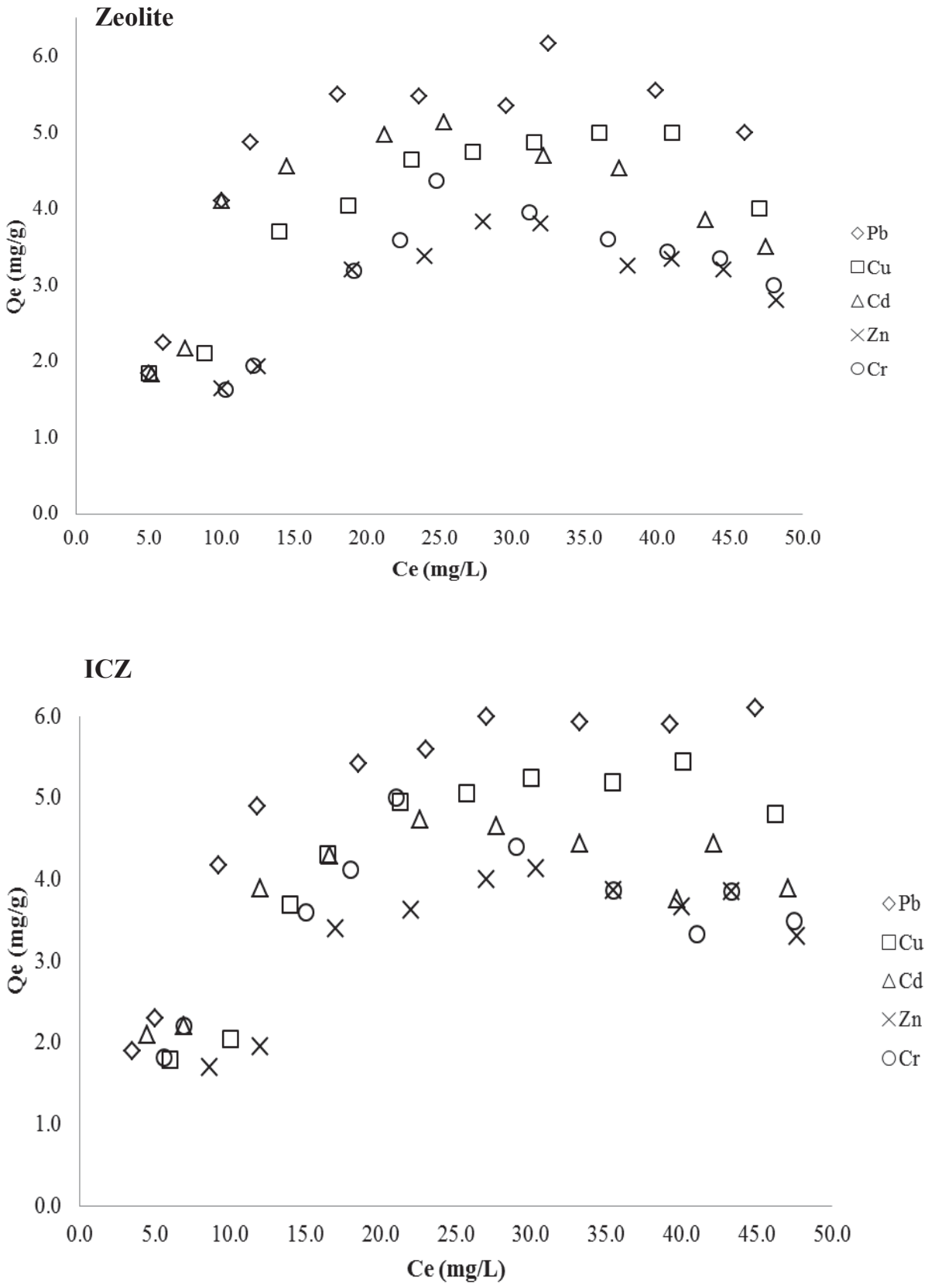

Figure 6.8. Batch adsorption isotherms for metals mixture on zeolite and ICZ at ionic strength 10^{-3} M $NaNO_3$ and pH 6.5

Table 6.2. Langmuir adsorption isotherm parameters for heavy metals (HM) adsorption on zeolite and ICZ at pH 6.5 and ionic strength 10^{-3} M $NaNO_3$

	HM	Individual metal (C_e = 0 – 50 mg/L)			Metals mixture (C_e = 0 – 30 mg/L)		
		Qmax (mg/g)	K_L (L/mg)	R^2	Qmax (mg/g)	K_L (L/mg)	R^2
Zeolite	Pb	9.97	0.083	0.985	6.54	0.139	0.922
	Cu	8.53	0.200	0.937	4.34	0.417	0.743
	Cd	6.72	0.840	0.992	4.20	0.810	0.897
	Zn	5.83	0.095	0.985	3.72	0.163	0.847
	Cr	5.03	0.103	0.990	4.01	1.001	0.821
ICZ	Pb	11.16	0.157	0.982	7.63	0.059	0.938
	Cu	9.33	0.095	0.946	6.11	0.099	0.780
	Cd	7.24	0.110	0.976	4.42	0.442	0.951
	Zn	6.22	0.095	0.985	4.61	0.105	0.859
	Cr	5.47	0.092	0.983	3.89	0.594	0.932

Table 6.3. Freundlich isotherm model parameters for the adsorption of heavy metals on zeolite and iron coated zeolite (ICZ) from solutions containing individual and mixed metals at an ionic strength of 10^{-3} M $NaNO_3$ and pH 6.0 and coefficients of determination for the Freundlich isotherm fit to data (R^2)

Metals		Individual metal			Metal mixture		
		K_F $(mg/g)(L/mg)^{1/n}$	n	R^2	K_F $(mg/g)(L/mg)^{1/n}$	n	R^2
Zeolite	Pb	1.01	1.81	0.972	1.18	2.21	0.738
	Cu	1.61	2.37	0.905	1.09	2.42	0.612
	Cd	1.04	2.24	0.982	1.51	3.28	0.450
	Zn	1.00	2.36	0.958	1.21	2.56	0.546
	Cr	1.05	2.68	0.966	0.80	2.38	0.508
ICZ	Pb	2.29	2.21	0.985	1.28	2.21	0.876
	Cu	1.85	1.09	0.964	0.81	1.93	0.722
	Cd	2.17	1.17	0.924	1.60	3.45	0.595
	Zn	1.06	2.33	0.961	1.31	2.23	0.678
	Cr	2.52	1.01	0.974	1.40	3.40	0.512

Table 6.4. The Dubinin–Radushkevick isotherm model parameters for the adsorption of individual and mixed heavy metals (5 mg/L) on zeolite and iron coated zeolite (ICZ) from solutions containing mixed metals at an ionic strength of 10^{-3} M $NaNO_3$ and pH 6.0 and coefficients of determination for the Langmuir isotherm fit to data (R^2)

Metals		Individual metal			Metal mixture		
		q_m (mg/g)	β (mol^2/kJ^2)	R^2	q_m (mg/g)	β (mol^2/kJ^2)	R^2
Zeolite	Pb	6.04	2×10^{-6}	0.831	5.77	6×10^{-6}	0.971
	Cu	4.71	4×10^{-7}	0.870	4.39	5×10^{-6}	0.682
	Cd	5.46	5×10^{-7}	0.526	4.62	5×10^{-6}	0.772
	Zn	4.27	4×10^{-6}	0.793	3.62	1×10^{-5}	0.815
	Cr	3.74	3×10^{-6}	0.745	3.93	2×10^{-5}	0.805
ICZ	Pb	7.40	5×10^{-7}	0.862	5.74	3×10^{-6}	0.930
	Cu	5.22	3×10^{-6}	0.828	4.97	8×10^{-6}	0.783
	Cd	6.06	3×10^{-6}	0.789	4.29	2×10^{-6}	0.746
	Zn	4.40	3×10^{-6}	0.740	4.02	1×10^{-5}	0.865
	Cr	3.92	3×10^{-6}	0.733	4.10	5×10^{-6}	0.823

The adsorption capacities of zeolite (Table 6.2) are comparable to those reported for zeolites from other countries. For example, a zeolite from Greece had Langmuir adsorption capacities (mg/g) of 3.5, 4.1, 4.6, and 5.9 for Zn, Cr, Cd, and Cu, respectively (Alvarez-Ayuso et al., 2003). Another study done in South Korea revealed that a zeolite had Langmuir adsorption capacities (mg/g) of 6.5, 7.1, and 8.9 for Cu, Cd, and Pb, respectively (Jeon et al., 2012). The adsorption capacities of ICZ (Table 6.2) are higher than those of zeolites and many other low-cost adsorbents. For example, Mishra and Patel (Mishra and Patel, 2009) reported Langmuir adsorption capacity values (mg/g) of 4.5, 5.0, 5.5, and 7.6 for Pb adsorption at pH 6.0 on kaolin, fly ash, blast furnace slag, and bentonite, respectively. The corresponding values for Zn were 3.1, 5.8, 3.3, and 9.1, respectively. The values reported for Cr and Pb adsorption on fly ash in another study at pH 5 and 6 were 4.4 and 2.5 mg/g, respectively (Gupta et al., 2003). However, the adsorption capacities of ICZ are lower than those of nano-sized metal oxides, carbon nanotubes and commercial ion exchangers (Hua et al., 2012; Rao et al., 2007; Sounthararajah et al., 2015). Nevertheless, the advantages of zeolite and ICZ over the other adsorbents are their low cost and their ability to be conveniently used directly in fixed-bed columns, because they have larger particles and better physical stability. The adsorption capacities of ICZ were not very much higher than zeolite probably because the loading of fe onto the zeolite was not high. Higher Fe loadings may increase the adsorption capacities further. Future studies need to test this suggestion.

The Langmuir maximum adsorption capacity order for the metals in the single metal and mixed metals systems was Pb > Cu > Cd > Zn, Cr. The adsorption capacities for all metals except for Cr were higher for ICZ than for zeolite on both single metal and mixed metals system. Doula et al (2009) also reported that the adsorption of Cu was higher than Zn on a zeolite and a Fe-modified zeolite in single and mixed metals systems. For both metals the adsorption of Fe-modified zeolite was higher than that of zeolite. The adsorption capacities of ICZ were not very much higher than zeolite probably because the loading of Fe onto the zeolite was not high. Higher Fe loadings may increase the adsorption capacities. Future studies need to test this.

The reason for ICZ having higher adsorption capacities than zeolite, despite the higher ZPC of the former, is that ICZ has iron oxide which specifically adsorbs heavy metals (Loganathan et al., 2012). The mechanism of adsorbing heavy metals on zeolite is predominantly outer-sphere complexation (non-specific adsorption) via the ion exchange

process where the counter balanced alkali and alkalai earth metal ions, Ca^{2+}, Mg^{2+}, Na+, and K+ in the exchangeable sites on zeolite are replaced by heavy metal ions (Dimirkou and Doula, 2008). Some heavy metal ions can also adsorb onto the terminal Al-OH and Si-OH surface sites by inner-sphere complexation (specific adsorption) by releasing protons (H^+) (Dimirkou and Doula, 2008; Qiu and Zheng, 2009). In the case of ICZ the presence of iron oxides on the zeolite surface would have further increased the adsorption of heavy metals by inner-sphere complexation due to abundant Fe-OH sites in the iron oxides. Strong affinity of iron oxides to heavy metals has been documented in many studies (McBride, 1989). At high pH (pH 6-7), depending on the metal) the removal of large amounts of heavy metals is due to adsorption of metal hydroxide (MOH^+, where M represents metal) species from solution and surface precipitation of metal hydroxide (Loganathan et al., 2012). Metal hydroxide species have higher affinity than divalent metal ions for adsorption on aluminosilicate and metal oxide surfaces.

The order of the adsorption capacities of the metals (Pb > Cu > Cd > Zn and Cr) can be explained by the first hydrolysis constant of the metals (MOH^+ formation) and solubility product of the metal hydroxides. The lower the first hydrolysis constant, the greater the proportion of MOH^+ which has stronger adsorption than M^{2+} among the various metal species in solution. High solubility product favours precipitation of metals, especially on the surface of adsorbents which can occur at a pH lower than the pH of precipitation in solutions (Loganathan et al., 2012). Lead hydroxide has the highest solubility product and lowest first hydrolysis constant; consequently it had the highest adsorption capacity (Sounthararajah et al., 2015). The second metal which had the highest adsorption capacity was Cu. The reason for this is that it has the second highest solubility product and second lowest hydrolysis constant.

6.3.2.2. Batch adsorption kinetics modelling

Adsorption of all metals from single metal and mixed metals solutions on both zeolite and ICZ increased with time and reached equilibrium only at approximately 20 h. The kinetic adsorption data fitted satisfactorily to both pseudo-first and pseudo-second order models for both single and mixed metals system (Table 6.5 and Table 6.6). The models predicted equilibrium adsorption capacities were approximately equal to the corresponding

experimental values for both models. When the R^2 values were considered, however, the pseudo-second order model appeared to fit the data better than the pseudo-first order model. The better fit of the pseudo-second order model suggests that chemical process may be the rate-limiting step in the adsorption (Nur et al., 2014).

The intra-particle diffusion model plot of the data is shown in Figure 6.9. According to Weber and Morris (1963), if intra-particle diffusion occurs the plot would be linear and if the plot passes through the origin then the rate limiting process is only the intra-particle diffusion. The data, however, exhibited two or more linear portions (Figure 6.9). The first linear portion up to 4 hours was a fast step which can be attributed to heavy metal transport by film diffusion and adsorption on the external surfaces. This is followed by a slow step where intra-particle diffusion of heavy metal through the pores and channels of the adsorbent occurs which is represented by the second straight line. As the entire plot was not linear and did not pass through the origin, both film diffusion and intra-particle diffusion appeared to have occurred simultaneously during the adsorption process. The third step which occurred beyond 16 hours was the equilibrium stage where the adsorption sites were saturated and the intra-particle diffusion process was nearly completed.

Table 6.5. Pseudo-first order and pseudo-second order kinetics models parameters for the adsorption of heavy metals (HM) onto zeolite and ICZ from single metal solutions at pH 6.5 and ionic strength 10^{-3} M $NaNO_3$

Zeolite

HM	Initial conc. (mg/L)	q_e exp.	Pseudo-first order			Pseudo-second order		
			q_e (mg/g)	K_1x10^{-2} (min^{-1})	R^2	q_e (mg/g)	K_2x10^{-2} (min^{-1})	R^2
Pb	5.04	4.6	5.39	0.27	0.893	6.17	0.19	0.998
Cu	5.23	4.0	2.90	0.15	0.924	4.61	0.27	0.997
Cd	5.12	4.6	4.57	0.24	0.962	5.32	0.39	0.999
Zn	5.10	4.0	3.25	0.25	0.953	4.54	0.46	0.999
Cr	4.87	2.5	3.15	0.20	0.992	4.04	0.42	1.000

ICZ

HM	Initial conc. (mg/L)	q_e exp.	Pseudo-first order			Pseudo-second order		
			q_e (mg/g)	K_1x10^{-2} (min^{-1})	R^2	q_e (mg/g)	K_2x10^{-2} (min^{-1})	R^2
Pb	4.89	5.1	4.08	0.16	0.984	5.29	0.21	1.000
Cu	5.23	4.9	3.05	0.21	0.983	4.92	0.35	0.992
Cd	5.10	4.6	3.79	0.23	0.951	4.13	0.67	0.991
Zn	5.09	4.0	3.22	0.24	0.954	3.96	0.81	0.943
Cr	5.11	3.6	2.01	0.21	0.783	2.56	0.99	0.984

Table 6.6. Pseudo-first order and pseudo-second order kinetics models parameters for the adsorption of heavy metals (HM) onto zeolite and ICZ from mixed metal solutions at pH 6.5 and ionic strength 10^{-3}M $NaNO_3$

Zeolite

HM	Initial conc. (mg/L)	q_e exp.	Pseudo-first order			Pseudo-second order		
			q_e (mg/g)	K_1x10^{-2} (min^{-1})	R^2	q_e (mg/g)	K_2x10^{-2} (min^{-1})	R^2
Pb	4.86	4.7	4.32	0.20	0.922	5.57	0.067	0.994
Cu	4.89	3.5	3.14	0.20	0.882	3.61	0.094	0.983
Cd	4.85	3.7	3.45	0.23	0.983	4.30	0.067	0.981
Zn	4.78	3.2	2.88	0.19	0.961	3.96	0.20	0.941
Cr	5.01	2.5	1.51	0.17	0.964	2.42	0.067	1.000

ICZ

HM	Initial conc. (mg/L)	q_e exp.	Pseudo-first order			Pseudo-second order		
			q_e (mg/g)	K_1x10^{-2} (min^{-1})	R^2	q_e (mg/g)	K_2x10^{-2} (min^{-1})	R^2
Pb	5.12	5.0	4.65	0.18	0.972	6.03	0.06	0.994
Cu	5.23	3.7	2.93	0.19	0913	4.18	0.05	0.982
Cd	5.10	4.0	4.38	0.19	0.932	4.81	0.08	0.991
Zn	4.89	4.0	5.41	0.24	0.731	5.36	0.16	0.981
Cr	5.07	3.01	2.84	0.17	0.972	3.55	0.13	0.993

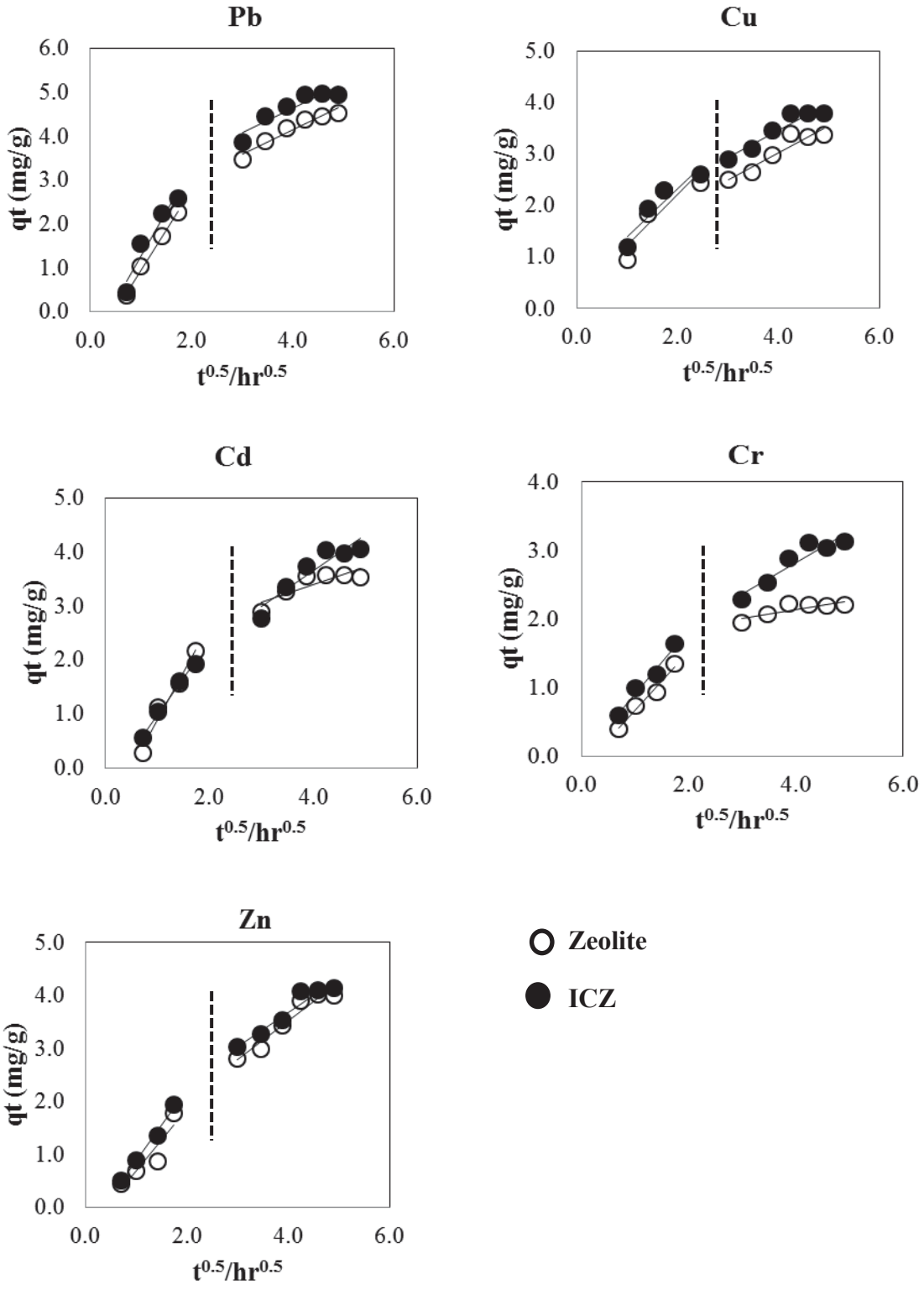

Figure 6.9. Intra-particle diffusion model

6.3.3. Fixed-bed column experiments

6.3.3.1 Breakthrough curves and modelling

Adsorption of single and mixed heavy metals by zeolite and ICZ is presented in the form of breakthrough curves (Figures 6.10 and Figure 6.11). The heavy metals breakthrough generally occurred faster and the breakthrough curve was steeper for Cr and Zn than the other metals. The time to reach the plateau of C_t/C_o was significantly higher for Pb than Cd, Cu, Zn and Cr. The breakthrough was slowest and the breakthrough curve was least steep for Pb. Jeon et al. (Jeon et al., 2012) reported similar results for a zeolite and an iron-coated zeolite removing Cd, Cu, and Pb in column experiments where the breakthrough was not very different between Cu and Cd. However, there was no breakthrough for Pb when up to 800 bed volumes were tested. It is hypothesised that Pb was removed in greater quantities, compared to other metals, because of its solution chemistry which was discussed under batch adsorption results. The order of column adsorption capacities calculated from the breakthrough curves (Pb > Cd, Cu > Zn > Cr) agreed fairly well with that obtained from the batch adsorption experiments (Table 6.7). Furthermore, the metals removal efficiencies were higher for ICZ (1.17-2.28 mg/g for the single metal system and 0.76-1.03 mg/g for the mixed metals system) than for zeolite (0.81-1.67 mg/g for the single metal system and 0.35-0.63 mg/g for the mixed metals system) as observed in the batch adsorption study. ICZ had higher removal efficiencies because of the presence of iron oxides.

The Thomas model satisfactorily described the breakthrough behaviour of the different heavy metals in both zeolite and ICZ (R^2 = 0.876-0.959) (Table 6.7). The model predicted adsorption capacities (q_o) were approximately the same as the corresponding adsorption capacities calculated from the breakthrough curves. For all metals, the q_o values were higher for single than mixed metals system reflecting the competition for adsorption between metals in the later system.

Although the column adsorption capacities calculated from the breakthrough curves and Thomas model predicted adsorption capacities (Table 6.7) followed the same order as the batch Langmuir adsorption capacities (Table 6.2) for the different metals, the former were much lower than the latter. This is probably due to two reasons. Firstly, the metals flowing through the columns have not reached equilibrium unlike in the batch equilibrium

experiment. Secondly, the column adsorption was determined at a lower influent solution metals concentration than the metals concentrations at which Langmuir adsorption maxima were determined.

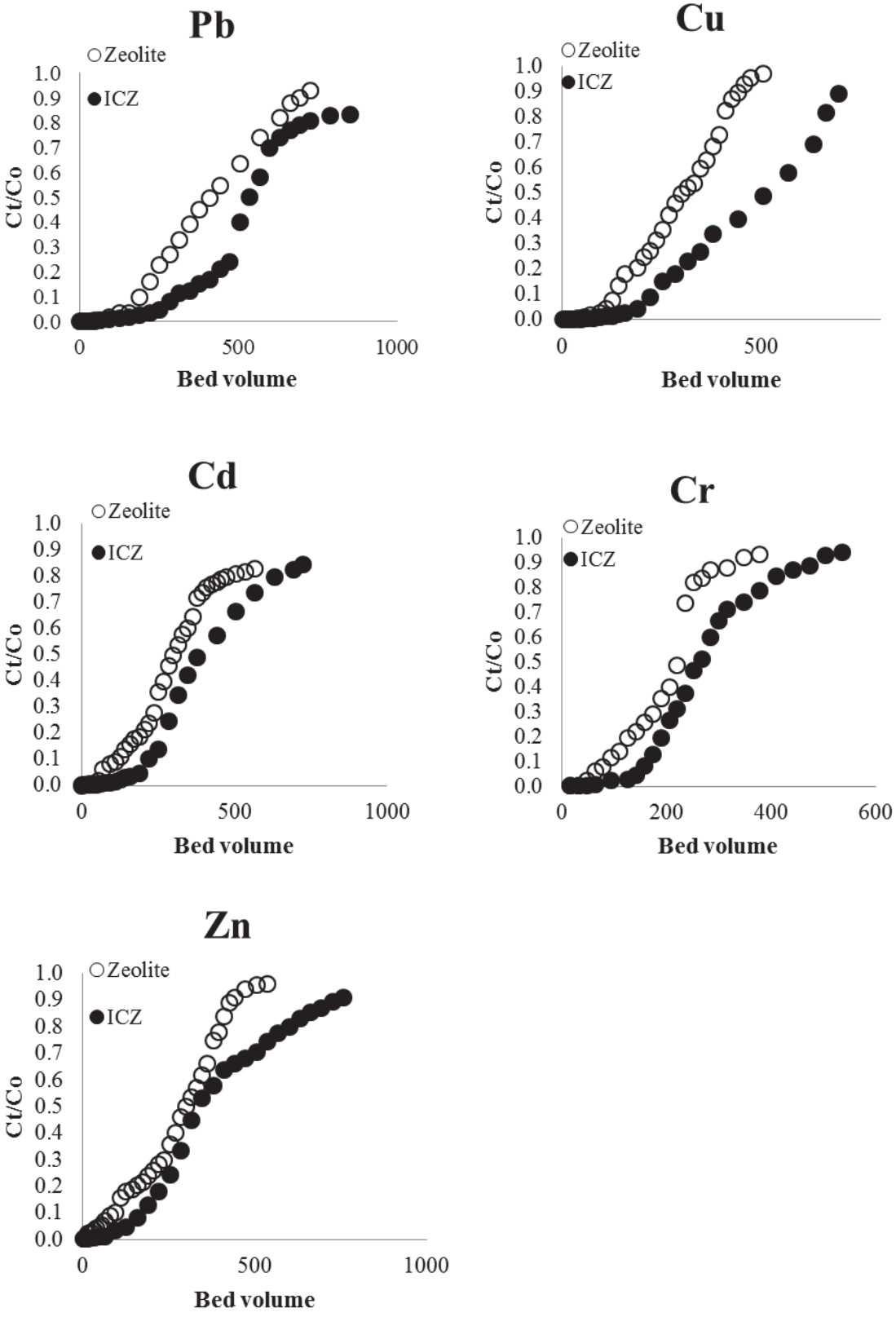

Figure 6. 10. Breakthrough curves of column experiments for individual metals at pH 6.5

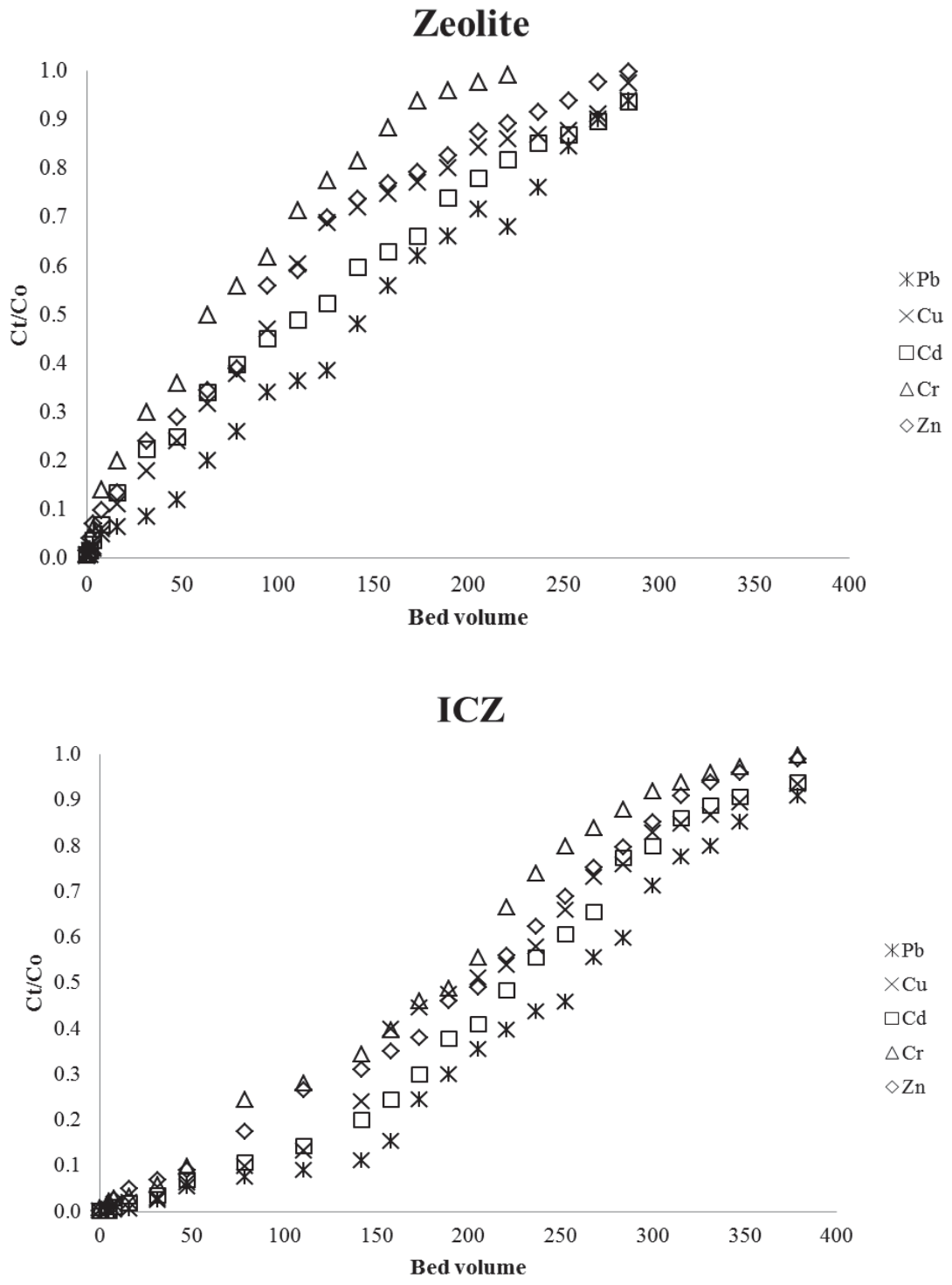

Figure 6.11. Breakthrough curves of column experiments for metals mixture at pH 5.0

Table 6.7. Breakthrough adsorption capacities and Thomas model parameters for column adsorption of heavy metals (HM) from single (pH 6.0) and mixed metals solution (pH 5.0)

		Individual metal				Metals mixture			
	HM	Breakthrough adsorption capacity q_e^* (mg/g)	q_o^{**} (mg/g)	k_{Th}^{**} (mL/min.mg)	R^{2**}	Breakthrough adsorption capacity q_e^* (mg/g)	q_o^{**} (mg/g)	k_{Th}^{**} (mL/min.mg)	R^{2**}
Zeolite	Pb	1.67	1.61	0.62	0.924	0.63	0.61	1.16	0.899
	Cd	1.32	1.29	0.66	0.894	0.52	0.52	1.06	0.876
	Cu	1.15	1.14	0.88	0.949	0.48	0.49	1.20	0.879
	Zn	1.19	1.10	0.70	0.959	0.45	0.41	1.28	0.917
	Cr	0.81	0.74	1.12	0.945	0.35	0.32	1.72	0.924
ICZ	Pb	2.28	2.03	0.54	0.959	1.03	0.95	1.04	0.954
	Cd	1.89	1.82	0.58	0.933	0.93	0.86	1.08	0.940
	Cu	1.70	1.70	0.66	0.948	0.89	0.83	1.04	0.946
	Zn	1.66	1.61	0.50	0.919	0.83	0.75	1.06	0.933
	Cr	1.17	1.08	0.92	0.949	0.76	0.67	1.14	0.957

qe: breakthrough adsorption capacity (mg/g), qo: maximum adsorption capacity (mg/g)

**: Thomas model parameters*

6.3.3.2. Desorption of metals and regeneration of zeolite and ICZ

Desorption of metals previously adsorbed on zeolite and ICZ columns by elution with 0.1 M HCl removed 62-90% and 58-85% of adsorbed metals on zeolite in the first and second cycles of adsorption/desorption, respectively (Table 6.8). The corresponding values for ICZ were 64-93% and 49-85%, respectively. Desorption peaked at around 10-15 bed volumes (40-60 min) and was completed in less than 40 bed volumes (Figure 6.12, Table 6.8). Despite a large percentage of adsorbed metals being desorbed, the adsorption capacities declined in the second cycle, particurlarly for ICZ. Han et al. (Han et al., 2009) reported that the adsorption capacity of an iron oxide-coated zeolite for Cu decreased in the second cycle after desorption of Cu by 1 M HCl. The reason for the higher reduction in adsorption capacities of ICZ compared to zeolite is probably because some iron oxide coatings in ICZ dissolved in the acidic condition of 0.1 M HCl. The Fe concentration in the leachate from the ICZ column was about 80 times higher compared to that in zeolite (Table 6.8). Fe dissolved from the iron coatings in the first cycle was 10% of Fe originally present in ICZ (Fe content in ICZ = 8%, total Fe in desorbed solution = 0.081 mg/g). In comparison, Fe dissolved in the second cycle was much lower (0.75%). Although the regeneration of ICZ reduced the adsorption capacity, partly because of the iron coatings being dissolved, the adsorption capacity of the regenerated ICZ was still higher than that of the original zeolite (Figure 6.13).

Table 6. 8. Heavy metals adsorption and their desorption by 0.1 M HCl in zeolite and ICZ fixed-bed columns and leaching of Fe during desorption (column height 12 cm, adsorption and desorption flow velocity 1.0 m/h, adsorption after 300 bed volumes, desorption after 40 bed volumes)

Zeolite (Z)								
HM	1st cycle				2nd cycle			
	Adsorption (mg/g)	Desorption (mg/g)	Desorption (%) *	Fe in leachate (mg/g Z)	Adsorption (mg/g)	Desorption (mg/g)	Desorption (%) *	Fe in leachate (mg/g Z)
Pb	0.63	0.57	90	0.001	0.52	0.44	85	0.001
Cu	0.48	0.31	65	0.001	0.34	0.21	62	0.001
Cd	0.52	0.37	71	0.001	0.37	0.23	62	0.001
Zn	0.45	0.28	62	0.001	0.34	0.21	62	0.001
Cr	0.35	0.23	66	0.001	0.26	0.15	58	0.001

ICZ								
HM	1st cycle				2nd cycle			
	Adsorption (mg/g)	Desorption (mg/g)	Desorption (%) *	Fe in leachate (mg/g ICZ)	Adsorption (mg/g)	Desorption (mg/g)	Desorption (%) *	Fe in leachate (mg/g ICZ)
Pb	1.03	0.96	93	0.081	0.61	0.52	85	0.006
Cu	0.89	0.69	78	0.081	0.53	0.33	62	0.006
Cd	0.93	0.65	70	0.081	0.54	0.35	65	0.006
Zn	0.83	0.62	75	0.081	0.48	0.33	69	0.006
Cr	0.76	0.49	64	0.081	0.47	0.23	49	0.006

** % desorption = Amount desorbed/Amount adsorbed × 100*

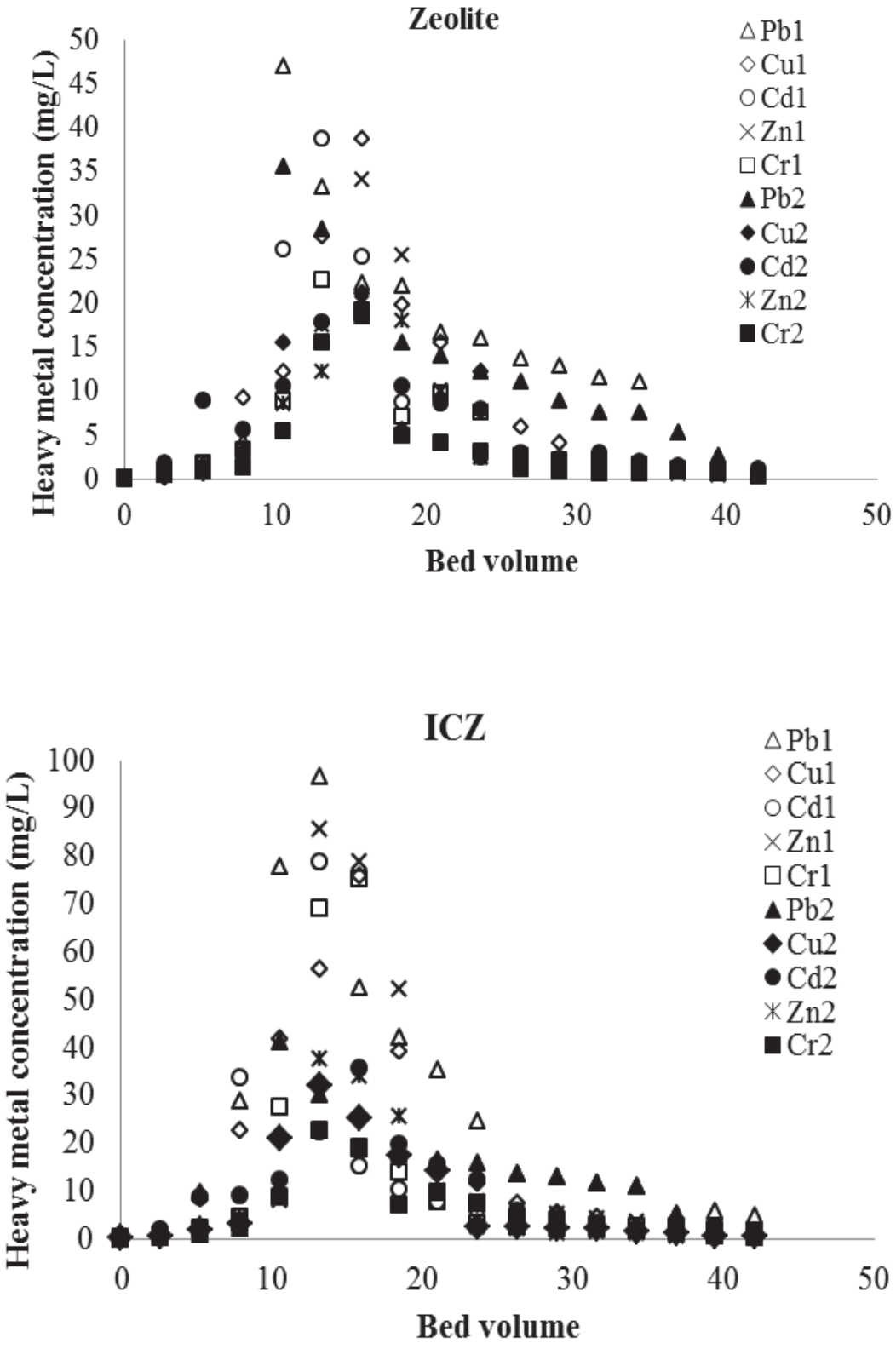

Figure 6.12. Heavy metals concentrations in desorbed solutions from zeolite and ICZ columns and Fe concentration in desorbed solutions of ICZ column for 2 adsorption and desorption cycles (open symbols- cycle 1; closed symbols- cycle 2)

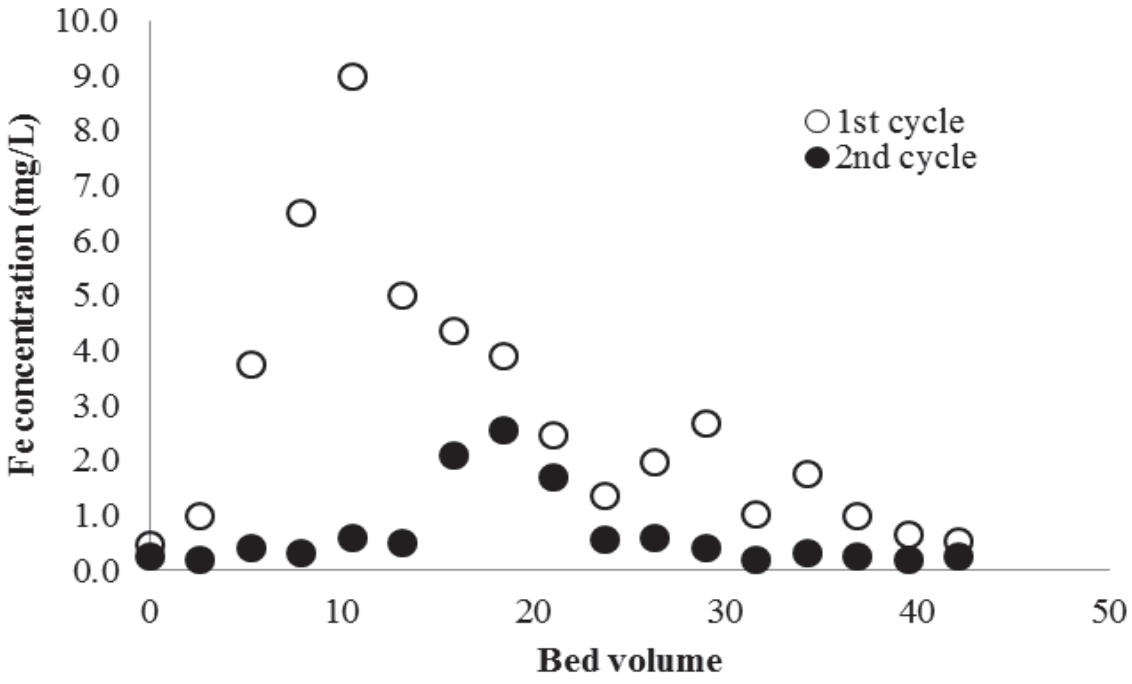

Figure 6.13. Heavy metals concentrations in desorbed solutions from zeolite and ICZ columns and Fe concentration in desorbed solutions of ICZ column for 2 adsorption and desorption cycles (open symbols- cycle 1; closed symbols- cycle 2)

6.4. Conclusions

Iron oxide coating of an Australian zeolite (ICZ) increased the heavy metal adsorption capacity compared to natural zeolite in both batch and column adsorption capacity experiments whether adsorption was from individual or mixed metals solution. The adsorption reaction can be satisfactorily described by both the pseudo-first-order and the pseudo-second-order kinetic models with the data fit slightly better for the latter model, suggesting a chemical adsorption. Data fit to a diffusion model suggested that adsorption was also governed by intra-particle diffusion. The Langmuir adsorption capacity of the metals for both ICZ and Z at pH 6.5 was Pb > Cu > Cd > Cr, Zn. The column adsorption capacity followed the order of Pb > Cd > Cu > Zn > Cr as calculated from the breakthrough curves as well as using Thomas model. In the mixed metals adsorption the adsorption capacity decreased at high concentrations of metals probably due to competition between metals for adsorption. Overall, both zeolite and ICZ displayed a high affinity for Pb, Cd and Cu, but

were less effective at removing Zn and Cr. Leaching of used ICZ and zeolite columns with 0.1 M HCl, desorbed a large percentage of the adsorbed metals and dissolved 10% Fe from the ICZ. However, the adsorption capacities got reduced in the second adsorption/desorption cycle, more so for ICZ, probably due to dissolution of some iron coatings in the acidic conditions of HCl. Despite this, the adsorption capacity of the regenerated ICZ was still higher than that of the original zeolite.

CHAPTER 7

INDUSTRIAL BY-PRODUCT ADSORBENTS FOR REMOVING HEAVY METALS FROM WATER

CHAPTER 7

INDUSTRIAL BY-PRODUCT ADSORBENTS FOR REMOVING HEAVY METALS FROM WATER

7.1. Introduction

The Asian Pacific region is subject to rapid changes and economic growth. One of the consequences is rapid industrialisation and urbanisation of the population. This puts high pressure on waters by increasing use and pollution. One of the economic means of removing heavy metals from water is the use of low-cost adsorbents. Several review papers have summarized the adsorption capacities of heavy metals on low-cost adsorbents (Ahmaruzzaman, 2008; Ahmaruzzaman, 2011; Babel and Kurniawan, 2003; Bailey et al., 1999; Gupta and Ali, 2012; Kurniawan et al., 2006; Wang et al., 2003). Among the low-cost adsorbents, industrial by-products played a very important role in the metal removal process not only because of their low cost but also of their disposal problem causing environmental pollution which is partly solved by using this process.

Fly ash is a by-product of coal industry and has been widely used as a low-cost adsorbent for the removal of heavy metals. The use of fly ash for removal of heavy metals from industrial wastewaters was reported many decades ago (Gangoli et al., 1975; Grover and Narayanaswamy, 1982). Removal of Cr ions, including Cr^{6+} and Cr^{3+} using fly ash has been investigated by several researchers and the effects of initial concentrations, fly ash dosage, contact time, and pH on the removal of Cr were reported (Bhattacharya et al., 2006; Kelleher et al., 2002; Panday et al., 1985; Rao et al., 2002). Bhattacharya et al. (2006, 2008) studied the removal of Cr^{6+} and Zn^{2+} from aqueous solutions using fly ash (Bhattacharya et al., 2008) and found that fly ash had a higher adsorption capacity for Zn^{2+}, as compared to Cr^{6+}. It was observed that the percentage removal of Cr^{6+} by fly ash is affected by its concentration in aqueous solution, temperature, particle size, and pH.

According to Bayat (2002), the higher the Ca content in the fly ash the higher the adsorption capacity of heavy metals (Zn^{2+}, Cu^{2+}, Cd^{2+}, Pb^{2+}, Ni^{2+}, Cr^{3+}, and Cr^{6+}). This researcher demonstrated that the adsorption capacity of Turkish fly ashes for 6 heavy metals were in the order: $Zn^{2+} > Cu^{2+} > Ni^{2+}$ and $Pb^{2+} > Cd^{2+} > Cr^{2+}$. The high Pb^{2+} removal observed in the experiments was attributed to precipitation, with a moderate contribution from physical adsorption and/or other mechanisms. Adsorption of heavy metals on fly ash was best described by the Langmuir model (Banerjee et al., 2003; Bayat, 2002; Bhattacharya et al., 2008; Hui et al., 2005). Bhattacharya et al. (2008) compared the adsorption capacity of fly ash with that of 6 other adsorbents and found that its adsorption capacity was (23.9 mg/g) nearly the same as adsorption capacities of other adsorbents (19.6 – 26.3 mg/g). The adsorption of Cr^{3+} on fly ash was endothermic and kinetic studies suggested that the overall rate of adsorption was explained by pseudo-second order model (Bhattacharya et al., 2008b; Kelleher et al., 2002; Wu et al., 2008). Apak et al. (1998) compared the adsorption capacity of fly ash and red mud and showed that fly ash had lower adsorption capacity than red mud for the removal of Cu, Pb and Cd. They also studied the single metal and mixed metals (competitive adsorption) adsorption of Pb^{2+}, Cu^{2+} and Cd^{2+} by fly ash and showed that the adsorption affinity of the metals in both the single and mixed metals systems followed the order $Cu^{2+} > Pb^{2+} > Cd^{2+}$. They explained this as due to energetic reasons in which hydroxo-metal complexes and hydroxides formed at a pH just below the precipitation limit in solution tend to adsorb on hydrous oxide-type sorbents with higher affinity. The degree of the insolubility of the metal hydroxides (expressed as the pK_{so} of the corresponding metal hydroxide) approximately followed the same order of adsorption of the metals.

Panday et al. (1985) reported that coal fly ash from thermal power plant had high adsorption capacity for Cu^{2+} and could be used as a low-cost adsorbent for the removal of Cu from water. The presence of organic pollutants such as humic acid significantly affected the heavy metals removal capacity of fly ash. In the presence of humic acid, complexation of humic with heavy metal decreased the adsorption capacity of the latter (Wang et al., 2008).

Steel plant produces large volumes of blast furnace slag as a by-product, causing a serious disposal problem. Blast furnace slag has high adsorption capacity for heavy

metals because of the presence of Al and Fe oxides in them (Dimitrova and Mehandgiev, 1998; Gupta, 1998). Dimitrova (1996) studied the adsorption of Cu^{2+}, Ni^{2+} and Zn^{2+} ions from simulated wastewater using blast-furnace slag and found that the Freundlich adsorption constant related to the adsorption capacities for Cu^{2+}, Ni^{2+} and Zn^{2+} were 8.2×10^{-3}, 4.2×10^{-3}, and 5.2×10^{-3} $(mg/g)(L/mg)^{1/n}$, respectively. They explained that these high adsorption capacities as due to metals adsorbing as hydroxide complexes and the formation of insoluble compounds on the internal surface of adsorbent. Feng et al. (2004) investigated Cu^{2+} and Pb^{2+} removal from simulated wastewater using iron slag and/or steel slag and found that the adsorption of both metals on the two slags satisfactorily followed the Langmuir isotherm. The maximum adsorption capacity (88 mg/g for Cu^{2+} and 95 mg/g for Pb^{2+}) was obtained at pH 5.5 (for Cu^{2+}) and 6.0 (for Pb^{2+}) on iron slag. For steel slag, the corresponding values for Cu^{2+} and Pb^{2+} were 16 and 32 mg/g, respectively. Another study by Mishra and Tiwari (2009) showed that sodium hydroxide treated fly ash and furnace slag had high adsorption capacities for Pb^{2+} and Zn^{2+}. Base treatment can dissolve the minerals in carbon and thus increase the pore volume and surface area of fly ash sample, leading to an increase in adsorption. Langmuir adsorption capacities for Pb^{2+} and Zn^{2+} in single metal system for fly ash were 4.98 and 5.82 mg/g, respectively and furnace slag were 5.52 and 3.25 mg/g, respectively. The metals removal observed in these experiments was attributed to precipitation, with a moderate contribution from physical adsorption or other mechanisms.

Table 7.1 presents adsorption capacities of heavy metals on fly ash and furnace slag reported in literature. The literature shows that in most cases, the equilibrium adsorption of heavy metals on fly ash and furnace slag generally followed the Langmuir adsorption isotherm and kinetics data followed the pseudo-second order model.

Most studies on heavy metals removal by fly ash and furnace slag have been performed in batch experiments and only a few have been reported in fixed bed column systems which are more relevant to real operating treatment systems in natural waters (Bhattacharya et al., 2008; Mishra and Patel, 2009). Moreover, simultaneous removal of several heavy metals from their mixtures in both batch and column adsorption conditions is rare. The simultaneous removal of several heavy metals is important as

most wastewaters contain more than one heavy metal and there can be competition for adsorption between metals. So, this study aimed to determine the adsorptive removal efficiencies in single and mixed metals systems in twater using column adsorption conditions.

This study was undertaken to investigate the adsorption of five heavy metals (Cu, Cd, Pb, Zn and Cr) using fly ash and furnace slag in single and mixed metals solutions. The specific aims of this study were to (i) study the feasibility of using fly ash and furnace slag as adsorbents for the removal of the five different heavy metal ions from aqueous solutions in single and mixed metals systems, (ii) study the effect of initial pH on the adsorption process, (iii) model the equilibrium and kinetic batch adsorption data, and (iv) investigate the breakthrough curves obtained in the column adsorption study and describe the data using Thomas model.

Table 7. 1. Literature on comparison of heavy metals removal efficiencies of fly ash and furnace slag adsorbents

Adsorbent	Adsorbate	Adsorption method	pH, temp.	Langmuir adsorption capacity (mg/g)	Best kinetic model	Best equilibrium model	References
Fly ash impregnated Fe	Zn^{2+}	Batch	6.5, 30–60°C	6.5–13.3	Intraparticle diffusion	Langmuir isotherm	Banerjee et al. (2003)
Fly ash impregnate Al	Zn^{2+}	Batch	6.5, 30–60°C	7.5-15.5	Intraparticle diffusion	Langmuir isotherm	Banerjee et al. (2003)
Fly ash	Zn^{2+}	Batch	6.5, 30–60°C	7.0–15.4	Intraparticle diffusion	Langmuir isotherm	Banerjee et al. (2003)
Fly ash	Zn^{2+}	Batch	2.0-8.0; 10-30°C	0.25 – 2.8	Intraparticle diffusion	Langmuir isotherm	Bayat (2002)
Fly ash	Cd^{2+}	Batch	2.0-8.0; 10-30°C	0.25 – 2.8	Intraparticle diffusion	Langmuir isotherm	Bayat (2002)
Bagasse fly ash	Cd^{2+}	Batch	6.0; 30°C	1.24-2.00		Langmuir isotherm	Gupta et al. (2003)
Fly ash	Zn^{2+}	Batch	6.0-7.5; 25°C	0.068 – 0.75	Pseudo-2nd-order	Langmuir isotherm	Weng and Huang (2004)
Fly ash	Zn^{2+}	Batch	-	14.30	Pseudo-2nd-order	Langmuir isotherm	Bhattacharya et al. (2006)
Fly ash	Zn^{2+}	Batch	30 - 50°C	1.24 – 2.00	Pseudo-2nd-order	Langmuir isotherm	Gupta et al. (2003)
Coal fly ash	Zn^{2+}	Batch	-	4.64	Pseudo-2nd-order	Langmuir isotherm	Weng and Huang (2004)
Fly ash	Pb^{2+}	Batch	25°C	47.3		Langmuir isotherm	Wang et al. (2009)
Fly ash washed	Pb^{2+}	Batch	25°C	483.4	Pseudo-2nd-order		Ricou et al. (1998)
Fly ash acid	Pb^{2+}	Batch	25°C	437.0	Pseudo-2nd-order		Ricou et al. (1998)
Fly ash	Cu^{2+}	Batch	20°C	0.34-1.35	Pseudo-2nd-order		Bayat (2002)
Fly ash	Cu^{2+}	Batch	20 °C	0.09-1.25	Pseudo-2nd-order		Bayat (2002)
Bagasse fly ash	Cu^{2+}	Batch	30÷50°C	2.26-2.36	Pseudo-2nd-order		Gupta and Ali (2000)
Fly ash	Cu^{2+}	Batch	5.0; 25°C	2.2-2.8	Pseudo-2nd-order	Langmuir isotherm	Lin and Chang (2001)
Fly ash	Cu^{2+}	Batch	25°C	82.7		Langmuir isotherm	Wang et al. (2009)
Fly ash	Cr^{3+}	Batch	20÷40°C	53.6-102.4		Langmuir isotherm	Cetin and Pehlivan (2007)
Bagasse fly ash	Cr^{3+}	Batch	-	4.25			Gupta et al. (2001)
Fly ash	Cr^{6+}	Batch	2.0; 30°C	1.4			Banerjee et al. (2003)
Fly ash impregnated Al	Cr^{6+}	Batch	2.0; 30°C	1.8			Banerjee et al. (2003)
Fly ash impregnate Fe	Cr^{6+}	Batch	2.0; 30 °C	1.7			Banerjee et al. (2003)
Fly ash	Cr^{6+}	Batch	2.0÷3.0; 30 °C	23.86	Pseudo-2nd-order		Bhattacharya et al. (2008)

Table 7.1 (Cont.)

Furnace slag	Zn^{2+}	Batch	4.2; 25 °C	103.33			
Furnace slag	Cu^{2+}	Batch	4.2; 25 °C	133.35			Dimitrova (1996)
Furnace slag	Ni^{2+}	Batch	4.2; 25 °C	55.76			
Furnace slag	Pb^{2+}	Batch	4.2; 25 °C	133.35			Dimitrova and Mehandgiev (1998)
Clarified slag	Zn^{2+}	Batch	25 °C	1..53		Langmuir isotherm	Bhattacharya et al. (2006)
Steel slag	Cu^{2+}	Batch	30 °C	11.23	Pseudo-2nd-order		Gupta (1998)
Blast furnace slag	Cu^{2+}	Batch	30 °C	10.57	Pseudo-2nd-order	Langmuir isotherm	Ortiz et al. (2001)
Steel slag	Pb^{2+}	Batch	30 °C	40	Pseudo-2nd-order	Langmuir isotherm	Srivastava et al. (1997)
Iron slag	Cu^{2+}	Batch	3.5÷8.5; 30 °C	88.50	Pseudo-2nd-order	Langmuir isotherm	Feng et al. (2004)
Activated slag	Cu^{2+}	Batch	3.5÷8.5; 30 °C	88.50	Pseudo-2nd-order	Langmuir isotherm	Feng et al. (2004)
Furnace slag	Cr^{6+}	Batch	1.0; 30 °C	1.45	Pseudo-2nd-order	Langmuir isotherm	Srivastava et al. (1997)
Furnace slag	Cr^{6+}	Batch	1.0; 40 °C	1.76	Pseudo-2nd-order	Langmuir isotherm	Srivastava et al. (1997)
Activated slag	Ni^{2+}	Batch	30 °C	112.2	Pseudo-2nd-order	Langmuir isotherm	Erdem et al. (2004)

7.2. Materials and methods

7.2.1. Adsorbents

Fly ash and furnace slag (Figure 7.1) were obtained from Coal Ash Development Association of Australia Inc and Australasian (iron and steel) Slag Association (ASA), respectively. Furnace slag used in this study was produced from BlueScope Steel in Port Kemble, NSW, Australia, which is an abundant by-product in steel-making process. The chemical compositions of these materials are presented in Table 7.2. Fly ash had higher SiO_2 and Al_2O_3 contents than furnace slag but the latter had higher CaO and Fe_2O_3 contents.

Zeta potentials of the adsorbents were measured in 10 mL suspensions containing 1.0 g adsorbent at different pHs after shaking the suspensions for 8 hours. Zeta potential was measured using a Zetasizer nano instrument (Nano ZS Zen3600, Malvern, UK) after measuring the final pH. Surface area and porosity were determined by nitrogen-sorption measurements carried out at 77 K with a Micromeritics 3 Flex surface characterisation analyser. The BET method was used to calculate the specific surface area of the adsorbents. The pore size distribution was derived from the adsorption branch of the isotherm by using the Barrett–Joyner–Halenda (BJH) method.

The furnace slag was treated with hydrogen peroxide at 60°C for 24 h to oxidize the adhering organic matter. It was then washed with de-ionized water, dried at 100°C, powdered, and sieved to produce desired particle sizes (100–150, 150–300 and 300–450 μm) and then 150-300 μm size of furnace slag was chosen for the study. The fly ash obtained from Coal Ash Development Association of Australia Inc had a particle size of 10-20 μm and this adsorbent was used in this study.

Figure 7. 1. Fly ash and furnace slag used in the study

Table 7. 2. The chemical composition (%) of fly ash and furnace slag

	MnO	Fe_2O_3	Al_2O_3	SiO_2	CaO	MgO	Cr_2O_7	Other
Fly ash	-	1.26	25.90	56.04	2.20	0.94	-	13.66
Furnace slag	3.29	28.83	0.18	22.33	32.73	10.00	0.20	2.44

7.2.2. Batch experiments

7.2.2.1. Equilibrium adsorption

Adsorption of heavy metals onto the adsorbents was studied in batch experiments by shaking 0.01 to 2.0 g of adsorbents with metals, each at an initial concentration of 5 mg/L, in 100 mL solutions at a pH of 6.5 and ionic strength of 10^{-3} M $NaNO_3$ at 25 ± 2^{o}C for 24 h and filtering the suspensions. The filtrates were analysed for heavy metals concentrations using a Microwave Plasma-Atomic Emission Spectrometer (MP-AES- 4100 Agilent) and amounts of metals adsorbed were determined as described in Chapter 6. Similar experiments were conducted at the pH range of 2.0 – 9.0 to determine the effect of pH on adsorption. The

adsorption data were fitted to the Langmuir, Freundlich and Dubinin–Radushkevick adsorption isotherms which were described in Chapter 6.

7.2.2.2. Kinetic of adsorption

Kinetics of adsorption were studied by shaking 100 mL nitrate solution of each metal at a concentration of 5 mg/L and 0.5 g/L adsorbent dose for different times (10 min to 14 h) at an ionic strength of 10^{-3} M $NaNO_3$ and pH 6.5 at 25 ± 2°C. Amounts of metals adsorbed were determined as in 7.2.2.1.

7.2.2.3. Effect of pH on adsorption

In order to investigate the effects of pH on metal ion adsorption, the pH of the metal ion solution (5 mg/L in 100 mL) was adjusted to different values (2, 3, 4, 5, 6, 7, 8 and 9) by adding required amounts of dilute NaOH or HCl solution. pH was measured using a HQ40d portable pH meter. 0.5 g of adsorbent was added to the pH adjusted solution and the suspensions were agitated in a flat shaker at a shaking speed of 120 rpm for 12 h at room temperature (25 ± 2°C) and the amounts of metals adsorbed were determined as described in 7.2.2.1.

7.2.3. Column experimental set-up

The fixed-bed column used for the experiments consisted of 2.0 cm inner diameter Pyrex glass tubes. Column adsorption experiments were conducted by passing solutions of Zn, Cu, Cd, and Pb at concentrations of 5 mg/L each metal through the column containing 80 g of furnace slag and 80 g of sand mixed together and packed to a height of 12 cm. Column experiment was not conducted on fly ash because it was not possible to pack fly ash in the column and maintain a constant flow of solution through the column. The fly ash formed a cake and blocked the water flow.

Tap water was spiked with heavy metals, one metal at a time, at a concentration of 5 mg/L each, at pH 5.0. Tap water (ionic strength of 95.1 mg/L) was utilised instead of distilled water at the ionic strength of 10^{-3} M $NaNO_3$ as in the batch study because large volumes of distilled water that were required for the long-term column study were not available. Experiments

were conducted by filtering metals-spiked tap water at a velocity of 20 mL/min (1.0 m/h) in the gravity flow mode with two peristaltic pumps; one before the water enters the column and the other when the water leaves the column as described in Chapter 6. The empty bed contact time (EBCT) at this filtration velocity was 15.7 min. Samples were collected at 1 h and thereafter every 2 h and analysed for pH and heavy metals concentrations. The experiments were repeated with a mixture of heavy metals with each metal at a concentration of 5 mg/L. The maximum column adsorption capacity, q_{total} (mg) for a given feed concentration is equal to the area under the plot of the adsorbed metal concentration, C_{ad} (Cad = C_o − C) (mg/L) versus time (t, min) (C_o is inlet heavy metal concentration, C is outlet heavy metal concentration) and was calculated manually from the breakthrough curves using Microsoft Excel spread sheet according to Equation (1) where Q is the flow rate of the solution (L/min):

$$q_{total} = \frac{Q}{1000} \int_{t=0}^{t=60} C_{ad} dt \qquad (1)$$

The effluents were collected periodically for 60 h and analysed for heavy metals using MP-AES.

7.3. Results and discussions

7.3.1. Characterization of furnace slag and fly ash

Fly ash is a heterogeneous material consisting largely of small spheres, formed by the condensation of aluminous and siliceous glass droplets in the air. BET surface area of fly ash was 2.82 m^2/g while that of furnace slag was 1.06 m^2/g.

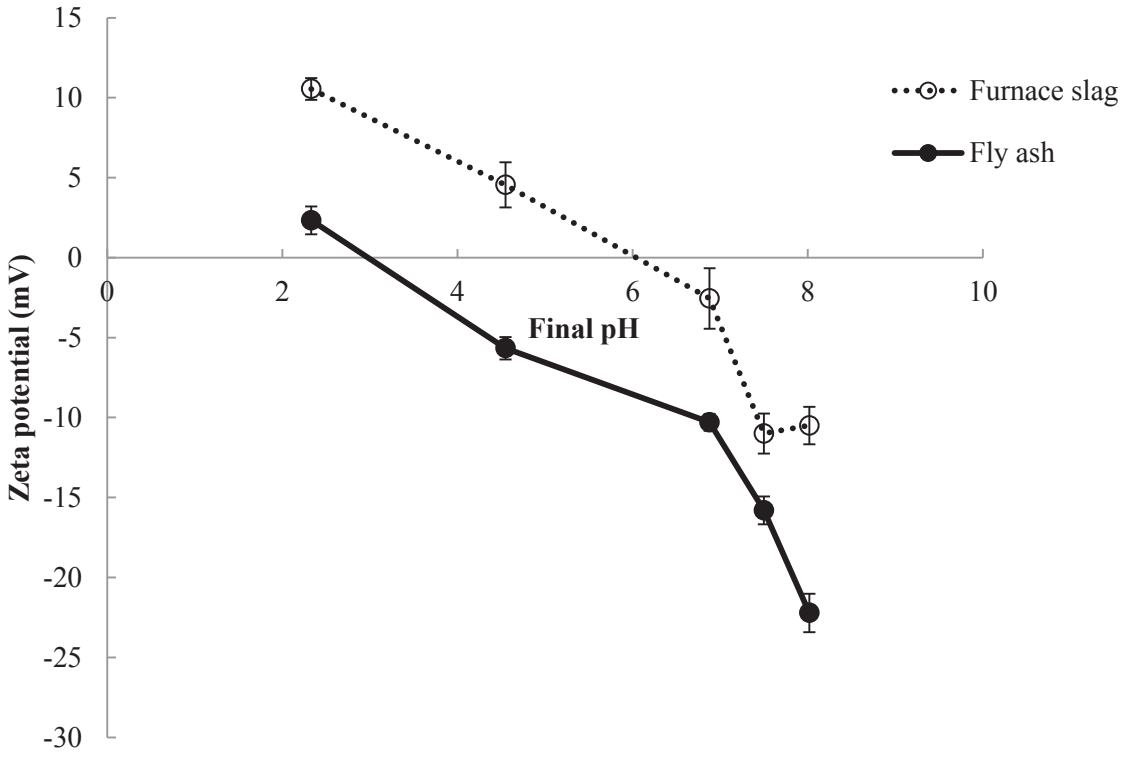

Figure 7. 2. Zeta potential of fly ash and furnace

Zeta potential values showed that the fly ash and furnace slag particles were positively charged at low pH's and negatively charged at high pH's (Figure 7.2). The point of zero charge (PZC) of fly ash was at a pH of 3.0 and that of furnace slag was at a pH of 6.0. Therefore, it can be expected that positively charged metal ions are likely to adsorb by Coulombic forces (outer-sphere complexation) onto the negatively charged fly ash particles at pH above 3.0 and above pH 6.0 in furnace slag. However, adsorption by other forces (inner-sphere complexation) can occur at all pHs independent of the PZC. The high content of SiO_2 in fly ash (Table 7.2) might have resulted in the low PZC of fly ash. In comparison to fly ash, the furnace slag had a higher PZC, probably due to the high contents of Fe and Ca oxides. SiO_2 is known to have PZC of 3.6 (Hommer 2009), Fe_2O_3 of pH 7.9 (Nagata et al. 2009) and CaO 10.5 (Azgomi. 2014).

7.3.2. Effect of pH on adsorption

Increase of pH increased metals adsorption. For fly ash, abrupt increase in adsorption of all metals occurred at pH 5.5-7.0, whereas for furnace slag, this occurred at pH 4.0-6.0 (Figures 7.3 and 7.4). The lower pH range where abrupt increase in adsorption occurs for furnace stag cannot be due to increase in negative surface charges on the adsorbent because the pH at which negative charges start to increase was higher for furnace slag compared to fly ash (Figure 7.2). There is practically no removal of metals at pH lower than 3.0 which may be due to the presence of high concentration of H^+ at low pH that compete with the metals and lower number of negative surface charge on the adsorbents. The abruption increase in adsorption at pH 4.0-7.0 is due to the formation of metal hydroxide precipitation on the surface of the adsorbents and adsorption of metal hydroxide complex (MOH^+) whose concentration increase at pH 5.0-7.0 depending on the metal (Sounthararajah et al. 2015).

The pH of precipitation is governed by the solubility product of the metal hydroxide (pK_{so}) and pH of metal hydroxide complex formation which is determined by the first hydrolysis constant (pK_1) (Table 7.3). The higher the pK_{so} value, the lower is the pH of metal hydroxide precipitation. Chromium hydroxide having the lowest pK_{so} value (Table 7.3) precipitates at higher pH and therefore the abrupt increase in adsorption occurs at a higher pH than other metals. The trend is opposite of Pb which has the highest pK_{so} value. Similarly, the lower the pK_1 value, the lower is the pH at which metal hydroxide complex starts to form.

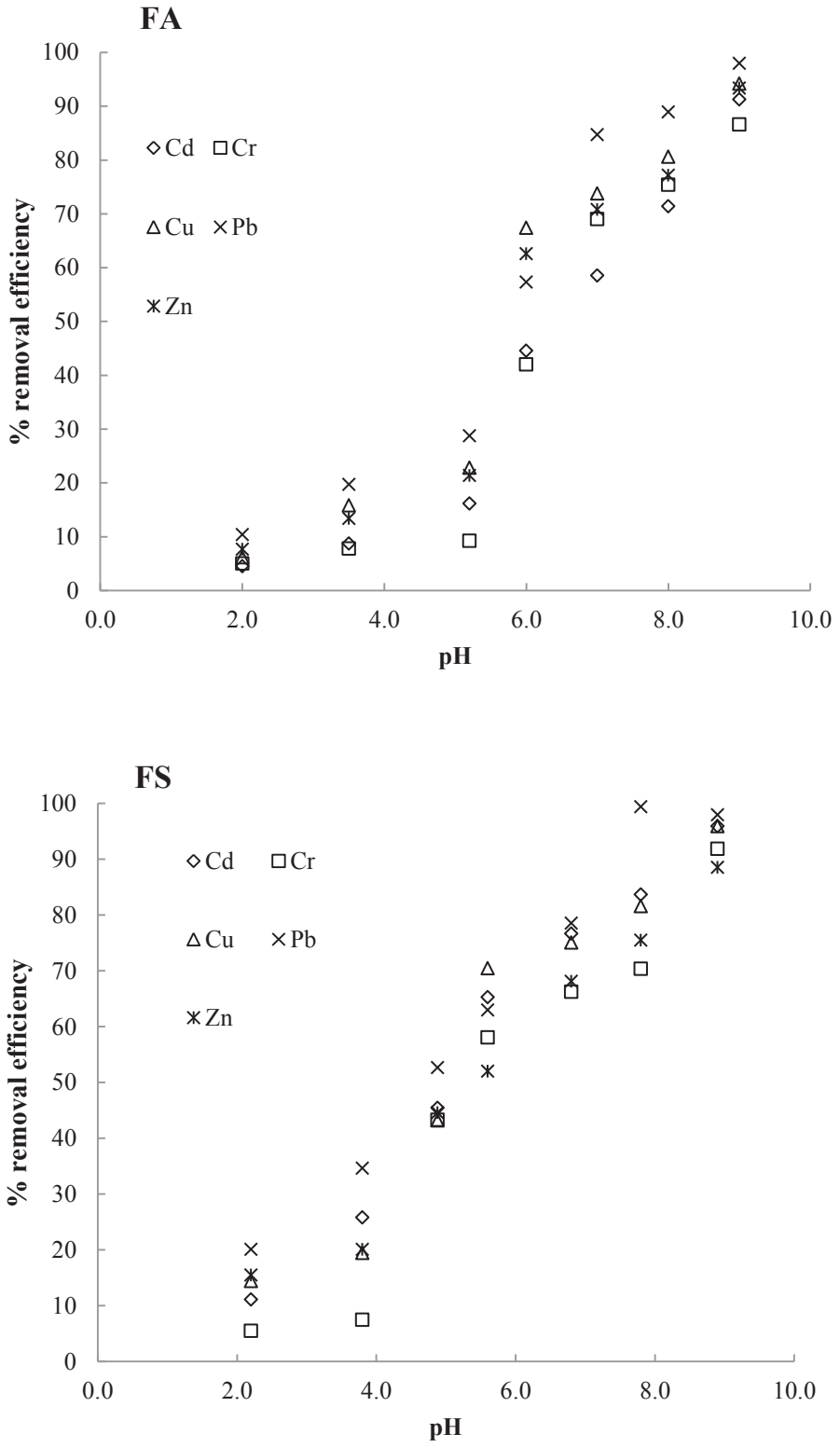

Figure 7. 3. Effect of pH on the adsorption of heavy metals by fly ash (FA) and furnace slag (FS)

Table 7.3. Some characteristics of heavy metal ions

Metal	Solubility products of metal hydroxides (pK_{so})	First hydrolysis constants (pK_1)	References
Zn^{2+}	16.5	8.96	Walker et al. (2012)
Cu^{2+}	19.3	7.96	Rao (2011)
Cd^{2+}	14.4	10.08	Barnum (1983)
Pb^{2+}	19.9	7.71	Baes (1976)
Cr^{2+}	9.6*	8.30**	*Rao et al. (1998) **Orlov et al. (2013)

7.3.3 Equilibrium adsorption batch study

The adsorption experiments for different doses of adsorbents were carried out at the concentration of 5 mg/L for all metals at pH 6.5. The plots of amount adsorbed vs equilibrium metal concentration are shown in Figure 7.4. As the concentration of heavy metals increased, the amount adsorbed on furnace slag and fly ash increased to reach a maximum of 3.3-3.8 and 3.0-3.5 mg/g, respectively. Equilibrium adsorption of all metals at pH 6.5 was successfully described using Langmuir, and Freundlich models and poorly by Dubinin-Radushkevich model. Freundlich model fitted the data slightly better than the Langmuir model (Table 7.4). The Langmuir maximum adsorption capacities for the metals followed the order, Pb > Cu > Cd, Zn and Cr. Despite furnace slag having a higher PZC than fly ash the adsorption capacities for the metals were generally higher for furnace slag (4.3 – 5.2 mg/g) than for fly ash (3.4 – 5.1 mg/g). This shows that electrostatic adsorption was not the main mechanism of adsorption. Also, despite the surface area of fly ash was higher than that of furnace slag, the adsorption capacities were lower for fly ash. Therefore, rather than total surface available for adsorption, the number of active sites available for adsorption is important. The reason for furnace slag to have higher adsorption capacities is that furnace slag has higher content of iron oxide which specifically adsorbs heavy metals. The Langmuir adsorption capacities of both fly ash and furnace slag are lower than those of zeolite and ICZ reported in Chapter 6 (Table 6.3).

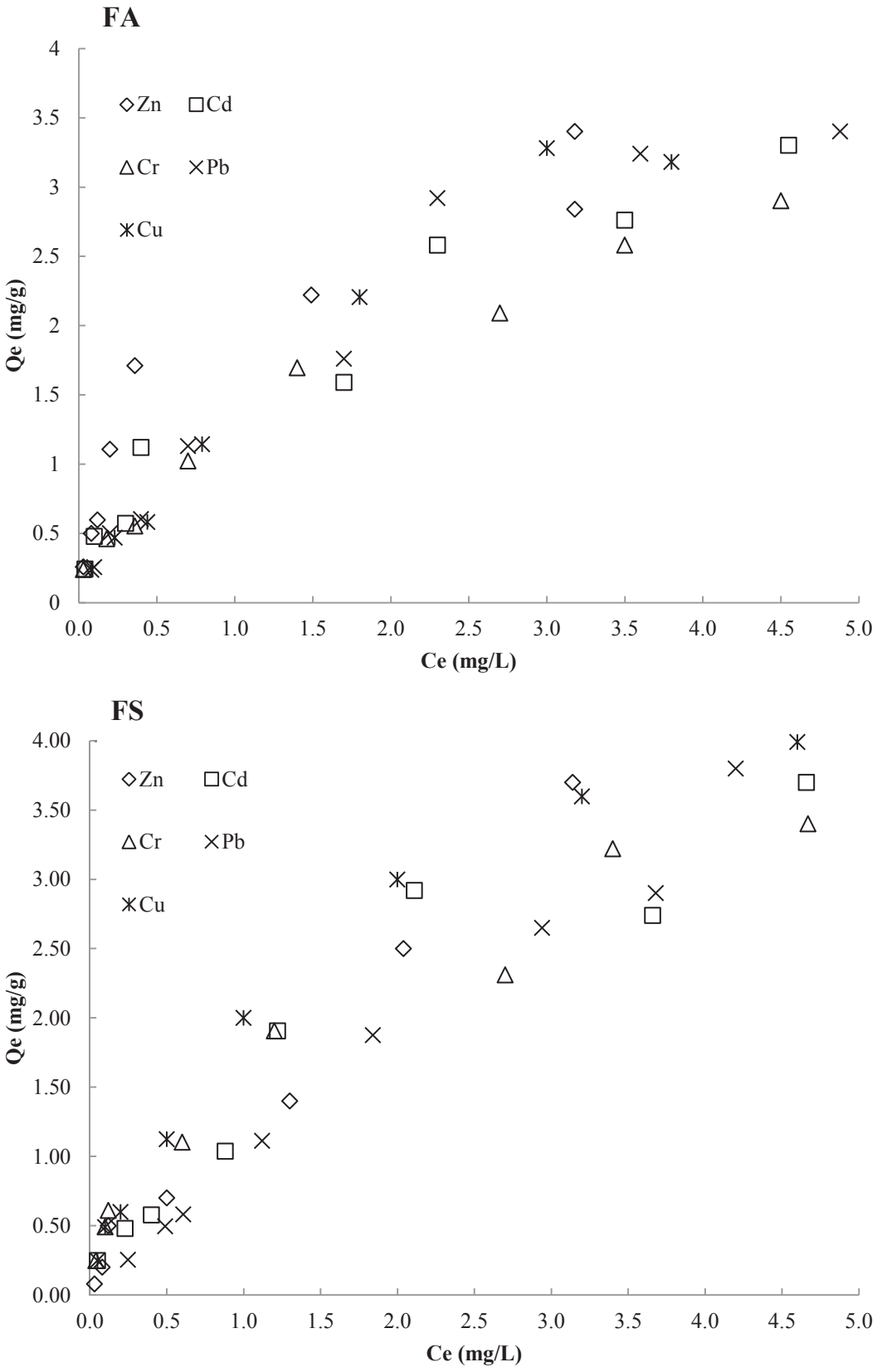

Figure 7.4. Batch adsorption isotherms for metals on fly ash (FA) and furrnace slag (FS) at ionic strength 10^{-3} M $NaNO_3$ and pH 6.5

Table 7.4. Adsorption isotherm parameters for heavy metals adsorption on fly ash (FA) and furnace slag (FS)

		Langmuir			Freundlich			Dubinin–Radushkevick		
	Metals	q_{max} (mg/g)	K_L (L/mg)	R^2	n	K_F(mg/g) L/mg)$^{1/n}$	R^2	q_m (mg/g)	β (mol^2/kJ^2)	R^2
FA	Cd	3.78	0.86	0.8906	1.86	1.44	0.9670	2.03	4×10^{-8}	0.8069
	Cr	3.53	0.73	0.9172	1.90	1.26	0.9754	1.63	3×10^{-8}	0.6871
	Cu	4.49	0.44	0.8843	1.60	1.19	0.9916	1.94	6×10^{-8}	0.7721
	Pb	5.11	0.42	0.9091	1.46	1.33	0.9804	2.32	7×10^{-8}	0.8349
	Zn	3.40	0.62	0.8714	1.67	1.13	0.9435	2.86	6×10^{-8}	0.5761
FS	Cd	5.05	0.44	0.7939	1.58	1.37	0.9549	1.92	4×10^{-8}	0.6766
	Cr	4.83	0.47	0.9023	1.51	1.33	0.9075	2.06	5×10^{-8}	0.7647
	Cu	5.22	0.68	0.9773	1.62	1.77	0.9890	2.62	5×10^{-8}	0.8670
	Pb	4.93	0.86	0.8999	1.80	1.83	0.9925	2.54	3×10^{-8}	0.8527
	Zn	4.26	0.78	0.8960	1.99	1.53	0.9806	1.92	2×10^{-8}	0.6922

q_{max}:maximum amount of the adsorbate per unit weight of the adsorbent (mg/g); K_L: Langmuir constants; K_F and n: Freundlich constants; q_m: the monolayer capacity; β: activity coefficient; R^2: coefficient of determination

7.3.4. Kinetic adsorption batch study

In adsorption kinetics, the adsorption capacity increased with increasing reaction time until it reached equilibrium (Figure 7.5). For both adsorbents, rapid removal of all heavy metals occurred in the first 2 hours, and then it slowed down and reached equilibrium at approximately 8 hours. This may be due to the fact that initially all adsorbent sites were vacant and the heavy metals concentration gradient was high. Later, the metal uptake rate by adsorbent decreased significantly, due to the decrease in number of adsorption sites as well as heavy metals concentration. The adsorption data for all metals on fly ash showed that for both adsorbents, the pseudo-second order kinetic model generally described the experimental data better than the pseudo-first order model (R^2 = 0.98 - 0.99 for pseudo-second order model compared to R^2 = 0.82 – 0.94 for pseudo-first order model) (Table 7.5). For the furnace slag, also the data fit was better for pseudo-second order model (R^2=0.93-0.98) than pseudo-first order (R^2 = 0.87 - 0.94) for Cd, Cu, Cr and Zn. For Pb, the R^2 value of the pseudo-second order model fit was 0.73 compared to pseudo-first order model fit value of 0.94. However, the values of q_e calculated from both the models were different from the experimental values of q_e. The better fit of data to pseudo-second order model suggests that chemisorption process could be the rate-limiting step in the adsorption process (Nur et al., 2014). Heavy metal adsorption on many other adsorbents has also been reported in literature to fit better to this model than pseudo-first order model (Dimitrova and Mehandgiev, 1998; Mishra and Patel, 2009). However, the large differences in the experimental and model values for q_e indicate that this model may not be accurate in describing the kinetic data. Other models need to be tested to find a more accurate model fit to the data.

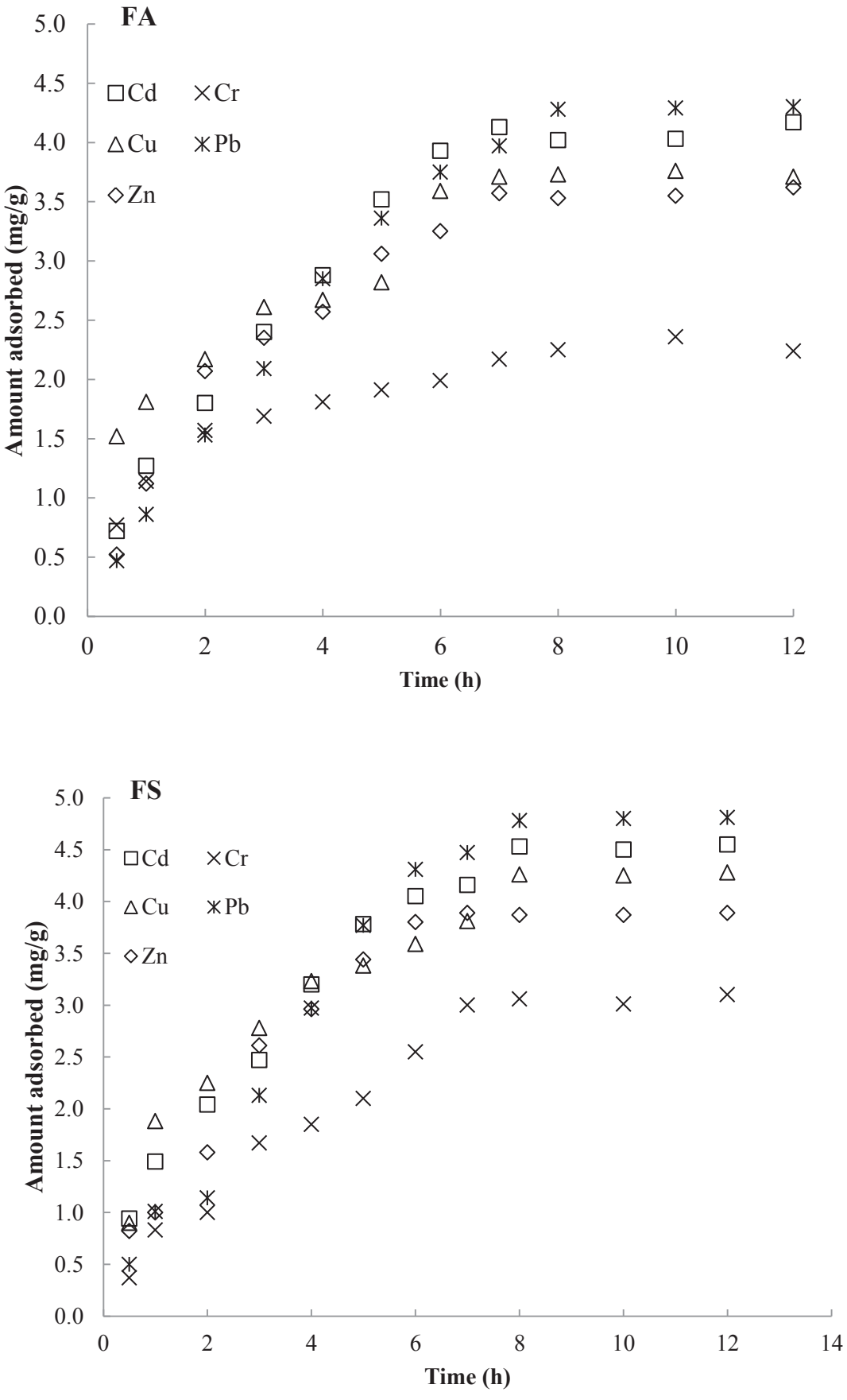

Figure 7.5. Kinetics of heavy metal adsorption on fly ash (FA) and furnace slag (FS)

Table 7.5. Pseudo-first order and pseudo-second order kinetic models parameters for the adsorption of heavy metals on fly ash (FA) and furnace slag (FS)

			Pseudo-first-order			Pseudo-second-order		
	Metals	q_e exp (mg/g)	q_e (mg/g)	$K_1 \times 10^{-2}$ (min^{-1})	R^2	q_e (mg/g)	$K_2 \times 10^{-2}$ (g /mg. min)	R^2
FA	Cd	4.10	2.90	0.34	0.8419	1.76	-	0.9851
	Cr	2.25	1.43	0.14	0.8241	1.06	-	0.9803
	Cu	3.71	3.86	0.31	0.8914	2.07	1.07	0.9844
	Pb	4.30	4.81	0.28	0.9443	2.34	0.31	0.9828
	Zn	3.62	3.02	0.24	0.9138	1.79	1.53	0.9760
FS	Cd	4.55	7.12	0.52	0.9226	5.96	0.05	0.9795
	Cr	3.10	4.79	0.44	0.9091	4.92	0.08	0.9288
	Cu	4.28	5.66	0.46	0.9008	5.18	0.08	0.9918
	Pb	4.81	11.14	0.58	0.9379	9.72	0.01	0.7315
	Zn	3.89	3.41	0.35	0.8672	5.28	0.06	0.9549

q_e: amount of heavy metals adsorbed at equilibrium (mg/g); K_1: equilibrium rate constant of pseudo-first-order sorption (min^{-1}); K_2: equilibrium rate constant of pseudo-second-order sorption (g/mg. min); R^2: coefficient of determination

7.3.5. Column experiment on furnace slag

In order to investigate the adsorptive removal capacities of furnace slag column, heavy metals solutions with 5 mg/L initial concentration were treated in column containing furnace slag mixed with clean sand. The results showed that furnace slag appeared better in removing Pb^{2+} and Cd^{2+} than other metals. The breakthrough curves of metals are closer to each other in single metals system than in mixed metals system (Figure 7.6 and 7.7).

Thomas model satisfactorily described the breakthrough curves obtained for single as well as mixed metals systems (R^2 = 0.86-1.00) (Table 7.6). The values obtained for adsorption

capacities (q_o) from the models are approximately equal to those calculated from the breakthrough curves. Both the model and breakthrough values were higher for each metal in the single metal system than in the mixed metals system. This is due to the competition for adsorption between metals in mixed metals system. Lower adsorption capacities for metals in mixed metals system than in single metals system were also reported for heavy metals adsorption on other adsorbents (Sounthrarajah et al. 2015). The column adsorption capacities are slightly lower than the respective the Langmuir adsorption capacities obtained from the batch study for furnace slag (Table 7.4). Sounthrarajah et al. (2015) also reported lower column values than batch values for heavy metals adsorption on granular activated carbon and explained this as due to equilibrium for adsorption not attaining in column study unlike in batch study (Sounthrarajah et al. 2015).

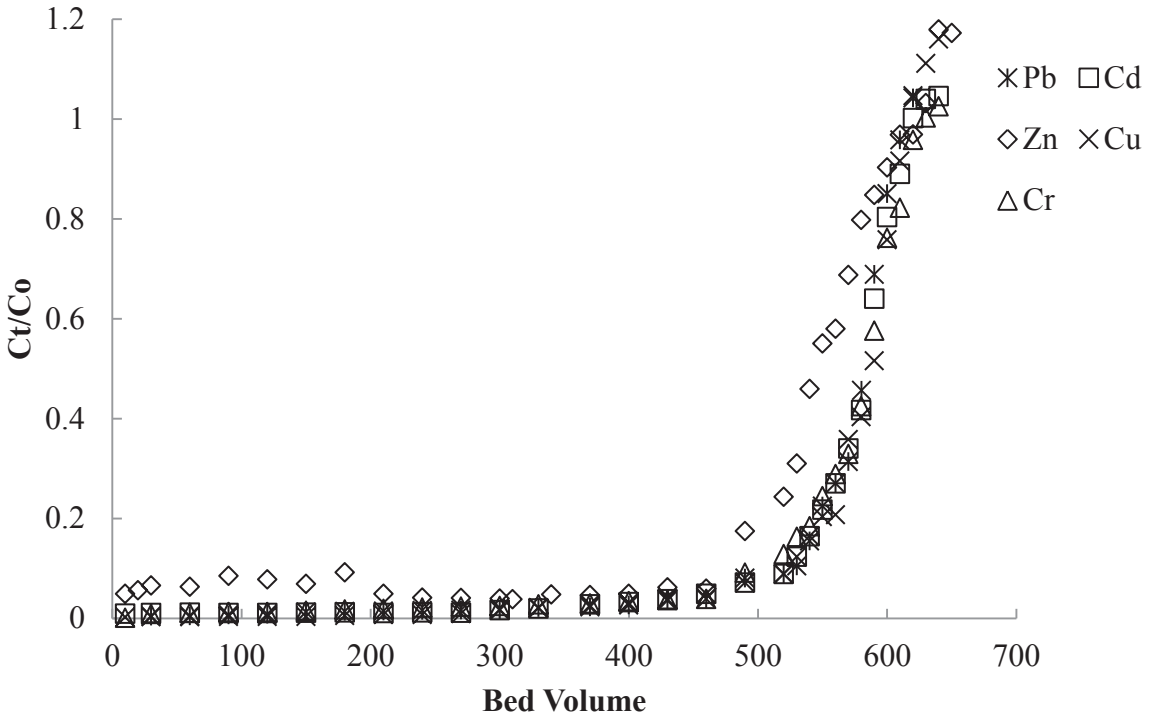

Figure 7. 6. Breakthrough curves of heavy metals in furnace slag + sand column in single metal system at pH 6.0

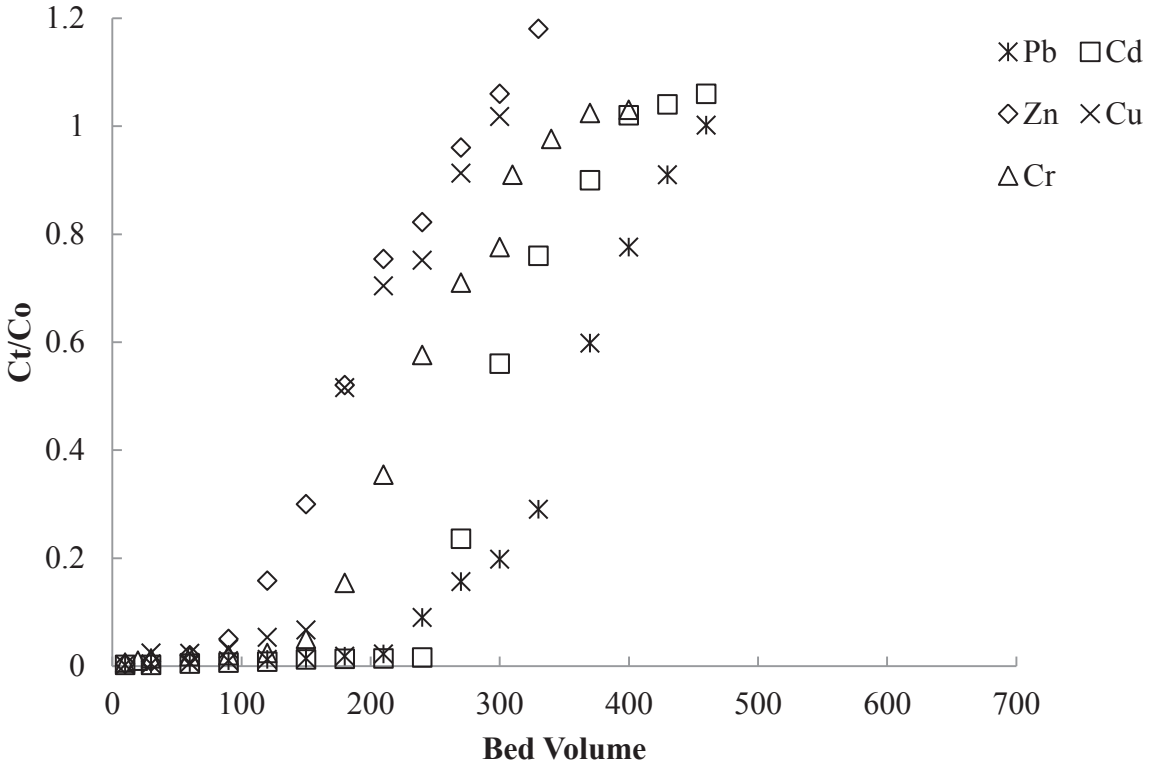

Figure 7. 7. Breakthrough curves of heavy metals in furnace slag + sand column in mixed metals system at pH 5.0

Table 7. 6. Breakthrough adsorption capacities and Thomas model parameters for furnace slag column adsorption of heavy metals (HM) from single (pH 6.0) and mixed metals solution (pH 5.0)

	Individual metal				Metals mixture			
HM	Breakthrough adsorption capacity q_e[1] (mg/g)	q_o (mg/g)	k_{Th} (mL/min.mg)	R^2	Breakthrough adsorption capacity q_e (mg/g)	q_o (mg/g)	k_{Th} (mL/min.mg)	R^2
Pb	4.05	3.52	1.54	0.9761	2.31	2.12	0.62	0.9587
Cd	3.68	3.47	1.56	0.9508	2.16	1.94	0.76	0.8613
Cu	4.11	3.47	1.54	0.9063	1.67	1.17	0.94	0.9118
Zn	3.73	3.46	1.60	0.9058	1.86	1.07	1.08	0.9955
Cr	3.55	3.43	2.08	0.9413	1.62	1.39	0.82	0.9572

qe: breakthrough adsorption capacity (mg/g),

q_o: Thomas adsorption capacity (mg/g) K_{Th}: Thomas rate constant (mL/min.mg)

7.4. Conclusions

Heavy metals can be serious pollutants of natural water bodies causing health risks to humans and aquatic organisms. A study was conducted to remove five heavy metals from water by adsorption onto an iron blast furnace slag and a fly ash in batch and column experiments. In batch experiment increase of pH increased adsorption of all metals with abrupt increase adsorption occurred in the pH range 4.0-6.0. Equilibrium adsorption of all metals at pH 6.5 was successfully modelled using Langmuir, Freundlich and Dubinin-Radushkevich models, with Freundlich model fitting the data the best. Langmuir adsorption maximum for fly ash ranged 3.4 - 5.1 mg/g with the adsorption capacity for the metals in the order: Pb > Cu > Cd, Zn, Cr. The corresponding values for furnace slag were 4.3 - 5.2 mg/g, and the order of adsorption capacities, Pb, Cu, Cd > Cr > Zn. The kinetics of adsorption fitted well to both the pseudo-first order and pseudo-second order models, but the fit was slightly better for the pseudo-second order model.

Column study showed that the adsorption capacities of metals were generally less in mixed metals system than in single metals system, probably due to metals competition for adsorption. The column adsorption data for both the single metal system and mixed metal system fitted reasonably well to Thomas model. The adsorption capacity predicted by the Thomas model in single metal system was also highest (4.1 mg/g) for Cu^{2+} and lowest for Zn^{2+} (3.6 mg/g). Overall the study showed that the industrial by-products, fly ash and blast furnace slag are effective low-cost adsorbents for the removal of Pb, Cu, Cd, Cr, and Zn from water. Further studies on these adsorbents are recommended in pilot plant scale experiments. Column experiments were conducted only on furnace slag. It was not possible to conduct column study on fly ash because of problems of caking of this material in columns during water flow. A suitable material is required to mix it with fly ash and use in columns to avoid the caking problem.

CHAPTER 8

CONCLUSIONS AND RECOMMENDATIONS

CHAPTER 8

CONCLUSIONS AND RECOMMENDATIONS

8.1. General summary

The main objective of the research was to (i) compare the concentration distribution, composition, possible sources and potential toxicity of heavy metals and PAHs found in Road-deposited sediments (RDS), water baseline sediments (WBS) and baseline soils (BLS) around Kogarah Bay in Sydney, (ii) determine potential mobility and bioavailability of heavy metals using a sequential chemical extraction method, (iii) determine possible sources of heavy metals and PAHs using statistical methods, (iv) determine the toxicity of the RDS and BLS elutriates using *Artemia salina*, Microtox® and different bioassays, and (v) test various low-cost adsorbents including industrial by-products for the removal of heavy metals.

8.2. Heavy metal concentrations, distributions, and sources in RDS

Contaminants from vehicles and activities associated with road and highway construction and maintenance are washed from roads and roadsides when it rains or snow melts. A large amount of this runoff pollutants are carried directly to natural water bodies. RDS are known to contain several inorganic and organic pollutants such as heavy metals and metalloids and polycyclic aromatic hydrocarbons (PAH). These pollutants are derived from vehicle exhaust emission, vehicle tyres, brakes and body frames, asphalt road surface, road fences, etc. Many of the heavy metals, metalloids and PAHs are acutely and chronically toxic and carcinogenic and known to have adverse effects on humans and aquatic ecosystems. Samples of RDS, WBS and BLS collected from Kogarah area Showed that Zn, Cu, V, Cr, and Sb concentrations were found to be the highest in RDS compared to those in BLS. The heavy metal concentrations were similar in WBS and BLS. Pollution Index (PI), a measure of metal enrichment was high (> 5) for Zn, Cu, V, Cr, and Sb in RDS. The possible sources of Zn, Cu, Cr and Sb were suggested to be vehicle brakes and tyre wear and the source of V was asphalt road surface. Metals concentrations in the mobile fraction (exchangeable) of RDS were: Fe > Mn, Zn > Cu, Pb > Cr, Ni, V, Cd, Sb. However, themobile fraction concentration as a % of total, was highest for Cd and lowest for Fe. Ecological risk as assessed byAustralia and New

Zealand Interim Sediment Quality criteria and the method developed by Hakanson (1980) was low to medium in RDS and low in BLS and WBS. Of the TEs in RDS, Cu had the highest potential ecological risk whereas Zn had the lowest.

8.3. PAHs concentrations, distribution, and sources in RDS

RDS is an important sink for PAHs originating from vehicle transport activity and road surface abrasion. This makes RDS a significant source of PAHs entering neighbouring water bodies as a result of stormwater runoffs and wind dispersion. The samples used for heavy metals study were also used for the PAH study to determine the concentration, distribution, sources and potential toxicity of PAHs compounds in RDS. The total concentration of 16 PAHs did not differ much between RDS, WBS, and BLS (RDS: 1.65 to 4.00 mg/kg; WBS: 0.49-5.19 mg/kg; NS: 0.40 to 7.49 mg/kg). However, the PAH composition and source from where they originated differed between these three sites. PAHs in RDS, WBS, and BLS were dominated by relatively high molecular weight compounds with more than three fused benzene rings, indicating that high temperature combustion processes were their predominant sources. The proportion of high molecular weight PAHs with 5 or 6 rings were higher in BLS than in RDS, whereas the low molecular weight PAHs proportions were higher in RDS. PAHs in RDS were derived both from petrogenic and pyrogenic sources while in BLS they were mainly from pyrogenic sources. The health risk of PAH exposure is very important to understand especially urban surface dust in urbanized densely populated areas. However, the potential toxicities of PAHs calculated using toxicity equivalent quotient calculated based on the relative toxicity values of individual PAHs proposed by Nisbet and LaGoy (1992) were all low.

8.4. RDS bioavailability and toxicity

Bioavailability and toxicity of pollutants in extracts from RDS and BLS was performed with an objective of characterizing toxicity of size-fractions by *Artemia salina* nauplii, Microtox® and cell culturing bioassay to measure the metabolic effects of the cells. Solvent and sea water elutriates of RDS and BLS were tested for the toxicity. Total PAH concentrations ranged from 0.16-0.20 mg/kg (BLS) to 1.25-2.37 mg/kg dry weight (RDS) and showed much higher in RDS than in BLS. Fine particle fraction had higher concentrations of PAH and heavy metal than coarser fractions. Median effect concentration (EC50) of RDS elutriate samples in Microtox® was significantly higher than BLS samples and increase of toxicity

with time suggests that the toxicity comes probably from metals. For spiked metals and PAHs, the toxicity to *Artemia* was significantly higher when they were tested in clean water than in elutriates. Mortality of *Artemia salina* nauplii varied with the type of heavy metal and PAH species. Low molecular weight PAH compounds showed higher toxicity for *Artemia* than high molecular weight PAH compounds. AhR CAFLUX toxicity bioassay suggests the similar trend of toxicity for the different particle sizes but it was significantly different between RDS and BLS samples. The p53 GeneBLAzer® assay showed no cytotoxic or genotoxic effects from any elutriates or solvent extracts of RDS or BLS.

8.5. Remediation of heavy metals in RDS stormwater runoff

An Australian zeolite with (Iron coated zeolite, ICZ) and without iron-coating, was used to remove five heavy metals from aqueous solutions using adsorption in batch and column experiments. The batch study showed that the Langmuir adsorption capacities of heavy metals on zeolite and ICZ at pH 6.5 and ionic strength 10^{-3} M $NaNO_3$ were in the order Pb > Cu > Cd > Cr, Zn for single metal (5.0–11.2 mg/g) and for mixed metals solution (3.7–7.6 mg/g). Langmuir adsorption capacity of ICZ was higher than zeolite for both single and mixed metals. The kinetic adsorption data fitted reasonably well to the pseudo-second order model for both zeolite and ICZ. Breakthrough adsorption capacity for single and mixed heavy metals in zeolite and ICZ column order was Pb > Cd > Cu > Zn > Cr. 0.1 M HCl satisfactorily desorbed the metals from zeolite and ICZ. The column adsorption data were fairly well described by Thomas model, with the order of Thomas adsorption capacity following a similar trend as in the batch study. Leaching of used ICZ and zeolite columns with 0.1 M HCl, desorbed a large percentage of the adsorbed metals and dissolved 10% Fe from the ICZ. However, the adsorption capacities got reduced in the second adsorption/desorption cycle, more so for ICZ, probably due to dissolution of some iron coatings in the acidic conditions of HCl. The study concluded that ICZ is a potential adsorbent for removing heavy metals from water.

Industrial by-products are low-cost materials for use as adsorbents to remove pollutants. Blast furnace slag (steels industry by-product) and fly ash (coal industry by-product) were used as adsorbents to remove heavy metals from water in both batch and column experiments. Increase of pH increased adsorption of all metals. Equilibrium adsorption of all metals was successfully modelled using Langmuir, Freundlich and Dubinin-Radushkevich models, with Freundlich model fitting the data the best. Langmuir adsorption maximum at pH 6.5 for fly

ash ranged 3.4 - 5.1 mg/g with the adsorption capacity for the metals in the order, Pb > Cu > Cd, Zn, Cr. The corresponding values for furnace slag were 4.3 - 5.2 mg/g, and the order of adsorption capacities was Pb, Cu, Cd > Cr > Zn. The kinetics of adsorption fitted well to both the pseudo-first order and pseudo-second order models, but the fit was slightly better for the pseudo-second order model. The column experiment with furnace slag indicated that column process can be used for treating polluted waters containing mixture of heavy metals.

8.6. Recommendations for future studies

The following recommendations are made for any future study on this important topic:

a. More studies are required to compare the metals and PAHs concentrations between RDS, WBS, and BLS within a single catchment area and determine the contribution of RDS on the metals and PAHs accumulation in the neighbouring water sediments.

b. Health risk assessment of RDS and BLS should be determined using different biological methods.

c. DNA damage experiments can be conducted to investigate the potential toxicity of RDS elutriates to aquatic organisms. More toxicity studies also need to be done for heavy metals and PAH compounds to determine the effect of light to exposed organisms especially in field scale condition.

d. Future research needs to explore highly efficient, low cost adsorbents such as industrial and agricultural wastes for the removal of heavy metals and PAHs compounds. Fly ash from coal industry and furnace slag from steel industry were studied in this thesis. Other common low cost adsorbents such as agricultural waste, red mud from Al industry can be studied.

e. Surface modifications of the adsorbents can be explored to increase the capacity, selectivity and strength of adsorption without significantly increasing the cost of such modification.

f. Investigate the effects of different factors such as pH, temperature, co-ions on adsorption and derived thermo dynamic parameters for adsorption. Use of continuous membrane

filtration adsorption hybrid system to remove heavy metals and PAHs compounds need to be explored.

REFERENCES

Aatmeeyata, Sharma M (2010). Polycyclic aromatic hydrocarbons, elemental and organic carbon emissions from tire-wear. Science of The Total Environment, 408: 4563-4568.

Abdel Salam OE, Reiad NA, ElShafei MM (2011). A study of the removal characteristics of heavy metals from wastewater by low-cost adsorbents. Journal of Advanced Research, 2: 297-303.

Abernethy S, Mackay D (1987). A discussion of correlations for narcosis in aquatic species. QSAR in Environmental Toxicology. Springer, 1-16.

Adams WJ, Rowland CD (2003). Aquatic toxicology test methods. Handbook of Ecotoxicology, 2: 19-38.

Agarwal T, Khillare PS, Shridhar V, Ray S (2009). Pattern, sources and toxic potential of PAHs in the agricultural soils of Delhi, India. Journal of Hazardous Matterials, 163: 1033-1039.

Ahmaruzzaman M (2008). Adsorption of phenolic compounds on low-cost adsorbents: A review. Advances in Colloid and Interface Science, 143: 48-67.

Ahmaruzzaman M (2011). Industrial wastes as low-cost potential adsorbents for the treatment of wastewater laden with heavy metals. Advances in Colloid and Interface Science, 166: 36-59.

Ahmed F, Bibi MH, Ahmed HI (2007). Environmental assessment of Dhaka City (Bangladesh) based on trace metal contents in road dusts. Environmental Geology 51, 975–985.

Aichner B, Glaser B, Zech W (2007). Polycyclic aromatic hydrocarbons and polychlorinated biphenyls in urban soils from Kathmandu Nepal. Organic Geochemistry, 38: 700-715.

Akher MS, Madany IM (1993) Heavy metals in street and house dust in Bahrain. Water, Air and Soil Pollution, 66, 111–119.

Al-Khasman OA (2007) The investigation of metal concentrations in street dust samples in Aqaba city, Jordan Environmental Geochemistry Health, 29, 197–207.

Allen JO, Dookeran NM, Smith KA, Sarofim AF, Taghizadeh K, Lafleur AL (1996). Measurement of polycyclic aromatic hydrocarbons associated with size-segregated atmospheric aerosols in Massachusetts. Environmental Science and Technology, 30: 1023-1031.

Allen S, Brown PA (1995). Isotherms analyses for single component and multi-component metal sorption onto lignite. Journal Chemical Technology Biotechnology, 62: 17–24.

Alvarez-Ayuso E, Garcıa-Sánchez A, Querol X (2003). Purification of metal electroplating waste waters using zeolites. Water Research, 37: 4855-4862.

Amato F, Querol X, Johansson C, Nagl C, Alastuey A (2010). A review on the effectiveness of street sweeping, washing and dust suppressants as urban PM control methods. Science of the Total Environment, 408: 3070-3084.

Amodu OS, Ntwampe SKO, Ojumu TV (2013). Bioavailability of high molecular weight polycyclic aromatic hydrocarbons using renewable resources: INTECH Open Access Publisher.

ANZECC (1997). ANZECC Interim Sediment Quality Guidelines. Report for the Environmental Research Institute of the Supervising Scientist. Sydney, Australia. Australian and New Zealand Environment and Conservation Council.

ANZECC (2000). ANZECC Water Quality Guidelines. Report for the Environmental Research Institute of the Supervising Scientist. Sydney, Australia. Australian and New Zealand Environment and Conservation Council.

Apak R, Tütem E, Hügül M, Hizal J (1998). Heavy metal cation retention by unconventional sorbents (red muds and fly ashes). Water Research, 32: 430-440.

Arfsten DP, Schaeffer DJ, Mulveny DC (1996). The effects of near ultraviolet radiation on the toxic effects of polycyclic aromatic hydrocarbons in animals and plants: A Review. Ecotoxicology and Environmental Safety, 33: 1-24.

Aryal R, Baral B, Vigneswaran S, Naidu R, Loganathan P (2011). Seasonal influence on urban dust PAH profile and toxicity in Sydney, Australia. Water Science and Technology, 63: 2238-2243.

Aryal R, Lee B-K. Characteristics of suspended solids and micropollutants in first-flush highway runoff. Water, Air, and Soil Pollution: Focus, 2009; 9: 339-346.

Aryal R, Vigneswaran S, Kandasamy J, Naidu R (2010). Urban stormwater quality and treatment. Korean Journal of Chemical Engineering, 27: 1343-1359.

Atanassova I (1999). Competitive effect of copper, zinc, cadmium and nickel on ion adsorption and desorption by soil clays. Water, Air and Soil Pollution, 113 (1/4): 115–125.

Atienza D, Calbet A, Saiz E, Alcaraz M, Trepat I (2006). Trophic impact, metabolism, and biogeochemical role of the marine cladoceran Penilia avirostris and the co-dominant copepod Oithona nana in NW Mediterranean coastal waters. Marine Biology, 150: 221-235.

Australian Protection Agency Report (2003): http://www.scew.gov.au/archive/air/pubs/atem/at_rev_pahs_health_review_200305.pdf

Babel S, Kurniawan TA (2003). Low-cost adsorbents for heavy metals uptake from contaminated water: a review. Journal of Hazardous Materials, 97: 219-243.

Backhaus T, Scholze M, Grimme L (2000). The single substance and mixture toxicity of quinolones to the bioluminescent bacterium *Vibrio fischeri*. Aquatic Toxicology, 49: 49-61.

Bäckström M, Nilsson U, Håkansson K, Allard B, Karlsson S (2003). Speciation of heavy metals in road runoff and roadside total deposition. Water, Air, and Soil Pollution, 147: 343-366.

Baes CF, Mesmer RE (1976). Hydrolysis of Cations, Wiley, New York.

Bailey SE, Olin TJ, Bricka RM, Adrian DD (1999). A review of potentially low-cost sorbents for heavy metals. Water Research, 33: 2469-2479.

Baker HM, Massadeh AM, Younes HA (2009). Natural Jordanian zeolite: removal of heavy metal ions from water samples using column and batch methods. Environmental Monitoring and Assessment, 157: 319-330.

Bakker MI, Casado B, Koerselman JW, Tolls J, Kolloffel C (2000). Polycyclic aromatic hydrocarbons in soil and plant samples from the vicinity of an oil refinery, Science of the Total Environment, 263: 91-100.

Banerjee S, Jayaram R, Joshi M (2003). Removal of nickel (II) and zinc (II) from wastewater using fly ash and impregnated fly ash. Separation Science and Technology, 38: 1015-1032.

Baptista LF, Migueal ED (2005) Geochemistry and risk assessment of street dust in Luanda, Angola: A tropical urban environment. Atmospheric Environment, 39, 4501–4512.

Baral S, Das N, Ramulu T, Sahoo S, Das S, Chaudhury GR (2009). Removal of Cr (VI) by thermally activated weed Salvinia cucullata in a fixed-bed column. Journal of Hazardous Materials, 161: 1427-1435.

Barnum DW (1983). Hydrolysis of cations. Formation constants and standard free energies of formation of hydroxy complexes. Inorganic Chemistry, 22: 2297–2305.

Baumard P, Budzinski H, Garrigues P (1998). PAHs in Arcachon bay, France: origin and biomonitoring with caged organisms. Marine Pollution Bulletin, 36: 577-586.

Bay S, Jones BH., Schiff K, Washburn L (2003). Water quality impacts of stormwaterdischarges to Santa Monica Bay. Marine Environmental Research, 56: 205–223.

Bayat B (2002). Combined removal of zinc (II) and cadmium (II) from aqueous solutions by adsorption onto high-calcium Turkish fly ash. Water, Air, and Soil Pollution, 136: 69-92.

Bayat B (2002). Comparative study of adsorption properties of Turkish fly ashes: I. The case of nickel (II), copper (II) and zinc (II). Journal of Hazardous Materials, 95: 251-273.

Beasley G, Kneale P (2002). Reviewing the impact of metals and PAHs on macroinvertebrates in urban watercourses. Progress in Physical Geography, 26: 236-270.

Béze LE, Rose J, Mouillet V, Farcas F, Masion A, Chaurand P, Bottero JY (2012). Location and evolution of the speciation of vanadium in bitumen and model of reclaimed bituminous mixes during ageing: Can vanadium serve as a tracer of the aged and fresh parts of the reclaimed asphalt pavement mixture? Fuel, 102: 423–430.

Bhatnagar A, Sillanpää M (2011). A review of emerging adsorbents for nitrate removal from water. Chemical Engineering Journal, 168: 493-504.

Bhattacharya AK, Mandal S, Das S (2006). Adsorption of Zn (II) from aqueous solution by using different adsorbents. Chemical Engineering Journal, 123: 43-51.

Bhattacharya AK, Naiya TK, Mandal SN, Das SK (2008). Adsorption, kinetics and equilibrium studies on removal of Cr (VI) from aqueous solutions using different low-cost adsorbents. Chemical Engineering Journal, 137: 529-541.

Bhattacharya S, Shoda LK, Zhang Q, Woods CG, Howell BA, Siler SQ (2012). Modeling drug and chemical induced hepatotoxicity with systems biology approaches. Frontiers in physiology, 3.

Bihari N, Hamer B, Kralj-Bilen B (2006). PAH content, toxicity and genotoxicity of coastal marine sediments from the Rovinj area, Northern Adriatic, Croatia. Science of the Total Environment, 366: 602-611.

Birch GF (2011). Contaminated soil and sediments in a highly developed catchment-estuary system (Sydney estuary, Australia): An innovative stormwater remediation strategy. Journal of Soils and Sediments, 11: 194-208.

Birch GF, McCready S (2009) Catchment sources of heavy metal contamination and influence on the quality of receiving basin sediments in Port Jackson, Australia. Science of the Total Environment, 407: 2820–2835.

Birch GF, Scollen A (2003) Trace elements in road dust, gully pots and parkland soils in a highly urbanised sub-catchment of Port Jackson, Australia. Australian Journal of Soil Research, 41: 1329–1342.

Blust R, Baillieul M, Decleir W (1995). Effect of total cadmium and organic complexing on the uptake of cadmium by the brine shrimp, Artemia franciscana. Marine Biology, 123: 65-73.

Borek S, Samardakiewicz S, Wozny A (1998). The effect of pH of water on lead toxicity in *Lemna minor* L. Biological Bulletin of Poznań, 1.

Boström C-E, Gerde P, Hanberg A, Jernström B, Johansson C, Kyrklund T (2002). Cancer risk assessment, indicators, and guidelines for polycyclic aromatic hydrocarbons in the ambient air. Environmental Health Perspectives, 110: 451.

Bott TL, Standley LJ (2000). Transfer of Benzo[a]pyrene and 2,2‘,5,5‘-Tetrachlorobiphenyl from Bacteria and Algae to Sediment-Associated Freshwater Invertebrates. Environmental Science and Technology, 34: 4936-4942.

Botta C, Di Giorgio C, Sabatier AS, De Méo M (2009). Effects of UVA and visible light on the photogenotoxicity of benzo [a] pyrene and pyrene. Environmental Toxicology, 24: 492-505.

Boyd GR, Palmeri JM, Zhang S, Grimm DA (2004). Pharmaceuticals and personal care products (PPCPs) and endocrine disrupting chemicals (EDCs) in stormwater canals and Bayou St. John in New Orleans, Louisiana, USA. Science of the Total Environment, 333: 137-148.

Braune M, Wood A (1999). Best management practices applied to urban runoff quantity and quality control. Water Science and Technology, 39: 117-121.

Brown B, Rattigan B (1970). Toxicity of soluble copper and other metal ions to Elodea canadensis. Environmental Pollution, 20: 303-314.

Brown JN, Peake BM (2006). Sources of heavy metals and polycyclic aromatic hydrocarbons in urban stormwater runoff. Science of the Total Environment, 359: 145-155.

Bryan G, Langston W (1992). Bioavailability, accumulation and effects of heavy metals in sediments with special reference to United Kingdom estuaries: a review. Environmental Pollution, 76: 89-131.

Bucheli TD, Blum F, Desaules A, Gustafsson O (2004). Polycyclic aromatic hydrocarbons, black carbon, and molecular markers in soils of Switzerland. Chemosphere, 56: 1061-1076.

Budzinski H, Jones I, Bellocq J, Pierard C, Garrigues P (2007). Evaluation of sediment contamination by polycyclic aromatic hydrocarbons in the Gironde estuary. Marine Chemistry, 58: 85-97.

Burton GA, Pitt R, Clark S (2000). The role of traditional and novel toxicity test methods in assessing stormwater and sediment contamination. Critical Reviews in Environmental Science and Technology, 30: 413-447.

Burton Jr GA (2002). Sediment quality criteria in use around the world. Limnology, 3: 65-76.

Butler JD, Butterworth V, Kellow SC, Robinson HG (1984). Some observations on the polycyclic aromatic hydrocarbon (PAH) content of surface soils in urban areas, Science of the Total Environment, 33: 75-85.

Cabal B, Ania C, Parra J, Pis J (2009). Kinetics of naphthalene adsorption on an activated carbon: comparison between aqueous and organic media. Chemosphere, 76: 433-438.

Cetin S, Pehlivan E (2007). The use of fly ash as a low cost, environmentally friendly alternative to activated carbon for the removal of heavy metals from aqueous solutions. Colloids and Surfaces A: Physicochemical and Engineering Aspects, 298: 83-87.

Chang S, Wang K, Chang H, Ni W, Wu B, Wong R, Lee H (2009) Comparison of source identification of metals in road-dust and soil. Soil and Sediment Contamination 18, 669–683.

Chapman PM, Barrick RC, Neff JM, Swart RC (1987). Four independent approaches to developing sediment quality criteria yield similar values for model contaminants. Environmental Toxicology and Chemistry, 6: 723-725.

Charlesworth S, Everett M, McCarthy R, Ordonez A, De Miguel E (2003) A comparative study of heavy metal concentration and distribution in deposited street dusts in a large and a small urban area: Birmingham and Coventry, West Midlands, UK. Environment International, 29, 563–573.

Chen F, Pu L (2007) Relationship between trace elements and basic properties of agricultural soils in Kunshan County. Soils, 39: 291–296.

Chen LG, Ran Y, Xing BS, Mai BX, He JH, Wei XG (2005). Contents and sources of polycyclic aromatic hydrocarbons and organochlorine pesticides in vegetable soils of Guangzhou, China. Chemosphere, 60: 879-890.

Chen Z, Ngo HH, Guo W (2013). A critical review on the end uses of recycled water. Critical Reviews in Environmental Science and Technology, 43: 1446-1516.

Cheung Y, Neller A, Chu K, Tam N, Wong C, Wong Y (1997). Assessment of sediment toxicity using different trophic organisms. Archives of Environmental Contamination and Toxicology, 32: 260-267.

Chial B, Persoone G (2003). Cyst-based toxicity tests- Application of ostracod soilid-phase microbiotest for toxicity monitoring of contaminated soils. Environmental Toxicology, 18 (5): 347–352.

Choi K, Meier PG (2001). Toxicity evaluation of metal plating wastewater employing the Microtox® assay: a comparison with cladocerans and fish. Environmental Toxicology, 16: 136-141.

Chowdhury ZZ, Zain SM, Rashid AK, Rafique RF, Khalid K (2013). Breakthrough curve analysis for column dynamics sorption of Mn(II) ions from wastewater by using Mangostana garcinia peel-based granular-activated carbon. Journal of Chemistry, 1:58-68.

Clement B, Raevel V, Renard O (2010). Ecotoxicological assessment of road runoffresidues for aquatic surface ecosystems in a scenario of reuse. Journal of Soils and Sediments, 10: 1255–1266.

Cortazar E, Bartolome L, Arrasate S, Usobiaga A, Raposo JC, Zuloaga O, Etxebarria N (2008). Distribution and bioaccumulation of PAHs in the UNESCO protected natural reserve of Urdaibai, Bay of Biscay. Chemosphere, 72: 1467-1474.

Crisafully R, Milhome MAL, Cavalcante RM, Silveira ER, De Keukeleire D, Nascimento RF (2008). Removal of some polycyclic aromatic hydrocarbons from petrochemical wastewater using low-cost adsorbents of natural origin. Bioresource Technology, 99: 4515-4519.

Crisinei A, Delaunay L, Rossel D, Tarradellas J, Meyer H, Saiah H (1994). Cyst-based ecotoxicological tests using Anostracans: Comparison of two species of Streptocephalus. Environmental Toxicology and Water Quality, 9: 317-326.

Davis AP, Shokouhian M, Ni S (2001). Loading estimates of lead, copper, cadmium, and zinc in urban runoff from specific sources. Chemosphere, 44: 997-1009.

De Cooman W, Florus M, Vangheluwe M, Janssen C, Heylen S, De Pauw N (1999). Sediment characterisation of rivers in Flanders. The Triad approach. Proceedings: CATS. 4, 351-367.

De Miguel E, Llamas JF, Chacon E, Berg T, Larssen S, Royset O, Vadset M (1997) Origin and patterns of distribution of trace elements in street dust: unleaded petrol and urban lead. Atmospheric Environment, 31, 2733–2740.

Deshpande V, Bhoskar PDB (2012). Characterization and dielectric study of zeolite ZSM5. International Journal of Engineering Research and Technology. 1. ESRSA Publications.

Diamond SA, Mount DR, Burkhard LP, Ankley GT, Makynen EA, Leonard EN (2000). Effect of irradiance spectra on the photoinduced toxicity of three polycyclic aromatic hydrocarbons. Environmental Toxicology and Chemistry, 19: 1389-1396.

Dimirkou A, Doula MK (2008). Use of clinoptilolite and an Fe-overexchanged clinoptilolite in Zn^{2+} and Mn^{2+} removal from drinking water. Desalination, 224: 280-292.

Dimitrova SV (1996). Metal sorption on blast-furnace slag. Water Research, 30: 228-232.

Dimitrova SV (2002). Use of granular slag columns for lead removal. Water Research, 36: 4001-4008.

Dimitrova SV, Mehandgiev DR (1998). Lead removal from aqueous solutions by granulated blast-furnace slag. Water Research, 32: 3289-3292.

Domene X, Alcaniz JM, Andres P (2008). Comparison of solid-phase and eluate assays to gauge the ecotoxiclogical risk of organic wastes on soil organisms. Environmental Pollution, 151 (3): 549–558.

Dong TTT, Lee B-K (2009). Characteristics, toxicity, and source apportionment of polycylic aromatic hydrocarbons (PAHs) in road dust of Ulsan, Korea. Chemosphere, 74: 1245-1253.

Doong RA, Lin YT (2004). Characterization and distribution of polycyclic aromatic hydrocarbon contaminations in surface sediment and water from Gaoping River, Taiwan. Water Research, 38: 1733-1744.

Doula M, Ioannou A, Dimirkou A (2002). Copper Adsorption and Si, Al, Ca, Mg, and Na Release from Clinoptilolite. Journal of Colloid and Interface Science, 245: 237-250.

Doula MK (2007). Synthesis of a clinoptilolite–Fe system with high Cu sorption capacity. Chemosphere, 67: 731-740.

Doula MK (2009). Simultaneous removal of Cu, Mn and Zn from drinking water with the use of clinoptilolite and its Fe-modified form. Water Research, 43: 3659-3672.

Drapper D, Tomlinson R, Williams P (2000). Pollutant concentrations in road runoff: Southeast Queensland case study. Journal of Environmental Engineering, 126: 313-320.

Du Y, Gao B, Zhou H, Ju X, Hao H, Yin S (2013) Health risk assessment of heavy metals in road dusts in urban parks of Beijing, China. Procedia Environmental Sciences, 18: 299–309.

Duong TT, Lee B-K (2011). Determining contamination level of heavy metals in road dust from busy traffic areas with different characteristics. Journal of Environmental Management, 92: 554-562.

Dvorak P, Benova K, Vitek J (2012). Alternative biotest on Artemia franciscana. Journal of Ecotoxicology and Environmental Safety, 23: 51-74.

Elnabarawy MT, Welter AN, Robideau RR (1986). Relative sensitivity of three daphnid species to selected organic and inorganic chemicals. Environmental Toxicology and Chemistry, 5: 393-398.

Erdem E, Karapinar N, Donat R (2004). The removal of heavy metal cations by natural zeolites. Journal of Colloid and Interface Science, 280: 309-314.

Eriksson E, Baun A, Scholes L, Ledin A, Ahlman S, Revitt M (2007). Selected stormwater priority pollutants-a European perspective. Science of the Total Environment, 383: 41-51.

Escher B, Leusch F (2012). Bioanalytical Tools In Water Quality Assessment: IWA publishing.

Escher BI, Allinson M, Altenburger R, Bain PA, Balaguer P, Busch W (2013). Benchmarking organic micropollutants in wastewater, recycled water and drinking water with in vitro bioassays. Environmental Science and Technology, 48: 1940-1956.

Essumang DK, Dodoo DK, Obiri S, Oduro AK (2006). Analysis of Polycyclic aromatic hydrocarbons in street soil dust in Kumasi Metropolis of Ghana. Environmental Monitoring Assessment, 121: 401-408.

Evans KM, Gill RA, Robotham PWJ (1990). The PAH and organic content of sediment particle size fractions. Water, Air, and Soil Pollution, 51: 13-31.

Everaarts J (1995). DNA integrity as a biomarker of marine pollution: Strand breaks in seastar (*Asterias rubens*) and dab (*Limanda limanda*). Marine Pollution Bulletin, 31: 431-438.

Faiz Y, Tufail M, Javed M, Chaudhry M, Siddique N (2009) Road dust pollution of Cd, Cu, Ni, Pb and Zn along Islamabad Expressway, Pakistan. Microchemistry Journal, 92, 186–192.

Fang GC, Chang CN, Wu YS, Fu PPC, Yang IL, Chen MH (2004). Characterization, identification of ambient air and road dust polycyclic aromatic hydrocarbons in central Taiwan, Taichung. Science of the Total Environment, 327: 135-146.

Feng D, Van Deventer J, Aldrich C (2004). Removal of pollutants from acid mine wastewater using metallurgical by-product slags. Separation and Purification Technology, 40: 61-67.

Fernandez M, I'Haridon J (1994). Effects of light on the cytotoxicity and Genotoxicity of Benzo(a)pyrene and an oil refinery effluent in the newt. Environmental and Molecular Mutagenesis, 24: 124-136.

Figi R, Nagel O, Tuchschmid M, Lienemann P, Gfeller U, Bukowiecki N (2010) Quantitative analysis of heavy metals in automotive brake linings: A comparison between wet-chemistry based analysis and in-situ screening with a handheld X-ray fluorescence spectrometer. Analytica Chimica Acta, 676, 46–52.

Gaete H, Silva J, Riveros A, Soto E, Troncoso L, Bay-Schmith E (1996). Combined effect and ecological risk of Zn, Cu and Cr present in the San Vicente Harbor, Chile. Gayana Oceanologia, 4: 99-107.

Gajbhiye S, Hirota R (1990). Toxicity of heavy metals to brine shrimp Artemia salina. Journal of the Indian Fisheries Association, 20: 43-50.

Gangoli N, Markey D, Thodos G (1975). Removal of heavy metal ions from aqueous solutions with fly ash. Proceedings of the 2nd National Conference on Complete Water Reuse, Chicago, IL, USA.

García-Flores E, Wakida F, Espinoza-Gomez J (2013). Sources of polycyclic aromatic hydrocarbons in urban storm water runoff in Tijuana, Mexico. International Journal of Environmental Research, 7: 387-394.

Gelboin HV (1969). A microsome-dependent binding of benzo [a] pyrene to DNA. Cancer Research, 29: 1272-1276.

Georgiou CD, Papapostolou I, Grintzalis K (2009). Protocol for the quantitative assessment of DNA concentration and damage (fragmentation and nicks). Nature Protocols, 4: 125-131.

Gong Z, Alef K, Wilke B-M, Li P (2007). Activated carbon adsorption of PAHs from vegetable oil used in soil remediation. Journal of Hazardous Materials, 143: 372-378.

Greenstein D, Tiefenthaler L, Bay S (2004). Toxicity of parking lot runoff after appli-cation of simulated rainfall. Archives of Environmental Contaminant Toxicology, 47 (2): 199–206.

Grimalt J, Canton L, Alonso B (1992). Spatial and temporal variance of hydrocarbon pollution data in a coastal river-influenced sedimentary system. Environmental Science Technology, 26: 2240-2251.

Gromaire-Mertz MC, Garnaud S, Gonzalez A, Chebbo G (1999). Characterisation of urban runoff pollution in Paris. Water Science and Technology, 39: 1-8.

Grover M, Narayanaswamy M (1982). Removal of hexavalent chromium by adsorption on fly ash. Journal of Instrumental Engineering (India), Part EN: Environmental Engineering, 504: 36-39.

Gunawardana C, Goonetilleke A, Egodawatta P, Dawes L, Kokot S (2012) Source characterisation of road dust based on chemical and mineralogical composition. Chemosphere 87, 163–170.

Guney M, Onay TT, Copty NK (2010). Impact of overland traffic on heavy metal levels in highway dust and soils of Istanbul, Turkey. Environmental Monitoring and Assessment, 164: 101-110.

Gupta VK (1998). Equilibrium uptake, sorption dynamics, process development, and column operations for the removal of copper and nickel from aqueous solution and wastewater using activated slag, a low-cost adsorbent. Industrial and Engineering Chemistry Research, 37: 192-202.

Gupta VK, Ali I (2000). Utilisation of bagasse fly ash (a sugar industry waste) for the removal of copper and zinc from wastewater. Separation and Purification Technology, 18: 131-140.

Gupta VK, Ali I (2012). Environmental Water: Advances in Treatment, Remediation and Recycling: Newnes.

Gupta VK, Gupta M, Sharma S (2001). Process development for the removal of lead and chromium from aqueous solutions using red mud- an aluminium industry waste. Water Research, 35: 1125-1134.

Gupta VK, Jain C, Ali I, Sharma M, Saini V (2003). Removal of cadmium and nickel from wastewater using bagasse fly ash- a sugar industry waste. Water Research, 37: 4038-4044.

Gupta VK, Sharma S (2003). Removal of zinc from aqueous solutions using bagasse fly ash-a low cost adsorbent. Industrial and Engineering Chemistry Research, 42: 6619-6624.

Guzzella L (1998). Comparison of test procedures for sediment toxicity evaluation with Vibrio fischeri bacteria. Chemosphere 1998, 37: 2895-2909.

Hadjispyrou S, Kungolos A, Anagnostopoulos A (2001). Toxicity, Bioaccumulation, and Interactive Effects of Organotin, Cadmium, and Chromium on *Artemia franciscana*. Ecotoxicology and Environmental Safety, 49: 179-186.

Hakanson L (1980) An ecological risk index for aquatic pollution control. A sedimentological approach. Water Research, 14: 975–1001.

Hamidpour M, Kalbasi M, Afyuni M, Shariatmadari H, Holm PE, Hansen HCB (2010). Sorption hysteresis of Cd (II) and Pb (II) on natural zeolite and bentonite. Journal of Hazardous Materials, 181: 686-691.

Han R, Zou L, Zhao X, Xu Y, Xu F, Li Y (2009). Characterization and properties of iron oxide-coated zeolite as adsorbent for removal of copper (II) from solution in fixed bed column. Chemical Engineering Journal, 149: 123-131.

Han YM, Du P, Cao J, Posmentier ES (2006) Multivariate analysis of heavy metal contamination in urban dusts of Xi'an, Central China. Science of The Total Environment, 355: 176–186.

Hao R, Wan HF, Song YT, Jiang H, Peng SL (2007). Polycyclic aromatic hydrocarbons in agricultural soils of the southern subtropics, China. Pedosphere, 17: 673-680.

Harris SL, Levine AJ (2005). The p53 pathway: positive and negative feedback loops. Oncogene, 24: 2899-2908.

Hassanien MA, Abdel-Latiff NM (2008). Polycyclic aromatic hydrocarbons in road dust over Greater Cairo, Egypt. Journal Hazardous Materials, 151: 247-254.

Haugland T, Ottesen RT, Volden T (2008). Lead and polycyclic aromatic hydrocarbons (PAHs) in surface soil from day care centres in the city of Bergen, Norway. Environmental Pollution, 153: 266–272.

Hjortenkrans D, Bergbäck B, Häggerud A (2006). New metal emission patterns in road traffic environments. Environmental Monitoring and Assessment, 117: 85-98.

Honda K, Mizukami M, Ueda Y (2007). Residue level of polycyclic aromatic hydrocarbons in Japanese paddy soils from 1959 to 2002. Chemosphere, 68: 1763-1771.

Hua M, Zhang S, Pan B, Zhang W, LL, Zhang Q (2012). Heavy metal removal from water/wastewater by nanosized metal oxides: a review. Journal of Hazardous Materials, 211: 317-331.

Huang X-D, Dixon DG, Greenberg BM (1995). Increased polycyclic aromatic hydrocarbon toxicity following their photomodification in natural sunlight: Impacts on the duckweed Lemna gibba L. G-3. Ecotoxicology and Environmental Safety, 32: 194-200.

Hui KS, Chao CYH, Kot SC (2005). Removal of mixed heavy metal ions in wastewater by zeolite 4A and residual products from recycled coal fly ash. Journal of Hazardous Materials, 127: 89-101.

Hurst MR, Balaam J, Chan-Man YL, Thain JE, Thomas KV (2004). Determination of dioxin and dioxin-like compounds in sediments from UK estuaries using a bio-analytical

approach: chemical-activated luciferase expression (CALUX) assay. Marine Pollution Bulletin, 49: 648-658.

Hutchinson T (1975). Heavy metal toxicity and synergism to floating aquatic weeds. International Association of Theoretical and Applied Limnology, 19: 2102–2111.

Hwang H-M, Foster GD (2006). Characterization of polycyclic aromatic hydrocarbons in urban stormwater runoff flowing into the tidal Anacostia River, Washington, DC, USA. Environmental Pollution, 140: 416-426.

Ikenaka Y, Sakamoto M, Nagata T, Takahashi H, Miyabara Y, Hanazato T (2013). Effects of polycyclic aromatic hydrocarbons (PAHs) on an aquatic ecosystem: acute toxicity and community-level toxic impact tests of benzo [a] pyrene using lake zooplankton community. Journal Toxicology Science, 38: 131-136.

Invitrogen TFS (2010). Invitrogen p53 CellSensor® p53RE-bla HCT-116 cell-based protocol.

Ireland D.S, Burton G.A, Hess GG (1996). In situ toxicity evaluations of turbidity and photoinduction of polycyclic aromatic hydrocarbons. Environmental Toxicology Chemistry, 15: 574–581.

Jamil TS, Ibrahim HS, El-Maksoud IA, El-Wakeel S (2010). Application of zeolite prepared from Egyptian kaolin for removal of heavy metals: I. Optimum conditions. Desalination, 258: 34-40.

Jeon C-S, Park S-W, Baek K, Yang J-S, Park J-G (2012). Application of iron-coated zeolites (ICZ) for mine drainage treatment. Korean Journal of Chemical Engineering, 29: 1171-1177.

Jiang XD, Wang GZ, Li SJ, He JF (2007). Heavy metal exposure reduces hatching success of Acartia pacifica resting eggs in the sediment. Journal of Environment Science (China), 19: 733-7.

Jiang YF, Wang XT, Wang F, Jia Y, Wu MH, Sheng GY, Fu JM (2009). Levels, composition profiles and sources of polycyclic aromatic hydrocarbons in urban soil of Shanghai, China. Chemosphere, 75: 1112-1118.

Jiao WT, Lu YL, Wang TY, Li J, Han JY, Wang G (2009). Polycyclic aromatic hydrocarbons in soils around Guanting Reservoir, Beijing, China. Chemical Ecology, 25: 39-48.

Jin L, Gaus C, Escher BI (2015). Adaptive stress response pathways induced by environmental mixtures of bioaccumulative chemicals in dugongs. Environmental Science and Technology, 49(11): 6963-6973.

Jiries A (2003). Vehicular contamination of dust in Amman, Jordan. The Environmentalist, 23: 205-210.

Joshi UM, Vijayaraghavan K, Balasubramanian R (2009) Elemental composition of urban street dusts and their dissolution characteristics in various aqueous media. Chemosphere, 77: 526–533.

Jusoh A, Su Shiung L, Ali Na, Noor M (2007). A simulation study of the removal efficiency of granular activated carbon on cadmium and lead. Desalination, 206: 9-16.

Kadıoğlu YK, Üstündağ Z, Solak AO, Karabıyıkoğlu G (2010). Sources of environmental pollution in Ankara (Turkey): Geochemistry and traffic effects-PEDXRF applications. Spectroscopy Letters, 43: 247-257.

Karbassi AR, Monavari SM, Bidhendi GRN, Nouri J, Nematpour K (2008). Metal pollution assessment of sediment and water in the Shur River. Environmental Monitoring Assessment, 147: 107–116.

Karlsson K, Viklander M (2008) Trace metal composition in water and sediment from catch basins. Journal of Environmental Engineering, 134: 870–878.

Kartal S, Aydin Z, Tokalioglu S (2006) Fractionation of metals in street sediment samples by using the BCR sequential extraction procedure and multivariate statistical elucidation of the data. Journal of Hazardous Materials, 132: 80–89.

Karthikeyan M, Satheeshkumar K, Elango K (2009). Removal of fluoride ions from aqueous solution by conducting polypyrrole. Journal of Hazardous Materials, 167: 300-305.

Kayhanian M, Stransky C, Bay S, Lau S-L, Stenstrom MK (2008). Toxicity of urban highway runoff with respect to storm duration. Science of the Total Environment, 389: 386-406.

Kelleher BP, O'Callaghan MN, Leahy MJ, O'Dwyer TF, Leahy JJ (2002). The use of fly ash from the combustion of poultry litter for the adsorption of chromium (III) from aqueous solution. Journal of Chemical Technology and Biotechnology, 77: 1212-1218.

Kennedy K, Macova M, Bartkow ME, Hawker DW, Zhao B, Denison MS (2010). Effect based monitoring of seasonal ambient air exposures in Australia sampled by PUF passive air samplers. Atmospheric Pollution Research, 1: 50-58.

Khalili NR, Scheff PA, Holsen TM (1995). PAH source fingerprints for coke ovens, diesel and gasoline engines, highway tunnels, and wood combustion emissions. Atmospheric Environment, 29: 533-542.

Khanal R, Furumai H, Nakajima F (2014). Toxicity assessment of size-fractionated urban road dust using ostracod *Heterocypris incongruens* direct contact test. Journal of Hazardous Materials, 264: 53-64.

Kim M, Mahlon C, Kennicutt II, Qian Y (2008). Source characterisation using compound composition and stable isotope ratio of PAHs in sediments from lakes, harbor, and shipping waterway. Science of the Total Environment, 389: 367-377.

Kocaoba S, Orhan Y, Akyüz T (2007). Kinetics and equilibrium studies of heavy metal ions removalby use of natural zeolite. Desalination, 214: 1-10.

Kong H, He J, Wu H, Wu H, Gao Y (2012). Phenanthrene Removal from Aqueous Solution on Sesame Stalk-based Carbon. Clean Soil, Air, Water, 40: 752-759.

Kragović M, Daković A, Sekulić Ž, Trgo M, Ugrina M, Perić J (2012). Removal of lead from aqueous solutions by using the natural and Fe (III)-modified zeolite. Applied Surface Science, 258: 3667-3673.

Krylov SN, Huang XD, Zeiler LF, Dixon DG, Greenberg BM (1997). Mechanistic quantitative structure–activity relationship model for the photoinduced toxicity of polycyclic aromatic hydrocarbons: I. Physical model based on chemical kinetics in a two-compartment system. Environmental Toxicology and Chemistry, 16: 2283-2295.

Kuo CY, Wang JY, Chang SH, Chen MC (2009) Study of metal concentrations in the environment near diesel transport routes. Atmospheric Environment 43, 3070–3076.

Kurniawan TA, Chan G, Lo W-H, Babel S (2006). Comparisons of low-cost adsorbents for treating wastewaters laden with heavy metals. Science of the Total Environment, 366: 409-426.

Laak TL, Agbo SO, Barendregt A, Hermens JLM (2006). Freely dissolved con-centrations of PAHs in soil pore water, measurements via solid-phase extraction and consequences for soil tests. Environmental Science Technology, 40 (4): 1307-1313.

Lau S-L, Han Y, Kang J-H, Kayhanian M, Stenstrom MK (2009). Characteristics of highway stormwater runoff in Los Angeles: metals and polycyclic aromatic hydrocarbons. Water Environment Research, 81: 308-318.

Lau SL, Stenstrom MK (2005). Metals and PAHs adsorbed to street particles. Water Research, 39: 4083-4092.

Lavens P, Sorgeloos P (1996). Manual On The Production And Use Of Live Food For Aquaculture: Food and Agriculture Organization (FAO).

Lee BK (2010). Sources, distribution and toxicity of polyaromatic hydrocarbons (PAHs) in particulate matter: INTECH Open Access Publisher.

Li GC, Xia XH, Yang ZF, Wang R, Voulvoulis N (2006). Distribution and sources of polycyclic aromatic hydrocarbons in the middle and lower reaches of the Yellow River, China. Environmental Pollution, 144: 985-993.

Li J, Shang X, Zhao Z, Tanguay RL, Dong Q, Huang C (2010). Polycyclic aromatic hydrocarbons in water, sediment, soil, and plants of the Aojiang River waterway in Wenzhou, China. Journal of Hazardous Materials, 173: 75-81.

Li JY, Tang JYM, Jin L, Escher BI (2013). Understanding bioavailability and toxicity of sediment-associated contaminants by combining passive sampling with in vitro bioassays in an urban river catchment. Environmental Toxicology and Chemistry, 32: 2888-2896.

Li XD, Poon CS, Liu PS (2001) Heavy metals contamination of urban soils and street dusts in Hongkong. Applied Geochemistry, 16: 1361–1368.

Li XH, Ma LL, Liu XF, Fu S, Cheng HX, Xu XB (2006). Polycyclic aromatic hydrocarbon in urban soil from Beijing, China. Journal of Environmental Science, 18: 944-950.

Lin CJ, Chang JE (2001). Effect of fly ash characteristics on the removal of Cu(II) from aqueous solution. Chemosphere, 44: 1185-1192.

Lindgren A (1996) Asphalt wear and pollution transport. Science of the Total Environment, (189/190): 281–286.

Liu C, Shang Y, Yin G (2006) Primary study on te pollution in farm soil of Chengdu city. Trace Element Science of Guangdong, 13: 41–45.

Liu W, Zhao J, Ouyang Z, Sorderlund L, Liu G (2005) Impacts of sewage irrigation on heavy metal distribution and contamination in Beijing, China. Environmental International, 31: 805–812.

Liu Y, Chen L, Zhao J, Wei Y, Pan Z, Meng XZ, Huang Q, Li W (2010). Polycyclic aromatic hydrocarbons in the surface soil of Shanghai, China: Concentrations, distribution and sources. Organic Geochemistry, 4: 355-362.

Loganathan P, Vigneswaran S, Kandasamy J (2013) Road-deposited sediment pollutants: A critical review of their characteristics source apportionment, and management. Critical Reviews in Environmental Science and Technology, 43: 1315–1348.

Loganathan P, Vigneswaran S, Kandasamy J, Bolan NS (2014). Removal and recovery of phosphate from water using sorption. Critical Reviews in Environmental Science and Technology, 44: 847-907.

Loganathan P, Vigneswaran S, Kandasamy J, Naidu R (2012). Cadmium sorption and desorption in soils: a review. Critical Reviews in Environmental Science and Technology, 42: 489-533.

Long ER (2006). Calculation and uses of mean sediment quality guideline quotients: a critical review. Environmental Science and Technology, 40: 1726-1736.

Long Y, Dai T, Wu Q (2013). Sources and distribution of polycyclic aromatic hydrocarbons in street dust from the Chang-Zhu-Tan Region, Hunan, China, Environmental Monitoring Assessment, 185: 1377-1390.

Lorenzi D, Entwistle JA, Cave M, Dean JR (2011). Determination of polycyclic aromatic hydrocarbons in urban street dust: implications for human health. Chemosphere, 83: 970-997

Lovei M (1998). Phasing Out Lead From Gasoline: Worldwide Experience and Policy Implications. Vol 397: World Bank Publications.

Lu X, Wang L, Lei K, Huang J, Zhai Y (2009) Contamination assessment of copper, lead, zinc, manganese and nickel in street dust of Baoji, NW China. Journal of Hazardous Materials, 161: 1058–1062.

Lynam DR, Pfeifer GD (1991) Human Health Effects Of Highway-Related Pollutants. In: 'Highway pollution, studies in Environmental Science 44'. (Eds RS Hamilton, RM Harrison), 259-280. (Elsevier: Amsterdam)

Ma J, Zhou Y (2011). Soil pollution by polycyclic aromatic hydrocarbons: a comparison of two Chinese cities. Journal of Environmental Science, 23:1518-1523.

Ma LL, Chu SG, Wang XT, Cheng HX, Liu XF, Xu XB (2005). Polycyclic aromatic hydrocarbons in the surface soils from outskirts of Beijing, China. Chemosphere, 58: 1355-1363.

MacDonald DD, Ingersoll CG, Berger T (2000). Development and evaluation of consensus-based sediment quality guidelines for freshwater ecosystems. Archives of Environmental Contamination and Toxicology, 39: 20-31.

Macken A, Giltrap M, Foley B, McGovern E, McHugh B, Davoren M (2008). A model compound study: the ecotoxicological evaluation of five organic contaminants employing a battery of marine bioassays. Environmental Pollution, 153: 627-637.

Macova M, Toze S, Hodgers L, Mueller JF, Bartkow M, Escher BI (2011). Bioanalytical tools for the evaluation of organic micropollutants during sewage treatment, water recycling and drinking water generation. Water Research, 45: 4238-4247.

Maher BA, Moore C, Matzka J (2008). Spatial variation in vehicle-derived metal pollution identified by magnetic and elemental analysis of roadside tree leaves. Atmospheric Environment, 42: 364-373.

Mahler BJ, Van Metre PC, Foreman WT (2014). Concentrations of polycyclic aromatic hydrocarbons (PAHs) and azaarenes in runoff from coal-tar- and asphalt-sealcoated pavement. Environmental Pollution, 188: 81-87.

Maltby L, Boxall A, Forrow DM, Calow P, Betton CI (1995). The effects of motorway runoff on freshwater ecosystems: 2. Identifying major toxicants. Environmental Toxicology and Chemistry, 14: 1093-1101.

Maltby L, Forrow DM, Boxall A, Calow P, Betton CI (1995). The effects of motorway runoff on freshwater ecosystems: 1. Field study. Environmental Toxicology and Chemistry, 14: 1079-1092.

Marsalek J, Rochfort Q, Brownlee B, Mayer T, Servos M (1999). An exploratory study of urban runoff toxicity. Water Science and Technology, 39: 33-39.

Marwood C, McAtee B, Kreider M, Ogle RS, Finley B, Sweet L, Panko J (2011). Acute aquatic toxicity of tire and road wear particles to alga, daphnid, and fish. Ecotoxicology, 20: 2079–2089.

Masih A, Taneja A (2006). Polycyclic aromatic hydrocarbons (PAHs) concentrations and related carcinogenic potencies in soil at a semi-arid region of India, Chemosphere, 65: 449-456.

McBride M (1989). Reactions controlling heavy metal solubility in soils. Advances in Soil Science. Springer, pp. 1-56.

McCready S, Birch G, Long E, Spyrakis G, Greely C (2006). An evaluation of Australian sediment quality guidelines. Archives of Environmental Contamination and Toxicology, 50: 306-315.

McCready S, Slee DJ, Birch JF, Taylor SE (2000). The distribution of polycyclic aromatic hydrocarbons in surficial sediments of Sydney Harbour, Australia. Marine Pollution Bulletin, 40: 999-1006.

McKenzie ER, Money JE, Green PG, Young TM (2009) Metals associated with stormwater-relevant brake and tyre samples. Science of the Total Environment, 407: 5855-5860.

Meharg AA, Wright J, Dyke H, Osborn D (2008). Polycyclic aromatic hydrocarbon (PAH) dispersion and deposition to vegetation and soil following a large scale chemical fire, Environmental Pollution, 99: 29-36.

Mielke HW, Wang G, Gonzales CR, Le B, Quach VN, Mielke PW (2001). PAH and metal mixtures in New Orleans soils and sediments, Science of the Total Environment, 281: 217-227.

Mielke HW, Wang G, Gonzales CR, Powell ET, Le B, Quach, V.N (2004). PAHs and metals in the soils of inner-city and suburban New Orleans, Louisiana, USA. Environmental Toxicological Pharmarcology, 18: 243-247.

Miller KP, Ramos KS (2001). Impact of cellular metabolism on the biological effects of benzo[a]pyrene and related hydrocarbons. Drug Metabolism Reviews, 33: 1-35.

Miller W, Peterson S, Greene J, Callahan C (1985). Comparative toxicology of laboratory organisms for assessing hazardous waste sites. Journal of Environmental Quality, 14: 569-574.

Mimura J, Fujii-Kuriyama Y (2003). Functional role of AhR in the expression of toxic effects by TCDD. Biochimica et Biophysica Acta (BBA)-General Subjects, 1619: 263-268.

Minceva M, Markovska L, Meshko V (2007). Removal of Zn^{2+}, Cd^{2+} and Pb^{2+} from binary aqueous solution by natural zeolite and granulated activated carbon. Macedonian Journal of Chemistry and Chemical Engineering, 26: 125-134.

Mishra PC, Patel RK (2009). Removal of lead and zinc ions from water by low cost adsorbents. Journal of Hazardous Materials, 168: 319-325.

Mohammed T, Loganathan P, Kinsela A, Vigneswaran S, Kandasamy J (2012). Enrichment, inter-relationship, and fractionation of heavy metals in road-deposited sediments of Sydney, Australia. Soil Research, 50: 229-238.

Molendijk J (2013). Improving water and sediment quality assessment using adaptive stress response assays and implementing more efficient methodologies. Faculty of Medicine Theses (Master thesis).

Mostafa A, Hegazi A, El-Gayar MS, Andersson J (2009). Source characterization and the environmental impact of urbasn street dusts from Egypt based on hydrocarbon distributions. Fuel, 88: 95-104.

Mozgawa W (2000). The influence of some heavy metals cations on the FTIR spectra of zeolites. Journal of Molecular Structure, 555: 299-304.

Murakami M, Nakajima F, Furumai H (2005). Size-and density-distributions and sources of polycyclic aromatic hydrocarbons in urban road dust. Chemosphere, 61: 783-791.

Murakami M, Sato N, Anegawa A, Nakada N, Harada A, Komatsu T (2008). Multiple evaluations of the removal of pollutants in road runoff by soil infiltration. Water Research, 42: 2745-2755.

Nadala M, Schuhmacher M, Domingo JL (2011). Levels of PAHs in soil and vegetation samples from Tarragona County, Spain. Environmental Pollution, 132: 1-11.

Nagy SR, Sanborn JR, Hammock BD, Denison MS (2002). Development of a green fluorescent protein-based cell bioassay for the rapid and inexpensive detection and characterization of Ah receptor agonists. Toxicological Sciences, 65: 200-210.

Nam JJ, Song BH, Eom KC, Lee SH, Smith A (2003). Distribution of polycyclic aromatic hydrocarbons in agricultural soils in South Korea. Chemosphere, 50: 1281-1289.

Nam JJ, Thomas GO, Jaward FM, Steinnes E, Gustafsson O, Jones KC (2008). PAHs in background soils from Western Europe: Influence of atmospheric deposition and soil organic matter. Chemosphere, 70: 1596-1602.

Neumann NF, Galvez F (2002). DNA microarrays and toxicogenomics: applications for ecotoxicology? Biotechnology Advances, 20: 391-419.

Newsted JL, Giesy JP (1987). Predictive models for photoinduced acute toxicity of polycyclic aromatic hydrocarbons to *Daphnia magna*, Strauss (Cladocera, Crustacea). Environmental Toxicology and Chemistry, 6: 445-461.

Nguyen TC, Ra J, Park K, Kim D, Kim S (2009). Toxicity of artificial runoff fostered with dry deposition particulates from industrial, commercial, and highway area in Gwangju, Korea. Water Science and Technology, 59(11): 2227–2235 .

Nisbet IC, LaGoy PK (1992). Toxic equivalency factors (TEFs) for polycyclic aromatic hydrocarbons (PAHs). Regulatory Toxicology and Pharmacology, 16: 290-300.

NOAA Administration (1999). Screening Quick Reference Tables (Squirts). Screening Quick Reference Tables, NOAA HAZMAT Report 99-1, Coastal Protection.

Nunes BS, Carvalho FD, Guilhermino LM, Van Stappen G (2006). Use of the genus *Artemia* in ecotoxicity testing. Environmental Pollution; 144: 453-462.

Nur T, Loganathan P, Nguyen T, Vigneswaran S, Singh G, Kandasamy J (2015). Batch and column adsorption and desorption of fluoride using hydrous ferric oxide: Solution chemistry and modeling. Chemical Engineering Journal, 247: 93-102.

Olette R, Couderchet M, Biagianti S, Eullaffroy P (2008). Toxicity and removal of pesticides by selected aquatic plants. Chemosphere, 70: 1414-1421.

Ordonez A, Loredo J, De Miguel E, Charlesworth S (2003) Distribution of heavy metals in the Street Dusts and Soils of an Industrial City in Northern Spain. Archives of Environmental Contamination Toxicology 44, 160–170.

Ortiz N, Pires M, Bressiani J (2001). Use of steel converter slag as nickel adsorber to wastewater treatment. Waste Management, 21: 631-635.

Ozaki H, Watanabe I, Kuno K (2004) Investigation of the heavy metals sources in relation to automobiles. Water, Air and Soil Pollution 157, 209–223.

Palacios M, Gomez M, Moldovan M, Morrison G, Rauch S, McLeod C (2000). Platinum-group elements: quantification in collected exhaust fumes and studies of catalyst surfaces. Science of the Total Environment, 257: 1-15.

Panday K, Prasad G, Singh V (1985). Copper (II) removal from aqueous solutions by fly ash. Water Research, 19: 869-873.

Parvez S, Venkataraman C, Mukherji S (2006). A review on advantages of implementing luminescence inhibition test (*Vibrio fischeri*) for acute toxicity prediction of chemicals. Environment International, 32: 265-268.

Pastorelli R, Guanci M, Cerri A, Negri E, La Vecchia C, Fumagalli F (1998). Impact of inherited polymorphisms in glutathione S-transferase M1, microsomal epoxide hydrolase, cytochrome P450 enzymes on DNA, and blood protein adducts of benzo (a) pyrene-diolepoxide. Cancer Epidemiology Biomarkers and Prevention, 7: 703-709.

Pathirana S, Connell DW, Vowles PD (1994). Distribution of polycyclic aromatic hydrocarbons (PAHs) in an urban roadway system. Ecotoxicology and Environmental Safety, 28: 256-269.

Peng C, Chen W, Liao X, Wang M, Ouyang Z, Jiao W, Bai Y (2011). Polycyclic aromatic hydrocarbons in urban soils of Beijing: Status, sources, distribution and potential risk. Environmental Pollution, 159: 802-808.

Peng C, Chen W, Liao X, Wang M, Ouyang Z, Jiao W, Bai Z (2012). Vegetative cover and PAHs accumulation in soils of urban green space. Environmental Pollution, 161: 36-42.

Pengchai P, Furumai H, Nakajima F (2004). Source apportionment of polycyclic aromatic hydrocarbons in road dust in Tokyo. Polycyclic Aromatic Compounds, 24: 773-789.

Pengchai P, Nakajima F, Furumai H (2005). Estimation of origins of polycyclic aromatic hydrocarbons in size-fractionated road dust in Tokyo with multivariate analysis. Water Science and Technology, 51: 169-175.

Perron MM, Burgess RM, Ho KT, Pelletier MC, Cantwell MG, Shine JP (2010). Bioavailability assessment of a contaminated field sediment from Patrick Bayou, Texas, USA: toxicity identification evaluation and equilibrium partitioning. Environmental Toxicology and Chemistry, 29: 742-750.

Persoone G, Janssen C (1993). Freshwater Invertebrate Toxicity Tests. Handbook of Ecotoxicology, 1: 51-65.

Phyu YL, Warne MSJ, Lim R (2005). Effect of river water, sediment and time on the toxicity and bioavailability of molinate to the marine bacterium *Vibrio fischeri* (Microtox®). Water Research, 39: 2738-2746.

Pies C, Hoffmann B, PetroWB, Sky J, Yang Y, Ternes TA, Hofmann T (2008). Characterization and source identification of polycyclic aromatic hydrocarbons (PAHs) in river bank soils. Chemosphere, 72: 1594-1601.

Ping LF, Luo YM, Zhang HB, Li QB, Wu LH (2007). Distribution of polycyclic aromatic hydrocarbons in thirty typical soil profiles in the Yangtze River Delta region, East China. Environmental Pollution, 147: 358-365.

Poulsen A, Chapman H, Leusch F, Escher B (2011). Application Of Bioanalytical Tools For Water Quality Assessment. Technical Report No. 41. Urban Water Security Research Alliance.

Prefecture S (2001). Water Quality Of Lake Biwa. Report

Prieto A, Zuloaga O, Usobiaga A, Bartolome L, Fernandez LA, Etxebarria N, Ciprain E, Alonso A (2008). Levels and spatial distribution of inorganic and organic contaminants in sediments along the Bilbao estuary. Marine Pollution Bulletin, 56: 2082-2105.

Qiu H (2010) Studies on the potential ecological risk and homology correlation of heavy metal in the surface soil. Journal of Agricultural Science 2, 194–201.

Qiu W, Zheng Y (2009). Removal of lead, copper, nickel, cobalt, and zinc from water by a cancrinite-type zeolite synthesized from fly ash. Chemical Engineering Journal, 145: 483-488.

Ramussen PE, Subramanian KS, Jessiman BJ (2001) A multi-element profile of housedust in relation to exterior dust and soils in the city of Ottawa, Canada. Science of the Total Environment 267, 125–140.

Rao GP, Lu C, Su F (2007). Sorption of divalent metal ions from aqueous solution by carbon nanotubes: a review. Separation and Purification Technology, 58: 224-231.

Rao M, Parwate A, Bhole A (2002). Removal of Cr^{6+} and Ni^{2+} from aqueous solution using bagasse and fly ash. Waste Management, 22: 821-830.

Rao SR (2011). Resource Recovery and Recycling from Metallurgical Wastes, Elsevier, Amsterdam.

Rauret G, Lopez-Sanchez J, Sahuquillo A, Rubio R, Davidson C, Ure A (1999). Improvement of the BCR three step sequential extraction procedure prior to the certification of new sediment and soil reference materials. Journal of Environmental Monitoring, 1: 57-61.

Rawson CA (2008). Ecological risk assessment of persistent organic pollutants in wetlands of the remediated Sydney Olympic Park, NSW, Australia. PhD thesis, University of Technology, Sydney, NSW Australia.

Ricou P, Lecuyer I, Le Cloirec P (1998). Removal of Cu^{2+} and Zn^{2+} and Pb^{2+} by adsorption onto fly ash and fly ash/lime mixing. Water Science and Technology, 39: 239-247.

Roberts MH, Hargis WJ, Strobel CJ, De Lisle PF (1989). Acute toxicity of PAH contaminated sediments to the estuarine fish, Leiostomus xanthurus. Bulletin of Environmental Contamination and Toxicology, 42: 142-149.

Robertson D, Taylor KG, Hoon SR (2003). Geochemical and mineral magnetic characterisation of urban sediment particulates, Manchester, UK. Applied Geochemistry, 18: 269-282.

Ruchaya B, Gullaya W, Ayako T, Takada H (2006). Distribution and origins of polycyclic aromatic hydrocarbons (PAHs) in riverine, estuarine, and marine sediments in Thailand. Marine Pollution Bulletin, 52: 942-956.

Ruiz M, López-Jaramillo L, Redondo M, Font G (1997). Toxicity assessment of pesticides using the Microtox test: application to environmental samples. Bulletin of Environmental Contamination and Toxicology, 59: 619-625.

Saeed SM, Shaker IM (2008) Assessment of Trace elements pollution in water and sediments and their effect on Oreochromis niloticus in the Northern Delta lakes, Egypt. 8th International Symposium in Tilapia in Aquaculture.

Saeedi M, Li LY, Salmanzadeh M (2012). Heavy metals and polycyclic aromatic hydrocarbons: pollution and ecological risk assessment in street dust of Tehran. Journal of Hazardous Materials, 227: 9-17.

Saltiene Z, Brukstiene D, Ruzgyte A (2002). Contamination of soil by polycyclic aromatic hydrocarbons (PAH) in some urban areas. Polycyclic Aromatic Compounds, 22: 23-35.

Sansalone J, Ying G (2008). Partitioning and granulometric distribution of metal leachate from urban traffic dry deposition particulate matter subject to acidic rainfall and runoff retention. Water Research, 42: 4146-4162.

Scanlon PF (1991) Effects of highway pollutants upon terrestrial ecosystems, in: "Highway Pollution, Studies in Environmental Science 44" (Eds RS Hamilton, RM Harrison), pp 281-338. (Elsevier: Amsterdam)

Schwar MJR, Moorcroft JS, Laxen DPH, Thompson M, Armorgie C (1988) Baseline metal-in-dust concentrations in Greater London. Science of the Total Environment, 68: 25-43.

Sezgin N, Ozcan HK, Demir G, Nemlioglu S, Bayat C (2003) Determination of heavy metal concentrations in street dusts in Istanbul E-5 highway. Environment International, 29: 979–985.

Sfriso A, Marcomini A, Zanett M (1995) Trace elements in sediments, SPM and phytozoobenthos of the lagoon of Venice. Marine Pollution Bulletine, 30: 116–124.

Shinya M, Tsuchinaga T, Kitano M, Yamada Y, Ishikawa M (2000). Characterization of heavy metals and polycyclic aromatic hydrocarbons inurban highway runoff. Water Science and Technology, 42: 201-208.

Simpson S, Batley GE, Chariton AA, Stauber JL, King CK, Chapman JC, Hyne RV, Gale SA, Roach AC, Maher WA (2005). Handbook of Sediment Quality Assessment. CSIRO-Bangor, NSW, Australia.

Skrbic B, Miljevic N (2002). An evaluation of residues at an oil refinery site following fires. Journal Environmental Science Health, 37: 1029-1039.

Slameňová D, Gábelová A, Chalupa I, Szabová E, Mikulášová M, Horváthová E (1999). Cytotoxic and genotoxic effect of inhibitor of vulcanisation N-cyclohexylthiophthalimide in a battery of in vitro assays. Mutation Research/Genetic Toxicology and Environmental Mutagenesis, 446: 35-48.

Smith SL, MacDonald DD, Keenleyside KA, Ingersoll CG, Field LJ (1996). A preliminary evaluation of sediment quality assessment values for freshwater ecosystems. Journal of Great Lakes Research, 22: 624-638.

Snowdon R, Birch GF (2004) The nature and distribution of copper, lead, and zinc in soils of a highly urbanised sub-catchment (Iron Cove) of Port Jackson, Sydney, Australia. Australian Journal of Soil Research 42, 329–338

Soclo H, Garrigues PH, Ewald M (2000). Origin of polycyclic aromatic hydrocarbons (PAHs) in coastal marine sediments: case studies in Cotonou (Benin) and Aquitaine (France) areas. Marine Pollution Bulletin, 40: 387-396.

Sojinu O, Wang J-Z, Sonibare O, Zeng EY (2010). Polycyclic aromatic hydrocarbons in sediments and soils from oil exploration areas of the Niger Delta, Nigeria. Journal of Hazardous Materials, 174: 641-647.

Sorgeloos P, Dhert P, Candreva P (2001). Use of the brine shrimp, *Artemia* spp., in marine fish larviculture. Aquaculture, 200: 147-159.

Sounthararajah D, Loganathan P, Kandasamy J, Vigneswaran S (2015). Adsorptive removal of heavy metals from water using sodium titanate nanofibres loaded onto GAC in fixed-bed columns. Journal of Hazardous Materials, 287: 306-316.

Sounthararajah D, Loganathan P, Kandasamy J, Vigneswaran S (2015). Effects of humic acid and suspended solids on the removal of heavy metals from water by adsorption onto granular activated carbon. International Journal of Environmental Research and Public Health, 12(9): 10475-10489.

Spehar R, Poucher S, Brooke L, Hansen D, Champlin D, Cox D (1999). Comparative toxicity of fluoranthene to freshwater and saltwater species under fluorescent and ultraviolet light. Archives of Environmental Contamination and Toxicology, 37: 496-502.

Spitzer T, Kuwatsuka S (1993). Residue levels of polynuclear aromatic compounds in urban surface soil from Japan. Journal of Chromatography A, 305-643.

Srivastava S, Gupta V, Mohan D (1997). Removal of lead and chromium by activated slag-A blast-Furnace waste. Journal of Environmental Engineering, 123: 461-468.

Srivastava VC, Mall ID, Mishra IM (2006). Equilibrium modelling of single and binary adsorption of cadmium and nickel onto bagasse fly ash. Chemical Engineering Journal, 117: 79-91.

Stalikas CD, Chaidou CI, Pilidis GA (1997). Enrichment of PAHs and heavy metals in soils in the vicinity of the lignite-fired power plants of West Macedonia. Science of Total Environment, 204: 135-46.

Stone M, Marsalek J (1996). Trace metal composition and speciation in street sediment: Sault Ste. Marie, Canada. Water, Air, and Soil Pollution, 87: 149-169.

Su MC, Christensen ER, Karls JF (1998). Determination of PAH sources in dated sediments from Green Bay, Wisconsin, by a chemical mass balance model. Environmental Pollution, 98: 411-419.

Sun Y, Zhou Q, Xie X, Liu R (2010) Spatial, sources and risk assessment of heavy metal contamination of urban soils in typical regions of Shenyang, China. Journal of Hazardous Materials 174, 455–462.

Sutherland R, Tolosa C (2000). Multi-element analysis of road-deposited sediment in an urban drainage basin, Honolulu, Hawaii. Environmental pollution, 110: 483-495.

Svensson B-M, Mathiasson L, Mårtensson L, Bergström S (2005). Artemia salina as test organism for assessment of acute toxicity of leachate water from landfills. Environmental Monitoring and Assessment, 102: 309-321.

Swartz RC (1999). Consensus sediment quality guidelines for polycyclic aromatic hydrocarbon mixtures. Environmental Toxicology and Chemistry, 18: 780-787.

Tabakci M, Yilmaz M (2008). Sorption characteristics of Cu (II) ions onto silica gel-immobilized calix arene polymer in aqueous solutions: batch and column studies. Journal of Hazardous Materials, 151: 331-338.

Takada H, Onda T, Ogura N (1990). Determination of polycyclic aromatic hydrocarbons in urban street dusts and their source materials by capillary gas chromatography. Environmental Science and Technology, 24: 1179-1186.

Tang J, Glenn E, Aryal R, Gernjak W, Chong M, Sidhu J (2012). Toxicity characterization of urban stormwater using bioanalytical tools. 2nd SETAC Australasia Conference. Society of Environmental Toxicology and Chemistry.

Tang J, Taulis M, Edebeli J, Leusch F, Jagals P, Jackson G (2014). Chemical and bioanalytical assessment of coal seam gas associated water. Environmental Chemistry, 12: 267-285.

Tang JY, Aryal R, Deletic A, Gernjak W, Glenn E, McCarthy D (2013). Toxicity characterization of urban stormwater with bioanalytical tools. Water Research, 47: 5594-5606.

Tang L, Tang XY, Zhu YG, Zheng MH, Miao QL (2005). Contamination of polycyclic aromatic hydrocarbons (PAHs) in urban soils in Beijing, China. Environmental International, 31: 822-828.

Tanner PA, Ma H-L, Yu PK (2008). Fingerprinting metals in urban street dust of Beijing, Shanghai, and Hong Kong. Environmental Science and Technology, 42: 7111-7117.

Taparcevska J, Markovska L, Koumanova B, Meshko V (2010). Diffusion models for adsorption kinetics of Zn^{2+}, Cd^{2+} and Pb^{2+} onto natural zeolite. Water Science and Technology, 62 (5): 1136–1142.

Taraldsen JE, Norberg-King TJ (1990). New method for determining effluent toxicity using duckweed (*Lemna minor*). Environmental Toxicology and Chemistry, 9: 761-767.

Taylor K (2007). Urban Environments. Environmental Sedimentology, John Wiley and Sons, 190-222.

Taylor KG, Owens PN (2009) Sediments in urban river basins: a review of sediment–contaminant dynamics in an environmental system conditioned by human activities. Journal of Soils and Sediments, 9: 281–303.

Tessier A, Campbell PG, Bisson M (1979). Sequential extraction procedure for the speciation of particulate trace metals. Analytical Chemistry, 51: 844-851.

Thorpe A, Harrison RM (2008). Sources and properties of non-exhaust particulate matter from road traffic: a review. Science of the Total Environment, 400: 270-282.

Tobiszewski M, Namieśnik J (2012). PAH diagnostic ratios for the identification of pollution emission sources. Environmental Pollution, 162: 110-119.

Treacy MM, Higgins JB (2007). Collection of Simulated XRD Powder Patterns for Zeolites Fifth Revised Edition: Elsevier.

Tronczynsky J, Munschy C, Moisan H, Guiot N, Truquet I, Olivier N, Men S, Furaut A (2004). Contamination of the Bay of Biscay by polycyclic aromatic hydrocarbons (PAHs) following the T/V ‘‘Erika’’ oil spill. Aquatic Living Resource, 17: 243-259.

Tsihrintzis VA, Hamid R (1997). Modeling and management of urban stormwater runoff quality: a review. Water Resources Management, 11: 136-164.

Tuzen M (2003) Investigation of heavy metal levels in street dust samples in Tokat, Turkey. Journal of Trace and Microprobe Techniques, 21: 513–521.

USA EPA (1993). Trimmed Spearman-Karber (TSK) Program version 1.5. Ecological Monitoring Research Division, Environmental Monitoring Systems Laboratory, U.S. Environmental Protection Agency, Cincinati, Ohio 45268.

USA EPA (1996). Whole Sediment Acute Toxicity Invertebrates, Freshwater. Ecological effects test guidelines.

USA EPA (2001). Methods for Collection, Storage and Manipulation of Sediments for Chemical and Toxicological Analyses: Technical Manual. U.S. Environmental Protection Agency, Office of Water, Washington, DC. EPA 823-B-01-002.

USA EPA (2002). Short-term Methods for Estimating the Chronic Toxicity of Effluents and Receiving Waters to Freshwater Organisms.

Utgikar VP, Chaudhary N, Koeniger A, Tabak HH, Haines JR, Govind R (2004). Toxicity of metals and metal mixtures: analysis of concentration and time dependence for zinc and copper. Water Research, 38: 3651-3658.

Valavanidis A, Vlachogianni T (2010). Metal pollution in ecosystems. Ecotoxicology studies and risk assessment in the marine environment. PhD Thesis. Department of Chemistry, University of Athens University Campus Zografou.

Valderrama C, Gamisans X, De las Heras X, Farran A, Cortina J (2008). Sorption kinetics of polycyclic aromatic hydrocarbons removal using granular activated carbon: Intraparticle diffusion coefficients. Journal of hazardous materials, 157: 386-396.

Van Metre PC, Mahler BJ (2003). The contribution of particles washed from rooftops to contaminant loading to urban streams. Chemosphere, 52: 1727-1741.

Vasseur P, Ferard J, Vial J, Larbaigt G (1984). Comparaison des tests Microtox et daphnie pour l'evaluation de la toxicite aigue d'effluents industriels. Environmental Pollution Series A, Ecological and Biological, 34: 225-235.

Venkataraman C, Friedlander SK (1994). Size distributions of polycyclic aromatic hydrocarbons and elemental carbon. 2. Ambient measurements and effects of atmospheric processes. Environmental Science and Technology, 28: 563-572.

Vidal CB, Barros AL, Moura CP, de Lima ACA, Dias FS, Vasconcellos LCG (2011). Adsorption of polycyclic aromatic hydrocarbons from aqueous solutions by modified periodic mesoporous organosilica. Journal of Colloid and Interface Science, 357: 466-473.

Viguri J, Verde J, Irabien A (2002). Environironmental assessment of polycyclic aromatic hydrocarbons (PAHs) in surface sediments of the Santander Bay, Northern Spain. Chemosphere, 48: 157-66.

Villaescusa I, Marti S, Matas C, Martine M, Ribó JM (1997). Chromium (VI) toxicity to luminescent bacteria. Environmental Toxicology and Chemistry, 16: 871-874.

Viñas L, Angeles Franco M, Antonio Soriano J, José González J, Pon J, Albaigés J (2010). Sources and distribution of polycyclic aromatic hydrocarbons in sediments from the Spanish northern continental shelf. Assessment of spatial and temporal trends. Environmental Pollution, 158: 1551-1560.

Vindimian E (2012). MSExcel Macro Regtox 7.06 Freely available from Eric Vindimian. IRSTEA, France.

Von Uexküll O, Skerfving S, Doyle R, Braungart M (2005). Antimony in brake pads-a carcinogenic component? Journal of Cleaner Production, 13: 19-31.

Walker JD, Newman MC, Enache M (2012). Fundamental QSARs for Metal Ions, CRC Press, Boca Raton.

Wan X, Chen J, Tian F, Sun W, Yang F, Saiki K (2006). Source apportionment of PAHs in atmospheric particulates of Dalian: factor analysis with nonnegative constraints and emission inventory analysis. Atmospheric Environment, 40: 6666-6675.

Wang C, Li J, Sun X, Wang L, Sun X (2009). Evaluation of zeolites synthesized from fly ash as potential adsorbents for wastewater containing heavy metals. Journal of Environmental Sciences, 21: 127-136.

Wang DG, Yang M, Jia HL, Zhou L, Li YF (2009). Polycyclic aromatic hydrocarbons in urban street dust and surface soil: comparisons of concentration, profile, and source. Archives of Environmental Contamination and Toxicology, 56: 173-180.

Wang DT, Meresz O (1982) (3rd Eds.). Occurrence and potential uptake of polynuclear aromatic hydrocarbons of highway traffic origin by proximally grown food crops. 3rd ed. New York: Springer Verlag.

Wang S, Peng Y (2010). Natural zeolites as effective adsorbents in water and wastewater treatment. Chemical Engineering Journal, 156: 11-24.

Wang S, Sheng Y, Feng M, Leszczynski J, Wang L, Tachikawa H (2007). Light-induced cytotoxicity of 16 polycyclic aromatic hydrocarbons on the US EPA priority pollutant list in human skin HaCaT keratinocytes: Relationship between phototoxicity and excited state properties. Environmental Toxicology, 22: 318-327.

Wang S, Terdkiatburana T, Tadé M (2008). Adsorption of Cu (II), Pb (II) and humic acid on natural zeolite tuff in single and binary systems. Separation and Purification Technology, 62: 64-70.

Wang S, Terdkiatburana T, Tadé M (2008). Single and co-adsorption of heavy metals and humic acid on fly ash. Separation and Purification Technology, 58: 353-358.

Wang S, Wu H (2006). Environmental-benign utilisation of fly ash as low-cost adsorbents. Journal of Hazardous Materials, 136: 482-501.

Wang W, Huang M, Kang Y, Wang H, Leung AOW, Cheung KC, Wong MH (2011). Polycyclic aromatic hydrocarbons (PAHs) in urban surface dust of Guangzhou, China: Status, sources and human health risk assessment. Science of Total Environment, 409: 4519-4527.

Wang W, Primbs T, Tao S, Simonich SL (2009). Atmospheric particulate matter pollution during the 2008 Beijing Olympics. Journal of Environmental Science Technology, 43: 5314-5320.

Wang YH, Lin SH, Juang RS (2003). Removal of heavy metal ions from aqueous solutions using various low-cost adsorbents. Journal of Hazardous Materials, 102: 291-302.

Watanabe H, Nakajima F, Kasuga I, Furumai H (2011). Toxicity evaluation of road dust in the runoff process using a benthic ostracod Heterocypris incongruens. Science of the Total Environment, 409: 2366-2372.

Weber CI (1991). Methods for measuring the acute toxicity of effluents and receiving waters to freshwater and marine organisms: Environmental Monitoring Systems Laboratory, Office of Research and Development, US EPA.

Weber W, Morris J (1963). Intraparticle diffusion during the sorption of surfactants onto activated carbon. American Society of Civil Engineers. Journal of Sanitary Engineering Division, 89: 53-61.

Wei B, Jiang F, Li X, Mu S (2010). Heavy metal induced ecological risk in the city of Urumqi, NW China. Environmental monitoring and assessment, 160: 33-45.

Wei B, Yang L (2010). A review of heavy metal contaminations in urban soils, urban road dusts and agricultural soils from China. Microchemical Journal, 94: 99-107.

Weiss P, Riss A, Gschmeidler E, Schentz H (1994). Investigation of heavy metal, PAH, PCB pattern and PCDDF profiles of soil samples from an industrialized urban area (Linz, upper Austria) with multivariate statistical methods. Chemosphere, 29: 2223-2236.

Wells PG, Lee K, Blaise C (1997). Microscale Testing In Aquatic Toxicology: Advances, Techniques, And Practice: CRC Press.

Weng CH, Huang C (2004). Adsorption characteristics of Zn (II) from dilute aqueous solution by fly ash. Colloids and Surfaces A: Physicochemical and Engineering Zeolite Aspects, 247: 137-143.

Wernersson AS, Dave G (1997). Phototoxicity identification by solid phase extraction and photoinduced toxicity to *Daphnia magna*. Archives of Environmental Contamination and toxicology, 32: 268-273.

Westerlund C, Viklander M, Backstrom M (2003). Seasonal variations in road runoff quality in Lule, Sweden. Water Science and Technology, 48: 93-101.

Westerlund K (2001). Metal Emissions From Stockholm Traffic-Wear Of Brake Linings. SLB-ANALYS.

White PA (2002). The genotoxicity of priority polycyclic aromatic hydrocarbons in complex mixtures. Mutation Research/Genetic Toxicology and Environmental Mutagenesis, 515: 85-98.

WHO (2011). World Health Organisation. Guideline for Drinking-Water Quality (4th Edition).

WHO (2015). International Public Health Hazards: Indian Legislative Provisions: World Health Organization.

Wik A, Nilsson E, Kallqvist T, Tobiesen A, Dave G (2009). Toxicity assessment of sequential leachates of tire powder using a battery of toxicity tests and toxicityidentification evaluations. Chemosphere, 77: 922–927.

Wislocki P, Wood A, Chang R, Levin W, Yagi H, Hernandez O (1976). High mutagenicity and toxicity of a diol epoxide derived from benzo[a]pyrene. Biochemical and Biophysical Research Communications, 68: 1006-1012.

Woodhead RJ, Law RJ, Matthiessen P (1999). Polycyclic aromatic hydrocarbons in surface sediments around England and Wales, and their possible biological significance. Marine Pollution Bulletin, 38: 773–790.

Wu D, Sui Y, He S, Wang X, Li C, Kong H (2008). Removal of trivalent chromium from aqueous solution by zeolite synthesized from coal fly ash. Journal of Hazardous Materials, 155: 415-423.

Xi Z, Chen B (2014). Removal of polycyclic aromatic hydrocarbons from aqueous solution by raw and modified plant residue materials as biosorbents. Journal of Environmental Sciences, 26: 737-748.

Xu J, Yu Y, Wang P, Guo W, Dai S, Sun H (2007). Polycyclic aromatic hydrocarbons in the surface sediments from Yellow River, China. Chemosphere, 67: 1408-1414.

Yan J, Wang L, Fu PP, Yu H (2004). Photomutagenicity of 16 polycyclic aromatic hydrocarbons from the US EPA priority pollutant list. Mutation Research, 557: 99-108.

Yang SYN, Connell DW, Hawker DW, Kayal SI (1991). Polycyclic aromatic hydrocarbons in air, soil and vegetation in the vicinity of an urban roadway. Science of the Total Environment,102: 229-240.

Yang T, Liu Q, Li H, Zeng Q, Chan L (2010). Anthropogenic magnetic particles and heavy metals in the road dust: Magnetic identification and its implications. Atmospheric Environment, 44: 1175-1185.

Yang Y, Zhang XX, Korenaga T (2002). Distribution of polynuclear aromatic hydrocarbons (PAHs) in the soil of Tokushima, Japan. Water Air Soil Pollution, 138: 51–60.

Yin CQ, Jiang X, Yang XL, Bian YR, Wang F (2008). Polycyclic aromatic hydrocarbons in soils in the vicinity of Nanjing, China. Chemosphere, 73: 389-94.

Yongming H, Peixuan D, Junji C, Posmentier ES (2006) Multivariate analysis of heavy metal contamination in urban dust of Xi'an, Central China. Science of the Total Environment 355, 176–186.

Yunker MB, Macdonald RW, Vingarzan R, Mitchell RH, Goyette D, Sylvestre S (2002). PAHs in the Fraser River basin: a critical appraisal of PAH ratios as indicators of PAH source and composition. Organic Geochemistry, 33: 489-515.

Zakaria MP, Takada H, Tsutsumi S, Ohno K, Yamada J, Kouno E (2002). Distribution of polycyclic aromatic hydrocarbons (PAHs) in rivers and estuaries in Malaysia: a widespread input of petrogenic PAHs. Environmental Science and Technology, 36: 1907-1918.

Zechmeister H, Dullinger S, Hohenwallner D, Riss A, Hanus-Illnar A, Scharf S (2006). Pilot study on road traffic emissions (PAHs, heavy metals) measured by using mosses in a tunnel experiment in Vienna, Austria. Environmental Science and Pollution Research, 13: 398-405.

Zeng F, Cui K, Xie Z, Wu L, Luo D, Chen L (2009). Distribution of phthalate esters in urban soils of subtropical city, Guangzhou, China. Journal of Hazardous Materials, 164: 1171-1178.

Zereini F, Wiseman C, Püttmann W (2007). Changes in palladium, platinum, and rhodium concentrations, and their spatial distribution in soils along a major highway in Germany from 1994 to 2004. Environmental Science and Technology, 41: 451-456.

Zhan, Y., Lin, J., and Zhu, Z. (2011). Removal of nitrate from aqueous solution using etylpyridinium bromide (CPB) modified zeolite as adsorbent, Journal of Hazardous Materials, 186: 1972 - 1978.

Zhang HB, Luo YM, Wong MH, Zhao QG, Zhang GL (2006). Distributions and concentrations of PAHs in Hong Kong soils. Environmental Pollution,14: 107-110.

Zhang J, Liu G, Wang R, Liu J (2015). Distribution and source apportionment of polycyclic aromatic hydrocarbons in bank soils and river sediments from the middle reaches of the huaihe river, China. Clean, Soil, Air, Water, 43(8):1207-1214.

Zhang MK, Wang H (2009) Concentrations and chemical forms of potentially toxic metals in road-deposited sediments from different zones of Hangzhou, China. Journal of Environmental Science, 21: 625–631.

Zhang W, Zhang S, Yue D, Wan C, Ye Y, Wang X (2008). Characterization and loading estimation of polycyclic aromatic hydrocarbons in road runoff from urban regions of Beijing, China. Environmental Toxicology and Chemistry, 27: 31-37.

Zhao B, Baston DS, Khan E, Sorrentino C, Denison MS (2010). Enhancing the response of CALUX and CAFLUX cell bioassays for quantitative detection of dioxin-like compounds. Science China Chemistry, 53: 1010-1016.

Zhao L, Hou H, Shangguan Y, Cheng B, Xu Y, Zhao R (2014). Occurrence, sources, and potential human health risks of polycyclic aromatic hydrocarbons in agricultural soils of the coal production area surrounding Xinzhou, China. Ecotoxicology and Environmental Safety, 108: 120-128.

Zhao Z, Rate AW, Tang S, Bi H (2007) Characteristic of trace element distribution in agricultural soils of Hainan island and its environment significances. Journal of Agro-Environment Science, 27: 182–187.

https://www.thermofisher.com/au/en/home/life-science/drug-discovery/target-and-lead-identification-and-validation/g-protein-coupled-html/gpcr-cell-based-assays/geneblazer-substrate-loading-kits.html

US EPA (1992) Ecological Risk Assessment: Technical Overview http://www.epa.gov/oppefed1/ecorisk_ders/

APPENDIX

APPENDIX

Appendix 1.

Table 1. Concentrations of heavy metals in RDS and BLS (solid phase)

	RDS (mg/kg)					
mg/kg	< 75	< 150	< 300	< 425	< 600	total
Cr	39	30	11	9.6	35	30
Cu	270	47	25	31	38	210
Cd	15	14	12	13	12	13
Pb	150	210	200	18	32	48
Ni	12	8.5	5.4	5.2	16	10
Zn	320	170	170	79	110	270
	BLS (mg/kg)					
mg/kg	< 75	< 150	< 300	< 425	< 600	total
Cr	2.3	0.55	0.42	0.44	0.3	0.5
Cu	1.2	0.84	0.75	0.57	0.6	0.63
Cd	1.7	1.1	1.5	1.2	0.8	1.2
Pb	8.7	8.2	6.7	5.5	6.8	6.6
Ni	0.6	0.5	0.5	0.5	0.5	0.5
Zn	3.9	3.4	2.8	2.3	2.5	2.6

APPENDIX

Appendic 2.

Table 2. Concentrations of PAHs in RDS and BLS (solid phase)

RDS μg/kg	< 75	< 150	< 300	< 425	< 600	Total
Nap	0.030	0.054	0.041	0.034	0.030	0.047
Ace	0.015	0.019	0.019	0.010	0.010	0.015
Acenap	0.010	0.010	0.010	0.010	0.010	0.010
F	0.029	0.026	0.024	0.023	0.023	0.027
Phe	0.220	0.210	0.180	0.110	0.150	0.240
Ant	0.047	0.034	0.035	0.019	0.022	0.048
Fl	0.440	0.350	0.310	0.180	0.210	0.460
Pyr	0.430	0.400	0.340	0.200	0.220	0.520
BaA	0.160	0.120	0.120	0.077	0.073	0.180
Chr	0.210	0.190	0.170	0.110	0.100	0.270
BkF	0.280	0.180	0.180	0.120	0.120	0.210
BaP	0.140	0.082	0.085	0.055	0.059	0.100
IND	0.088	0.052	0.059	0.034	0.037	0.082
DBA	0.041	0.019	0.025	0.014	0.021	0.031
BghiP	0.110	0.100	0.089	0.047	0.048	0.130
BLS μg/kg	< 75	< 150	< 300	< 425	< 600	Total
Nap	0.010	0.010	0.010	0.010	0.021	0.010
Ace	0.010	0.010	0.010	0.010	0.010	0.010
Acenap	0.010	0.010	0.010	0.010	0.010	0.010
F	0.010	0.011	0.013	0.012	0.014	0.011
Phe	0.013	0.015	0.018	0.016	0.027	0.015
Ant	0.010	0.010	0.010	0.010	0.010	0.010
Fl	0.010	0.010	0.010	0.010	0.010	0.010
Pyr	0.010	0.010	0.010	0.010	0.010	0.010
BaA	0.011	0.013	0.016	0.013	0.016	0.013
Chr	0.022	0.015	0.010	0.010	0.011	0.010
BkF	0.020	0.020	0.020	0.020	0.020	0.020
BaP	0.010	0.013	0.015	0.012	0.014	0.011

APPENDIX

IND	0.010	0.010	0.010	0.010	0.010	0.010
DBA	0.010	0.010	0.012	0.010	0.011	0.010
BghiP	0.010	0.010	0.010	0.010	0.010	0.010

** Fl: Fluoranthrene; Phe: Phenanthrene; Pyr: Pyrene; Chr: Chrysene; B(b&k)F: Benzo(b-k)fluoranthrene;*

*** Detection limit for MP-AES (Agilent 4100): < 0.001 mg/L for all metals; *** GC-MS recovery was 86 - 100 % for PAHs compounds*

Appendix 3.

Table 3. Summary of heavy metals concentration in the urban runoff

HMs concentration (μg/L)	Gromaire-Mertz et al. (1999)	Shinya et al. (2000)	Drapper et al. (2000)	Beasley and Kneale (2002)	Westerlund et al. (2003)	Bäckström et al. (2003)	Lau et al. (2009)	Aryal and Lee (2009)
Country	France	Japan	Australia	UK	Sweden	Sweden	USA	Japan
Cadmium	0.6	-	-	0.7-220	0.0	0.05	1.3	4-5
Chromium	-	73	-	3.3-30	-	-	2.8	-
Copper	61	620	0.03-0.34	15-1250	2.7	13.3	66.0	7-27
Lead	133	567	0.08-0.62	30-150	0.1	7.5	4.9	5-23
Nickel	-	56	-	3-70	0.5	-	15.7	1-7
Zinc	550	-	0.15-1.85	58-130	13.9	89.3	415	-

(-): not detected

APPENDIX

Appendix 4.

Table 4. Summary of PAHs concentration in the urban runoff

PAHs concentration (µg/L)	Van Metre and Mahler (2003)	Hwang and Foster (2006)	Zhang et al. (2008)	Lau et al. (2009)	Meland et al. (2010)	García-Flores et al. (2013)	Mahler et al. (2014)
Country	USA	USA	China	USA	Norway	Mexico	USA
Napthalene	0.013-0.018	17.7-59.0	38.5	< 0.001	0.013	186.8	221.2
Acenapthylene	-	2.09-25.2	10.2	< 0.001	0.015	26.9	576.8
Acenapthene	-	3.68-28.8	4.5	< 0.001	0.18	52.9	1357.8
Fluorene	0.014-0.029	8.79-152	25.8	< 0.001	0.13	93.5	8345.8
Phenanthrene	0.38-0.96	26.1-338	112.7	0.015	0.034	342.5	9522.0
Anthracene	0.04-0.10	5.43-119	24.3	0.001	-	129.3	8932.0
Fluoranthene	1.2-2.4	86.5-1380	136.9	0.028	-	180.5	12160.0
Pyrene	0.9-1.8	65.6-774	86.2	0.068	0.225	361.9	7157.0
Benz[a]anthracene	0.24-0.62	22.2-337	12.5	0.016	-	79.1	4116.0
Chrysene	0.7-1.6	48.6-519	29.6	0.047	-	278.5	3795.0
Benzo(b)fluoranthene	-	57.7-733	15.1	0.016	0.043	138.1	3563.0
Benzo(k)fluoranthene	-	32.4-404	10.0	0.007	-	74.0	2708.0
Benzo(a)pyrene	0.43-0.98	27.8-446	4.5	0.015	-	161.6	1715.0
Indeno(1,2,3 cd)pyrene	-	37.1-505	2.0	< 0.001	-	113.9	1740.0

APPENDIX

Dibenzo(a,h)anthracene	0.086-0.19	6.94-134	ND	< 0.001	-	55.1	1210.0
Benzo(ghi)perylene	-	15.0-548	1.7	0.038	0.083	169.5	682.5
Total PAHs	9.8-1.9	1510-12.500	548.2	0.281	67802	2444.0	0.561

(-): not detected

APPENDIX

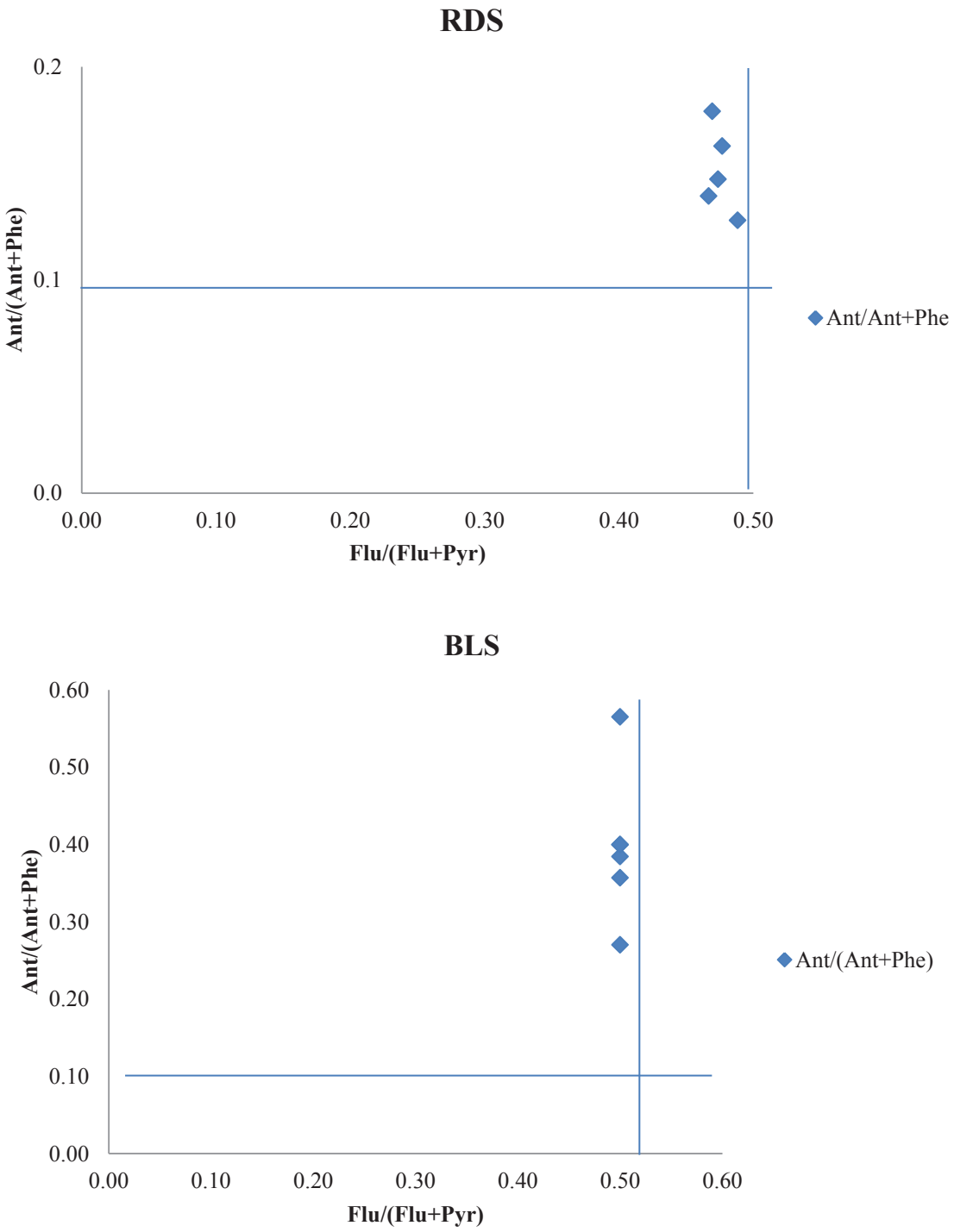

Figure 1. Diagnostic PAHs ratios in RDS and BLS (petrogenic sources, pyrogenic sources).

APPENDIX

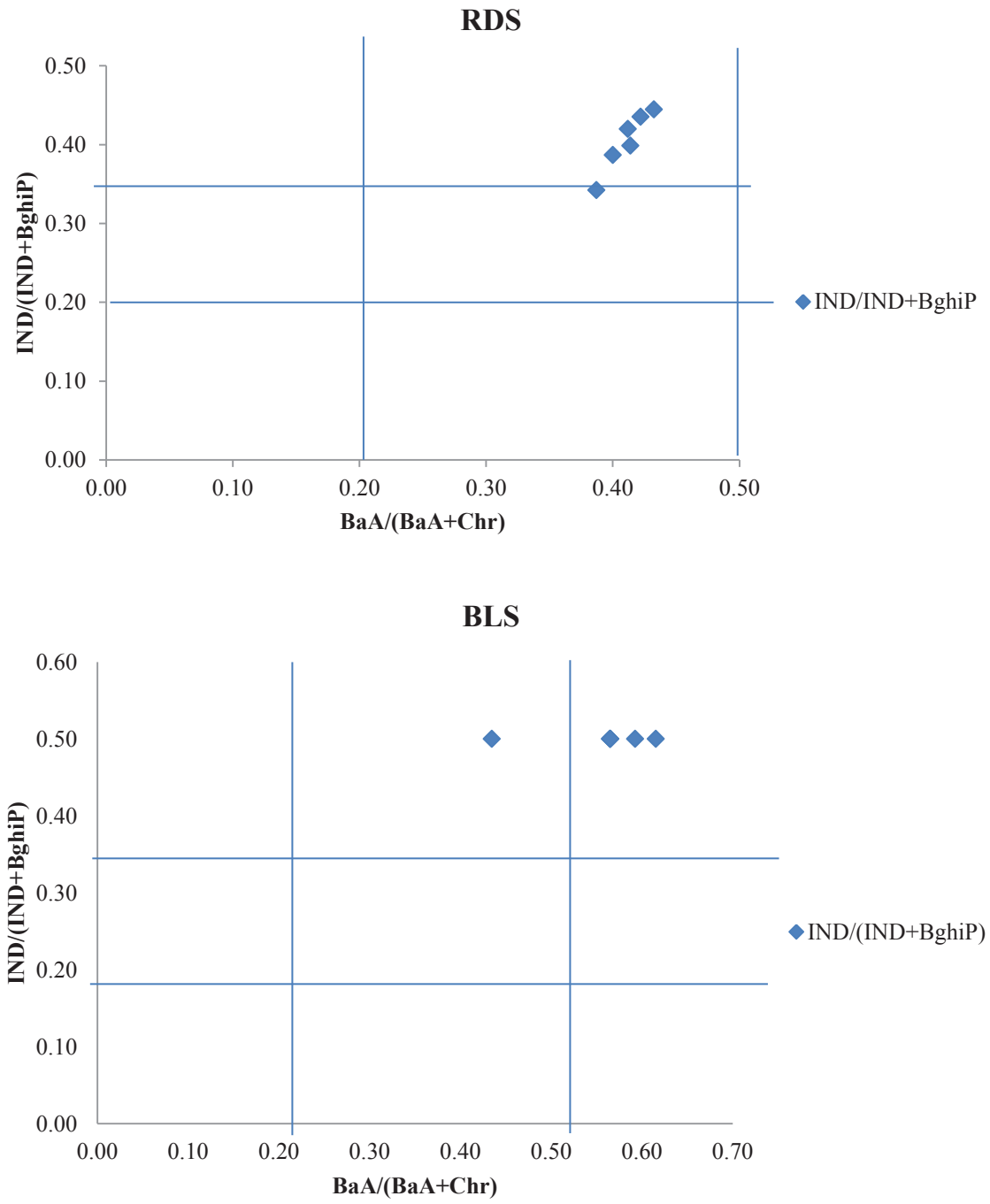

Figure 2. Diagnostic PAHs ratios in RDS and BLS (petrogenic sources, pyrogenic sources).

Appendix 5.

Table 5. Diagnostic PAHs ratios in RDS and NS (petro - petrogenic sources, pyro -pyrogenic sources, mixed – mixed sources)

	Flu/Flu+Pyr	Ant/Ant+Phe	BaA/BaA+Chr	IND/IND+BghiP
RDS1	0.51	0.18	0.43	0.44
RDS2	0.47	0.14	0.39	0.34
RDS3	0.48	0.16	0.41	0.40
RDS4	0.47	0.15	0.41	0.42
RDS5	0.49	0.13	0.42	0.44
RDS5	0.47	0.18	0.40	0.39
NS1	0.50	0.57	0.43	0.50
NS2	0.50	0.40	0.57	0.50
NS3	0.50	0.36	0.62	0.50
NS4	0.50	0.38	0.57	0.50
NS5	0.50	0.27	0.59	0.50
NS5	0.50	0.40	0.57	0.50

Appendix 6. TOC correlation with total PAHs in RDS of Commenarra Parkway

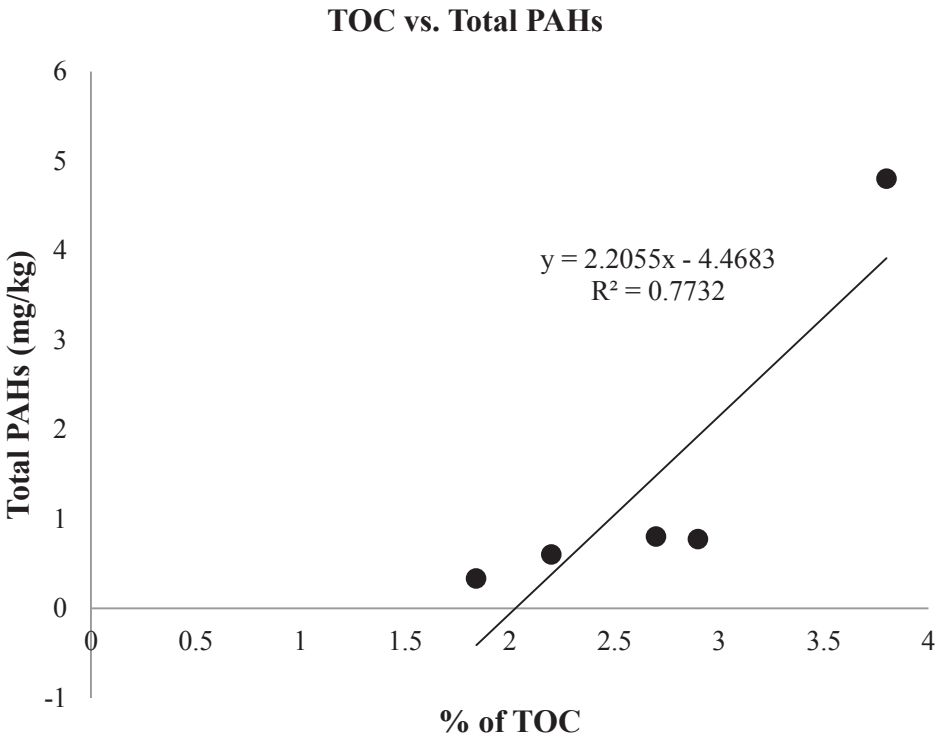

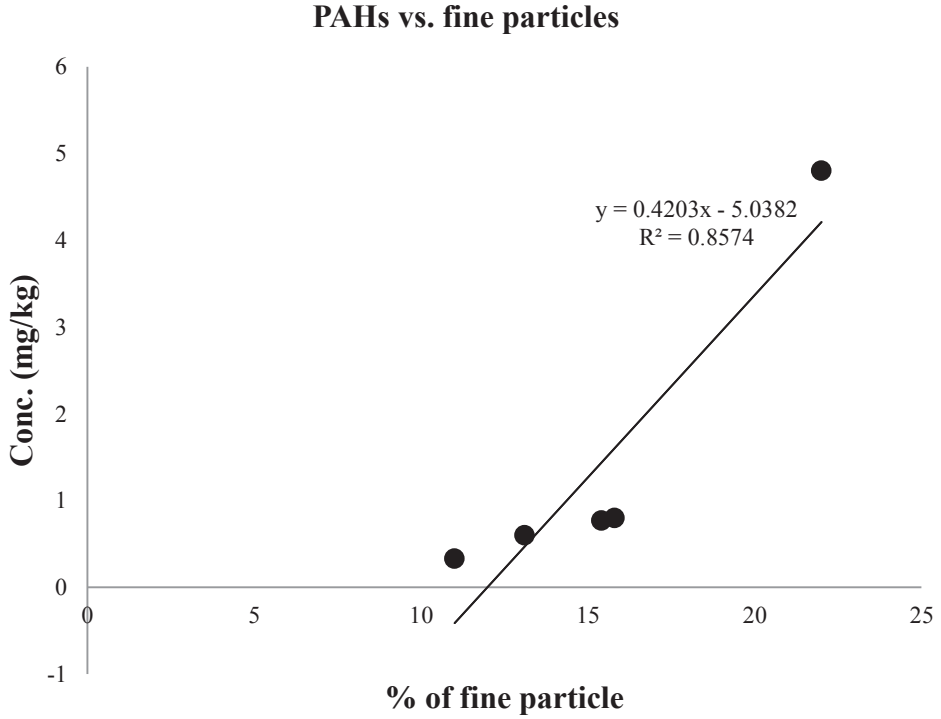

APPENDIX

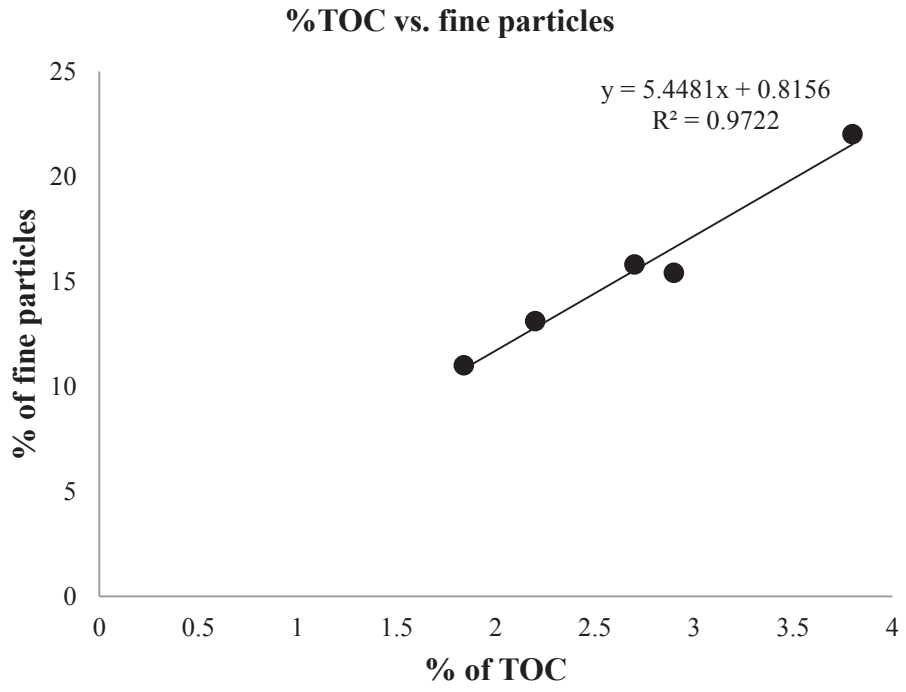

Figure 3. TOC relationship with fine particles and PAHs concentrations in RDS

Appendix 7. Characteristic of furnace slag and fly ash

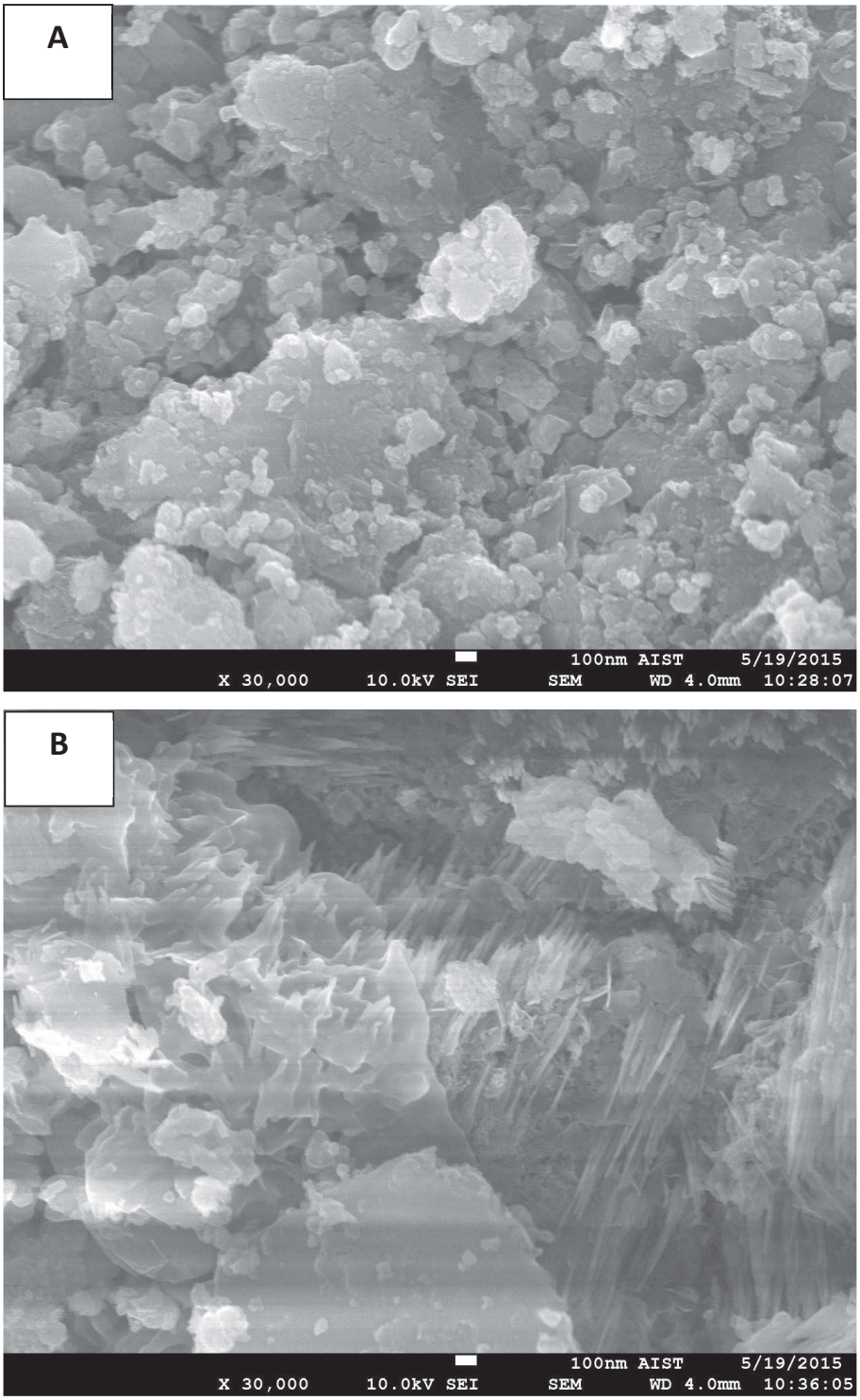

Figure 4. SEM images of furnace slag (A) and saturated slag (B)

APPENDIX

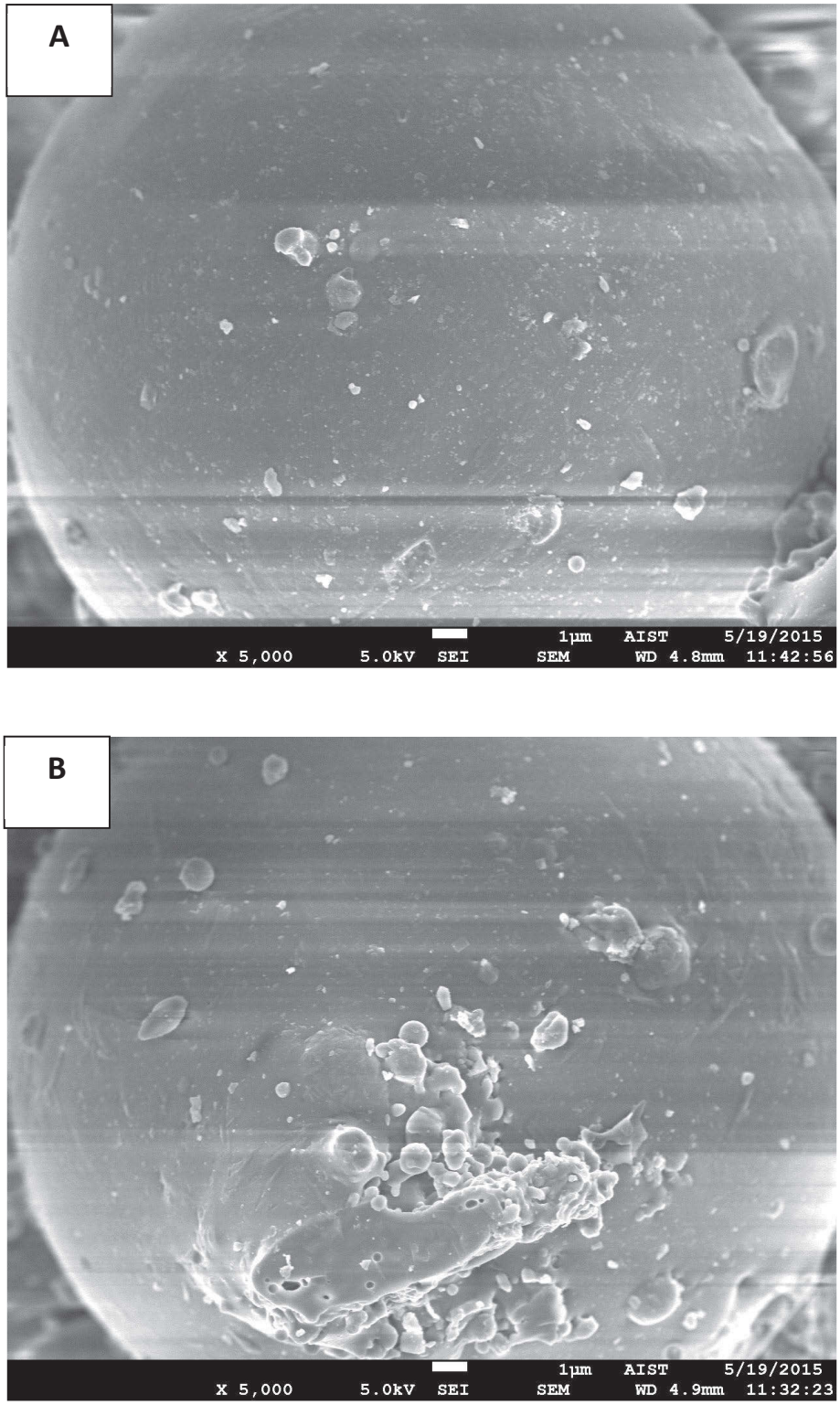

Figure 5. SEM images of fly ash (A) and saturated fly ash (B)

APPENDIX

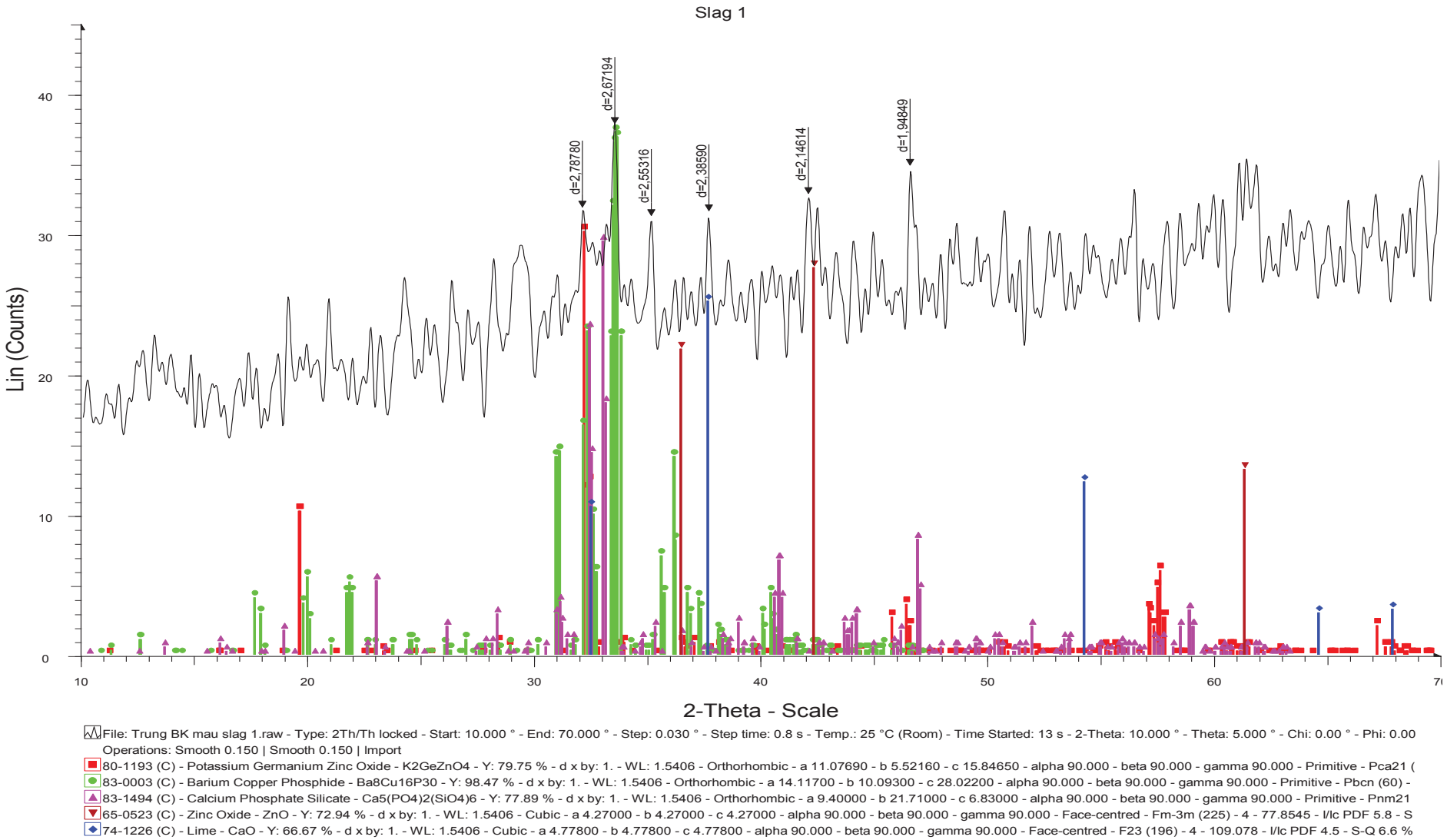
Slag 1
d=2,78780
d=2,67194
d=2,55316
d=2,38590
d=2,14614
d=1,94849
Lin (Counts)
0
10
20
30
40
10
20
30
40
50
60
2-Theta - Scale
File: Trung BK mau slag 1.raw - Type: 2Th/Th locked - Start: 10.000 ° - End: 70.000 ° - Step: 0.030 ° - Step time: 0.8 s - Temp.: 25 °C (Room) - Time Started: 13 s - 2-Theta: 10.000 ° - Theta: 5.000 ° - Chi: 0.00 ° - Phi: 0.00
Operations: Smooth 0.150 | Smooth 0.150 | Import
80-1193 (C) - Potassium Germanium Zinc Oxide - K2GeZnO4 - Y: 79.75 % - d x by: 1. - WL: 1.5406 - Orthorhombic - a 11.07690 - b 5.52160 - c 15.84650 - alpha 90.000 - beta 90.000 - gamma 90.000 - Primitive - Pca21 (
83-0003 (C) - Barium Copper Phosphide - Ba8Cu16P30 - Y: 98.47 % - d x by: 1. - WL: 1.5406 - Orthorhombic - a 14.11700 - b 10.09300 - c 28.02200 - alpha 90.000 - beta 90.000 - gamma 90.000 - Primitive - Pbcn (60) -
83-1494 (C) - Calcium Phosphate Silicate - Ca5(PO4)2(SiO4)6 - Y: 77.89 % - d x by: 1. - WL: 1.5406 - Orthorhombic - a 9.40000 - b 21.71000 - c 6.83000 - alpha 90.000 - beta 90.000 - gamma 90.000 - Primitive - Pnm21
65-0523 (C) - Zinc Oxide - ZnO - Y: 72.94 % - d x by: 1. - WL: 1.5406 - Cubic - a 4.27000 - b 4.27000 - c 4.27000 - alpha 90.000 - beta 90.000 - gamma 90.000 - Face-centred - Fm-3m (225) - 4 - 77.8545 - I/Ic PDF 5.8 - S
74-1226 (C) - Lime - CaO - Y: 66.67 % - d x by: 1. - WL: 1.5406 - Cubic - a 4.77800 - b 4.77800 - c 4.77800 - alpha 90.000 - beta 90.000 - gamma 90.000 - Face-centred - F23 (196) - 4 - 109.078 - I/Ic PDF 4.5 - S-Q 6.6 %

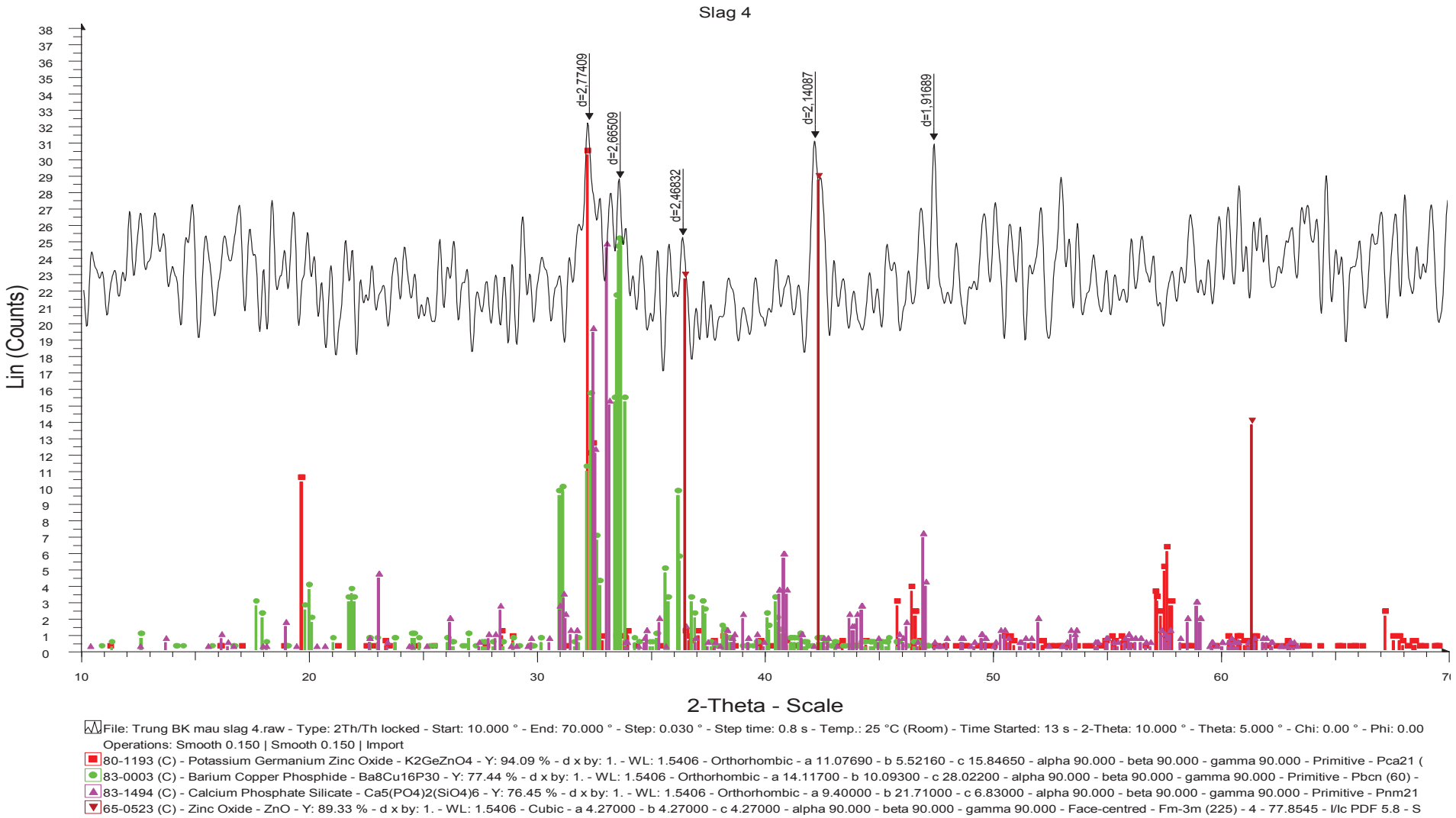
Slag 4
Lin (Counts)
2-Theta - Scale
d=2,77409
d=2,66509
d=2,46832
d=2,14087
d=1,91689
File: Trung BK mau slag 4.raw - Type: 2Th/Th locked - Start: 10.000 ° - End: 70.000 ° - Step: 0.030 ° - Step time: 0.8 s - Temp.: 25 °C (Room) - Time Started: 13 s - 2-Theta: 10.000 ° - Theta: 5.000 ° - Chi: 0.00 ° - Phi: 0.00
Operations: Smooth 0.150 | Smooth 0.150 | Import
80-1193 (C) - Potassium Germanium Zinc Oxide - K2GeZnO4 - Y: 94.09 % - d x by: 1. - WL: 1.5406 - Orthorhombic - a 11.07690 - b 5.52160 - c 15.84650 - alpha 90.000 - beta 90.000 - gamma 90.000 - Primitive - Pca21 (
83-0003 (C) - Barium Copper Phosphide - Ba8Cu16P30 - Y: 77.44 % - d x by: 1. - WL: 1.5406 - Orthorhombic - a 14.11700 - b 10.09300 - c 28.02200 - alpha 90.000 - beta 90.000 - gamma 90.000 - Primitive - Pbcn (60) -
83-1494 (C) - Calcium Phosphate Silicate - Ca5(PO4)2(SiO4)6 - Y: 76.45 % - d x by: 1. - WL: 1.5406 - Orthorhombic - a 9.40000 - b 21.71000 - c 6.83000 - alpha 90.000 - beta 90.000 - gamma 90.000 - Primitive - Pnm21
65-0523 (C) - Zinc Oxide - ZnO - Y: 89.33 % - d x by: 1. - WL: 1.5406 - Cubic - a 4.27000 - b 4.27000 - c 4.27000 - alpha 90.000 - beta 90.000 - gamma 90.000 - Face-centred - Fm-3m (225) - 4 - 77.8545 - I/Ic PDF 5.8 - S

APPENDIX

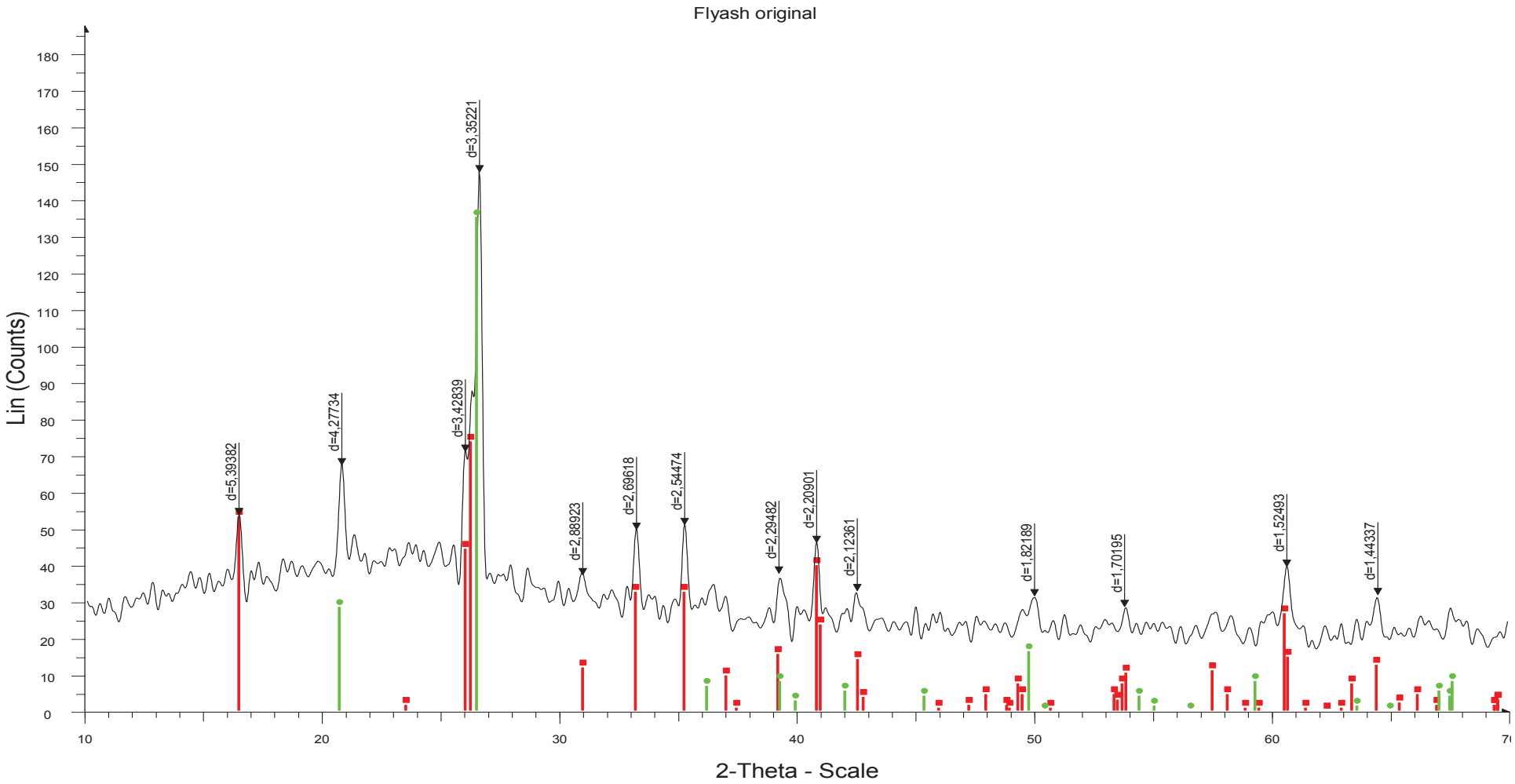
Flyash original
Lin (Counts)
2-Theta - Scale
d=5,39382
d=4,27734
d=3,42839
d=3,35221
d=2,88923
d=2,69618
d=2,54474
d=2,29482
d=2,20901
d=2,12361
d=1,82189
d=1,70195
d=1,52493
d=1,44337
File: Trung BK mau flyash original.raw - Type: 2Th/Th locked - Start: 10.000 ° - End: 70.000 ° - Step: 0.030 ° - Step time: 0.8 s - Temp.: 25 °C (Room) - Time Started: 14 s - 2-Theta: 10.000 ° - Theta: 5.000 ° - Chi: 0.00 ° -
Operations: Smooth 0.150 | Smooth 0.150 | Import
83-2187 (D) - Quartz - SiO2 - Y: 91.67 % - d x by: 1. - WL: 1.5406 - Hexagonal - a 4.96500 - b 4.96500 - c 5.42400 - alpha 90.000 - beta 90.000 - gamma 120.000 - Primitive - P3121 (152) - 3 - 115.795 - I/Ic PDF 3.1 - S-Q
89-2814 (C) - Mullite - synthetic - Al(Al.83Si1.08O4.85) - Y: 50.00 % - d x by: 1. - WL: 1.5406 - Orthorhombic - a 7.58400 - b 7.69300 - c 2.89000 - alpha 90.000 - beta 90.000 - gamma 90.000 - Primitive - Pbam (55) - 2 - 1

APPENDIX

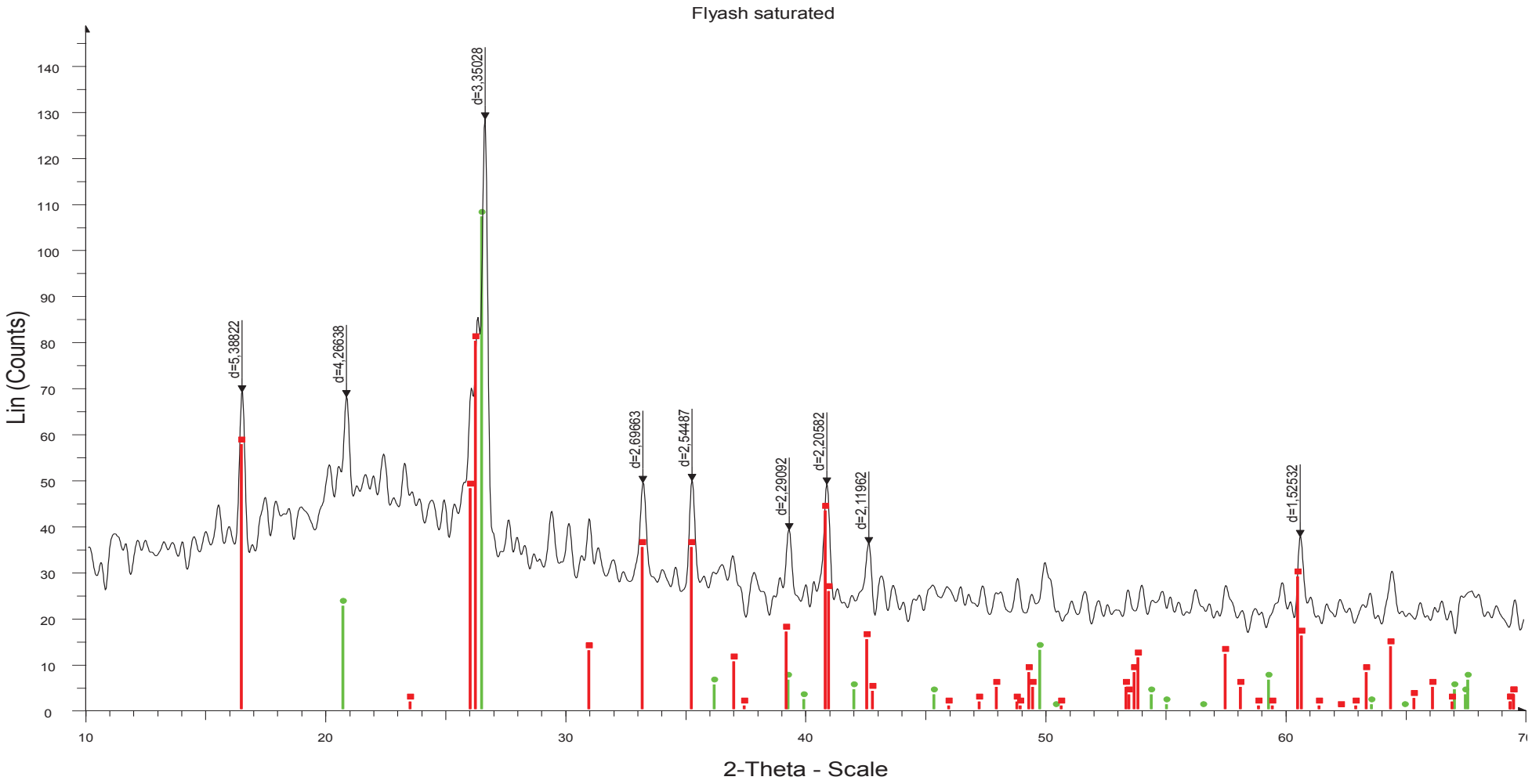
Flyash saturated
Lin (Counts)
2-Theta - Scale
d=5,38822
d=4,26638
d=3,35028
d=2,69663
d=2,54487
d=2,29092
d=2,20582
d=2,11962
d=1,52532
File: Trung BK mau flyash saturated.raw - Type: 2Th/Th locked - Start: 10.000 ° - End: 70.000 ° - Step: 0.030 ° - Step time: 0.8 s - Temp.: 25 °C (Room) - Time Started: 13 s - 2-Theta: 10.000 ° - Theta: 5.000 ° - Chi: 0.00 ° -
Operations: Smooth 0.150 | Smooth 0.150 | Import
83-2187 (D) - Quartz - SiO2 - Y: 83.47 % - d x by: 1. - WL: 1.5406 - Hexagonal - a 4.96500 - b 4.96500 - c 5.42400 - alpha 90.000 - beta 90.000 - gamma 120.000 - Primitive - P3121 (152) - 3 - 115.795 - I/Ic PDF 3.1 - S-Q
89-2814 (C) - Mullite - synthetic - Al(Al.83Si1.08O4.85) - Y: 62.39 % - d x by: 1. - WL: 1.5406 - Orthorhombic - a 7.58400 - b 7.69300 - c 2.89000 - alpha 90.000 - beta 90.000 - gamma 90.000 - Primitive - Pbam (55) - 2 - 1

APPENDIX

Furnace slag

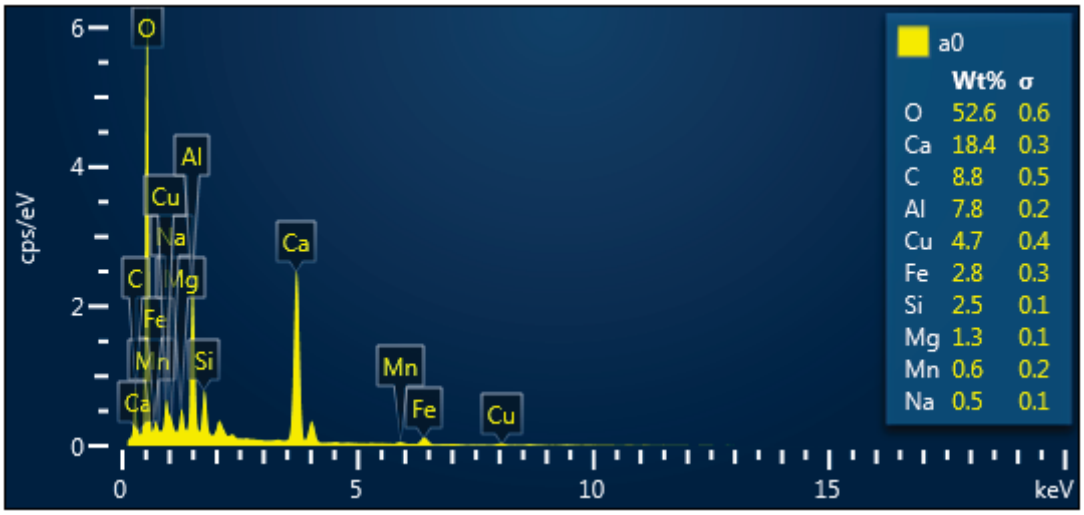

Saturated furnace slag

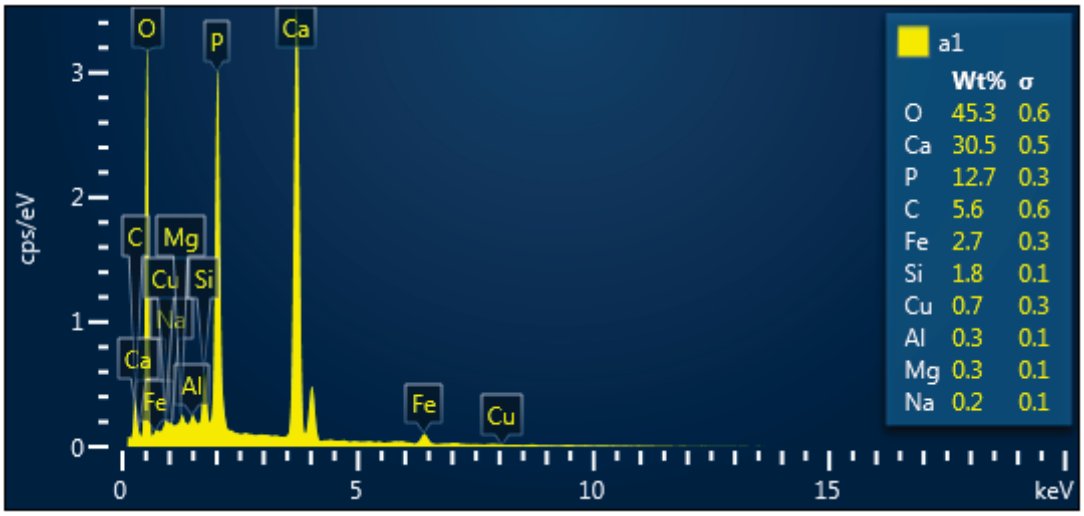

APPENDIX

Fly ash

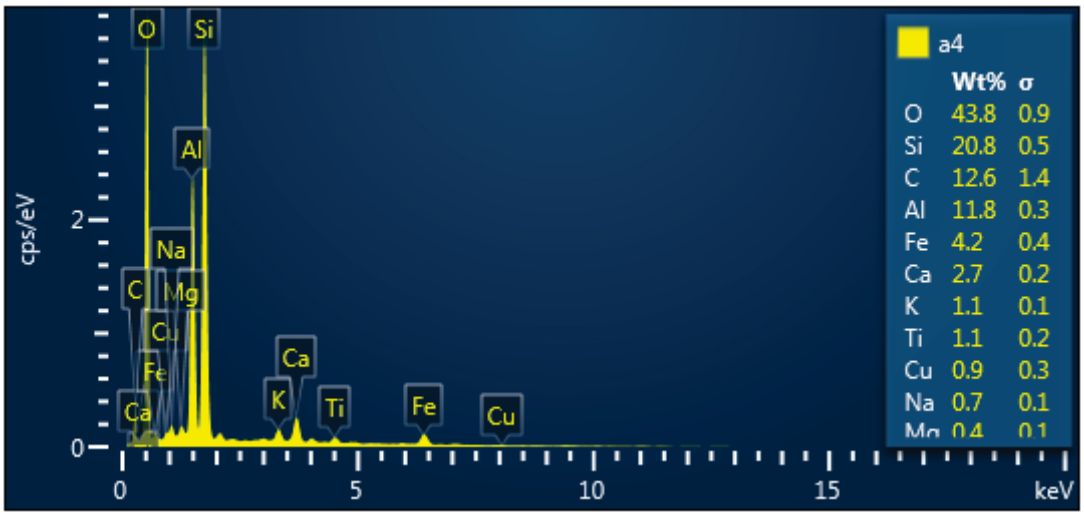

Saturated fly ash

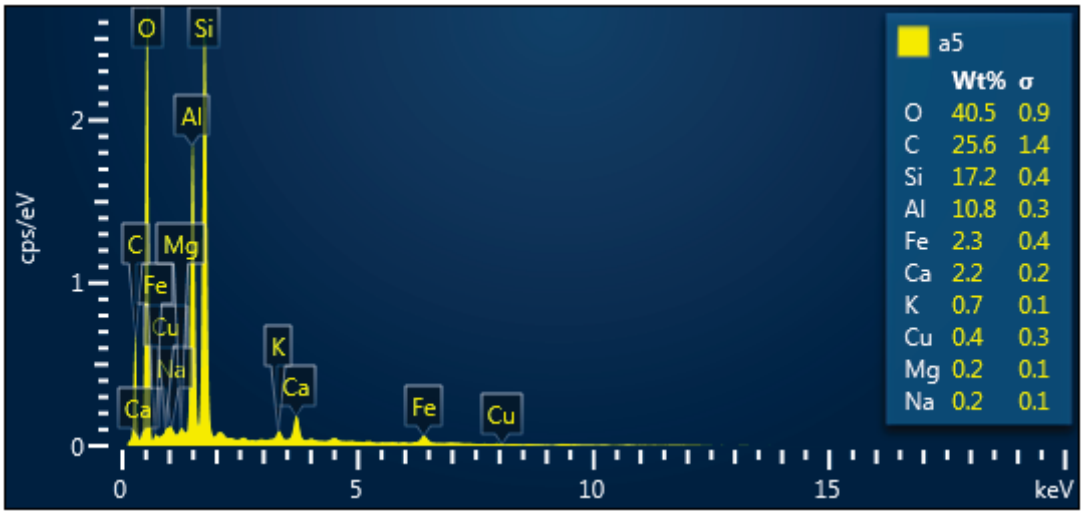

Quantachrome® ASiQwin™- Automated Gas Sorption Data Acquisition and Reduction
© 1994-2012, Quantachrome Instruments
version 3.0

Analysis			Report			
Operator:	Vien KH Vat lieu	Date:2014/01/21	Operator:	Vien KH Vat lieu	Date:2014/01/21	
Sample ID:	furnace slag	Filename:	Furnace slagall.qps			
Sample Desc:		Comment:				
Sample Weight:	5.9039 g	Instrument:	Autosorb iQ Station 1			
Approx. Outgas Time:	6.0 hrs	Final Outgas Temp.:	200 °C	Extended info:	Available	
Analysis gas:	Nitrogen	Non-ideality:	6.58e-05 1/Torr	CellType:	9mm w/o rod	
Analysis Time:	0:20 hr:min	Bath temp.:	77.35 K			
Analysis Mode:	Standard			VoidVol Remeasure:	on	
VVrm(1):	v=0 @ t=0	VVrm(2):	v=0 @ t=0			
VoidVol. Mode:	He Measure	Cold Zone V:	7.39032 cc	Warm Zone V:	13.8279 cc	

Multi-Point BET

Data Reduction Parameters Data

Adsorbate	Thermal Transpiration: on	Eff. mol. diameter (D):	3.54 Å	Eff. cell stem diam. (d):	4.0000 mm
	Nitrogen	Temperature	77.350K		
	Molec. Wt.: 28.013	Cross Section:	16.200 Å²	Liquid Density:	0.808 g/cc

Multi-Point BET Data

Relative Pressure [P/Po]	Volume @ STP [cc/g]	1 / [W((Po/P) - 1)]	Relative Pressure [P/Po]	Volume @ STP [cc/g]	1 / [W((Po/P) - 1)]
4.99380e-02	0.2125	1.9787e+02	2.01153e-01	0.2930	6.8769e+02
7.72157e-02	0.2319	2.8868e+02	2.51000e-01	0.3155	8.4995e+02
1.02090e-01	0.2462	3.6853e+02	3.01005e-01	0.3391	1.0161e+03
1.51082e-01	0.2701	5.2725e+02			

BET summary

Slope =	3246.481
Intercept =	3.675e+01
Correlation coefficient, r =	0.999985
C constant=	89.332
Surface Area =	1.061 m²/g

APPENDIX

Surface area of Fly ash: 2.823 m^2/g

Quantachrome® ASiQwin™- Automated Gas Sorption Data Acquisition and Reduction
© 1994-2012, Quantachrome Instruments
version 3.0

Analysis			Report		
Operator:	Vien KH Vat lieu	Date:2014/01/21	Operator: Vien KH Vat lieu		Date:2014/01/21
Sample ID:	Flyash1	Filename:	Flyash 1.qps		
Sample Desc:		Comment:			
Sample Weight:	0.5545 g	Instrument:	Autosorb iQ Station 1		
Approx. Outgas Time:	3.3 hrs	Final Outgas Temp.:	200 °C	Extended info:	Available
Analysis gas:	Nitrogen	Non-ideality:	6.58e-05 1/Torr	CellType:	9mm w/o rod
Analysis Time:	0:22 hr:min	Bath temp.:	77.35 K		
Analysis Mode:	Standard			VoidVol Remeasure:	on
VVrm(1):	v=0 @ t=0	VVrm(2):	v=0 @ t=0		
VoidVol. Mode:	He Measure	Cold Zone V:	3.23035 cc	Warm Zone V:	13.7491 cc

Multi-Point BET

Data Reduction Parameters Data

Adsorbate	Thermal Transpiration: on	Eff. mol. diameter (D):	3.54 Å	Eff. cell stem diam. (d):	4.0000 mm
	Nitrogen	Temperature	77.350K		
	Molec. Wt.: 28.013	Cross Section:	16.200 Å²	Liquid Density:	0.808 g/cc

Multi-Point BET Data

Relative Pressure [P/Po]	Volume @ STP [cc/g]	1 / [W((Po/P) - 1)]	Relative Pressure [P/Po]	Volume @ STP [cc/g]	1 / [W((Po/P) - 1)]
4.79755e-02	0.5664	7.1186e+01	2.04031e-01	0.7924	2.5883e+02
7.96040e-02	0.6266	1.1044e+02	2.54072e-01	0.8500	3.2062e+02
1.05123e-01	0.6680	1.4070e+02	3.04199e-01	0.9048	3.8661e+02
1.54017e-01	0.7327	1.9881e+02			

BET summary

Slope =	1221.504
Intercept =	1.195e+01
Correlation coefficient, r =	0.999865
C constant=	103.199
Surface Area =	2.823 m²/g

APPENDIX

Furnace slag

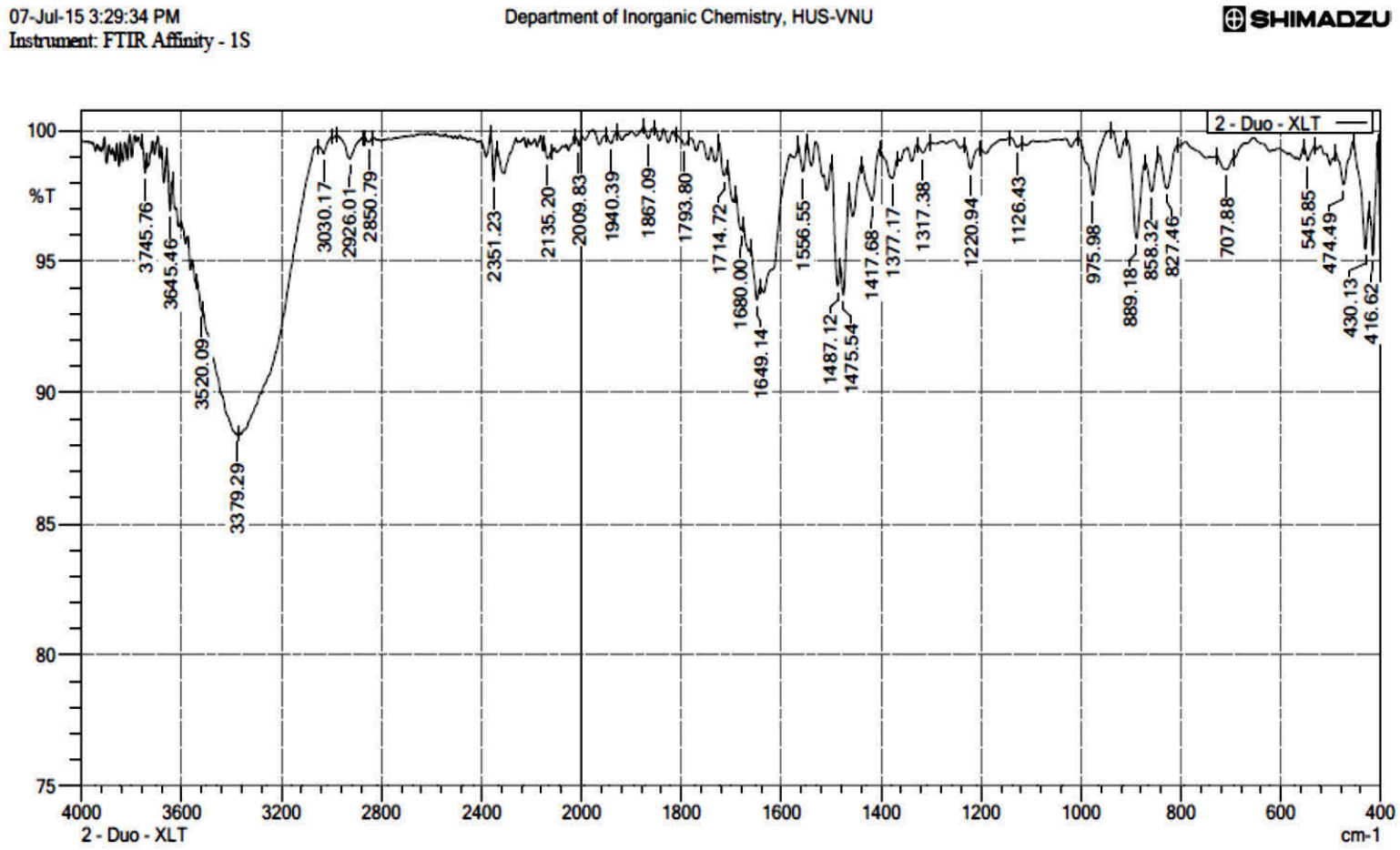

APPENDIX

Fly ash